

**BIOLOGICAL ACTIVITIES OF *CURCUMA PURPURASCENS* BL.
RHIZOME EXTRACT USING *IN VITRO* AND *IN VIVO* MODELS**

ELHAM ROUHOLLAHI

**THESIS SUBMITTED IN FULFILLMENT OF THE
REQUIREMENTS FOR THE DEGREE OF DOCTOR OF
PHILOSOPHY**

**FACULTY OF MEDICINE
UNIVERSITY OF MALAYA
KUALA LUMPUR**

2016

UNIVERSITY OF MALAYA

ORIGINAL LITERARY WORK DECLARATION

Name of Candidate: Elham Rouhollahi

Passport No:

Registration/Matric No: MHA 120053

Name of Degree: PhD

Title of Thesis: Biological activity of *Curcuma purpurascens* *BI.* rhizome extract using *in vitro* and *in vivo* models

Field of Study: pharmacology

I do solemnly and sincerely declare that:

(1) I am the sole author/writer of this Work;

(2) This Work is original;

(3) Any use of any work in which copyright exists was done by way of fair dealing and for permitted purposes and any excerpt or extract from, or reference to or reproduction of any copyright work has been disclosed expressly and sufficiently and the title of the Work and its authorship have been acknowledged in this work;

(4) I do not have any actual knowledge nor ought I reasonably to know that the making of this work constitutes an infringement of any copyright work;

(5) I hereby assign all and every rights in the copyright to this work to the University of Malaya ("UM"), who henceforth shall be owner of the copyright in this work and that any reproduction or use in any form or by any means whatsoever is prohibited without the written consent of UM having been first had and obtained;

(6) I am fully aware that if in the course of making this work I have infringed any copyright whether intentionally or otherwise, I may be subject to legal action or any other action as may be determined by UM.

Candidate's Signature

Date

Witness's Signature

Date

Name:

Designation

ABSTRACT

Curcuma purpurascens BI. is a medicinal plant from the Zingiberaceae family, which is widely used as a spice and in folk medicine for the treatment of wounds, scabies, itching, fever, cough and boil. In this study, chemopreventive properties of dichloromethane and hexane extracts of *C. purpurascens* BI rhizome (DECPR and HECPR) on azoxymethane-induced colonic aberrant crypt foci (ACF), gastroprotective and wound healing potential in rats were been evaluated. The acute toxicity test of DECPR and HECPR in rats, carried out in two doses, i.e. 2 and 5 g/kg, showed that these two plant extracts were safe even at a high dose (5 g/kg). DECPR apoptosis-inducing effect was investigated against HT-29 colon cancer cell line utilising a bioassay-guided approach. The chemoprotective experiment was performed in five groups of rats: negative control, positive cancer control, DECPR (250, 500 mg/kg) and reference drug (5-fluorouracil) group. Methylene blue staining of colon specimens showed that treatment with of DECPR at both doses significantly reduced the colonic ACF formation compared with the positive cancer control group. Immunohistochemistry analysis showed down-regulation of PCNA and Bcl-2 proteins and up-regulation of Bax protein after administration of DECPR compared with the positive cancer control group. In addition, an increase in the levels of enzymatic antioxidants and a decrease in the malondialdehyde (MDA) level of the colon tissue homogenates were observed, suggesting the suppression of lipid peroxidation levels. These findings substantiate the usage of *Curcuma purpurascens* BI. in ethno- medicine against cancer.

For wound healing experiment *Sprague Dawley* rats were randomly divided into four groups: vehicle control, HECPR (100-200 mg/ml), and positive control with excisional wound

Created on the neck area. Wounds were topically dressed twice a day with HECPR for 20 days. On the 20th day, animals were sacrificed and immunohistochemical and histological processes including Hematoxylin & Eosin and Masson Trichrome stains were carried out. The antioxidant activity, namely catalase, glutathione peroxidase and superoxide dismutase, and MDA were measured in wound tissue homogenate. Macroscopic and microscopic analysis of wounds demonstrated a significant wound healing activity shown by HECPR at two doses (100-200 mg/ml). Treatment of wounds with HECPR caused significant surge in antioxidant activity and decrease in the MDA level of wound tissues compared with positive control. The immunohistochemical evaluation revealed conspicuous up-regulation of Hsp70 in treated wounds with HECPR, suggesting that the anti-inflammatory effect of HECPR. Furthermore, HECPR exhibited a promising wound healing potential towards excisional wound models in rats.

The gastroprotective effect of hexane extract of HECPR was investigated against ethanol-induced gastric injury models in rats. The antiulcer study in rats (five groups, n=6) was performed with two doses of HECPR (200 and 400 mg/kg) and with omeprazole (20 mg/kg), as a standard antiulcer drug. Gross and histological features showed the antiulcerogenic characterizations of HECPR. There was significant suppression on the ulcer lesion index of rats pretreated with HECPR, which was comparable to the omeprazole effect. Oral administration of HECPR to rats resulted in a significant increase in the level of nitric oxide and antioxidant activity, including catalase, glutathione, and superoxide dismutase associated with attenuation in gastric acidity, and compensatory effect on the loss of gastric wall mucus. In addition, pretreatment of rats with HECPR caused significant reduction in the level of MDA (a marker for oxidative stress), which is associated with an increase in prostaglandin E2 activity. Immunohistochemical staining also demonstrated that HECPR induced the down-regulation of Bax and up-regulation of Hsp70 proteins after pretreatment. Collectively, the present results suggest that HECPR

has promising antiulcer potential, which could be attributed to its suppressive effect against oxidative damage and preservative effect toward gastric wall mucus. The current study suggests that *Curcuma purpurascens* BI. Extracts are safe and have anti-cancer activity, cancer prevention, significant gastroprotective activity and excision wound-healing potential.

University of Malaya

ABSTRAK

Curcuma purpurascens BI adalah tumbuhan ubatan daripada famili Zingiberaceae yang digunakan secara meluas sebagai bahan rempah dan perubatan tradisional. Dalam kajian ini, ciri-ciri pencegahan kimia oleh ekstrak diklorometin dan heksana bagi rizom *C. purpurascens* BI (DECPR dan HECPR) ke atas crypt foci kolon yang tidak normal yang dirangsang oleh azoxymetin (ACF), keupayaan gastro dan penyembuhan luka pada tikus telah dinilai. Ujian toksisiti akut terhadap DECPR dan HECPR pada tikus telah dijalankan dengan dua dos iaitu 2 and 5 g/kg, yang mana, ia menunjukkan bahawa ekstrak ini selamat digunakan, walaupun pada dos yang lebih tinggi daripada 5 g/kg. Kesan DECPR untuk merangsang apoptosis telah disiasat terhadap titisan sel kanser kolon HT-29 dengan menggunakan pendekatan berpandukan bioasai. Eksperimen ini telah dibahagikan kepada lima kumpulan tikus: kawalan negatif, kawalan kanser, DECPR (250, 500 mg/kg), dan kawalan positif (5-fluorouracil). Pewarnaan biru metilin ke atas spesimen kolorektal menunjukkan bahawa aplikasi DECPR pada kedua-dua dos berkurang secara signifikan bagi pembentukan ACF koloni berbanding dengan kumpulan kawalan kanser. Analisis immunohistokimia menunjukkan pengawalturan-rendah bagi protein-protein PCNA dan Bcl-2 dan pengawalturan-tinggi bagi protein Bax selepas pemberian DECPR berbanding dengan kumpulan kawalan kanser. Tambahan pula, peningkatan aras enzim antioksidan dan penurunan aras malondialdehid (MDA) ke atas tisu homegenat kolon mencadangkan berlakunya penindasan aras protein lipid peroksidasi. Penemuan ini menyokong penggunaan *Curcuma purpurascens* BI dalam perubatan etho menentang kanser.

Tikus *Sprague Dawley* telah dibahagikan secara rawak kepada empat kumpulan: kawalan negatif, HECPR (100-200 mg/ml), dan kawalan positif dengan pemotongan luka tercipta pada kawasan leher. Luka-luka dirawat secara luaran dua kali untuk sehari selama 20 hari. Pada hari ke-20, haiwan-haiwan telah dikorbankan dan penilaian

imunohistokimia dan histologi termasuklah pewarnaan Hematoxylin & Eosin dan Masson Trichrome telah diproses. Aktiviti-aktiviti antioksidan seperti katalase, perosidasi glutathione dan superoksida dismutase, dan MDA telah diukur pada homegenat tisu luka. Analisis makroskopik dan mikroskopik bagi luka-luka menunjukkan aktiviti luka penyembuhan yang signifikan ditunjukkan oleh HECPR. Rawatan ke atas luka dengan krim mengandungi HECPR telah menyebabkan peningkatan aktiviti antioksidan dan penurunan aras MDA secara signifikan bagi tisu-tisu luka berbanding dengan kawalan negatif. Penilaian imunohistokimia mendedahkan pengawalturan-tinggi yang ketara ke atas HECPR. HECPR mempamerkan keupayaan penyembuhan luka yang baik ke atas model pemotongan luka pada tikus.

Kesan pencegahan gastro telah disiasat menggunakan ekstrak etil asetat HECPR terhadap model kecederaan gastrik teransang etanol pada tikus. Kajian antiulser pada tikus (lima kumpulan, n=6) telah dipersembahkan dengan dua dos HECPR (200 dan 400 mg/kg) dan dengan omeprazole (20 mg/kg), sebagai dadah piawai antiulser. Ciri-ciri kasar dan histologi menunjukkan pencirian antiulserogenik ke atas HECPR. Terdapat penindasan yang signifikan bagi indeks ulser ke atas tikus yang dipra-rawat dengan HECPR, di mana ia setanding dengan kesan omeprazole. Pemberian HECPR secara oral kepada tikus-tikus menyebabkan peningkatan signifikan aras nitrik oksida dan aktiviti-aktiviti antioksidan, termasuklah katalase, glutathione, dan superoksida dismutase yang dikaitkan dengan pengurangan asiditi gastrik dan kesan penggantian ke atas kehilangan mukus dinding gastrik. Sebagai tambahan, prarawatan pada tikus-tikus dengan HECPR menyebabkan penurunan signifikan aras MDA (penanda bagi tekanan oksidatif) yang dikaitkan dengan peningkatan aktiviti prostaglandin E2. Pewarnaan imunohistokimia juga menunjukkan bahawa HECPR telah meransang pengawalturan-rendah bagi protein Bax dan pengawalturan rendah bagi protein Hsp70 selepas prarawatan. Secara pengumpulan, keputusan-keputusan terkini mencadangkan bahawa HECPR mempunyai

keupayaan antiulser yang baik, yang mana mungkin penyebab kepada kesan penindasan terhadap kerosakan oksidatif dan kesan pemeliharaan ke arah mukus dinding gastrik. Kajian ini menunjukkan ekstrak *Curcuma purpurascens* BI. adalah selamat digunakan dan menunjukkan aktiviti anti-kanser, pelindung system pencernaan yang signifikan dan berpotensi untuk menyembuhkan luka luaran.

University of Malaya

ACKNOWLEDGMENT

First, I would like to thank God for giving me this chance to continue my study at higher level despite facing difficulties and helping me to overcome all of them.

My gratitude particularly goes to my supervisor, Professor Dr. Zahurin Mohamed for giving me this opportunity of doing my research project under their supervision and also sincere thanks for their everlasting and heartfelt guidance and kind attention. I am deeply indebted to my supportive supervisor by encouraging me in all steps of doing my research from the beginning to the end.

In addition, I would like to express my sincere thanks to Professor Dr. Mahmood Ameen Abdulla, Dr. Soheil Zorofchian Moghadamtousi and Dr. Chung Yeng Looi, for his kind guidance and cooperation and to all my laboratory mates who were by my side in this effort, especially during the stressful times.

I want to express my great appreciation to my beloved family members, my dear father and mother for their support and understanding.

TABLE OF CONTENTS

ABSTRACT	iii
ABSTRAK	vi
ACKNOWLEDGMENT	ix
TABLE OF CONTENTS	x
LIST OF FIGURES	xiv
LIST OF TABLES	xix
1 CHAPTER 1: INTRODUCTION	1
1.1 Cancer	1
1.2 Colon Cancer.....	1
1.3 Gastric Ulcer	3
1.4 Wound Healing	6
1.5 Hypothesis of the Research	7
1.6 Objectives of the Study	8
1.6.1 General Objectives	8
1.6.2 Specific Objectives.....	8
2 CHAPTER 2: LITERATURE REVIEW	9
2.1 Colorectal Cancer.....	9
2.1.1 Signs and Symptoms of Colorectal Cancer.....	10
2.1.2 Cause of Colorectal Cancer.....	10
2.1.3 Inflammatory bowel disease.....	11
2.1.4 Diagnosis.....	11
2.1.5 Pathology of Colorectal Cancer	12
2.1.6 Aberrant Crypt Foci (ACF).....	14
2.1.7 Azoxymethane AOM	16
2.1.7.1 Metabolism of AOM in Colon Cancer.....	18
2.1.7.2 Mechanisms of AOM in Colon Cancer.....	18
2.1.8 Mechanism of Action of 5-Flurouracil.....	22
2.2 Gastric Ulcer	25
2.2.1 Definition	25
2.2.2 Possible Etiology and Risk Factors of Gastric Ulcer	26
2.2.2.1 Acid Output.....	26
2.2.2.2 Nonsteroidal Anti-Inflammatory Drugs.....	26
2.2.2.3 Life Style Factors	26
2.2.2.4 Genetics.....	26
2.2.2.5 <i>Helicobacter pylori</i> Infection.....	27
2.2.3 Drugs for Gastric Ulcer Treatment.....	27
2.2.4 Gastroprotective Factors and Gastric Mucosal Integrity.....	28
2.3 Wound Healing	33

2.3.1	Definition	33
2.3.2	Phases of Wound Healing	34
2.3.2.1	Hemostasis	35
2.3.2.2	Inflammation	37
2.3.2.3	Cellular Migration and Proliferation	39
2.3.2.4	Protein Synthesis and Wound Contraction.....	40
2.3.2.5	Remodeling	42
2.3.3	Wound Healing Factors.....	44
2.3.3.1	Infection	44
2.3.3.2	Local Blood Supply.....	45
2.3.3.3	Malnutrition and Healing Delay.....	45
2.3.3.4	Age	48
2.3.3.5	Reactive Oxygen Species (ROS).....	48
2.3.4	Apoptosis.....	50
2.4	Medicinal Plants.....	54
2.4.1	<i>C. Purpurascens</i>	54
3	CHAPTER 3: METHODOLOGY	57
3.1	Plant Collection and Preparation of Extracts	57
3.2	Evaluation of the Antioxidant Capacity of the Crude Extract	57
3.2.1	Scavenging Activity of DPPH	57
3.2.2	Ferric Reducing Antioxidant Power (FRAP) Assay	58
3.2.3	Total phenolic Content (TPC) Evaluation.....	58
3.3	<i>In Vitro</i> Anti-Cancer Study	59
3.3.1	Cell Lines and Culture Conditions	59
3.3.2	Cell Proliferation Assay	59
3.3.3	Lactate Dehydrogenase (LDH) Release Assay	60
3.3.4	Cytoskeletal Arrangement Assay	60
3.3.5	Reactive Oxygen Species (ROS) Generation Assay	60
3.3.6	Multiple Cytotoxicity Assay	61
3.3.7	DNA Fragmentation Assay	61
3.3.8	Caspase-3/7, -8 and -9 Activities Assay.....	61
3.3.9	Quantitative PCR Analysis for Bax, Bcl-2 and Bcl-xl.....	62
3.3.10	Western Blotting	62
3.4	<i>In Vivo</i> Experiment.....	63
3.4.1	Animals and Ethical Issues	63
3.4.2	Acute toxicity study	63
3.4.3	Colon Cancer.....	66
3.4.3.1	Experimental Protocols	66
3.4.3.2	Assessment of ACF.....	66
3.4.3.3	Immunohistochemistry	67
3.4.3.4	Activity of Antioxidant Enzymes.....	67

3.4.3.5	Malondialdehyde.....	67
3.4.3.6	Western blotting.....	68
3.4.4	Gastroprotective Ability of the <i>C. purpurascens</i> Extract.....	70
3.4.4.1	Animals and Ethical Issues	70
3.4.4.2	Experimental Design.....	70
3.4.4.3	Determination of the Mucosal Content and Gastric Juice Acidity.....	72
3.4.4.4	Macroscopic Analysis of Lesions	72
3.4.4.5	Determination of Lipid Peroxidation Activity	72
3.4.4.6	Determination of Superoxide Dismutase (SOD) Activity.....	73
3.4.4.7	Nitric Oxide Level.....	73
3.4.4.8	Histological Evaluation of Gastric Lesions.....	73
3.4.4.9	Immunohistochemical Evaluation.....	74
3.4.5	Wound Healing Ability of <i>C. Purpurascens</i> Extract	76
3.4.5.1	Excision wound model.....	76
3.4.5.2	Grouping, Ointment Administration and Wound Closure Percentage.....	77
3.4.5.3	Histological Evaluation	77
3.4.5.4	Immunohistochemistry Analysis.....	77
3.4.5.5	Enzymatic Activities	78
3.4.5.6	Lipid Peroxidation.....	78
3.4.5.7	Statistical Analysis	79
4	CHAPTER 1: RESULTS.....	81
4.1	Antioxidant Properties of DECPR and HECPR.....	81
4.1.1	DPPH Scavenging Activity of DECPR and HECPR.....	81
4.1.2	FRAP Capacity of DECPR and HECPR.....	81
4.1.3	Total Phenolic Content of DECPR and HECPR.....	82
4.2	In vitro results.....	83
4.2.1	MTT Cell Viability Assay.....	83
4.2.2	Cytotoxic Effects of DECPR and HECPR by LDH Release Assay	85
4.2.3	Induction of Cytoskeletal Rearrangement and Nuclear Fragmentation by DECPR 86	
4.2.4	Reactive Oxygen Species (ROS) Generation.....	88
4.2.5	Effect of DECPR on Nuclear Morphology, Membrane Permeability, Mitochondrial Membrane Potential (MMP) and Cytochrome C Release.....	90
4.2.6	Induction of Caspases Activation by DECPR.....	93
4.2.7	Induction of DNA Fragmentation by DECPR	93
4.2.8	Changes in Expression of Apoptosis-Associated Molecules by DECPR 94	
4.3	In Vivo Results	97
4.3.1	Safety of DECPR and CPRHE.....	97
4.3.2	Colon Cancer Chemoprevention Results	106
4.3.2.1	Analysis of Rat's Body Weight and Serum Biochemistry Parameter.....	106
4.3.2.2	Counting the Aberrant Crypt Foci (ACF)	109
4.3.2.3	Topographic Views of Colon	111

4.3.2.4	Histological Classification of ACF	113
4.3.2.5	Immunohistochemistry Analysis.....	115
4.3.2.6	Western Blot.....	121
4.3.2.7	Antioxidant Activities of Homogenized Colon.....	121
4.3.3	Gastroprotective Ulcer	123
4.3.3.1	PH of Gastric Content and Determination of Mucus Production.....	123
4.3.3.2	Macroscopic Evaluation of Gastric Lesions.....	125
4.3.3.3	Assessment of Stomach Malondialdehyde and Superoxide Dismutase..	127
4.3.3.4	Assessment of Nitric Oxide Level	127
4.3.3.5	Histological Assessment of Gastric Lesions by Haematoxylin and Eosin Staining	129
4.3.3.6	Histological Examination by Periodic Acid-Schif (PAS).....	131
4.3.3.7	Immunohistochemistry.....	133
4.3.4	Wound Healing Evaluation Parameters	136
4.3.5	Wound Area Contraction	136
4.3.5.1	Histological Evaluations of Healed Wound Area	140
4.3.5.2	Masson's Trichrome Staining of Healed Wound in Rats.....	142
4.3.5.3	Immunohistochemistry.....	144
4.3.5.3.1	Topical Application of HECPR Effect on Bax Expression.....	144
4.3.5.4	Antioxidant Evaluation in the Healed Wound Area.....	147
4.3.5.5	HECPR Attenuated the MDA Level	150
4.3.6	Gas Chromatography Profile of DECPR and HECPR.....	151
5	CHAPTER 5: DISCUSSION	190
5.1	Antioxidant Activity.....	190
5.2	<i>In vitro</i> studies.....	191
5.3	Colon Cancer <i>In Vivo</i>	193
5.4	Gastric ulcer	198
5.5	Wound healing	201
6	CHAPTER 6: CONCLUSION.....	206
	REFERENCES.....	208
	PUBLICATION.....	233
	Appendix A	234
	Appendix B	235
	Appendix C	237
	Appendix D	239
	Appendix E	246
	Appendix F.....	252
	Appendix G.....	257

LIST OF FIGURES

Figure 1.1: Colorectal cancer occurs in a multi-step process.....	2
Figure 2.1: Histology of colon tissue stained with H&E stain.....	13
Figure 2.2: Sequential pathological stages and molecular events in colon cancer (Corpt 2002).....	15
Figure 2.3: Chemical structure of azoxymethane (methyl-methylimino-oxidoazanium).....	17
Figure 2.4: Azoxymethane (AOM) involvement in the mechanism of colon cancer (Chen & Huang 2009b).....	19
Figure 2.5: Chemical structure of 5-Fluorouracil (5-FU) (Zhang & Kim, 2008).....	24
Figure 2.6: Gastric ulcer (Marks, 2012).....	25
Figure 2.7: Phases of wound healing (Monaco & Lawrence, 2003).....	35
Figure 2.8: Cutaneous wound healing at day 3 after injury.....	39
Figure 2.9: Cutaneous wound healing at day five after injury.	42
Figure 2.10: Cutaneous wound healing in remodeling phase.	44
Figure 3.1: flow chart of acute toxicity study.	65
Figure 3.2: Study flow chart for the chemoprevention ability of the extract of <i>C. purpurascens</i>.....	69
Figure 3.3: The gastroprotective ability of the <i>C. purpurascens</i> extract study flow chart	75
Figure 3.4: The excision wound model on day 0, before starting treatments....	76
Figure 3.5: Study flow chart for the wound healing ability of the <i>C. purpurascens</i> extract.....	80

Figure 4.1: DPPH free radical scavenging activities of HECPR and DECPR compared with the standards, Ascorbic acid, and Trolox.....	81
Figure 4.2: Ferric reducing power (FRAP) of the DECPR and HECPR.....	82
Figure 4.3: Total phenol content (TPC) of DECPR and HECPR.....	83
Figure 4.4: Lactate dehydrogenase (LDH) assay of DECPR on HT-29 cells.....	85
Figure 4.5: Induction of Cytoskeletal Rearrangement and Nuclear Fragmentation by DECPR	87
Figure 4.6: ROS generation in the presence of DECPR	89
Figure 4.7: Effect of DECPR on nuclear morphology	91
Figure 4.8: Effect of DECPR on membrane permeability mitochondrial membrane potential (MMP) and Cytochrome C release	92
Figure 4.9: Effect of DECPR on caspase 3/7, 8, and 9 activation in HT-29 cells	93
Figure 4.10: DECPR induced DNA fragmentation in HT-29	94
Figure 4.11: Quantitative RT-PCR analysis of apoptosis-associated genes in HT-29 cells.....	95
Figure 4.12: Western blot analysis of DECPR on HT-29 cells.....	96
Figure 4.13: Histological sections of kidney and liver tissue treated with DECPR	98
Figure 4.14: Histological sections of kidney and liver tissue treated with HECPR	99
Figure 4.15. Effect of DECPR on ACF formation in proximal and distal parts of the colons separated from the treated rats.....	111
Figure 4.16: Topographic views of colon mucosa of group treated with DECPR	112

Figure 4.17: Histological study of colon cancer in the rat treated with DECPR	114
Figure 4.18: Immunohistochemical analyses of the expression of PCNA in the colon tissues treated with DECPR	116
Figure 4.19: Immunohistochemical analyses of the expression of PCNA in the colon tissues treated with DECPR	117
Figure 4.20: Immunohistochemical expression of Bax in colon tissues of control and experimental groups of rats	118
Figure 4.21: Immunohistochemical expression of Bcl-2 in colon tissues of control and experimental groups of rats	120
Figure 4.22: Western blot analysis of PCNA, Bax and Bcl-2	121
Figure 4.23: Effect of DECPR on antioxidant enzyme activities and on MDA	122
Figure 4.24. Gross evaluation of stomach in rats	126
Figure 4.25: Effect of HECPR on the level of SOD, Nitric oxide, MDA in ethanol induces gastric ulcer,	128
Figure 4.26: Histological study of ulcer in rats treated with HECPR	130
Figure 4.27: Stomach histological evaluation by Periodic Acid- Schiff (PAS)	132
Figure 4.28: Immunohistochemical examination of Hsp70	134
Figure 4.29: Immunohistochemical examination of Bax	135

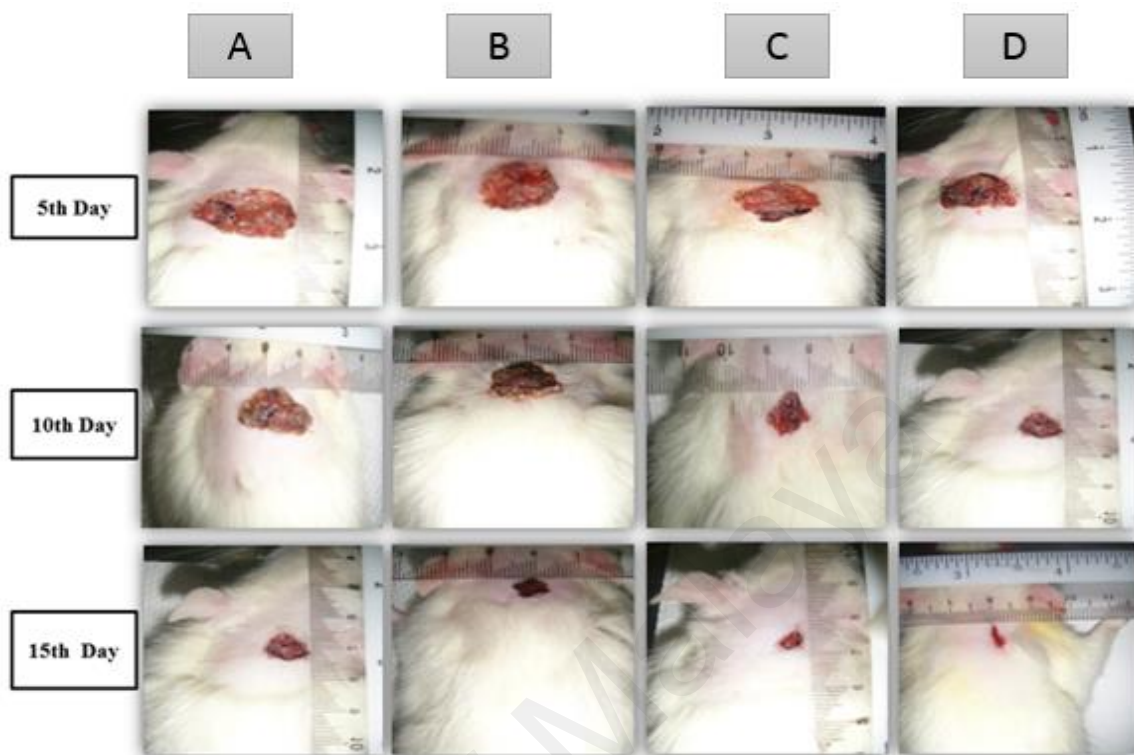


Figure 4.30: Gross appearance of excision wound healing area in rats138

Figure 4.31. Effect of topical treatment of HECPR on rats139

Figure 4.32: Histopathological view of excision wound healing after H & E staining at two magnifications.....141

Figure 4.33: Photomicrographs of healed wound stained with Masson Trichrome at two magnifications143

Figure 4.34: Bax and Hsp70 staining of wound area146

Figure 4.35: Effects of HECPR on CAT, GPX and SOD level in the healed wound area in the rats.....149

Figure 4.36: The MDA level in wounds tissues homogenates from four groups of rats151

Figure 4.37 : A gas chromatogram of the chemical constituents of DECPR...152

Figure 4.38: A gas chromatogram of the chemical constituents of HECPR....152

**Figure 4.39: Chemical structure of Ar-turmerone (peak NO.4) Identified in
DECPR.....154**

University of Malaya

LIST OF TABLES

Table 2.1: Taxonomy of Curcuma purpurascens BI	74
Table 3.1: The experimental design and specifications	66
Table 4.1: Anti- proliferative activity of Curcuma purpurascens BI. on some normal and cancer cells	84
Table 4.2: Effects of DECPR on renal function test.....	100
Table 4.3: Effects of HECPR on renal function test	101
Table 4.4: Effects of the DECPR on liver function test	102
Table 4.5: Effects of the HECPR on liver function test	103
Table 4.6: Effects of the DECPR on hematological parameters	104
Table 4.7: Effects of the HECPR on hematological parameters.....	105
Table 4.8: Effect of DECPR on rat's body weight in AOM-induced colon cancer.....	106
Table 4.9: Effect of DECPR on liver function test in AOM-induced colon cancer.....	107
Table 4.10: Effect of DECPR on renal function test in AOM-induced colon cancer study	108
Table 4.11. Effect of DECPR on AOM-induced colon ACF in rats.....	110
Table 4.12. Gastroprotective effect of HECPR against ethanol-induced gastric injury.....	124
Table 4.13: The possible compounds in DECPR were characterized using a GC-MS-TOF analysis	153
Table 4.14: The possible compounds in HECPR were characterized using a GC-MS-TOF analysis	153

LIST OF ABBRVIATIONS

ABBREVIATION	DESCRIPTION
ADP	Adenosine diphosphate
AKT	Kinase / protein kinase B
ANOVA	Analysis of variance
ALP	Alkaline phosphatase
ALT	Alanine aminotransferase
ANOVA	Analysis of variance
AOM	Azoxymethane
AST	Aspartate aminotransferase
ACF	Aberrant crypt foci
ATCC	American Type Culture Collection
ATP	Adenosine triphosphate
Bad	BCL-2-associated death protein
Bak	BCL-2 Homologous antagonist killer
BAO	Basal acid output
BAX	BCL-2-associated X
BCAC	Beta-Catenin-Accumulated Crpts
BCL2	B-cell leukemia / lymphoma-2
BHT	Butylated hydroxytoluene
CAT	Catalase
CCK2 receptors	Cholecystokinin 2 receptors
COX	Cyclooxygenase
CYP2E1	Cytochrome P450 2E1
DECPR	Dichloromethane extract of <i>Curcuma purpurascens</i> BI. rhizome
DMEM medium	Dulbecco's Modified Eagle Medium
DMSO	Dimethyl sulfoxide
DNA	Deoxy ribonucleic acid
DPPH	2, 2-diphenyl-1-picrylhydrazyl
ECL	Enterochromaffin like cell
EGFs	Epidermal growth factors
ELISA	Enzyme-linked immunosorbent assay
EtOH	Ethanol
FADD	Fas-associated death domin
FAM	6-carboxyfluorescein
FBS	Fetal bovine serum
FC	Flavonoid content
FeIII-TPTZ	Ferritri pyridyl triazine
FeII-TPTZ	Ferrous tripyridyl triazine
FGF	Fibroblast growth factor
FGF-2	Fibroblast growth factor-2
FRAP	Ferric reducing antioxidant power
GPx	Glutathione peroxide
H & E stain	Hematoxylin-eosin stain
H2O2	Hydrogen peroxide
HCL	Hydrochloric acid

HD	High dose
HECPR	Hexane extract of <i>Curcuma purpurascens</i> BI. rhizome
HeLa	Human cervical carcinoma cell line
HGF	Hepatocyte growth factor
HPRT1	Hypoxanthine phosphoribosyl transferase1.
HPLC	High performance liquid chromatography
IFN- α	Interferon- alpha
IP	Intraperitoneal
Kg	Kilogram
IgG	Immunoglobulin G
IgM	Immunoglobulin M
IL-1	Interleukin 1
IL-12	Interleukin 12
IL-2	Interleukin 2
IL-4	Interleukin 4
IL-6	Interleukin 6
IL-8	Interleukin 8
LC-MS	Liquid chromatography-mass spectrometry
LD	Low dose
LDL	Low density lipoprotein
LPO	Lipid peroxidation
LPS	Lipopolysaccharide
LTC4	Leukotriene C4
LTD4	Leukotriene D4
LTE4	Leukotriene E4
MAPK	Mitogen-activated protein kinase Malondialdehyde
LTs	Leukotrienes
MDA	Malondialdehyde
MDF	Mucin Developed Foci
Min	Minute/s
ml	Millilitre
mM	Micromole
Mm	Millimere
mmol	Millimole
MMPs	Matrix metalloproteinase
MTT	3-(4,5-dimethylthiazol-2-yl)-2,5-diphenyltetrazolium bromide
NADPH	Nicotinamide adenine dinucleotide phosphate
NF- κ B	Nuclear factor kappa B
NK	Natural killer cell
NO	Nitric oxide
NSAIDs	Nonsteroidal anti-inflammatory drugs
NCCLS	National committee for clinical laboratory standards
nm	nanometre
P value	Level of significance
PBMC	Peripheral blood mononuclear cells
PBS	Phosphate buffer saline

PDGF	Platelet-derived growth factor
PGD2	Prostaglandin D2
PGE2	Prostaglandin E2
PGF2 α	Prostaglandin F2 α
PI3	Phosphoinositide-3
PPIs	Proton pump inhibitors
RAW264.7	A murine macrophage cell line RAW264.7
RNA	Ribonucleic acid
ROS	Reactive oxygen species
RT-PCR	Real time polymerase chain reaction
S.D	Standard deviation
SD rats	Sprague Dawley rats
SEM	Standard error of the mean
SOD	Superoxide dismutase
SPARC	Secreted protein acidic rich in cysteine
TAMRA	6-carboxy-tetramethyl-rhodamine
TBARS	Thiobarbituric acid reactive substance
TE-2	Esophageal cancer cells
TGF- α	Transforming growth factors α
TGF- β	Transforming growth factor-beta
Th1 cell	T helper cell type1
Th2 cell	T helper cell type2
TIMPs	Inhibitors of metalloproteinase
Tm	Melting temperature
T.P	Total protein
TPC	Total phenolic content
TPTZ	Pyridyl triazine
TRAIL	TNF-related apoptosis-inducing ligand

CHAPTER 1: INTRODUCTION

1.1 Cancer

Cancers are recognized by increased mass of cells in a tissue (tumour), which occur due to gene abnormalities that change subsequent pathways or products. These changes influence cell properties to cancerous type. A malignant cancer is however defined as an invasive and metastatic disease with uncontrolled cell proliferation, which is, differentiated from benign condition with self-limited status (non-invasive or metastatic) (Beahrs & Henson, 1992).

1.2 Colon Cancer

Colorectal cancer includes all cancers that originate from the cecum to the anus and it can be subdivided to colon cancer, which ranges from caecum to the sigmoid (approximately 15 cm above the anal verge) and rectal cancer that ranges from the recto-sigmoid to the anus (Vainio et al., 2003). Colon cancer is the main cause of cancer-related deaths and morbidity in the USA and other parts of the world (Moghadamtousi et al., 2015b). A high incidence of colon cancer has been shown in the Western industrialized countries. Colorectal cancer is the third most common cause of cancer deaths in Malaysia. Malaysian Ministry of Health confirms an increase in colorectal cancer admission rates from 8.1% in 1995 to 11.9% in 2014. Previous studies highlighted dietary factors as the main etiology for colorectal cancer (Kushi et al., 2002). Similar to other cancers, colorectal cancer occurs when changes exist due to several genes, which in turn, alter the regulatory pathway, in which cancerous cells are not able to perform the normal functions. Additionally, the cancerous changes are specific to the tumor development and are potentially considered as an indicator of specific stages due to histological changes (Ebert et al., 2005) (Figure 1.1).

It is confirmed that the risk of colorectal cancer increases in patients with inflammatory bowel disease (Danese & Mantovani., 2010), and therefore inflammation is commonly considered as the primary cause of colorectal cancer. Patients with chronic inflammatory bowel disease possibly express a higher incidence for colorectal cancer. For instance, Crohn's disease and Ulcerative colitis are the two most common inflammatory bowel diseases that leads to high incidence of colon cancer (Li et al., 2008).

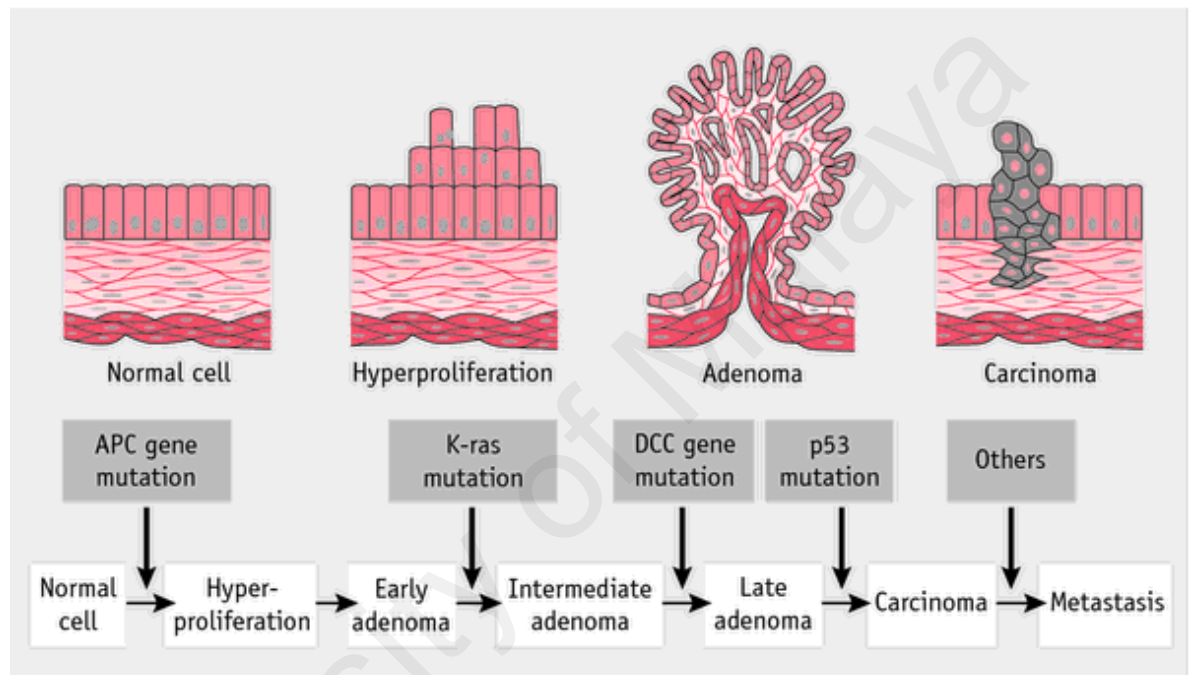


Figure 1.1: Colorectal cancer occurs in a multi-step process.

(Corpet & Tache, 2002)

Apparently, surgical excision is the best option to treat colon cancer, however, many patients who have undergone therapeutic resection, develop tumor recurrences, thus, other approaches to prevent and treat cancer are required. There is a great opportunity to prevent colon cancer in a stepwise process, because it takes 5-20 years from initiation to adenoma formation stage, and another 5-15 years until an invasive stage begins. It is worth noting that the risk factors and symptoms of colorectal cancer subdivisions are identical but the overall treatment strategy is different.

Azoxymethane (AOM) and its precursor compound, dimethyl hydrazine, are alkylating agents. They bind to methyl or alkyl groups of guanine (G) residues in DNA structure causing G to adenine (A) transition mutations and consequently DNA mutation occur (Dipple, 1995).

Aberrant crypt foci (ACF) are putative pre-neoplastic lesions of colon found in both animals models and humans (Cheng & Lai 2003). The ACF function as intermediate biomarkers to rapidly assess the chemopreventive potential of several agents like naturally occurring agents against colon cancer (Corpet & Tache, 2002). These lesions are hyper proliferative, which are located in human colon and they are carcinogen-treated laboratory creatures that share common features with colon tumors (Corpet & Taché, 2002).

Additionally, the ACF are alleged to be precursors of colon cancers and colonic carcinogenesis biomarkers (Takayama et al., 1998). The ACF are monoclonal collection of strange crypts that are always formed in reaction to carcinogen exposure in a dose-dependent manner (Bird, 1987). The crypt progenitor cells develop apoptosis within 6–8 hours of post exposure to AOM in response to DNA damage. Progenitor cells that avoid apoptosis then begin a proliferative response after 48–72 hours (Hirose et al., 1996). It seems that these aberrant crypts foci are formed as monoclonals (Hirose et al., 1996) and are developed by a process of incomplete crypt fissioning (Siu et al., 1999).

1.3 Gastric Ulcer

Gastric ulcer is one of the most common diseases, which is defined as localized breaches of the gastric tissues that shows tissue destruction to the depth of the muscolaris mucosa (Tarnawski et al., 2001).

Gastric ulcer is one of the most broadly distributed, severe and chronic diseases in the world. For instance, about 10% of the Western world's population express gastric ulcer disease (Barkun & Leontiadis, 2010). In Asia and in the South Pacific regions, gastric

ulcer was diagnosed in about 11.5% of the population (Scott et al., 2013). Additionally, gastric ulcer is considered as a major reason of morbidity and healthcare costs, due to stress, alcohol consumption, nutritional deficiencies, usage of many drugs such as non-steroidal anti-inflammatory drugs like aspirin and indomethacin that cause gastric ulcer in the long-term (Fattaha & Abdel-Rahman, 2000).

There are some Medicines like antacids, H₂-antagonists and proton pump inhibitor (PPI) to treat gastric ulcer. The H₂- antagonists and PPIs like omeprazole, ranitidine and famotidine currently function as gastric acid secretion inhibitors. It should be noted that all of these drugs show side effects, namely, diarrhea, hypercalcemia (which can lead to kidney failure), kidney stones, and osteoporosis (Widenhouse et al., 2002). Antacids are not sufficient to prevent and heal gastric ulcer; therefore, they are seldom used as anti-ulcer medicine (Eid et al., 2010). The stomach is continuously exposed to many potentially harmful agents. Pepsin and hydrochloric acid are considered as endogenous factors to mainly threaten the gastric mucosa (Widenhouse et al., 2002). The reflux of alkaline duodenal containing pancreatic enzymes with bile as endogenous factors additionally harms the stomach (Li, et al., 2007). As severe exogenous factors, cigarette smoking, drugs specially steroids, aspirin, and non-steroidal anti-inflammatory drugs (NSAIDs) cause mucosal excitations and therefore cause mucosal injury to happen. The presence of certain agents in the gastric mucosal defense line efficiently enables the stomach to protect itself against the excited factors. The mucus and bicarbonate that is excreted through the surface of epithelial cells, prostaglandins, and gastric mucosal blood flow are important to maintain the gastric mucosal safety (Bansal et al., 2011).

The gastric mucus is able to trap bacteria and excrete it in feces. Additionally, the gastric mucus is able to reduce mucosal damage, which is caused by bacteria and immunocytes because it contains antioxidant activity (Grisham et al., 1987). Eicosanoids bioactive lipids including prostaglandins, leukotrienes, and thromboxanes are important in gastric

physiology. Prostaglandins regularly inhibit secretion of gastric acid and preserve of mucosal blood flow (Wallace & McKnight, 1990).

Transforming growth factor (TGF- β) and epidermal growth factor (EGF) are known to potentially maintain integrity of gastric mucosal. The first one mainly functions as a mediator in interactions of epithelial cells and regulates proliferation, inflammation, and tissue repair in the human gastrointestinal tract. The expression of TGF- β increases after acute epithelial injury and in inflammatory bowel disease (Qiao et al., 2006).

Generation and scavenge of free radical is usually balanced in the body. There are two main factors to confront free radicals in the physiological defense system; known as endogenous enzyme systems, such as superoxide dismutase, catalase, glutathione reductase, and coenzyme Q, and exogenous factors, such as vitamin C, vitamin E, selenium, and β -carotene. All the above-mentioned molecules mainly function as an antioxidant to fight against oxidative stress because they are able to convert reactive oxygen species (ROS) into stable and harmless compounds or scavenge ROS with a redox-based mechanism (Brambilla et al., 2008). The scavenge and overall regulation of ROS levels to maintain the physiological homeostasis are done through enzymatic and non-enzymatic antioxidant protection systems, namely, catalase (CAT), superoxide dismutase (SOD), and glutathione peroxide (GPx). An increased concentration of alteration metal (Fe/Cu) ions, ischemia-reperfusion, or drug metabolism generates ROS and suppresses the cellular antioxidant defense leading to an oxidative stress (Verma et al., 2013).

Recently, people have turned to traditional medicine to treat diseases with medicinal plants, these medicinal plants have been shown to produce secondary metabolites, such as flavonoids, alkaloids, terpenoids, tannins, and other compounds which can protect the body against a variety of diseases. Furthermore, many medications have originated from plants. For instance, taxol as an anticancer drug is extracted from the Yew tree

(Slichenmyer & Von Hoff, 1991), artemisinin as an antimalarial drug is extracted from *Artemisia annua* leaves and carbenoxolone has been used as an antiulcer drug, and it is extracted from *Glycyrrhiza glabra*. Therefore, researchers are interested to use natural compounds from plants in order to investigate new medications that can treat gastric ulcer more effectively with less side effects and also natural compounds are more safer, cheaper, and more accessible than synthetic compounds (Borrelli & Izzo, 2000).

1.4 Wound Healing

An open wound is defined as a type of damage, in which the skin is cut, torn, or ruptured whereas a closed wound occurs with blunt force trauma to the skin that results in contusion. From a pathology point of view, wound is specifically referred to as a sharp injury that harms the dermis of the skin (Acconcia et al., 2006). There are many kinds of acute skin wounds including incision wounds, damages of incomplete thickness, and wounds without special tissue. Dissimilar wounds have a diverse phase process to heal, but the phases still remain the same (Monaco & Lawrence 2003). The process of wound healing is composed of a series of events, which happens in a precisely controlled way and is different from wound to wound. There is some overlap in the phases of the wound process. To make it accurate and clear, there are five phases of hemostasis, namely, inflammation, cellular migration and proliferation, protein synthesis and wound contraction, and finally remodeling phase. The process of wound healing involves the activity of a complex network of blood cells, tissues, growth factors, and cytokines, which overall increases cellular activity and subsequently raise metabolic demand for nutrients. It seems that nutritional deficit disrupts the healing process of the wound, which indicates that several nutritional agents that necessarily repair the wound is likely improve the healing time and tissue repair. For instance, vitamin A is necessary to form epithelial and bone tissues, in addition to immune function. Vitamin C is also essential for collagen formation, as a tissue antioxidant, and affects immune function. Another example is

vitamin E, which is the principal lipid soluble antioxidant found in the skin (Simon et al., 2000). Excess ROS result in the killing of fibroblasts and skin lipids will be less flexible. Because of these, the general role of antioxidant seem to be significant in the effective treatment and management of wounds. Antioxidants diminish these adversative effects of wounds through eliminating products of inflammation (Houghton et al., 2005). In the mechanism of antioxidant defense, the extracts or compounds directly interact with hydrogen peroxide instead of changing the cell membranes and controlling damage. Compounds offer a broad capacity to scavenge radicals in order to improve the wound-healing process, thus researchers attempt to explore the use of natural products in order to treat the wound. Some possible signals for cell expulsion in tissue repair during process of wound healing have been suggested, however, it is necessary to study the mechanism of cell death during the process. Those cells involved in each phase of wound die through one of the three possible mechanisms as follows: emigration, necrosis, and apoptosis (Houghton et al., 2005). The Bcl-2 family proteins for instance, either promote or prohibit apoptosis and eighteen proteins of the Bcl-2 family have been so far determined to affect the apoptosis pathway. The proteins of BAX, Bad, and Bak are known as pro-apoptotic proteins, whereas Bcl-2 and Bcl-xl are anti-apoptotic proteins. Apoptosis mainly functions to synchronize the cell population that rapidly changes and are involved in the process of tissues healing. In the majority of wounds, proliferation controls the increased speed of the wound closure, and it can lead to pathologic tissue repair if the balance between increase and decrease in cellular numbers is lost.

1.5 Hypothesis of the Research

The present study might offer important facts in order to solve the existing problems to treat human colon cancer in Malaysia. It is expected that DECPR will affect colon cancer cells through the induction of apoptosis without damaging normal colon cells. The hypothesis is that the mechanism of the extracts as anti-cancer is via the induction of

apoptosis through either cellular mitochondria signalling or extrinsic signalling pathways. The present research hypothesized that DECPR possess cytotoxic effect on one human colon cancer cell line HT29 and an anti-proliferative effect on AOM-induced colon cancer in rat. In addition the purpose of this study was to determine the role of hexane extract of *C.purpurascens* rhizome (HECPR) on the gastroprotective ability of ethanol-induced gastric ulcers and wound healing in rats.

1.6 Objectives of the Study

1.6.1 General Objectives

The main objective of this study is to evaluate the chemoprotective effects of *C.purpurascens* rhizome dichloromethane extract DECPR against AOM-induced aberrant crypt foci using rats as the experimental model and to investigate the effects of *C.purpurascens* rhizome hexane extract HECPR on gastroprotective and wound healing activities.

1.6.2 Specific Objectives

1. To investigate the antioxidant activity (DPPH and FRAP assays), total phenolic and total flavonoid contents *in vitro*.
2. To investigate the acute toxicity of DECPR and HECPR and the effects of these extracts on the liver and kidney functions.
3. To determine the *in vitro* cytotoxicity of the DECPR on HT29 cells.
4. To investigate the chemoprotective effect of DECPR against AOM-induced aberrant crypts foci (ACF) in rats and to study the mechanism of action.
5. To evaluate the gastroprotective ability of HECPR ethanol-induced gastric ulcers in rats.
6. To evaluate the wound healing potential of HECPR against on experimental rats grossly and histologically.

CHAPTER 2: LITERATURE REVIEW

2.1 Colorectal Cancer

Colorectal cancer is the most common gastrointestinal cancer worldwide. Colorectal cancer is also referred to as colon cancer or large bowel cancer, and it includes cancerous growths in colon, rectum, and appendix. Colorectal cancer is the fourth leading cause of cancer death worldwide (Yusoff et al., 2012) and the incidence of colon cancer is increasing in many countries (Béjar et al., 2012) including the Asian regions (Sung et al., 2005). Nonetheless, about 60% of the diagnosed cases were from the developed countries. It is estimated that about 1.23 million new cases worldwide were clinically diagnosed with colorectal cancer in 2008, out of which, about 608,000 people died (Ferlay et al., 2010). In Malaysia, colorectal cancer is the third most common cancer among females and the most common cancer among males with the majority of patients aged above 50 years old. Colorectal cancer also causes the highest number of hospital discharge due to neoplasm related problems (Yusoff et al., 2012).

Early diagnosis of colorectal cancer can decrease mortality level and incidence of malignant neoplasm (Pignone et al., 2002). Mortality can be decreased through screening of faecal occult blood test (FOBT), sigmoidoscopy, and colonoscopy (Walsh & Terdiman, 2003), thus, many countries have prepared guidelines to add colorectal cancer screening in the national screening programme (Power et al., 2009), however, the screening program still seem slow in many countries, even in the developed countries. The Asia Pacific consensus has suggested colorectal cancer screening for people aged 50 years old and above in the Asian regions (Sung et al., 2008). In Malaysia, the guidelines to screen colorectal cancer were firstly introduced in 2001 (Yusoff et al., 2012), and it suggested an annual screening of individuals with average risk of colorectal cancer using FOBT. Nonetheless, there are available information on screening of cervical cancer and breast cancer but not of colorectal cancer in Malaysia. The uptake of Pap smear for

cervical cancer is only 26% while uptake for mammography in breast cancer is only 3.8% (Lim, 2002), therefore, the uptake of colorectal cancer screening is expected to be lower than cervical cancer, which therefore is the likely reason for why most of colorectal cancer patients presented late, when patients are already in an advanced stage (Goh et al., 2005).

2.1.1 Signs and Symptoms of Colorectal Cancer

Location of tumor in the bowel determines the signs, symptoms and level of spreading (metastasis) of colorectal cancer in the body. There are typical warning signs for colorectal cancer in people over 50 years old as follows: worsening constipation, blood in the stool, weight loss, fever, loss of appetite, nausea and vomiting. Among these symptoms, rectal bleeding or anemia are classified as high-risk symptoms in people aged 50 years and above (Astin et al., 2011) while other common symptoms such as weight loss and change in bowel function can be noticed if associated with blood (Adelstein et al., 2011a).

It is often possible to cure those cancers that are restricted within the colon wall with surgery while those cancers that widely spreads around the body is usually not curable and therefore, medical management has to focus on chemotherapy and improving quality of patients' life.

2.1.2 Cause of Colorectal Cancer

Most colorectal cancer cases occur due to lifestyles and due to age factor and only in a few cases are associated with genetic disorders. Colorectal cancer generally begins in the bowl lining and if left untreated, it can move into the muscle layers underneath to grow, and then through the bowel wall. In order to reduce the death caused by colorectal cancer, screening program is effective and recommended at age of 50 and should be continued until age of 75. Colonoscopy or sigmoidoscopy are usually used to diagnose localized bowel cancer.

There are some risk factors for colon cancer such as age, male gender, high intake of fat, alcohol or red meat, obesity, smoking, and lack of physical exercise. More than 75-95% of colon cancer cases happen in people with little or no genetic risk (Watson & Collins, 2011) and about 10% of the cases are related to insufficient activity (Lee et al., 2012). In addition the intake of alcohol of more than one drink per day appears to be a risk factor for the disease (Fedirko et al., 2011).

2.1.3 Inflammatory bowel disease

Ulcerative colitis and Crohn's disease are referred to as inflammatory bowel disease, and these conditions have been shown to increase the risk of colon cancer (Jawad et al., 2011). The greater the risk, the longer a patient has the disease (Xie & Itzkowitz, 2008) with worse severity of inflammation (Triantafillidis et al., 2009). Colonoscopy and aspirin are suggested to prevent these high risk cases (Xie & Itzkowitz, 2008). Inflammatory bowel disease cases annually have been shown to be a causal factor in less than 2% of the colon cancer cases. About 2% of people with Crohn's disease are at risk of colorectal cancer after having been exposed to the condition for 10 years, 8% after 20 years, and 18% after 30 years. In ulcerative colitis cases, about 16% present either as colon cancer or contributes as a cancer precursor over a period of 30 years (Triantafillidis et al., 2009).

2.1.4 Diagnosis

Colonoscopy or sigmoidoscopy are usually used to diagnose colorectal cancer, histopathology for tumor biopsy is another way of diagnosis. A computerized tomography (CT) scan is then used to determine the severity of the disease from chest, abdomen, and pelvis. In certain cases, other potential imaging tests such as positron emission tomography (PET) and magnetic resonance imaging (MRI) can also be used. In order to determine the level of spread of the tumor, involvement of lymph nodes, and

determination of the number of metastasis, colon cancer staging is then performed using classification of malignant tumors system (Wargovich et al., 2010).

Early detection is significant to improve the chance of survival for colon, rectal, or other cancers in long-term. For instance, a 5-year survival rate of > 90% was reported for colorectal cancer patients who were treated at an early stage but with a drop to 64% if the cancer has spread to adjacent organs and with a decrease to < 10% if the cancer moves to distant organs, such as liver and lungs (Wargovich et al., 2010).

Screening tests at early detection considerably improve the survival rates and it provides an "early warning system" for individuals with no symptoms or one or more symptoms. Previous studies showed that identification of intermediate biomarkers help to recognize very early stages of cancer development before an obvious tumor is formed. Progression of cancer lesion can be reversed or significantly slowed down with a proper intervention. Aberrant crypt foci, is considered as a promising candidate for an intermediate biomarker in colon cancer (Wargovich et al., 2010).

2.1.5 Pathology of Colorectal Cancer

The analysis of colon tissue by a biopsy or surgery aids to determine the pathology of the colorectal tumor. Type and grade of the colorectal cells are described in a pathology report. There are three types of cells involved in colorectal cancer, known as adenocarcinoma as the most common colon cancer cell type, making up 95% of the cases, lymphoma and squamous cell carcinoma as the other two rare types.

The appearance of colon in colorectal cancer is different in the two sides of the tissue. Colorectal cancer on the ascending colon and cecum (right side) seems to be exophytic and the tumour grows outwards from one location in the bowel wall, which rarely causes obstruction of feces with symptoms such as anemia. The tumor of the left side, however, is circumferential and can obstruct the bowel like a napkin ring.

As a malignant epithelial tumor, adenocarcinoma originates from glandular epithelium of the colorectal mucosa and then invades the wall, infiltrates the muscularis mucosae, the submucosa, and the muscularis propria. Tumor cells present irregular tubular structures, having pluristratification with multiple lumens and reduced stroma ("back to back" aspect). They are sometimes discohesive and secrete mucus, and attacks the interstitium thereby producing a lot of mucus/colloid (optically "empty" spaces). Mucinous (colloid) adenocarcinoma is poorly differentiated. If the mucus exists inside the tumor cell, it pushes the nucleus to the periphery, making the cells like a signet-ring shape. Adenocarcinoma may develop three degrees of differentiation, namely, well, moderately, and poorly differentiated, depending on glandular architecture, cellular pleomorphism, and mucosecretion of the predominant pattern (Figure 2.1).

Cyclooxygenase-2 enzyme (COX-2) is not usually found in healthy colon tissue, but since it is assumed to promote abnormal cell growth, most colorectal cancer tumors are positive for COX-2.

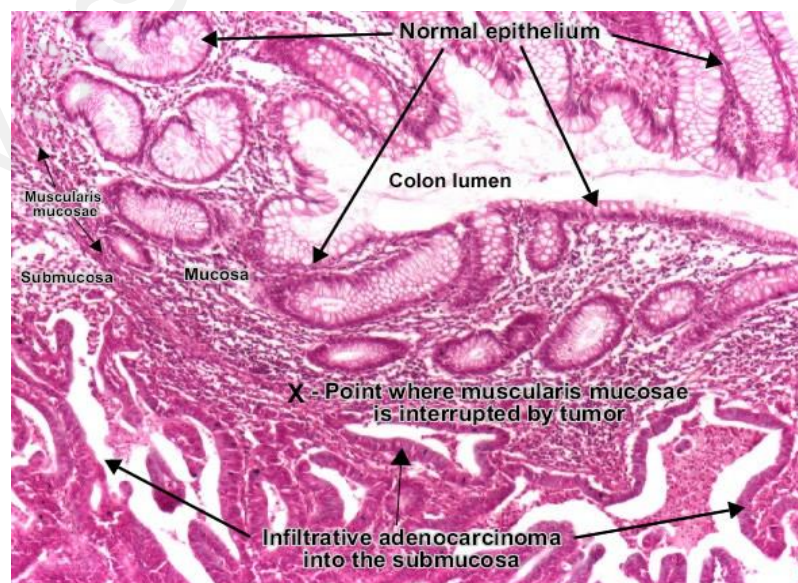


Figure 2.1: Histology of colon tissue stained with H&E stain

2.1.6 Aberrant Crypt Foci (ACF)

Bird (1987) first discovered aberrant crypt foci (ACF) and reported the role of ACF to understand the pathogenesis of colon cancer. Later Corpet and Tache (2002) treated mice with the carcinogen azoxymethane (AOM) and induced the growth of colonic crypts. They observed the crypts showed larger, thicker, and darker staining than the normal crypts when visualized with methylene blue. In another study by Wargovich et al (2010), the use of ACF was mentioned as a biomarker. They described ACF as a case for inclusion as a biomarker for colon cancer and studied the detection, gene abnormalities, and clinical usefulness of ACF (Wargovich et al., 2010).

Aberrant crypts clusters were also detected in the surrounding normal colonic mucosa of patients with colon cancer in 1991, which raised from the normal mucosal surface of the colon (Pretlow et al., 1991). The intestinal and colonic cells present a rapid turnover under normal conditions and therefore, it is assumed that aberrant crypts replicate at the same rate, if not faster than normal crypts. (Wargovich et al., 2010).

Many factors can affect the abovementioned inconsistency, namely, significant differences in sampling methods and analysis, and differences in proliferation of colonic epithelial cell (Jass et al., 2003). The replication of aberrant crypt is basically identical to that of normal crypts and the process begins at the bottom of the crypt, pushing cells upward and outwards in order to make new colonic crypts and to fill up the cells in the original crypt. This process is called budding and branching, known as crypt fission, forming larger size of foci over time (Fujimitsu et al., 1996). The crypt fission is found in different bowel diseases with varying rates (Figure 2.2).

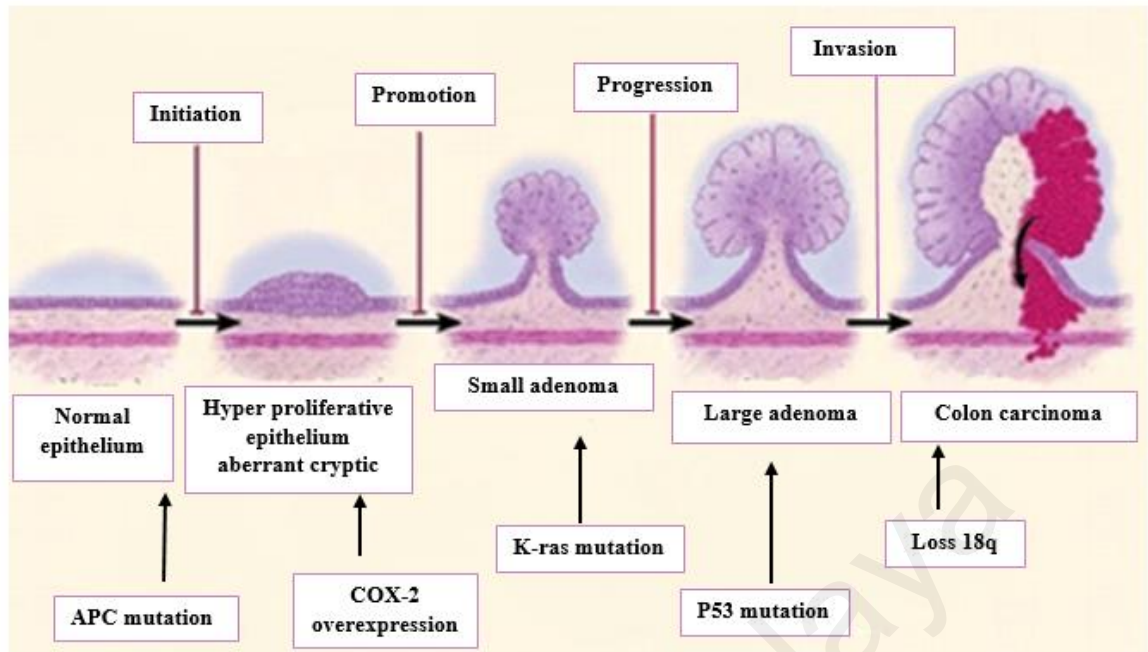


Figure 2.2: Sequential pathological stages and molecular events in colon cancer (Corpt 2002)

The ACF are usually visible at a magnification of 40x under a dissection microscope. Previous researches significantly described the main histopathological signatures of ACF, however, categorizing them seems very controversial (Gupta et al., 2009; Gupta et al., 2007). The ACF microscopically are categorized into dysplastic ACF and non-dysplastic ACF, which often harbor serrated hyperplastic ACF (Wargovich et al., 2010). The incidence of macroscopic tumors, colon cancers, colon adenomas, and adenocarcinomas induced by a chemical carcinogen was the gold standard endpoint to carry out chemoprevention in rodents before 1990. These standard endpoints are obviously relevant to cancer, however, there are three main disadvantages as follows:

- 1- A tumor needs a long time usually 5-8 months to develop.
- 2- Histology is required to confirm each tumor and this is time-consuming and costly.

3- Each animal provides little information for the study since each rat for instance has either no tumor or a tumor, therefore large groups of rats are required to carry out statistical analysis, usually 30 rats or more per each study group.

With regard to all these disadvantages, the ACF seems to have benefit as endpoint chemoprotective screening biomarkers since (i) all colon carcinogens can induce ACF in a dose- and species-dependant manner; (ii) modulators of colon carcinogenesis can modify the number and growth of ACF and the tumor outcome was predicted in many rodent studies; (iii) the ACF is correlated with risk of colon cancer, and size and number of adenoma in humans; (iv) from morphology and genotype point of views, the ACF were similar in human and animal colons, and many changes are similar in ACF and tumors; (v) some ACF show dysplasia and carcinoma in rodents and humans (Corpet & Taché, 2002).

Taken together, the ACF is therefore used as a preliminary endpoint in colon cancer chemoprevention studies, because it presents a simple and economical solution for preliminary screening of potential chemopreventive agents, allowing to quantitatively assess mechanisms of colon carcinogenesis.

2.1.7 Azoxymethane AOM

Azoxymethane (methyl-methylimino-oxidoazanium) is the oxide form of azoxymethane with molecular formula of $C_2H_6N_2O$ and the chemical structure is shown in Figure 2.3. Azoxymethane is a carcinogenic and neurotoxic chemical, which is widely used in biological research, and is especially effective to induce colon carcinomas (Corpet & Taché, 2002). In addition to water solubility in water, azoxymethane is sensitive to long exposure to air and high temperatures.

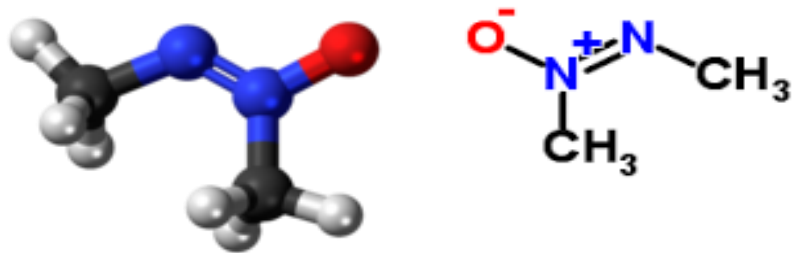


Figure 2.3: Chemical structure of azoxymethane (methyl-methylimino-oxidoazanium)

Previous researchers have used azoxymethane (methyl-methylimino-oxidoazanium) to induce foci of aberrant crypts in rats (Adler, 2005; Velmurugan et al., 2008). In a study on *Zingiber zerumbet*, for instance, the chemoprevention effect of zerumbone was explored using azoxymethane to induce aberrant crypt foci in male F344 rats. The ACF was induced by subcutaneous injections of AOM for two weeks in the rats (15 mg/kg body weight). The effects of zerumbone was assessed on cell proliferation and therefore silver-stained nucleolar organizer regions protein (AgNORs) in colonic cryptal cell nuclei was counted (Corpet & Taché, 2002).

Challa induced aberrant crypt foci with AOM and studied the effect of phytic acid and green tea to explore interactive suppression of the ACF (Challa et al., 1997). Magnuson carried out extensive research to study the increased susceptibility of adult rats to AOM-induced aberrant crypt foci (Magnuson et al., 2000). Verghese used dietary insulin and studied the suppression of AOM-induced ACF using dietary insulin (Verghese et al., 2002).

Azoxymethane is generally used to induce colon cancer with specific induction pattern similar to the pathogenesis of human sporadic colon cancer. The azoxymethane has been widely used to study the molecular biology, prevention, and treatment of colon cancer. From AOM carcinogenesis point of view, AOM is metabolised to

methylazoxymethanol by cytochrome P450 2E1 (CYP2E1) after administration, and it subsequently causes DNA mutations. Mutation of K-ras initiates the activation of the pathway, its downstream PI3K/Akt pathway, and mitogen-activated protein kinase (MAPK) pathway (Chen & weng, 2009b). Mutation of β -catenin prevents degradation by GSK-3 and therefore the subsequent accumulation causes cell proliferation, while transforming growth factor beta (TGF β) as a pro-apoptotic protein is also inhibited.

2.1.7.1 Metabolism of AOM in Colon Cancer

Azoxymethane does not directly interact with DNA and therefore it has to be activated *in vivo* during carcinogenesis. Azoxymethane is specifically metabolised by CYP2E1 isoform which belongs to cytochrome P450. In the first step, the hydroxylation of the methyl group of AOM occurs to form methylazoxymethanol (MAM), which then breaks down into formaldehyde and probably also into methyldiazonium, which is known to be a highly reactive alkylating species. Chemical alteration eventually causes alkylation of DNA guanine to O6-MEG and O4-methylthymine (Chen & Huang, 2009b). These mutations can then cause tumorigenesis via various key genes in intracellular signal pathways. The inhibition of CYP2E1 was reported to prevent chemical carcinogenesis, for instance through disulfiram, an agent used for avoidance therapy in alcohol abuse. In CYP2E1 knockout mice, O6-MEG formation and colon polyp numbers are reduced in response to AOM treatment (Chen & Huang, 2009b).

2.1.7.2 Mechanisms of AOM in Colon Cancer

Many activation pathways have been discovered to be involved in the mechanism of AOM-induced colon cancer (Figure 2.4), namely, K-ras, β -catenin, and TGF β , however, there is no unity to explain the mechanism of this model. K-ras is a small G-protein, which regulates both MAPK and PI3K/Akt intracellular signal pathways that subsequently regulate cell growth, proliferation, and glucose metabolism. K-ras plays a

key role in the carcinogenesis of colon cancer. Azoxymethane is reported to cause a K-ras gene transversion mutation from G: C to A: T at codon 12 deriving from O6-methyl-deoxyguanine adducts that changes glycine to aspartic acid, which then causes the activation of the K-ras protein.

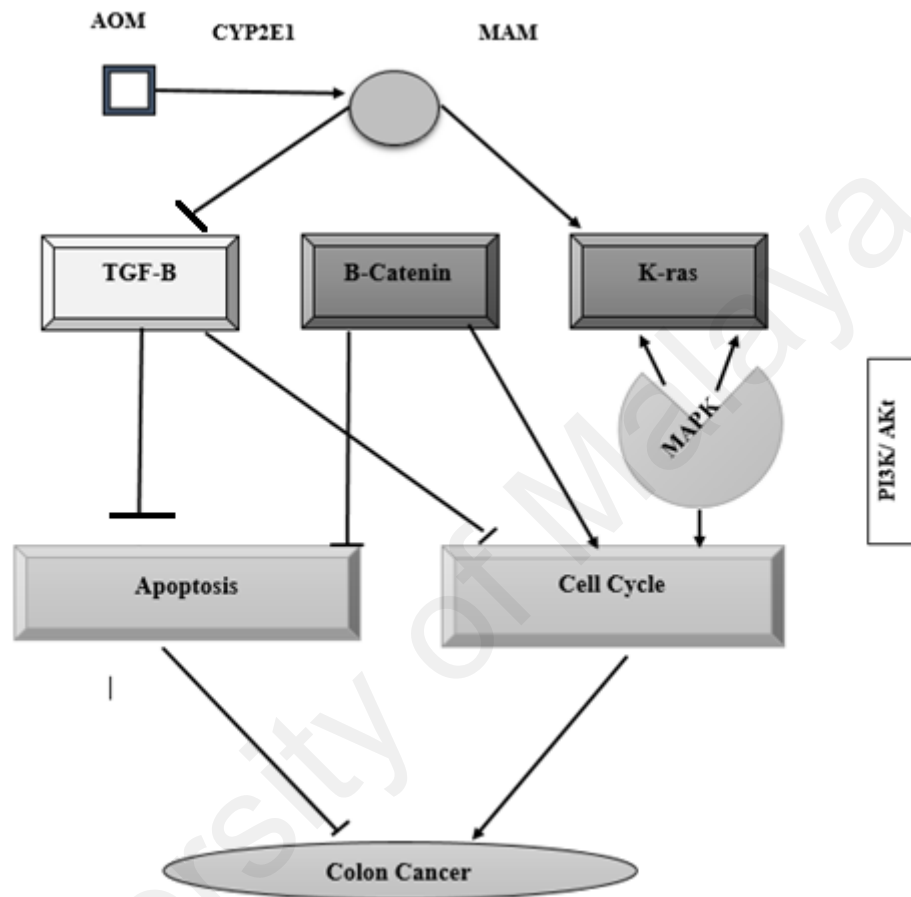


Figure 2.4: Azoxymethane (AOM) involvement in the mechanism of colon cancer (Chen & Huang 2009b)

Both pathways have important roles in the carcinogenesis of many types of cancers such as human colon cancer. pEGFR, pAkt, and pMAPK are elevated in colon tumours in comparison with normal colon tissue. The PI3K/Akt pathway is important in colon cancer and about 20% of patients show PIK3CA mutations. The activation of PI3K/Akt can cause an increase in cell survival pathways via phosphorylation of

downstream targets, including NF κ B, and Bcl-x1. PI3K/ Akt also stops p53 and the forkhead/Fas-ligand to reduce apoptosis (Messersmith et al., 2005).

PI3K/Akt deactivates glycogen synthase kinase 3 (GSK3) and activate cyclin D1 and c-myc to increase cell proliferation in the cell cycle pathway. PI3K/Akt also activates the mammalian target of rapamycin (mTOR), a conserved Ser/Thr kinase to elevate cell size. The increased level of mTOR activity in the AOM model has not been explored. COX2 was reported to be involved in the carcinogenesis of AOM in the downstream of PI3K/Akt. The activated Ras initiates stimulation of serine/threonine-selective protein kinase, known as Raf kinase, which is an oncogene. The encoded protein has regulatory and kinase domains. Ras binds to CR1 in regulatory region and phosphorylates CR2, which has serine/threonine in the structure. Subsequently, the CR3 in the kinase region is activated, and this in turn activates MAPK and ERK kinase. MAPK and ERK initiates carcinogenesis through target proteins like c-myc, CREB, RSK, Mc11, p16, Rb, and cyclins. Inhibition of the abovementioned pathways were reported to cause cancer cell death (Messersmith et al., 2005).

Overexpression of cell cycle promoters such as cyclin D1 might be involved in the AOM model. For instance, Cdk4 was discovered in the early stages in the AOM cancer-induced colon in mice.

β -catenin is an oncogenic protein, which is involved in cell adhesion and associates with cadherin or α -catenin to interact with the actin cytoskeleton. Free form of β -catenin is a co-transcriptional activator of genes in the Wnt signal pathway, which associates with the scaffolding proteins such as axin and Apc and is phosphorylated by GSK-3 β , resulting in degradation by the proteasome (Messersmith et al., 2005). The N-terminus of β -catenin is sometimes mutated, therefore it cannot form the complex and thus would be degraded. The level of free β -catenin is increased which then binds to the T-cell factor/lymphoid enhancer factor TCF/LEF to form a complex, then activating gene

transcription and cell proliferation through targeting *c-myc* and *cyclinD1* genes, as well-known carcinogens. Azoxymethane causes mutations at codons 33 and 41 of β -catenin, that codes for serine and threonine residues targeting for GSK-3 β phosphorylation. This mutation causes accumulation of β -catenin for the carcinogenesis. Previous researches have shown that AOM treatment increases both β -catenin and cyclin D (Chen & Huang, 2009a).

Isoforms 1, 2, and 3 of transforming growth factor- β (TGF β) inhibits cell growth, proliferation, and cell cycle progression indicating an anti-tumour effect. About 20–30% of colon cancer patients have shown defects in TGF β signalling, in which the activity of the TGF β pathway is reduced after AOM treatment, mediating AOM-induced colon cancer. Previous researches indicated a decrease in the active form of TGF β in AOM-treated mice (Chen & Huang, 2009a). The TGF- β induces apoptosis via many signalling pathways. Firstly, transforming growth factor β (TGF β) forms dimers and then binds to the type 2 receptor. The associated complex then phosphorylates the type 1 receptor, which in turn phosphorylates R-SMAD (receptor-regulated SMADs) to induce apoptosis. Secondly, the activated type 2 receptor binds to death associated protein 6 to cause apoptosis. Third, TGF β inhibits phosphorylation of p85 subunit of PI3K/Akt activated by Granulocyte-macrophage colony-stimulating factor (GM-CSF) in many myeloid leukemia cell lines, such as MV4-11, TF-1, and TF-1a (Chen & Huang, 2009a).

There are some significant markers in development of colorectal cancer via adenoma-carcinoma as follows: loss or mutation of APC gene which changes normal epithelium into hyper-proliferative epithelium and DNA methylation is responsible for the alteration of hyper-proliferative epithelium into early adenoma. Mutation of K-ras gene and loss of DCC causes early adenoma into dysplastic adenoma and loss of p53 function subsequently causes carcinoma. Despite the fact that adenoma-carcinoma concept is well established, not all adenomas will transform into carcinomas because

many may regress (Sillars-Hardebol et al., 2010). As a matter of fact, genetic alterations rather than order of a preferred sequence is basically responsible to determine the properties of tumor (Vogelstein et al., 1988).

Azoxymethane, PhIP, and other relevant heterocyclic amines can cause ACF in rats within a few weeks. The ACF assay is a quick method to screen compounds to effectively inhibit the development of colon cancer, and many other promising candidates for chemoprevention including plant extracts.

As previously mentioned, the development of colorectal cancer is dependent on several lifestyle factors as well as genetic factors, which together affect the digestive tract. Therefore, it is interesting for many researchers to identify when a normal colonic epithelium alters to a neoplastic, hyperplastic, or dysplastic form, as an early indicator of colon cancer. The ACF seems to be a colon cancer precursor and size and numbers of ACF are directly correlated with risk of developing colon cancer (Wargovich et al., 2010).

5-Fluorouracil (5-FU) is widely used as an anticancer drug to especially treat colon cancer, breast cancer, and head and neck cancer since 1957 (Grem, 2000). 5-FU is a heterocyclic aromatic organic compound similar to pyrimidine molecules of DNA and RNA. The 5-FU is an analogue of uracil with a fluorine atom at the C-5 position instead of hydrogen (Figure 2.5) (Rutman et al., 1954). Previous studies reported only one crystal structure for pure 5-FU that crystallizes with four molecules in the asymmetric unit showing a hydrogen-bonded sheet structure (Hulme et al., 2005). The 5-FU can interfere with nucleoside metabolism and thus is incorporated into RNA and DNA, causing cytotoxicity and cell death (Noordhuis et al., 2004).

2.1.8 Mechanism of Action of 5-Fluorouracil

Fluorouracil (5-FU) (trade name Adrucil among others) a medication which is used in the treatment of cancer. It is a suicide inhibitor and works through irreversible inhibition of thymidylate synthase. It belongs to the family of drugs called the

antimetabolites. It is also a pyrimidine analog. It is on the World Health Organization's List of Essential Medicines, the most important medications needed in a basic health system. Fluorouracil has been given systemically for anal, breast, colorectal, oesophageal, stomach, pancreatic and skin cancers (especially head and neck cancers). It has also been given topically (on the skin) for actinic keratosis, skin cancers and Bowen's disease and as eye drops for treatment of ocular surface squamous neoplasia. It is contraindicated in patients that are severely debilitated or in patients with bone marrow suppression due to either radiotherapy or chemotherapy. It is likewise contraindicated in pregnant or breastfeeding women. It should also be avoided in patients that do not have malignant illnesses.

The 5-Fluorouracil (5-FU) is converted to fluorodeoxyuridine monophosphate (FdUMP) in mammalian cells forming a stable complex with thymidylate synthase (TS) and thus inhibiting deoxythymidine monophosphate (dTMP) production. The dTMP is required for DNA replication and repair and therefore lack of dTMP causes cytotoxicity (Longley et al., 2003). In normal and tumor cells, dihydropyrimidine dehydrogenase (DPD)-mediated conversion of 5-FU to dihydrofluorouracil (DHFU) is the rate-limiting step of 5-FU catabolism. DPD breaks down up to 80% of administered 5-FU in the liver (He et al., 2008). Thymidylate synthetase (TS) is an essential enzyme to catalyze thymidylate biosynthesis and plays a role in the regulation of protein synthesis and apoptotic process (Chernyshev et al., 2007). TS catalyzes the methylation of deoxyuridine monophosphate (dUMP) to dTMP, where 5, 10-methylenetetrahydrofolate (CH₂THF) is the methyl donor and provides thymidylate for the reaction in DNA replication and repair (Roberts et al., 2006). There is a seriatim binding sequence in the reaction and dUMP binds at the active site before CH₂THF. The reaction is then started by the nucleophilic addition of Cys 146 in the active site (numbering of amino acid residues is based on the sequence of EcTS) to the pyrimidine C (6) atom of dUMP. At the startpoint of catalysis,

the binding position and substrate orientation specifically provide an efficient binding of the cofactor, and subsequently permit the formation of the ternary TS–dUMP–CH₂THF complex, and the reaction (Newby et al., 2006). Previous researches have shown that 5-FU presents the anticancer effects by inhibiting TS, but the pathways are not well understood. Previous researchers have highlighted that formation of ternary TS–FdUMP–CH₂THF complex depends on time and when the fluorine substituent cannot dissociate from the pyrimidine ring, the reaction stops, which inactivate the enzyme in a slowly reversible manner (Sotelo-Mundo et al., 2006). Reduction of dTMP causes depletion of deoxythymidine triphosphate (dTTP) in the downstream reactions, inducing perturbations in other deoxynucleotides' level (dATP, dGTP and dCTP). The imbalances of ATP/dTTP ratio specifically alter DNA synthesis and repair and cause lethal DNA damage (Danenberg, 1977). When dUMP is accumulated, it subsequently increases the levels of deoxyuridine triphosphate (dUTP), which can be misincorporated.

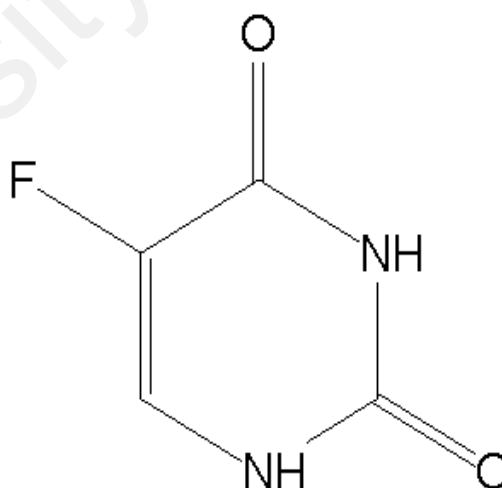


Figure 2.5: Chemical structure of 5-Fluorouracil (5-FU) (Zhang & Kim, 2008)

2.2 Gastric Ulcer

2.2.1 Definition

Gastric ulcer is known to be one of the most common diseases and it is defined as localized breaches of the gastric stomach with tissue destruction to the depth of muscularis mucosa (Figure 2.6) (Tarnawski et al., 2001). Gastric ulcer is widely distributed among the world's population and it is a chronic disease. In the Western world, about 10% of the population presents gastric ulcer disease (Barkun & Leontiadis, 2010), however, gastric ulcer was diagnosed in 11.5% among Asia and South Pacific population (Scott et al., 2013). Previous study in Malaysia consisted of 124 participants who were diagnosed with gastric ulcer, gastric erosions, and duodenal ulcer with 69.4% Malay, 24.2% Chinese, 2.4% Indian, 2.4% Kampuchean, and 1.6 % Thai ethnic origin. The study was carried out at North-eastern Peninsular Malaysia, where Malay is the major ethnic group, with more than 98% of the population, therefore, the Malay ethnic origin showed the major percentage of incidence of ulcer (Raj & Yap, 2001).

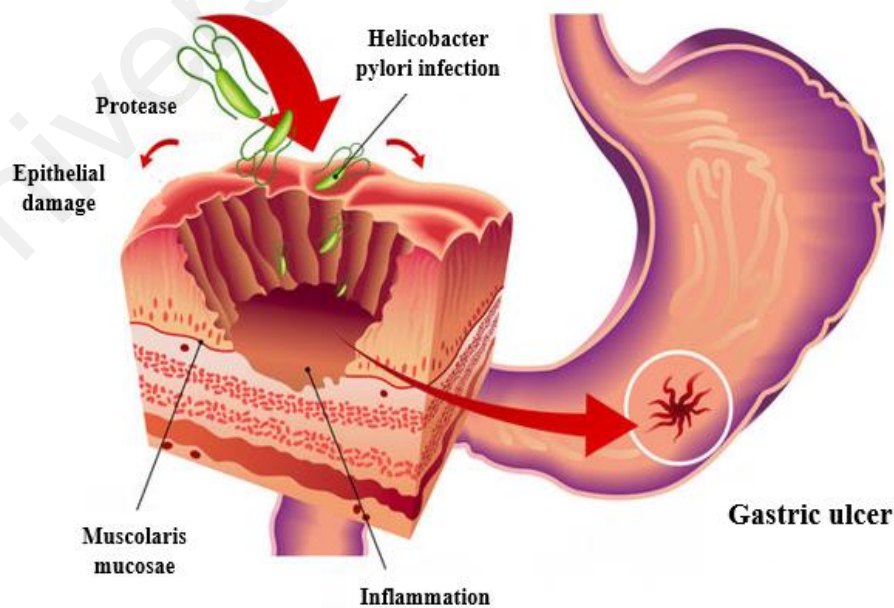


Figure 2.6: Gastric ulcer (Marks, 2012)

2.2.2 Possible Etiology and Risk Factors of Gastric Ulcer

2.2.2.1 Acid Output

Level of basal acid output (BAO) and maximal acid output are increased in up to one third of patients with gastric ulcer, forming a significant proportion of the patients. Additionally, gastric acidity is observed in some gastric ulcer patients because a high amount is sent to the end of the stomach, where most of gastric ulcers are observed (Aihara et al., 2003).

2.2.2.2 Nonsteroidal Anti-Inflammatory Drugs

Non-steroidal anti-inflammatory drugs (NSAIDs) are associated with gastrointestinal toxicity such as formation of gastric ulcer and duodenal ulcer. The NSAIDs cause gastric ulcer within three months of onset of therapy in about 4-10% of patients on daily therapeutic dose, with up to 1% of these cases being clinically significant. Some associated factors associated with increased risk of gastric ulcer with regards to NSAIDs are as follows: old age, female gender, and long-term use of NSAIDs (Laine et al., 2008).

2.2.2.3 Life Style Factors

Lifestyle can be considered as a risk factor for gastric ulcer. For instance, smoking may elevate gastric emptying and reduce formation of pancreatic bicarbonate, which in turn may cause gastric ulcer. Alcohol, in addition, may cause irritation of gastric mucosal and nonspecific gastritis. Diet was also considered as one of the main cause for gastric ulcer (Chisholm, 1998).

2.2.2.4 Genetics

In comparison with the control group with only 5-10% gastric ulcer, more than 20% of the patients indicated a family history of gastric ulcer. The genetic association is

however not clear. A rare genetic association between familial hyper pepsinogenemia type I (a genetic phenotype leading to enhanced secretion of pepsin) and gastric ulcer is reported, which indicates an association with gastric acid hyper secretion and gastric ulcer development (Blaser & Atherton, 2004).

2.2.2.5 *Helicobacter pylori* Infection

Helicobacter pylori (*H. pylori*) bacteria are small, spiral in shape, microaerophilic, and gram-negative rods. The existence of *H. pylori* in stomach and duodenum might be the most popular bacterial infection in the world (Blaser & Atherton, 2004). *H. pylori* infection is generally known as the most important etiology factor in pathological development of gastroduodenal ulcer (Chan & Leung, 2002).

2.2.3 Drugs for Gastric Ulcer Treatment

Many drugs have been found to be effective in gastric ulcer, by selectively affecting specific receptors, thereby leading to certain mechanisms in gastric ulcer therapy. These drugs can function to neutralize gastric acid secretion, scavenge free radical mediated by ulcerogenic agents or increase mucosal defenses. Antacids are known to be the first optional drugs to lessen heartburn and dyspepsia such as Maalox and Mylanta. The antacids do not avoid or cure gastric ulcers, but they are useful via two possible mechanisms; they can neutralize acidity environment inside stomach lumen with the association of three main compounds such as calcium, magnesium, and aluminum, they also may protect the mucosal layer of stomach by increasing secretion of bicarbonate and mucus (Chisholm, 1998).

Antibiotics can also be used to treat gastric ulcer caused by *H. pylori* (Hentschel et al., 1993). Amoxicillin, for example, is effectively used to lessen growth of bacteria and it has been extensively considered as a positive reference drug to assess antibacterial activity specifically *H. pylori* (Malfertheiner et al., 2007).

H₂ blockers drugs such as cimetidine and ranitidine typically treat gastric ulcer before proton pump inhibitors and antibiotic treatments were prepared against *H. pylori*. Their role is to suppress acid production via blocking histamine, which is a cytokine molecule, produced in the body to increase acid secretion in the stomach. Despite the fact that H₂ blockers such as cimetidine and ranitidine have been used by many researchers as a standard drug to carry out experiments for antiulcer evaluation, H₂ blockers are used to treat the symptoms of gastroesophageal reflux disease (GERD). These drugs, however, cannot treat gastric ulcers and they are only used to cure duodenal ulcers (Wallace, 2005).

Proton pump inhibitors (PPIs) are commonly administrated to gastric ulcers patients. They block the secretion of stomach acid through inhibiting H⁺/K⁺ ATPase enzyme, which regulates acid secretion in the parietal cell present in stomach glands. The main PPIs used to prevent and heal ulcer include omeprazole (Wallace, 2005). It is worth to noting that all these above mentioned drugs show side effects, mainly diarrhea, hypercalcemia (lead to kidney failure), kidney stones, and osteoporosis. Antacids are seldom used as anti-ulcer, because they are not adequate to prevent and heal (Eid et al., 2010). In this project, omeprazole was applied as a positive control group because it is extensively used as a standard drug to evaluate anti-ulcerogenic activity in several plant extracts. Previous studies used omeprazole as a positive control drug against ethanol induction model believing that omeprazole can increase cytoprotection and scavenge oxidative stress arbitrated by ethanol-induced ulcer (Alrashdi et al., 2012; Gupta et al., 2005).

2.2.4 Gastroprotective Factors and Gastric Mucosal Integrity

The stomach is continuously in contact to potentially risk factors, which are mainly harmful to the gastric mucosa as endogenous factors like pepsin and hydrochloric acid (Widenhouse et al., 2002). In addition, reflux of alkaline duodenal contents including

pancreatic enzymes with bile are dangerous endogenous factors. Cigarette smoking, drugs specially steroids, aspirin, and other NSAIDs are severe exogenous mucosal factors to cause mucosal damage (Weil et al., 2000). On the other hand there are many agents in the gastric mucosal defense line that help stomach to protect itself against these stimulatory factors. As for the defense agents, mucus and bicarbonate excreted by surface of epithelial cells, sulfhydryl compounds, prostaglandins, and gastric mucosal blood flow are important to keep the gastric mucosal safety (Abdelwahab et al., 2011). The gastrointestinal mucosa builds a barrier between the body and luminal environment, because it contains nutrients with high loads of potentially hostile microorganisms and toxins. Gastrointestinal tract barrier has two main parts as epithelial cell lining (the digestive tube) as the first part and secretions affect the epithelial cells and protect the barrier activity as the second part. Protection of an intact epithelium is therefore important to maintain the barrier integrity and involves an accurate balance between cell proliferation and cell death (Zorofchian Moghadamtousi et al., 2014). Gastric mucosa is continuously in contact with a mixture of endogenous and exogenous harmful agents such as gastric acid, bile, drugs, and microorganisms, which some of them such as mucus secretion, mucosal microcirculation, acid inhibition, prostaglandins, and inflammatory mediators are responsible to protect mucos (Abdelwahab et al., 2011).

The gastrointestinal epithelium coated with mucus synthesized by cells builds part of the epithelium. Mucus plays an important role to lessen shear stresses on the epithelium and associates to barrier function. The carbohydrates part on mucin molecules binds to bacteria to prevent epithelial colonization via aggregation and increasing clearance. Bicarbonate ion is secreted from apical faces of gastric and duodenal epithelial cells to maintain a neutral pH along the epithelial plasma membrane, despite the high acidic environment in the lumen (Ishrat et al., 2009).

Mucus is important to trap bacteria to excrete it in feces. It also shows that antioxidant activity decrease mucosal damage caused by bacteria and immunocytes. Mucus plays an important role in the mucosal surface to maintain a neutral and perform as a physical barrier versus luminal pepsin. Eicosanoids bioactive lipids such as prostaglandins (PG), leukotrienes, and thromboxanes are significant in gastric physiology. For example, prostaglandins often block secretion of gastric acid. Previous researches indicated the inhibitory effect of PGE₂ on acid output in the mice, rat, dog, monkey, and human. Prostaglandins from exogenous or endogenous source can stimulate mucosal defense mechanisms (Wallace, 2005). The PGE₂ and prostacyclin are essential to protect the gastric mucosal. Prostaglandins are significant to preserve mucosal blood flow (Wallace, 2005). They stimulate secretion of mucus and bicarbonate in the stomach (Hu et al., 2011).

When the stomach is exposed to 150mM HCl at pH 0.8 for a period of 5 min, production of luminal PGE₂ is increased seven folds as compared to basal values. Prostaglandins, therefore, maintain gastric mucosal integrity through activating secretion of mucus and bicarbonate, inhibiting acid secretion, mast cell activation, and apoptosis, as well as reducing leukocyte adherence to the vascular endothelium, elevating and preserving mucosal blood flow and finally inhibiting ischemia (Schaffer et al., 2011b).

Szabo et al., (1985) reported that vascular injury develop hemorrhagic erosions after intragastric administration of absolute ethanol to the rat using vascular tracers, which activates vascular permeability within 1-3min after one hour of absolute ethanol exposure. Visible hemorrhagic injury in gastric mucosa glands occurred due to noticeable lesions in the blood vessels and elevated vascular permeability. Vascular injury can be considered as pathogenic factor evidence in the growth of ethanol induced gastric hemorrhage decay. Additionally, the pretreatment with prostaglandin F₂ beta reduces ethanol injury. In another study by Tarnawski et al., (2008) the deep necrosis lesion in

the gastric mucus layer from absolute ethanol can completely stopped by 16,16-dimethyl PGE₂ (Rao et al., 2012). Robert et al. reported that pretreatment with 16, 16-dimethyl PGE₂ (10g/kg in 1ml) avoided the ethanol from histologic changes (Robert & Sporn, 1992). Serious mucosal damage to gastric glandular mucosa capillaries caused by absolute ethanol within 1 min in rat can be decreased by pretreatment with 0.5mg/100g PGF (Wilken et al., 2011). Many endocrine and paracrine agents have effect on normal proliferation of gastric epithelial cells in response to such damage as ulceration. Many enteric hormones enhance proliferation rates. Prostaglandins especially PGE₂ and prostacyclin have "cytoprotective" effect on the gastrointestinal epithelium, which shows that they are able to activate mucosal mucus and bicarbonate secretion to elevate mucosal blood flow and to restrict acid diffusion especially into the stomach epithelium.

There are some other factors with potential activity to preserve gastric mucosal integrity, namely epidermal growth factor, transforming growth factor-beta (TGF- β), fibroblast growth factor, and hepatocyte growth factor, which bind to a common receptor and activate proliferation of epithelial cell. Nitric oxide molecule has a critical function in mucosal integrity and barrier function (Bar-Sela et al., 2010). The superfamily of TGF- β signaling pathways basically regulates cellular processes such as differentiation, proliferation, migration, survival, and physiological processes including embryonic development, angiogenesis, and wound healing. Any changes in these pathways through somatic mutations or germ-line subsequently alter expression of the signaling pathways and often cause human disease (Yue et al., 2010). The TGF- β is critical as a mediator of the epithelial cell interactions to regulate epithelial cell proliferation, inflammation, and tissue repair in human gastrointestinal tract and thus the expression is elevated after acute epithelial damage in inflammatory bowel disease. The TGF- β null mice die 20 days after birth due to multifocal inflammatory disease in stomach and intestine (Yue et al., 2010). The gastric mucosa is continuously exposed to possibly harmful factors and mucosal

integrity is protected via a complicated system consisting of interacting mediators. Excessive amount of ethanol administration causes gastritis characterized by mucosal edema, cellular exfoliation, sub-epithelial hemorrhages, cell infiltration, inflammatory, and ulcer. Exogenous compounds, mainly acetylsalicylic acid, NSAIDs drugs, and high amount of ethanol trigger corrosive lesions in the gastrointestinal mucosa (May & Lawrence, 2001). Ethanol increases superoxide anion activity, lipid peroxidation, and hydroxyl radical production in the gastric mucosa (Bagchi et al., 1998). Acute ethanol stimulates DNA damage, oxidative stress, elevate xanthine oxidase activity, malondialdehyde level and reduce total glutathione level in gastric mucosal cells (Marotta et al., 1999). The ethanol- induced gastric mucosa damage is suggested to be related to oxidative stress, which interrupts energy metabolism of mitochondria and is critical in the pathogenesis of ethanol-induced gastric mucosa damage (Pan et al., 2008). The body is typically kept under an active balance of free radical production and scavenging. The physiological defense systems face free radicals through endogenous enzyme systems, including superoxide dismutase, catalase, glutathione reductase, and coenzyme Q, in addition to exogenous factors consisting of vitamin C, vitamin E, selenium, and β -carotene. The abovementioned molecules are significant antioxidant to fight against oxidative stress because they are able to convert reactive oxygen species (ROS) into stable and safe compounds or by scavenging ROS through a redox based mechanism (Brambilla et al., 2008). Physiological response to stressor increases function of hypothalamic pituitary adrenal axis and changes in gastrointestinal tissue, which subsequently increases the adrenocortical action and incidence of gastric ulceration. Oxidative stress is the main potential for the stress ulcers in the stomach (Suzuki et al., 2012). It activates either additional ROS generation or a reduction in antioxidant defenses. Oxidative stress is associated in gastric inflammation pathogenesis, ulcerogenesis and *H. pylori* infection, as well as in lifestyle-related diseases such as hypertension, atherosclerosis, ischemic heart

diseases, diabetes mellitus, and malignancies (Suzuki et al., 2011). Many gastrointestinal diseases' phenotypes such as peptic ulcer disease and gastro-paresis are relevant to antioxidant property dysfunction. The ethanol effect on gastric mucosa is multifaceted and complex, which can be relevant to a balance disruption between gastric mucosal protection and harmful agents. Gastric mucosa is exposed to gastric acid and pepsin, whereas gastroprotective agents maintain gastric mucous layer safety, microcirculatory system, bicarbonate, epidermal growth factor, prostaglandins, and epithelial cell recovery. Ethanol is harmful to the vascular endothelial cells in gastric mucosa and disturbs microcirculatory and hypoxia related to the overproduction of oxygen radicals (Suzuki et al., 2012). Generation of ROS is a series of reactions, which start with superoxide production and quickly dismutase to hydrogen peroxides. Free radicals directly or indirectly damage through reacting with other molecules in the cell. The scavenge and regulation of ROS levels in order to maintain physiological homeostasis is performed via enzymatic and non-enzymatic antioxidant protection systems such as superoxide dismutase (SOD), catalase (CAT), and glutathione peroxide (GPx). The presence of high concentration of alteration metal (Fe/Cu) ions, ischaemia reperfusion or drug metabolism generates ROS, which change the cellular antioxidant defense leading to oxidative stress (Verma et al., 2013).

2.3 Wound Healing

2.3.1 Definition

An open wound is generated when the skin is cut, torn or ruptured, whereas closed wound occurs when blunt force trauma to skin causes contusion. From pathology point of view, wound is particularly referred to a sharp injury, harmful to the dermis of the skin (Acconcia et al., 2006). Several types of acute skin wounds include incision wound, incomplete thickness damages, and lack of special tissue. Dissimilar wounds include

variety of phase process of healing (Monaco & Lawrence, 2003). Healing of wound basically consists of cascade of events, which happen in a precise and organized manner, specific to every wound. There are some overlapping in the phases of wound process. To make it accurate and clear, there are five phases, namely; hemostasis, inflammation, cellular migration and proliferation, protein synthesis and wound contraction, and remodeling phase. The process of wound healing involves the activity of a complex network of blood cells, tissues, growth factors, and cytokines, which overall increases cellular activity and subsequently raise metabolic demand for nutrients (Eisenbud et al., 2003). It seems that nutritional deficit disrupts the healing process of wound, which indicates that several nutritional agents that necessarily repair wound likely improve the healing time and the outcome. For instance, vitamin A is necessary to form epithelial and bone tissues, in addition to immune function. Vitamin C is also essential for collagen formation, tissue antioxidant, and immune function. Another examples is vitamin E, which is the principal lipid soluble antioxidant found in the skin (Simon et al., 2000). Taken together, researchers attempt to explore a medication based on natural sources in order to cure wound.

2.3.2 Phases of Wound Healing

Wound healing occurs in a series of events and some of them are overlapping. Wound healing is characterized by five phases namely; hemostasis, inflammation, migration of cell and proliferation, synthesis of protein and contraction of wound and finally remodeling phase (Figure 2-7).

Towards healing

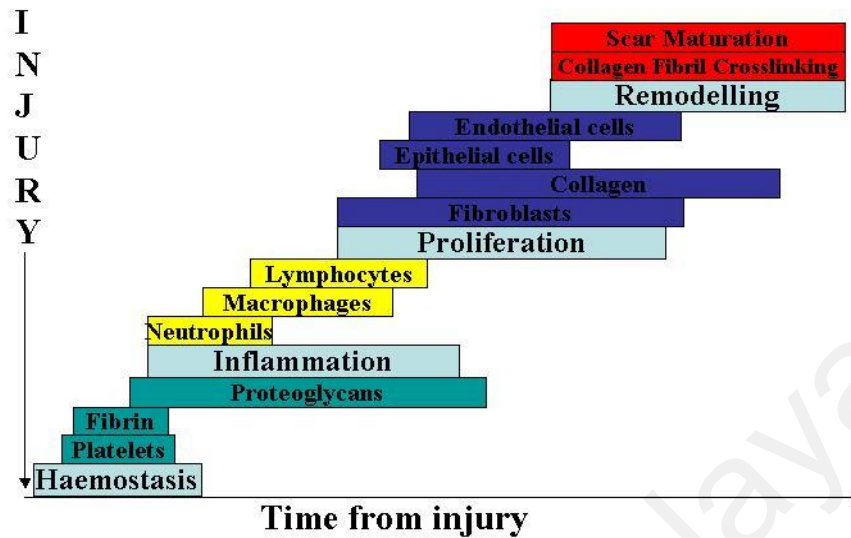


Figure 2.7: Phases of wound healing (Monaco & Lawrence, 2003)

The process of acute wound healing starting from hemostasis to the final phase of remodeling depends on a complicated interaction of several different acute wound-healing events. Cytokines is mainly important in wound healing and a major signal for different cell types and healing events (Monaco & Lawrence, 2003).

2.3.2.1 Hemostasis

All traumas are harmful to vascular parts and initiates molecular and cellular responses, which stimulate hemostasis. Hemostasis is critical to maintain the healing process. Vasoconstriction, platelet aggregation and fibrin deposition mainly contribute in hemostasis, which start from coagulation cascades. Formation of clot is the end result of hemostasis. The main component of clots is known as fibrin net including gathered platelets within surrounded cells (Lawrence, 1998). Losing of extra fluid and electrolyte from wound location and entrance of contaminates occur from external environment.

Fibrin is the main substance in wound medium of fibroblasts and other cells migration in healing process. Three characteristics for hemostasis phase are as follows:

2.3.2.1.1 Vasoconstriction

Vasoactive amines are released when vasoconstriction happens and dermis is penetrated. When sympathetic nervous system stimulates local norepinephrine, epinephrine then is released into the peripheral circulation. Further vasoconstriction is also associated to prostaglandins such as thromboxane, which can be secreted from damaged cells (Monaco & Lawrence, 2003).

2.3.2.1.2 Platelet Aggregation

Damaged cells release tissue factors, which proceed to platelet aggregation and fibrinogen. After aggregation and platelets adhesion inside cytoplasm, substances of alpha granules, dense bodies, and lysosomes are occurred (Cines et al., 1998). Several proteinaceous and immunomodulatory factors in the primary and late phases of healing are found within alpha granules. These factors mainly include adhesive proteins such as von willebrand factor VIII, fibrinogen, fibronectin, and thrombospondin as well as platelet derived growth factor (PDGF), fibroblast growth factor-2 (FGF-2), transforming growth factors α and β (TGF- α & TGF- β), platelet derived epidermal growth factors (EGFs), and endothelial cell growth factors. The TGF- β , PDGF, and FGF-2 are the main components. Calcium, serotonin, ADP, and ATP are essential compounds in the process of healing as well as those found inside dense bodies. These compounds are important to prompt coagulation cascades (Griendling et al., 2000).

2.3.2.1.3 Fibrin and the Coagulation Cascades

Coagulation cascades are composed of intrinsic and extrinsic factors. Extrinsic cascade is important in normal healing process. Thrombin is produced via activation of intrinsic and extrinsic pathways converting fibrinogen to fibrin. Thrombin then promotes

vascular permeability and extravascular migrations of inflammatory cells. Fibrin is important as a net for platelet plugs in addition to be a vital factor for temporary matrix changing quickly in the wound. Serum and platelets derived fibronectin coats the fibrin and activates fibronectin that produced through fibroblasts and epithelial cells (Dahlbäck, 2005).

2.3.2.2 Inflammation

Erythema, edema, heat, and pain are known as main features of inflammation. Increasing vascular permeability and constant movement of leukocytes to extravascular region provide inflammation at the tissue level (Figure 2.8). Moving the inflammatory cells to the damaged regions in order to kill bacteria and remove debris from dead cells and injured matrix is known as one of the main activity of inflammation, which assist to process repair mechanism (Li, et al., 2007).

Erythema and heat are considered as signs of inflammation, which occur immediately after injury because of vasodilatation, which in turn starts vasoconstriction inverting 10-15 min to the next wound. Infiltration of plasma from intravascular area to the extravascular chamber happens between endothelial cells of capillaries in wound and makes a gap (Monaco & Lawrence, 2003). Pain as a cardinal sign of inflammation and it starts from fluid accumulation in the area generating edema. Several factors are important to switch from vasoconstriction to vasodilation. Endothelial and mast cell derivative factors such as group of arachidonic acid metabolites refers to leukotrienes (LTs). Leukotriene B₄, for instance, is a strong chemotactic agent that stimulates aggregation of neutrophils, whereas LT₄, LTD₄, and LTE₄ result in vasoconstriction and increase vascular permeability, prostaglandins [PG I₂, PGD₂, PGE₂, and PGF₂α] and histamine contribution to vasodilation (Noli & Miolo, 2001). Movement of leukocytes to wound area is important to start the cellular response in inflammatory phase. At damage region,

neutrophils and monocytes are the main cells in early inflammatory phase, which immediately immigrate from capillaries into wound. Neutrophils are observed as high number at first, but later in inflammation, neutrophils number is declined and macrophages increased (Li, et al., 2007). Macrophages are known as the main controlling cell in inflammatory reaction because they phagocytize, digest, and kill pathogenic organisms, in addition to scavenge debris of tissues and destroy any neutrophil residues. There are certain enzymatic proteins and biologically active oxygen intermediates, which is released from monocyte or macrophage, allowing initiation of angiogenesis and production of granulation tissue (White et al., 2004). Macrophage also plays a role to release chemotactic factors including fibronectin, fibroblast growth factor, vascular endothelial growth factor, Platelet derived growth factor, TGF- α , and TGF- β , which are important in cell migration and proliferation, fibroblast attraction to the damage site, and matrix production. Macrophages are therefore considered as growth factor production factory and function in transition between inflammation and repair (Bosco et al., 2008).

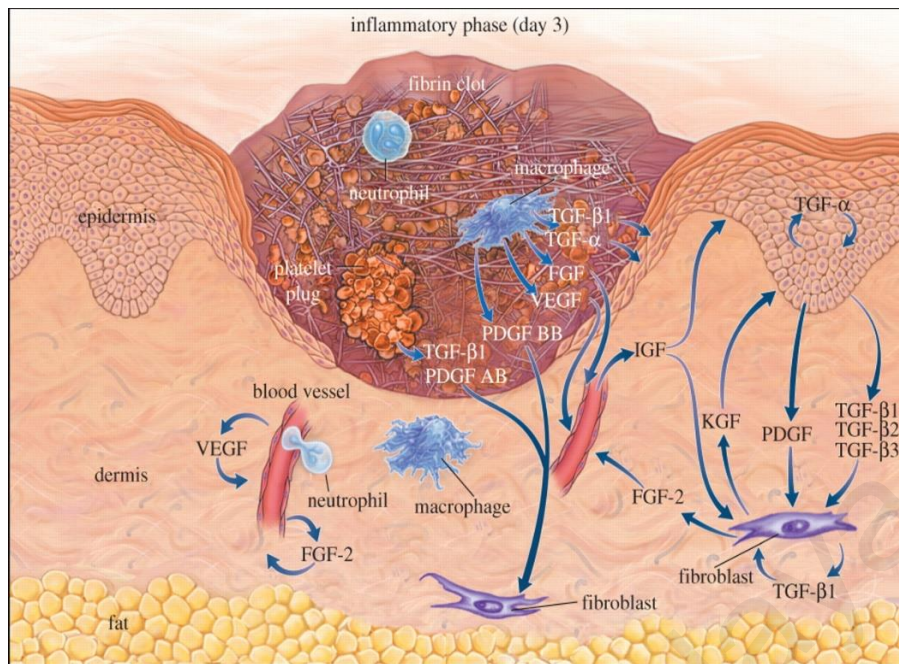


Figure 2.8: Cutaneous wound healing at day 3 after injury.

Growth factors are necessary for cell movement and wound healing. TGF- β 1, TGF- β 2, and TGF- β 3, TGF- α , fibroblast growth factor (FGF), vascular endothelial growth factor (VEGF), Platelet derived growth factor (PDGF), insulin like growth factor (IGF), and keratinocyte growth factor (KGF) are shown (Epstein & Ross, 1999).

2.3.2.3 Cellular Migration and Proliferation

Cellular medium of wounds are mainly different in the first week after acute wound, which include high infiltration of inflammatory cells to initial fibrin–fibronectin matrix and the main cells are fibroblasts and endothelial cells as healing continues. Building the epithelial surface and revascularization of the injured region are started within the first days after injury. Cytokine production is important in fibroplasia, epithelialization, and angiogenesis. Later, deactivation of cells is necessary via negative feedback mechanisms to heal normally (Diegelmann & Evans, 2004). Fibronectin and collagen are known as structural molecules in early extracellular matrix and are involved in formation of granulation tissue through supporting a scaffold and a reservoir for cytokines and growth factors. Collagens function as a support for intracellular matrix formation inside wound (Baum & Arpey, 2005). In the process of wound healing, modeling and establishing of new blood vessels is important and occurs at all stages of

repair process. Neutrophils and macrophages are also attracted via several angiogenic factors, which are secreted during hemostatic phase in order to increase angiogenesis (Takeshita et al., 1994).

2.3.2.4 Protein Synthesis and Wound Contraction

Protein synthesis and deposition and wound contraction are the main events that happen four to five days after wound occurs (Figure 2.9). Quality and quantity of deposition during healing process determine strength of a scar. As it was mentioned earlier, collagen provides more than 50% of protein constitutes in scar tissue and the production is essential in healing mechanism. Fibroblasts are responsible to synthesize collagen and other necessary proteins during repair process (Diegelmann & Evans, 2004).

There are many cytokines stimulate fibroblast to synthesize collagen, namely PDGF, TGF- β , and EGF. Several factors influence rate of collagen synthesis such as age, tension, pressure, and stress (Diegelmann & Evans, 2004; Velnar et al., 2009). Collagen synthesis continues to be high for 2-4 weeks and slows down later. Precipitation of collagen might cause healing aberration although there are some variations. Limited collagen deposition and defective healing happen in diabetic patients because of impaired inflammatory cells activation, which are correlated to lack of additional factors in healing process (Brem & Tomic-Canic, 2007). Fibrin and fibronectin are made of main initial wound matrix. Wound composition alters due to protein accelerations because fibrins as main component of matrix are replaced by collagen and proteoglycans. Several proteins are actively synthesized, namely proteoglycans as main component of mature matrix in order to improve cellular staffing and promote wound remodeling via thrombospondin I and SPARC (secreted protein acidic rich in cysteine). Wound contraction happens four to five days after initiation of wound and actively continues for about two weeks. Wound

contraction can also remain longer in open wounds for two weeks interval. Wound contraction is obvious in an open wound as it moves closer to each other.

In incisional wound, the contraction is not much clear. Contraction percentage varies based on anatomic sites, but it shows 0.6 to 0.75 mm on average per day. Contraction level is also influenced by wound shape; for example, four-sided wounds contract more rapid than round wounds, which are less possible to be exposed to risk of narrowing. Myofibroblasts mainly found at wound periphery as a feature of wound contraction at 2-3 weeks. Although myofibroblasts have been known as the “motor” to contract a wound, but recently, fibroblasts have been found to be essential for wound contraction. Several cytokines like TGF- β are involved in wound contraction (Huebener & Huebener, 2013). All cutaneous wounds can be healed through three main mechanisms of connective tissue matrix deposition, contraction, and epithelization. Simple wounds that can be closed by tape, sutures, or staples may be healed faster via main mechanism of connective tissue matrix deposition, collagen, proteoglycans, and attachment proteins form a new extracellular matrix. On the other side, open wounds mainly may be healed through contraction, in which the contact between cells and matrix move the tissue toward wound center. Although mechanism of wound contraction is not well understand but a complex interface between contractile fibroblasts, known as myofibroblasts and the matrix components seems to be necessary . Previous studies indicated the role of nerve growth and IL-8 as moderators in contraction response (Iocono et al., 2000).

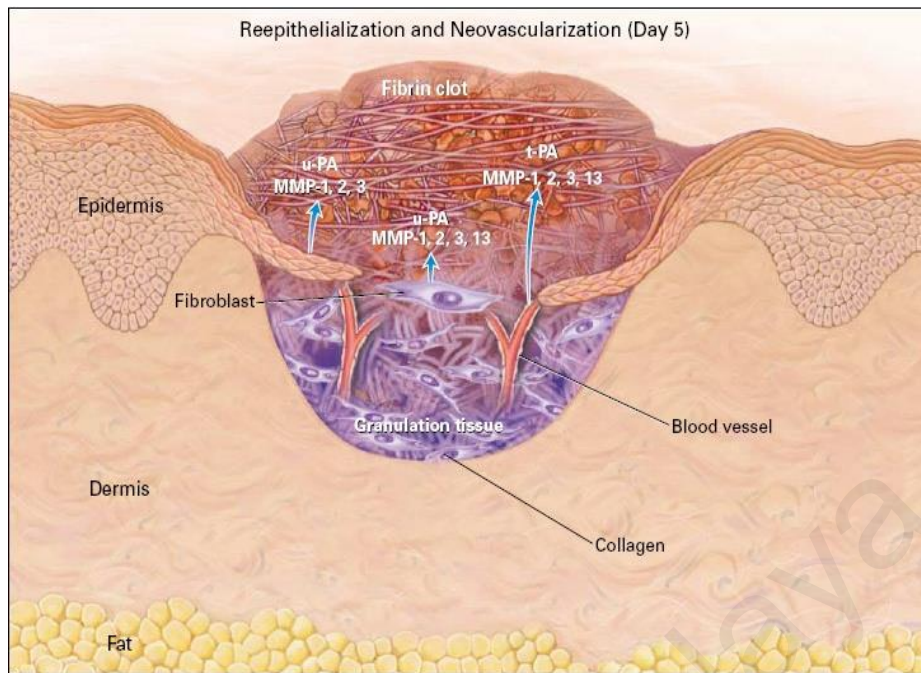


Figure 2.9: Cutaneous wound healing at day five after injury.

Blood vessels are appeared sprouting into the fibrin clot as epidermal cells cover the wound. Proteinase enzymes seem important for cell movement. In this phase, expression of urokinase type plasminogen activators (u-PA), MMP-1, 2, 3, and 13 (matrix metalloproteinases 1, 2, 3, and 13) and tissue plasminogen activator (t-PA) are shown (Epstein & Ross, 1999).

2.3.2.5 Remodeling

Scar remodeling happens about 21 days after wound has been already formed (Figure 2.10). Rate of collagen synthesis is reduced and reached to rate of collagen split-up. Factors such as interferon- γ , TNF- α , and collagen matrix are significantly important in down regulation of collagen synthesis. Matrix metalloproteinase (MMPs) plays a complex role during wound repair, because it eliminate non-vital tissue, stimulate blood vessel growth, migrate keratinocyte, regulate growth factor activity, and remodel connective tissue. MMPs is actively involved in breakdown of collagen molecules during remodeling process and other aspects of wound healing process (Gawronska-Kozak, 2011).

About 23 MMP genes have been so far identified in humans to break down extracellular matrices (Visse & Nagase, 2003). Several cells produce MMPs and

modulation occurs through tissue inhibitors of metalloproteinase (TIMPs), which so far four isoforms have been identified (Brew et al., 2000). The MMPs and TIMPs are kept balance in tissues and is controlled through cytokines excluding TGF- β , PDGF, and IL-1 (Haroon et al., 2000).

TIMP-1 and TIMP-2 are basically important in wound healing as they encourage cell proliferation, inhibit apoptosis, and prevent matrix MMPs, which impeded wound healing indirectly through degradation of growth factors and cytokines and directly through destruction of extracellular matrix proteins (Ching et al., 2011). Modification of extracellular matrix composition happens in wound remodeling. Collagen fibers provide nearly 80% of dry weight of normal human dermis and are the key proteins for strength, structure, and hardness of dermal tissue. In healthy adults, for instance, type I collagen and type III collagen consist of about 80% and 10% of collagen in dermis, respectively. Collagen quantity increases during repair and reaches to a maximum level between 2-3 weeks after injury. The dermis gradually reverse to normal phenotype with type I collagen after one year or longer. After wound is closed, type III collagen is degraded and type I collagen synthesis is increased. The process of dermis collagen transformation is controlled via production of new collagen and lysis of old collagen, basically performed by MMPs. In final phase of wound healing, the remodeling phase is responsible to improve new epithelium and make final scar tissue. Synthesis of extracellular matrix is started with granulation tissue development during proliferative and remodeling phases.

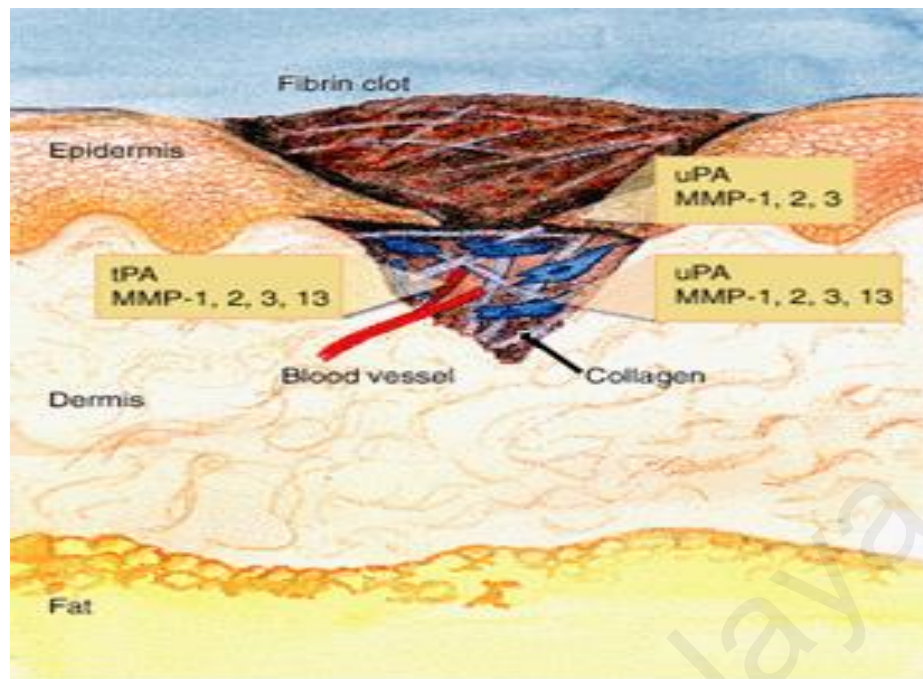


Figure 2.10: Cutaneous wound healing in remodeling phase.

The remodeling phase of wound healing is mediated by cytokine, which controls degradation of fibrillar collagen and other matrix proteins performed by serine proteases and MMPs. Granulation tissue is formed below the epithelium and made of inflammatory cells, fibroblasts, and newly formed and forming vessels (Grose et al., 2002).

2.3.3 Wound Healing Factors

Rate of wound healing might be influenced by local and systemic factors; the first one is referred to immediate wound environment while the latter refers to entire body (Guo & Dipietro, 2010).

2.3.3.1 Infection

It is usually observed that infected wounds are healed slowly. Infection defines a situation where bacteria are present in wound and generate an inflammatory host response. Exotoxins are secreted by living bacteria in wound, which is considered as waste products of active metabolism. Exotoxins are toxic molecules for cells and they inhibit normal activity of local cells or tissues. For instance, exotoxins may alter protein synthesis. Infected wounds have to be cleaned and systemic antibiotics are often required. Any foreign bodies in a wound can also be possibly correlated with infection (Guo & Dipietro, 2010). Inflammation is important to remove contaminant microorganisms and

is a normal phase of wound healing process. Bacteria and endotoxin increase proinflammatory cytokines as TNF- α , interleukin-1 and therefore elongate inflammatory phase, which cause wounds to remain in a chronic stage and fail to heal. Prolonged inflammation can cause an increase in MMPs level as a family of proteases that in turn reduces extracellular matrix (Menke et al., 2007).

2.3.3.2 Local Blood Supply

Oxygen is essential for cell metabolism especially energy production and wound healing process. Oxygen keeps wounds from infection as follows: activating angiogenesis, increasing keratinocyte differentiation, migration, and re-epithelialization, promoting fibroblast proliferation, and collagen production and encouraging wound contraction (Bishop, 2008; Rodriguez et al., 2008). In addition, superoxide, which is critical to kill microorganisms and produced via polymorphonuclear leukocytes depends on oxygen level. For example, when oxygenation is not repaired in wound, healing is reduced. Impermanent hypoxia after injury promotes wound healing but extended or chronic hypoxia interferes with wound healing. In acute wounds, in other words, hypoxia helps as a signal in wound healing progression. Hypoxia is able to activate cytokine and growth factors secreted from keratinocytes, macrophages, and fibroblasts including platelet derived growth factor, TGF- β , TNF- α , vascular endothelial growth factor, and endothelin-1, which all are important activators for cell proliferation, migration, chemotaxis, and angiogenesis in wound healing process (Menke et al., 2007).

2.3.3.3 Malnutrition and Healing Delay

Proteins are the main component for cell renewal, tissue growth, and restoration after injury. They significantly affect several wound healing phases via RNA and DNA synthesis, elastic tissue formation and collagen, nutrition of immune system, epidermal growth, and keratinization. Prolong protein malnutrition causes skin to be thinner and

wrinkled and therefore immunity level drops. Diabetic patients with protein malnutrition are at higher risk for mutilation (Dryden et al., 2013). Sufficient intake of protein is necessary for convenient wound healing. Delay in wound healing process due to protein depletion happens by extending inflammatory phase, which in turn inhibit synthesis of collagen and proteoglycan, fibroplasia, angiogenesis (proliferation phase), wound remodeling (Ruberg, 1984).

Dietary proteins provide all nine necessary amino acid and thus are considered as complete proteins, such as poultry, meat, fish, milk products, eggs, and soybeans. On the other hand, body requires sufficient amount of necessary amino acids, nitrogen and energy in order to produce the other eleven amino acids.

Certain amino acids are especially important for wound healing process, for instance, cysteine and methionine are involved in collagen and connective tissues synthesis. Arginine is assumed to be the main element to increase proliferation of collagen and thus immune reaction (Wild et al., 2010). Glutamine is significant for inflammatory cells proliferation and energy source (Dryden et al., 2013).

Carbohydrates are the main source of energy. Wound healing is a very energy consumer process; therefore carbohydrates are necessary in cells and tissues. Patients suffering from extensive wounds require an elevated intake of energy giving foods. When amount of carbohydrates is enough, the body does not require breaking down amino acids to produce energy (Medlin, 2012). Studies showed that glucose deficiency affects proliferation of fibroblast and lower levels of glucose significantly was found in wound fluid of patients with chronic wound (Han et al., 2004).

Fatty acids are subunits of fats. Certain components in cells and tissues (cell membranes) are made of fatty acids, which are needed for tissue regeneration. Fat

generally supply essential fatty acid, which are energy source for cell metabolism (Shingel et al., 2008).

Vitamins are vital micronutrients in diet. Vitamin A, D, E, and K are fat-soluble and may be stored in the body while vitamin B1-B11 and C are water-soluble and thus cannot be stored. Vitamin C, also known as ascorbic acid, is the main cofactor for synthesis of proteoglycans, collagen and other organic constituents of intracellular matrix of tissues such as skin, capillary walls, bones, and other connective tissues. Deficiency of ascorbic acid results in abnormal collagen fibers and thus alters intracellular matrix that in turn causes cutaneous lesions, reduces tensile strength of fibrous tissue, decreases adhesion of endothelium cells and finally affect the level of immunity (Biesalski, 2010).

Vitamin A is necessary to develop epithelial and bone tissues, better function immune system, and differentiate cells. Vitamin A promotes normal physiological wound repair mechanism and reverses inhibition of cutaneous and facial wound healing causes by corticosteroid. Vitamin A is beneficial for wound because it promotes early inflammatory phase, improves localization, stimulate immune response, enhance number of macrophages and monocytes cells in wound, support differentiation of epithelial cell and tranformation of collagenase function (Simon et al., 2000).

Minerals are inorganic nutrients that small amount of them are needed for health. For instance, zinc is an essential mineral for wound healing and re-epithelialization. About 300 enzymes require zinc for their cellular function. From molecular point of view, zinc is required for cell division, synthesis of DNA and proteinas well as regeneration and repair of tissues. Previous studies on zinc-deficient animals showed that zinc deficiency is correlated with delayed wound healing and reduced strength of animal wound that arises from decreased level of collagen and protein synthesis duringwound healing process. Zinc deficiency is associated by an immunodeficiency that results in infections.

Zinc affects keratinocytes, osteocytes, and leukocytes cells. In addition, certain concentration of zinc is needed for a specific cell response. Iron is known as a cofactor for prolyl and lysyl hydrolases for collagen synthesis and thus iron deficiency severely inhibits wound-healing process. Moreover, iron aids to transport oxygen by being part of hemoglobin structure and therefore helps to regenerate injured tissues (Brown & Phillips, 2010).

Water is critical for optimal wound healing because hydration promotes cell proliferation and migration through chemotactic gradients by cytokines, metal ions, and growth factors. In other words, dehydration hardens epidermal tissues and causes dermal necrosis that delays wound healing, elevating patient discomfort (Dryden & Shoemaker, 2013).

2.3.3.4 Age

Children and young adults usually have a good level of wound healing because they require competent nutrients and conventional requirements for growth and development. On the other side, elderly people may have longer period for wound healing due to small number of fibroblasts in tissues and reduced rate of collagen formation. In addition, wound contraction and re-epithelialization process are slower in old people. Diseases such a peripheral ischemia, heart disease, and diabetes mellitus may severely affect wound-healing process in old people, who have less mobility with elevated risk for pressure sore formation (Gosain & Dipietro, 2004).

2.3.3.5 Reactive Oxygen Species (ROS)

A variety of cytokines, growth factors, and hormones controls process of wound healing. Previous studies indicated that nitric oxide and reactive oxygen species (ROS) significantly regulates wound healing (Schwentker et al., 2002). ROS play an important role in protection against microbial invasion and intracellular signal transduction. For

instance, small amount of hydrogen peroxide is necessary for efficient angiogenesis during wound healing, while high amount of ROS can be toxic due to high reactivity. Hyperoxia and hypoxia conditions elevate formation of ROS, in which an excessive amount of ROS causes additional tissue damage (Guo & Dipietro, 2010). ROS are produced in all types of cells during normal metabolic processes such as respiratory system. Inflammatory cells produce high amount of NADPH oxidase in injured tissues with inflammation that in turn makes a certain level of ROS (Schreml et al., 2010).

Cells produce high reactive superoxide radical anion, which quickly converts to hydrogen peroxide (H_2O_2) and water. Many superoxide dismutase enzymes are responsible to carry out this conversion. Although, H_2O_2 is not a radical molecule, it causes severe cell injuries through production of hydroxyl radicals in the presence of iron or copper ions. Hydroxyl radicals are significantly harmful and cause oxidation of cellular macromolecules, therefore, H_2O_2 should be immediately detoxified by catalase and various peroxidases. If ROS is produced excessively or detoxified unsuccessfully, oxidative stress may happen, in which causes severe cell damage, premature aging, or neoplastic transformation. ROS is highly produced in wound to protect cells against bacteria (Kotani et al., 2007), however, a high number of neutrophils and ROS eliminate anti-protease substances that generally defend tissue and extracellular matrix. High concentration of ROS causes serious tissue injury and neoplastic transformation and thus reduces healing process by damaging cellular membranes, proteins, DNA, and lipids (Süntar et al., 2012). Large amount of ROS may kill fibroblasts and thus skin lipids would be less flexible. Taken together, antioxidants are significant to effectively treat and manage wounds through eliminating inflammation products (Houghton et al., 2005). On the most possible mechanism for antioxidant defense is direct interface of extracts or compounds with hydrogen peroxide in order to change cell membranes and control damage. Certain compounds present high radical scavenging capacity in order to increase

wound healing (Süntar et al., 2012). Previous studies have proposed many low molecular weight antioxidants to regulate redox environment in wounds healing process such as endogenous molecules including glutathione, uric acid, and lipoic acid and vitamin C and E, carotinoids, and phenolic compounds in food. Lack of these antioxidants in wound healing proves their significance (Simon et al., 2000).

2.3.4 Apoptosis

Previous studies have proposed certain signals in wound healing process for cells expulsion, but mechanisms of cell death are not well addressed. There are three possible mechanisms, in which cells die during injury, namely emigration, necrosis, and apoptosis. In pathologic tissue repair, necrosis occurs for extreme wounds and healing is done without serious inflammatory response and tissue injury. Tissue inflammation is activated by necrosis, thus reduced amount of wounds cellularity is not possibly regulated by necrosis (Greenhalgh, 1998). Cellular migration in wound seems to be waste of energy and therefore apoptosis is the reasonable mechanism to eliminate undesired cells during healing phases that can be done in a phagocytotic process without an inflammatory response. As a result, inflammatory cells are eliminated from wound via apoptosis. When appropriate amount of collagen is deposited at the end of proliferative phase, fibroblasts start to be apoptotic. Finally endothelial cells are disappeared and fibroblasts are remained. Previous studies have revealed an association between apoptosis and resolution of tissue repair during wound healing process. For instance, inflammatory cells have gone through apoptosis as early as 12 hours after wounding during early phase of tissue repair (Epstein, et al., 1999). An obvious apoptosis have been reported in inflammatory cells under margin of migrating epithelium and next to wound margin. Granulation tissue surrounded by an epithelium does not show any apoptosis. Minimum inflammatory cells infiltration and auxiliary fibroblasts was reported in open dermal wound without diabetic and diabetic mice covered by polyurethane dressing (Darby et al., 1997). Neutrophils,

macrophages, and lymphocytes inflammatory cells were found in open granulation tissue at the wound center. Apoptosis was found at transition zone under leading margin of epithelium across granulation tissue, which confirms the hypothesis that thymosin α 1 is responsible for inhibition of inflammation in the epithelium, supported by clinical findings. Closure of a wound with a graft is correlated with elimination of inflammatory cells in wound (Ashcroft et al., 2003; Rodero & Khosrotehrani, 2010). Apoptosis reduces cellular infiltration via switching between granulation tissue and scar in order to eliminate fibroblasts in the later stages of tissue repair. Apoptotic process can be permanently blocked if down regulation of fibroblast and myofibroblasts activity is delayed. Excessive activity of fibroblast may hardly estimate collagen synthesis and degradation and thus leads to formation of severe scar, which the accurate mechanisms are not known (Desmoulière et al., 1997).

Apoptosis regulates neutrophil response to injury, in which major injuries do not destroy tissues. After invading pathogens are eliminated, most neutrophils in wound tissue undergo apoptosis and are phagocytized by macrophages to avoid excessive inflammation (Rodero & Khosrotehrani, 2010). Several mechanisms are proposed for neutrophil apoptosis as such neutrophil apoptosis might be activated via TNF- α signaling pathway (Ohta et al., 1994). Neutrophils interaction via β 2 integrins (CD11b/CD18) promotes apoptosis and neutrophils migration to a monolayer of endothelial cells later induces apoptosis (Larsson et al., 2000). TGF- β 1 is probably involved in down regulation of inflammatory response. Previous studies on TGF- β 1 null knockout animals discovered its function in eliminating inflammatory cells (Desmoulière et al., 1995). They showed that mice without TGF- β 1 expression presents normal healthy status until three weeks of age, however, pups show lethal inflammatory response due to invasion of neutrophils, macrophages, and lymphocytes to all tissues. The inflammatory response is correlated with high level of expression of TNF- α and IL-1 β . Tissue repair process was reported

normal in these pups during the three weeks because knockout animals receive TGF- β 1 via mother's milk, which is stopped during weaning and thus animals fall sick due to inflammatory cell invasion (Sporn & Roberts, 1992).

Antiproliferative protein p53 is also involved in apoptosis of inflammatory cells throughout healing process (Fuchs & Steller, 2011). For instance, regulation of keratinocytes apoptosis attracts researchers' attention in dermatologic diseases. When keratinocytes are exposed to ultraviolet light (sunburn), cells apoptosis is quickly induced (Raskin, 1997). Eighteen members of Bcl-2 family were found to induce apoptosis pathway, either to promote or prohibit apoptosis. For example, BAX, Bad, and Bak are pro-apoptotic proteins, whereas Bcl-2 and BCL-xL are anti-apoptotic proteins. A decrease in BCL-xL expression and thus induction of apoptosis causes basement membrane to lose attachment. In a similar pattern, inhibition of EGF receptor's activity is associated with apoptosis and reduced expression of BCL-xL (Rai et al., 2005). Pena explored transgenic mice in order to study function of BCL-xL and BCL-xS, which reduces and stimulates apoptosis, respectively. They found out that overexpression of BCL-xL or BCL-xS cause normal epidermis in keratinocytes of mice. After ultraviolet irradiation, mice with BCL-xL overexpression showed mounting resistance to injury, while those with BCL-xS overexpression presented mounting sensitivity, which suggest different pathways for keratinocyte apoptosis in injury and normal differentiation (Pena et al., 1997).

A decrease in p53 levels via siRNA treatment in keratinocyte improves apoptosis responses to interferon-alpha (IFN- α) and interferon-gamma (IFN- γ), which indicates human keratinocyte cell line to interferon-stimulated apoptotic after exposure. Mechanism for the elevated apoptosis is associated with stimulation of TNF-related apoptosis-inducing ligand (TRAIL), and interaction with death receptors through

blocking the pathway by dominant negative Fas-Associated protein with Death Domain (FADD) or neutralizing antibody versus TRAIL, which reduces apoptosis response to IFN- α and IFN- γ (Pena et al., 1997).

Interferon reduces range of hypertrophic or keloid scarring. For instance, IFN- γ is reported to eliminate range of keloid formation (Durani & Bayat, 2008) or IFN- α 2b is found to decrease hypertrophic scar formation in burn patients (Harrop et al., 1995), who showed increased level of TGF- β in serum (Schmid et al., 1998). Findings from these studies suggest that fibroblast activity is controlled by an interaction between interferon and TGF- β in a maturing wound. Inducing collagenase by apoptosis signals regulates collagen degradation. Bian and Sun discovered that p53 molecule binds to promoter of type IV collagenase (matrix metalloproteinase 2) in human (Bian & Sun, 1997), which suggests apoptosis signals are involved in downregulation of collagen deposition via reducing fibroblast numbers (thus reducing collagen synthesis) and by promoting collagenase activity. Previous studies on effects of recombinant human TNF- α on collagen synthesis and gene expression in cultured fibroblasts confirm that TNF- α reduces transcription of collagen gene, expression of collagen mRNA, and thus collagen production in cultured fibroblasts (Solis-Herruzo et al., 1988).

Cellularity and extracellular matrix in the late phase of wound healing are decreased in granulation tissue of a mature scar. Studies suggest apoptosis as a mechanism or accelerate conversion of granulation tissue to scar. For example, Nakazono-Kusaba et al. discovered the effect of benzoyl staurosporine known as an inhibitor of protein kinase C on human keloid derived fibroblasts to understand treatment capability of keloid formation and they showed that benzoyl staurosporine can be considered as a candidate for antitumor factors because it can stimulate keloid fibroblast apoptosis via caspases-dependent pathway (Nakazono-Kusaba et al., 2004).

Taken together, apoptosis is important to rapidly synchronize altering populations of all cells, which are involved in tissue healing. In majority of wounds, control of cell proliferation facilitates wound closure. In some cases, imbalance number of cells leads to a pathologic tissue repair.

2.4 Medicinal Plants

Plants have been useful to provide food, dyes, perfume, gum, fiber, resin, and many other products for humans. Currently, ethnopharmacologists show interest to discover bioactive properties and phytochemical analysis in medicinal plant in order to cure several diseases. From therapeutic point of view, many medicinal plants can be utilized as a natural medicine in many biological mechanisms such as gastric ulcer and wound healing (Gupta et al., 2005). Previous study showed that plants have several bioactivities (Alam et al., 2009; Yadav et al., 2011).

2.4.1 *C. Purpurascens*

Curcuma purpurascens Bl., belonging to the Zingiberaceae family, is known as temu tis in Yogyakarta, Indonesia. *Curcuma purpurascens* Bl. is a rhizomatous herbaceous perennial plant of the ginger family, Zingiberaceae. It is native to Indonesia, requiring temperatures between 20 and 30 °C (68 and 86 °F) and a considerable amount of annual rainfall to thrive. Plants are gathered annually for their rhizomes and propagated from some of those rhizomes in the following season.

Curcuma purpurascens Bl. is one of the less known *Curcuma* species and is considered of minor importance. *C. purpurascens*, locally known as temu tis in Yogyakarta, Indonesia, is also known as Solo's (east of Yogyakarta) temu glenyeh or temu blenyeh, whose scientific name is *Curcuma soloensis* Val. . Villagers from the Kediri district of East Java plant *C. purpurascens* or temu tis at the base of Mount Wilis. The rhizomes are dried and ground before being sold to wholesalers as alternative

medicine. The powdered rhizomes are usually taken together with other herbs to treat ailments, such as cough and skin infections. Temu tiscan grow up to 1.75 m in height and usually flowers from October to February. Morphologically, the rhizomes of temu tis are similar to those of common turmeric (*Curcuma longa*). However, cross-sections of the rhizomes of temu tis are slightly bigger and paler in colour in comparison to common turmeric. Hence, the dried ground rhizomes of temu tis are often used to adulterate dried ground rhizomes of common turmeric and *Curcuma xanthorrhiza* (locally known as temulawak) for higher profit margins.

The rhizome of *C. purpurascens* were collected from Yogyakarta, Indonesia and a voucher specimen (KL 5793) was deposited at the herbarium of the Department of Chemistry, Faculty of Science, University of Malaya, Kuala Lumpur, Malaysia.

C. purpurascens is a herb with branched rhizome, outside and inside with orange-yellow color with whitish tips; leaf blades elliptical (55-70 cm × 19-23 cm), green but purple along the midrib above; inflorescence terminal on a leafy shoot, bracts pale green, coma bracts white at base and pale green towards the top or almost entirely white, outside pale brown spotted at the top; corolla about 5 cm long, white; labellum about 17 mm × 17 mm, pale creamy yellow with a dark yellow median, other staminodes pale creamy yellow, another with long spurs. *C. purpurascens* grows spontaneously in teak forest (Figure. 2-11) (Koller, 2009a).

In the current study, *Curcuma purpurascens* BI (*C. purpurascens*) rhizome extract was used to study anti-cancer activity, gastro protective potential, and ability of wound healing. Ethnopharmacological data have indicated usage of for many purposes such as food additive and medicinal agents. A wide variety of secondary metabolites such as alkaloids, tannins, terpenoids, and flavonoids have been discovered from *C. purpurascens* rhizome so far. *In vitro* studies revealed antioxidant activity, drugs potential, and dietary supplement in *C. purpurascens* BI rhizome. *C. purpurascens* rhizome have been utilized

to treat wounds, scabies, itch, fever, cough, and boils. Previous studies have isolated several active compounds such as 3,7-cyclodecadien-1-one, 3,7-dimethyl-10-(1-methylethylidene), α -Elemene, α -Elemenone, α -Turmerone, turmerone, curlone, benzofuran, and 6-ethenyl-4,5,6,7-tetrahydro-3,6-dimethyl-5-isopropenyl from rhizome of *C. purpurascens* (Rouhollahi, et al., 2014).



Figure 2.11: Curcuma purpurascens B

Table 2.1: Taxonomy of Curcuma purpurascens BI

systematics	
Domain	eukaryotes
Kingdom	plants
Division	fanerogamer
Class	Monocot flowering plants
Order	Zingiberales
Family	Zingiberaceae
Genus	<i>Curcuma</i>
Pea	<i>Curcuma purpurascens</i>

CHAPTER 3: METHODOLOGY

3.1 Plant Collection and Preparation of Extracts

The *C. purpurascens* rhizome studied in this work was collected from Yogyakarta, Indonesia, in 2012. A voucher specimen (KL 5793) was deposited in the herbarium of the Chemistry department, Faculty of Science, University of Malaya, Kuala Lumpur, Malaysia. The air-dried and powdered rhizomes (1.0 kg) were subjected to extraction using n-hexane followed by dichloromethane. The resulting filtrate of the rhizome was concentrated by a rotary evaporator at 40 °C. The extracts were stored at -20 °C. (Rouhollahi, et al., 2014).

3.2 Evaluation of the Antioxidant Capacity of the Crude Extract

3.2.1 Scavenging Activity of DPPH

The antioxidant power of the *C. purpurascens* rhizome crude extracts were determined using 2, 2-Diphenyl-1-picrylhydrazyl (DPPH) stable free radical scavenging assay. In the occurrence of an antioxidant which can donate an electron to DPPH, the purple hue which is usual for free DPPH radical decays and the change in absorbance at 517 nm can be read. This assay evaluates the free radical scavenging capability of the enquired specimen. The assay was conveyed out as described by (Gorinstein et al., 2003) with minor modification. In brief, 1 mg from each extracts were dissolved in 1 ml (DMSO), then diluted to five different concentrations (50, 25, 12.5, 6.25 and 3.125 µg/ml), Ascorbic acid and trolox were utilized as antioxidant standards. An amount of 5 µl of DPPH in triplicate was added and the decrease in absorbance value was assessed at 517 nm by UV 1601 spectrophotometer for 2 hours with 20 minutes gaps. The radical scavenging activity was calculated from the following equation and the outcomes were expressed as Mean ± Standard Error (SEM):

% of scavenging activity = (Abs blank – Abs sample) / Abs blank X100

3.2.2 Ferric Reducing Antioxidant Power (FRAP) Assay

The anti-oxidant power of *C. purpurascens* rhizome crude extracts were also determined using a test sensitive to its scavenging ability towards reactive oxygen species or reagents containing iron. In this regard, the ferric reducing anti-oxidant power (FRAP) of both plant extracts were determined using the method described by (Benzie & Strain, 1996), with a slight modification. The FRAP reagent was prepared by mixing 300 mM acetate buffer (3.1 mg sodium acetate /ml, pH 3.6), 10 mM 2,4,6-tripyridyl-S-triazine (TPTZ) (Merck , Darmstadt-Germany) and 20 mM FeCl₃.H₂O (5.4 mg/ml). The *C. purpurascens* rhizome crude extracts, and the following standards; gallic acid, quercetin, ascorbic acid , rutin , and 2,6-di-tert-butyl-4methyl phenol (BHT), were added in amounts of 10 µL of 0.1mg/ml silymarin and added into 300 µl of the reagent TPTZ separately in triplicate. The absorbance of the mixture was read using ELISA reader (UV 1601 spectrophotometer, Shimadzu, Kyoto, Japan) at 593 nm wavelengths at 0 minute and after 4 minutes. To compensate this deficiency, we performed the measurements in equivalent amounts obtained by scaling the administered doses up by 20 times, respectively. The reading from both plant extracts and were compared against those standards; gallic acid ,quercetin, qscorbic, rutin , and BHT (Asghar et al., 2008).

3.2.3 Total phenolic Content (TPC) Evaluation

The TPC of the *C. purpurascens* rhizome crude extract were determined by the Folin Denis calorimetric method using Folin-Ciocalteu reagent (Merck, Darmstadt, Germany) in gallic acid equivalent. An amount of 1 mg of each crude extract was added into 100 µl of Folin –Ciocalteu reagent, followed by incubating the mixture in the dark for 3 minutes. Then, 100 µl of sodium carbonate (1g/10 ml) solution was added to the mixture, and mixed thoroughly. The final mixture was re-incubated in the dark for 1 h. All

procedures were carried out in triplicate. Serial dilution of gallic acid (1 mg/ml DMSO) was used to produce linear standard curve and the absorbance was read at 750 nm.

3.3 *In Vitro* Anti-Cancer Study

3.3.1 Cell Lines and Culture Conditions

CCD841 (normal human colon epithelial cell line), HepG2 (human hepatoma cell line), HT-29 (human colon cancer cell line), MDA-MB-231 (human breast cancer cell line), PC-3 (human prostate cancer cell line) and WRL-68 (human hepatic cell line) were purchased from the American Type Culture Collection (ATCC, Manassas, VA, USA) and maintained in RPMI-1640 (Sigma, St. Louis, Mo, USA) supplemented with 10% fetal bovine serum (PAA Lab, Pashing, Austria), 100 U/ml penicillin and 100 mg/ml streptomycin (PAA Lab) in a humidified atmosphere with 5% CO₂ at 37 °C. Untreated medium containing vehicle DMSO (0.1%) was used as a negative control in this study.

3.3.2 Cell Proliferation Assay

In vitro cytotoxic effect of DECPR and HECPR was determined using MTT [3-(4, 5-dimethylthiazol-2-yl)-2, 5-diphenyltetrazolium bromide] assay as described by (Mosmann, 1983). In brief, cells (5×10^4 cells/ml) were treated with concentrations of DECPR and HECPR in a 96-well plate and incubated for 24 h. After incubation time, the MTT solution (5 mg/ml, 20 μ l) was added and the plate was incubated for 2 h. DMSO (100 μ l) was then used to dissolve the formazan crystals. The absorbance was measured at 570 nm with a microplate reader (Asys UVM340, Eugendorf, Austria). The suppressive effect of DECPR and HECPR was expressed as IC₅₀ value. Since DECPR showed the strongest suppressive effect towards HT-29 cells, we carried out further experiments only on the respective colon cancer cell. The anticancer drug, 5-Fluorouracil (5-FU) (Sigma, St. Louis, MO, USA) was used as a positive control towards HT-29 cells.

$\% \text{ cell viability} = (\text{abs of extract sample} - \text{abs of control}) / \text{abs of control} \times 100$

3.3.3 Lactate Dehydrogenase (LDH) Release Assay

Release of LDH from treated colon cancer cells was measured using Pierce LDH cytotoxicity assay kit (Thermo Scientific, Pittsburgh, PA, USA). Briefly, HT-29 cells were treated with different concentrations of DECPR for 24 h. To determine the LDH leakage, the supernatant of treated cells was transferred in 96-well plate. Triton X-100 (2%) as positive control was used to completely lyse the cells and release the maximum LDH. Then, the LDH reaction solution (100 μ l) was added to the cells for 30 min. The red color intensity presenting the LDH activity was measured at the absorbance of 490 nm using a Tecan Infinite 200 Pro (Tecan, Männedorf, Switzerland) microplate reader. The level of released LDH from treated colon cancer cells was expressed against a percentage of positive control.

3.3.4 Cytoskeletal Arrangement Assay

To determine the effect of DECPR on the cytoskeletal rearrangement, we used cellomics cytoskeletal rearrangement kit (Thermo Scientific, Pittsburgh, PA, USA) as described by (Liew et al., 2014). In brief, HT-29 cells at the exponential phase of growth were treated with different concentrations of DECPR for 24 h. Then, treated cells were fixed and stained with Hoechst and phalloidin dyes according to the vendor's instructions. At the end, the stained cells were examined for changes in cytoskeletal rearrangement using ArrayScan HCS system (Cellomics Inc, Pittsburgh, PA, USA).

3.3.5 Reactive Oxygen Species (ROS) Generation Assay

To determine the effect of DECPR on ROS generation in colon cancer cells, we carried out ROS assay. Briefly, HT-29 cells (1×10^4 cells/well) were seeded in a 96-well plate for 24 h. Then, colon cancer cells were treated with different concentrations of DECPR and incubated overnight. After the incubation time, treated cells were stained with dihydroethidium (2.5 μ g/ml, 50 μ l) and Hoechst 33342 (500 nM) for 30 min. Next,

cells were fixed with paraformaldehyde (3.5%) for 15 min and washed with PBS twice. Formation of ROS in treated cells was measured using a cellomics array scan HCS reader (Cellomics Inc, Pittsburgh, PA, USA).

3.3.6 Multiple Cytotoxicity Assay

The important characterizations of mitochondrial dependent apoptosis, including changes in cytochrome C release and mitochondrial membrane potential (MMP) in addition to cell membrane permeability were measured using a cellomics multiparameter cytotoxicity 3 kit as described in detail by Lövborg and colleagues (Rickardson et al., 2005). The fixed and stained HT-29 cells were exhaustively analyzed using the ArrayScan HCS system (Cellomics Inc, Pittsburgh, PA, USA).

3.3.7 DNA Fragmentation Assay

A suicide-track DNA ladder isolation kit (Calbiochem, San Diego, CA, USA) was used to observe DNA fragments (mononucleosome and oligonucleosomes) formed during apoptosis. In brief, HT-29 cells were seeded at the density of 5×10^4 cells/ml in a culture flask, and incubated for 24 h. They were then treated with DECPR at 12.5 and 25 $\mu\text{g/ml}$ concentrations for 24 h. The treated cells were trypsinized and centrifuged at 1,000 rpm for 10 min. The pellet was gently re-suspended in 55 μl of solution #1 (kit component). It was then mixed with 20 μl of re-suspension buffer. To detect the DNA ladder, the extracted DNA samples were run on the 1.5% agarose gel in a Tris-acetic-EDTA buffer. After electrophoresis, the gel was stained with Novel Juice Cat No. LD001-1000, visualized with a UV light transilluminator, and photographed.

3.3.8 Caspase-3/7, -8 and -9 Activities Assay

Activation of caspases was measured by bioluminescent assay using caspase-Glo 3/7, 8, and 9 assay kits (Promega, Madison, WI, USA), according to the manufacturers protocol. In brief, after seeding HT-29 cells in white-walled 96-well plates overnight, they

were treated with different concentrations of DECPR for 24 h. Then, 100 μ l caspase-Glo reagent was added to each well and incubated at 25 °C for 30 min. The activation of caspases in DECPR treated HT-29 cells caused the cleavage of aminoluciferin-labeled synthetic tetrapeptide, which provides the substrate for the luciferase enzyme. A Tecan Infinite 200 Pro (Tecan, Mannedorf, Switzerland) microplate reader was used to measure the luminescent intensity presenting the caspases activities.

3.3.9 Quantitative PCR Analysis for Bax, Bcl-2 and Bcl-xl

The gene expression of Bax, Bcl-xl and Bcl-2 in treated HT-29 cells were measured by quantitative RT-PCR assay analysis. Briefly, Zymo Research Quick-RNA MiniPrep kit (Zymo Research, Freiburg, Germany) was used to isolate total RNA from HT-29 cells after 24 h treatment with DECPR at IC₅₀ concentration. Next, complementary DNA was synthesized using high capacity RNA-to-cDNA kit (Applied Biosystems, Foster City, CA, USA), according to the vendor's protocol. Quantitative RT-PCR was performed with TaqMan fast advanced master mix and TaqMan gene expression assays using the Applied Biosystems Step One Plus Real-Time PCR (Applied Biosystems, Foster City, CA, USA). The IDs for TaqMan gene expression assays used in this study are Bax: Hs00180269_m1, Bcl-xl: Hs00236329_m1, Bcl-2: Hs00608023_m1 and GAPDH: Hs02758991_g1.

3.3.10 Western Blotting

To confirm the changes of mRNA expression detected from quantitative RT-PCR analysis, western blot assay was performed as described. In brief, after treatment of HT-29 cells (1×10^6 cells/ml) with DECPR at different concentrations for 24 h, cells were washed with PBS and lysed in ice-cold radio immuno precipitation assay buffer (RIPA, Thermo Scientific (Rockford, IL, USA). Protein separation was carried out on 10% resolving polyacrylamide gels (i.e., SDS-PAGE) followed by electroblotting at 25 mA

for 2 h. After transforming the proteins to polyvinylidene fluoride membrane (Pierce, Rockford, IL, USA), the membrane was blocked using a Blocker Casein (Pierce). The blots were incubated overnight with specific primary antibodies; β -actin 1:10000 (Cat: ab6276, Abcam), Bax 1:1000 (Cat: ab7977, Abcam), Bcl-2 (1:1000 Cat: ab18210, Abcam), Bcl-xl (1:1000 Cat: ab32310, Abcam), and then exposed to peroxidase-coupled secondary antibodies for 2 h. Subsequent detection of protein expression was carried out using the Fusion FX7 system (Vilber Lourmat, Eberhardzell, Germany).

3.4 *In Vivo* Experiment

3.4.1 Animals and Ethical Issues

Healthy adult male and female Sprague Dawley rats (six weeks old and 200–220 g weight) were provided from the animal house of the AEU (Animal Experimental Unit, University of Malaya). Rodents were housed in clean polyvinyl cages under the 12/12 h light-dark conditions of 50–60% humidity and a room temperature of 22–24 °C, Food and water ad libitum. All animals received care according to the criteria outlined in the Guide for the Care and Use of Laboratory Animals prepared by the United States National Academy of Sciences and published by the National Institutes of Health. The FOM Institutional Animal Care and Use Committee of University of Malaya approved all protocols involving the experiment (Ethics No. 2014-03-05/PHAR/R/ER).

3.4.2 Acute toxicity study

To determine a safe range of doses for DECPR and HECPR, toxicity evaluation was carried out as described by (Hajrezaie et al., 2012). In brief, 30 female rats, were divided into five groups labeled as the vehicle (5% Tween 20), low dose of DECPR and HECPR (2 g/kg) and high dose of DECPR and HECPR (5g/kg). The rats were fasted for 12 h prior to the dosing (water was accessible except for the last 2 h). Following the dosing, food was withheld for another 1 to 3 h. All signs of toxicities and mortality were

recorded during the period of two weeks. On day 15, the animals were sacrificed for hematological and histological analysis (Figure 3.1) (Hajrezaie et al., 2014).

University of Malaya

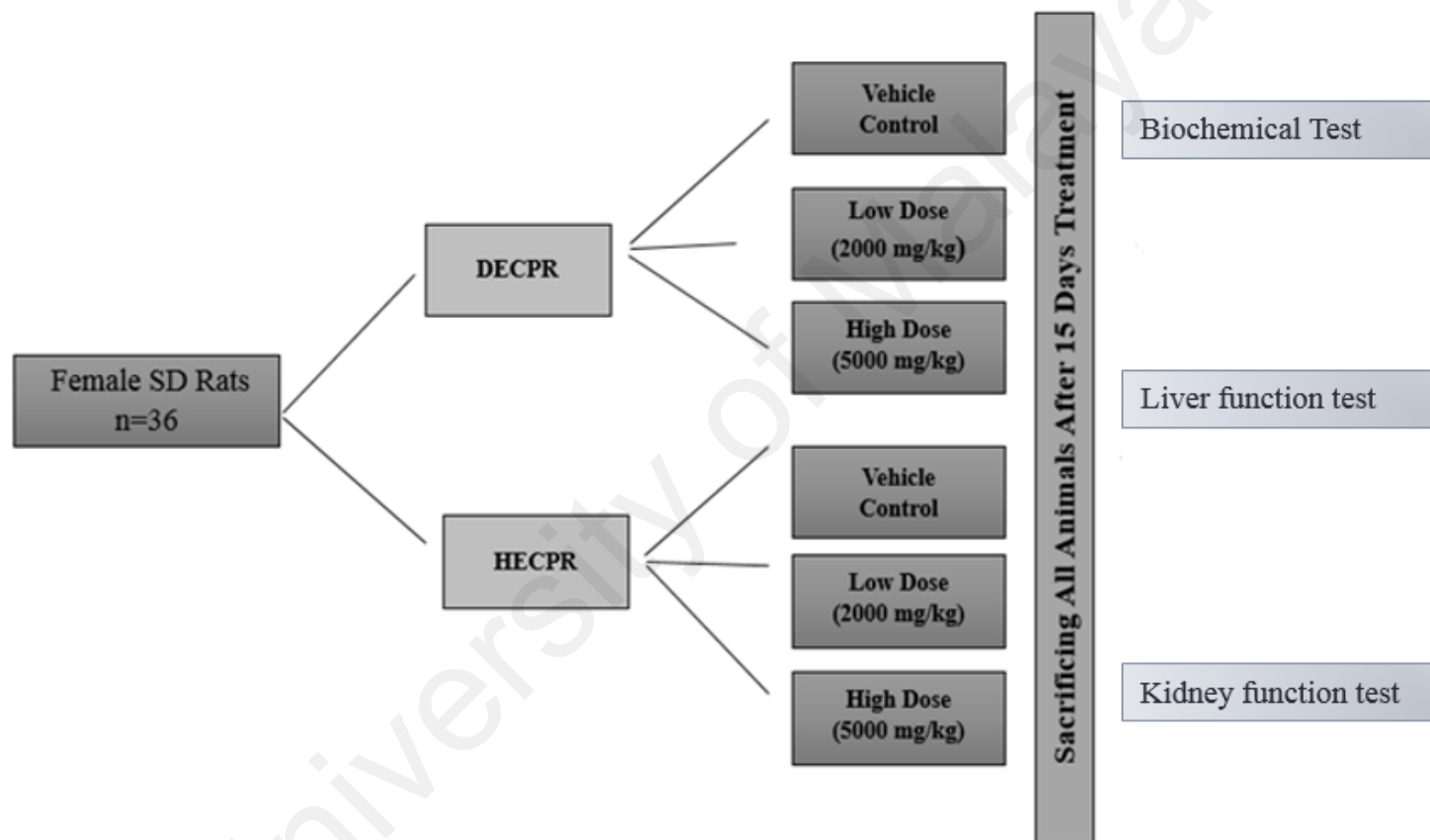


Figure 3.1: flow chart of acute toxicity study.

3.4.3 Colon Cancer

3.4.3.1 Experimental Protocols

The experiment was performed as described by (Shwter et al., 2014). Male rats were randomly divided into five group (n=6), namely, normal control, cancer control, low dose of DECPR, high dose of DECPR and drug control (Figure 3.2). To induce ACF formation, all of the rats, except normal control group, were subcutaneously injected with AOM (15 mg/kg) once a week for two consecutive weeks. Normal control rats were subcutaneously injected with normal saline (5 ml/kg). Then, rats were orally administered with DECPR or Tween-20 (10%) once a day for two months according to the “Treatment” column in Table 3-1, except for the rats in treatment control group. 5-Fluorouracil (5-FU, Sigma) at 35 mg/kg dose intra-peritoneally injection administrated for five consecutive days Table 3.1.

Table 3.1: The experimental design and specifications

Group	Description	Induction	Treatment
A	Normal control	normal saline (5 ml/kg)	10% Tween-20 (5 mg/kg)
B	Cancer control	AOM (15 mg/kg)	10% Tween-20 (5 ml/kg)
C	Low dose	AOM (15 mg/kg)	DECPR (250 mg/kg)
D	High dose	AOM (15 mg/kg)	DECPR (500 mg/kg)
E	Drug control	AOM (15 mg/kg)	5-FU (35 mg/kg)

3.4.3.2 Assessment of ACF

After two months of treatment, all rats were sacrificed with a over dose of ketamine and xylazine. The extracted colon of rats were opened longitudinally and rinsed with phosphate-buffered saline (PBS) prior to fixation between two filter papers in 10% buffered formalin for 24 h. Then, proximal and distal segments of samples with equal

length were stained with methylene blue (0.2%, Sigma) and enumeration of ACF was performed under a light microscope (Olympus, Tokyo, Japan)(Bird, 1987).

3.4.3.3 Immunohistochemistry

Immunohistochemical analyses of tissue sections were performed as described in details by (Bardi et al., 2014). In brief, after deparaffinizing and rehydrating tissue sections, sodium citrate buffer (10 mM) was employed to perform antigen retrieval for 10 min. Samples were then cooled in tris buffered saline (TBS) prior to use the commercial Dako ARK Peroxidase kit (DAKO, Carpinteria, CA, USA). Endogenous peroxidase was blocked using peroxidase blocking solution for 5 min followed by rinsing the samples. The slides were incubated with biotinylated primary antibodies against Bax (1:100), Bcl-2 (1:100) and PCNA (1:200) for 15 min and then supplemented with streptavidin-HRP for 30 min. Development of slides and counterstaining were performed using diaminobenzidine (DAB) substrate chromogen and hematoxylin. For PCNA expression as a tumor marker, the proliferation index (PI) was determined using the formula below.

3.4.3.4 Activity of Antioxidant Enzymes

To prepare the colon tissue homogenate, samples were washed and homogenized in ice-cold PBS (10%) using a Teflon homogenizer (Polytron, Heidolph, Germany). Then, samples were centrifuged at 4500 rpm for 15 min at 4 °C to dispose cell debris. The supernatant was then employed to examine antioxidant activities using assay kits for catalase (CAT), glutathione peroxidase (GPx) and superoxide dismutase (SOD) (Cayman Chemical, Ann Arbor, MI, USA), according to the manufacturer's instructions.

3.4.3.5 Malondialdehyde

To determine the level of oxidative stress in colon tissue homogenates, a commercial kit for thiobarbituric acid reactive substance (TBARS; Cayman Chemical Company) was used according to the vendor's instructions (Fraga et al., 1988).

3.4.3.6 Western blotting

Western blot analysis was performed as described in detail by (Hajrezaie et al., 2014). In brief, the colon tissues collected from rats were subjected to protein extraction using protein extraction buffer (Pierce Biotechnology Inc., Rockford, Illinois, USA). After quantifying the extracted protein using the Bradford method, samples (30 μ g) were run in a 10% SDS-PAGE gel followed by transformation to PVDF membranes (Pierce Biotechnology Inc.). Then, membranes were blocked using the blocker casein (Pierce Biotechnology Inc.) and samples were incubated overnight with specific primary antibodies: PCNA, Bax, Bcl-2 and β -actin which were procured from Abcam Inc. (Cambridge, MA, USA). After washing the samples with 0.1% TBST for 5 min, they were probed with the appropriate peroxidase-coupled secondary antibodies for 2 h. Bands were visualized using the Fusion FX7 system (Vilber Lourmat, Eberhardzell, Germany).

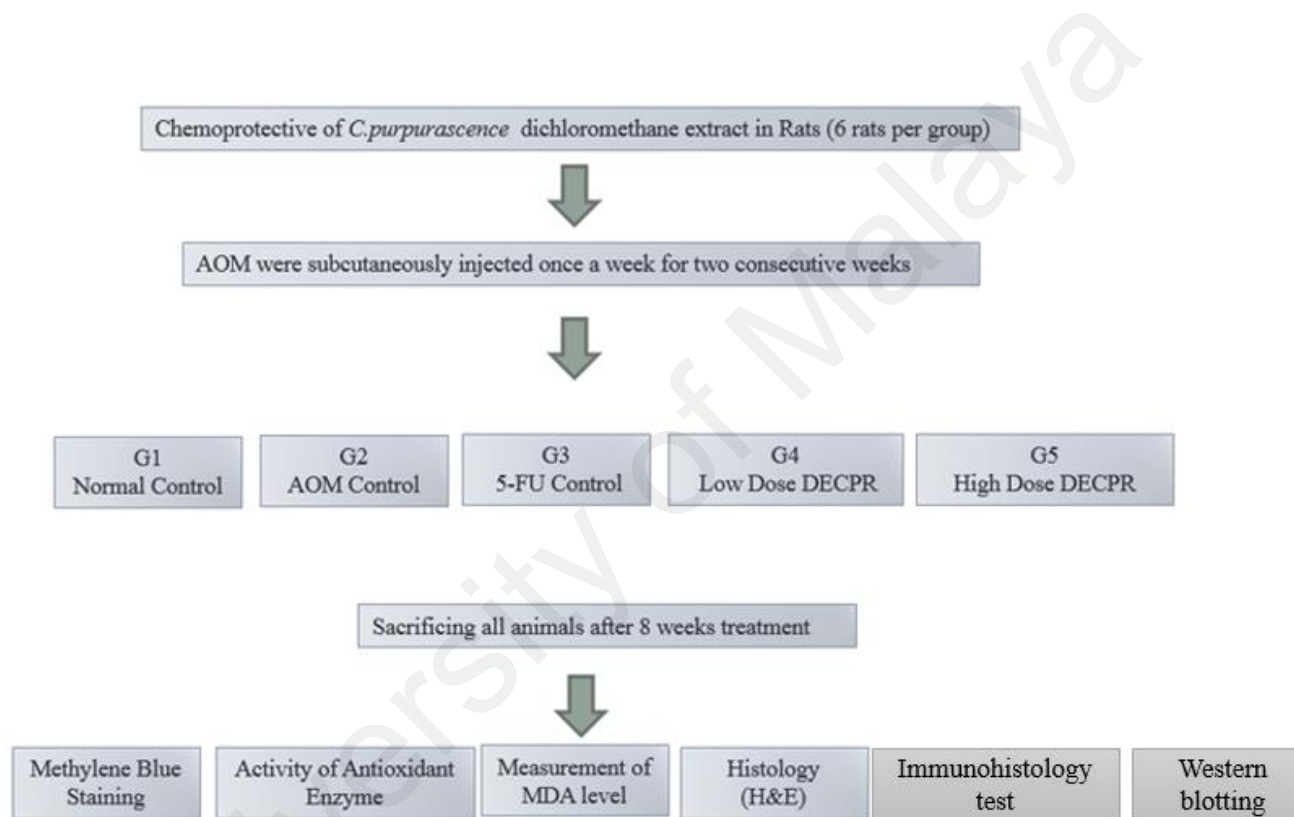


Figure 3.2: Study flow chart for the chemoprevention ability of the extract of *C. purpurascens*.

3.4.4 Gastroprotective Ability of the *C. purpurascens* Extract

3.4.4.1 Animals and Ethical Issues

Healthy Sprague Dawley female rats weighing between (200 g to 250 g) were used. Rats were obtained from the animal house, Faculty of Medicine, Kuala Lumpur. The animals were randomly divided into five groups (six rats/ group). The experimental protocol was approved by the Animal Ethics Committee (Ethics No. 2014-03-05/PHAR/R/ER). All rats were housed individually and maintained under standard conditions of humidity (50-60%), temperature ($22 \pm 3^{\circ}\text{C}$) and light (12h light: dark cycle) and fed chow diet and water ad libitum. Each rat was caged alone and fasted before treatment (food, but water was with-drawn overnight). Throughout the experiments, all criteria of taking care of animals were in line with the guidelines provided by the National Academy of Sciences and defined in the “Guide for the care and use of laboratory animals” (Rouhollahi, et al., 2014).

3.4.4.2 Experimental Design

The preventive potential of HECPR against superficial hemorrhagic mucosal lesions were investigated in the normal rats. Prior to the experiment, *Sprague Dawley* female rats were fasted for 24 h (water was accessible except for the last 2 h). Thirty rats were divided randomly into 5 groups of 6 rats each and pre-treated according to table 3.2. After 1 h of pre-treatment, all the rats were gavaged with 5% Tween 20 (5 ml/kg) or absolute ethanol (5 ml/kg) based on the animal experimental design. The rats were sacrificed 1 h later with an over-dose of xylazine and ketamine and their stomachs were immediately excised (Rouhollahi, et al., 2014).

Table 3.2: The gastroprotective ability of the *C. purpurascens* extract study

Groups	Name of group	Orally administration	Time	Orally administration
Group A	Vehicle control	5% Tween 20 (5 ml/kg)	After one hour	5 ml/kg 5% Tween 20
Group B	Ulcer control	5% Tween 20 (5 ml/kg)	After one hour	5 ml/kg absolute ethanol
Group C	Reference drug	20 mg/kg Omeprazole (5ml/kg)	After one hour	5 ml/kg absolute ethanol
Group D	pretreated group 200 mg/kg	200 mg/kg DECPR (5ml/kg)	After one hour	5 ml/kg absolute ethanol
Group E	pretreated group 400 mg/kg	400 mg/kg DECPR (5ml/kg)	After one hour	5 ml/kg absolute ethanol

3.4.4.3 Determination of the Mucosal Content and Gastric Juice Acidity

The stomach of each rat was dissected along the greater curvature, and pH-meter titration with 0.1 N NaOH was used to analyze the hydrogen ion concentration in the gastric contents were expressed in mEq/l value. Then, a glass slide was applied to gently scrape the gastric mucosa of the rats followed by the weighing of the obtained mucus with a precision electronic balance.

3.4.4.4 Macroscopic Analysis of Lesions

In accordance with several studies, ethanol-induced ulcers on the gastric mucosa were characterized as elongated bands of hemorrhagic lesions parallel to the long axis of the stomach (Kumar et al., 2013). The hemorrhagic damage of the stomach was determined by assessment of luminal surface. The protective potential (P%) of each pre-treatment was calculated using a planimeter ($10 \times 10 \text{ mm}^2$) and dissecting microscope (1.8 \times) where UC and UT were the ulcer area of the control and treated group, respectively. The measurement of ulcer area was performed as described in detail by (Abdelwahab et al., 2011).

3.4.4.5 Determination of Lipid Peroxidation Activity

To measure malondialdehyde (MDA) concentration, we carried out thiobarbituric acid reactive substance (TBARS) assay as described previously (Draper et al., 1993). In brief, the homogenated stomach (10% w/v) in 0.1 mol/l PBS was centrifuged at 4°C for 10 min. Then, the supernatant (3 ml) was mixed with 20% trichloroacetic acid solution and 0.67% 2-thiobarbituric acid followed by heating in a water-bath (95°C) for 30 min. Next, the MDA concentration of the obtained supernatant was determined spectrophotometrically at 532 nm. The protein concentrations were expressed as MDA $\mu\text{mol/g}$ protein using the Lowry method (Hartree, 1972).

3.4.4.6 Determination of Superoxide Dismutase (SOD) Activity

The activity of SOD enzyme was estimated by determining its potential to suppress the photochemical reaction of NBT (nitroblue tetrazolium), as previously described by Sun and colleagues (Sun et al., 1988). In this assay, the homogenated tissues were centrifuged twice at 4°C for 10 and 20 min. In a dark chamber, the reactant (1 ml, 50 mM phosphate buffer, 100 nM EDTA and 13 mM l-methionine, pH 7.8) was mixed with the resulting supernatant (30 µl), NBT (150 µl, 75 µM) and riboflavin (300 µl, 2 µM). The resulting solution was exposed to fluorescent light bulbs (15 W) for 15 min and the absorbance was determined at 560 nm wavelength using a spectrophotometer.

3.4.4.7 Nitric Oxide Level

To evaluate the effect of HECPR on nitric oxide (NO) generation in the gastrointestinal tract, Griess reaction was used to determine total nitrite/nitrate levels, as described by Tsikas and colleagues (Tsikas et al., 1997). In brief, the supernatant (50 µl) of the homogenated stomach was mixed with the Griess reagent. After 10 min, the subsequent colorimetric analysis was carried out at 540 nm using a Tecan Infinite 200 Pro microplate reader (Tecan, Männedorf, Switzerland). The generated NO in the culture supernatant was determined using a standard curve of sodium nitrite and results were expressed as µmoles nitrite/nitrate per gram of protein.

3.4.4.8 Histological Evaluation of Gastric Lesions

Histological analysis of the specimens of the gastric walls was carried out using 10% buffered formalin for the fixation. The samples were embedded in paraffin followed by 5 µm sectioning and staining with hematoxylin and eosin.

3.4.4.9 Immunohistochemical Evaluation

Immunohistochemical analysis of Bax and HSP70 proteins was carried out as previously described with some modifications (Hajrezaie et al., 2014). In brief, tissues were paraffinized in xylene and rehydrated using graded alcohol. The boiling sodium citrate buffer (10 mM) was used for antigen retrieval process followed by immunohistochemical staining according to the manufacture's instruction (Dakocytomation, USA). After blocking the endogenous peroxidase with peroxidase block, Bax (1:200) or Hsp70 (1:500) biotinylated primary antibodies were applied and the sections were incubated for 15 min. Next, sections were incubated with the appropriate amount of streptavidin–HRP for 15 min. The sections were then exposed to diaminobenzidine substratechromagen for 5 s, then dipped in weak ammonia (0.037 mol/L) for ten times. Brown stains on the slides indicated positive findings of the immunohistochemical staining as observed under a light microscope.

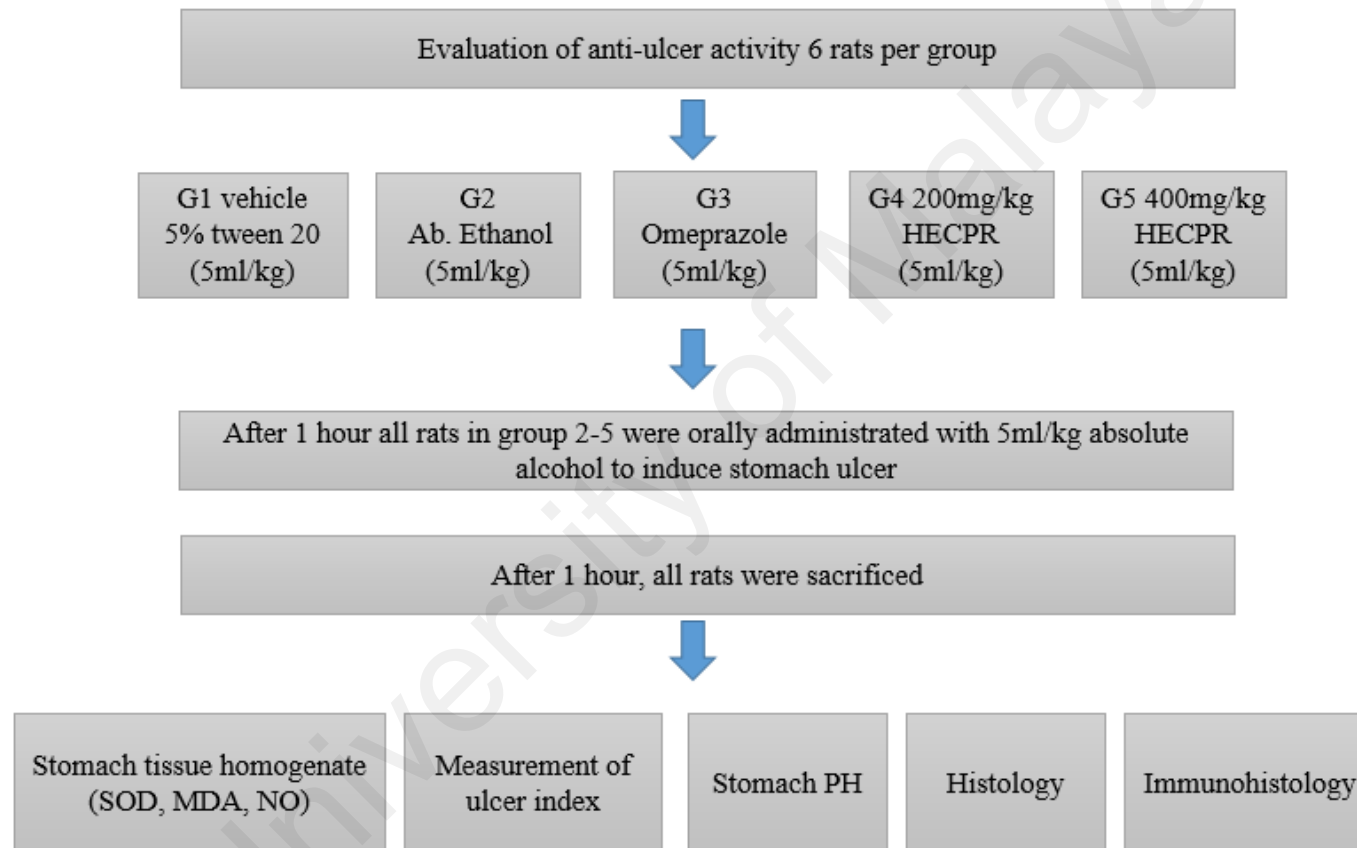


Figure 3.3: The gastroprotective ability of the *C. purpurascens* extract study flow chart

3.4.5 Wound Healing Ability of *C. Purpurascens* Extract

3.4.5.1 Excision wound model

The excision wound model was used to study the wound healing effect of HECPR in rats. The rats were generally anesthetized using intra-muscular injection of ketamine and xylazine prior to the wound creation. The necks of the rats were thoroughly shaved with sterile razor blade and disinfected with alcohol (70%). After marking an oval wound on the shaved necks of the rats, a full thickness of the excision wound (approx. 2.00 cm) with 2 mm depth was created without any damage to the muscle layer using a sterile surgical blade and disinfected scissors (Fig 3.4). The neck area was chosen for this experiment to preclude the rats from biting and stretching the wound area.

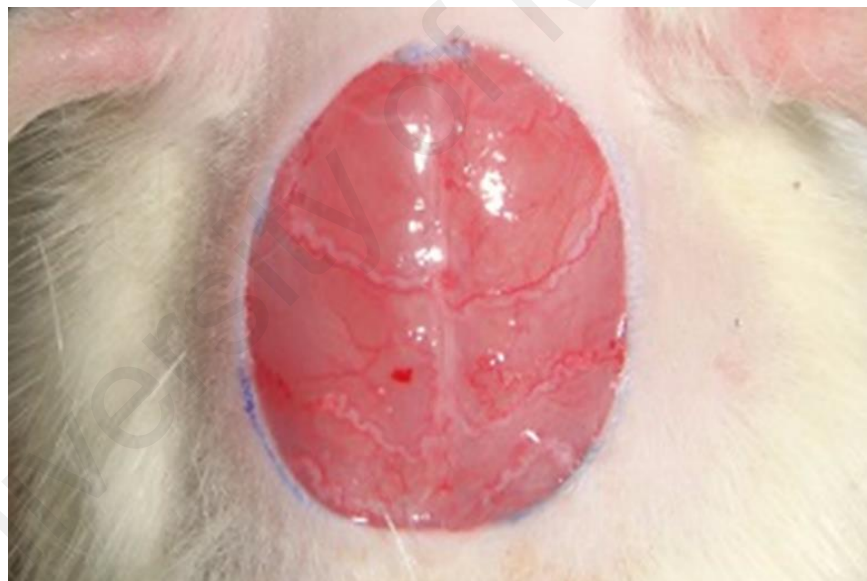


Figure 3.4: The excision wound model on day 0, before starting treatments

3.4.5.2 Grouping, Ointment Administration and Wound Closure Percentage

Four groups ($n = 6/\text{group}$) of rats were used for the experiment. Group A: wounds were treated with vehicle (negative control), group B: wounds were treated with HECPR (100 mg/kg, low dose), group C: wounds were treated with HECPR (200 mg/kg, high dose) and group D: wounds were treated with intrasite gel (1 g/kg). Starting from the day of wounding (day 0), treatment samples (0.2 ml) were topically dressed over the entire wound twice daily for 20 days. Wound contraction (mm^2) was measured by tracing margins of the wound using transparent graph papers on days 5, 10, 15 and 20. The evaluated surface area was then employed to determine the wound healing percentage of each rat through calculation of the wound reduction from the initial size (Tamri et al., 2014).

3.4.5.3 Histological Evaluation

On 20th day after surgery, the cross-sectional full-thickness specimens of skins were excised from healed wounds and surrounding tissues. Samples were fixed and processed using a paraffin tissue-processing machine (Leica, Germany), and then 5 μm sections were stained with Hematoxylin & Eosin (H & E) and Masson Trichrome stainings to examine the histopathological alterations.

3.4.5.4 Immunohistochemistry Analysis

The Bax and Hsp70 protein expressions were evaluated in each formalin-fixed paraffin-embedded wounded tissue section, as previously described in detail (Hajrezaie et al., 2014). Immunostaining was performed using the EGFR pharmDx kit (DakoCytomation; Carpinteria, CA, USA), according to the manufacturer's protocol. In brief, endogenous peroxidase activity was quenched using a peroxidase block. Tissue sections were then incubated with Bax (1:200, Cat: ab7977, Abcam, Cambridge, MA,

USA) and Hsp70 (1:500, Cat: ab2787, Abcam) biotinylated primary antibody for 15 min followed by another 15 min incubation with streptavidin–horseradish peroxidase. The sections were incubated with diaminobenzidine tetrahydrochloride for 5 min, and then counterstained with hematoxylin and 0.5% ammonia in water. The brown illustrations of samples under a light microscope demonstrated positive findings.

3.4.5.5 Enzymatic Activities

On day 20th after surgery, the granulation tissues (200 mg) were homogenized in Tris-buffer. The tissue homogenates were centrifuged at 6000 RPM for 20 min at 4°C and the supernatant was employed for the further assessment of the enzymatic activities. The commercial kits (Cayman, Ann Arbor, MI, USA) were applied to measure the activity of catalase (CAT) (Item NO. 707002, Cayman, USA), glutathione peroxidase (GPx) (Item NO.703102, Cayman, USA) and superoxide dismutase (SOD) (Item NO. 706002, Cayman, USA) in tissue homogenates, according to the vendor's protocol.

3.4.5.6 Lipid Peroxidation

Lipid peroxidation in wound tissue homogenates was determined by measuring malondialdehyde (MDA) content (Item NO. 10009055, Cayman, USA), a direct product formed as a result of peroxidation of lipids, using Wills method as previously described (Wills, 1966). MDA level was assayed in the form of thiobarbituric acid reactive substances and represented as nmol of MDA formed/mg protein. 1.1 Gas

Chromatography of *C. Purpurascens* Hexane and Dichloromethane Extracts

The gas chromatography analysis of *C. purpurascens* hexane and dichloromethane extracts were performed using an Agilent and LECO. RESTEK, Rxi-5MS capillary column (30 m, 0.25 mm i.d., 0.25 µm film thickness) and a mass spectrometer Pegasus HT High Throughput Time-of-flight mass spectrometry (TOFMS). The carrier gas was helium at a flow rate of 1 ml/min. Column temperature was initially 40 °C for 5 min, then

gradually increased to 160 °C at 4 °C/min, and finally increased to 280 °C at 5 °C/min and held for 10 min. For GC-MS detection an electron ionization system was used with ionization energy of 70 eV. The fraction was diluted 1:100 (v/v) with ethyl acetate and 1.0 µl of the diluted sample was injected automatically in split less mode. Injector temperature was set at 250 °C. Samples were identified from their mass spectra, by comparison of the retention times of peaks with interpretation of MS fragmentation patterns from the National Institute of Standards and Technology (NIST147) Mass Spectral Database(Karimian et al., 2014).

3.4.5.7 Statistical Analysis

Results were analyzed by one-way analysis of variance, followed by Tukey's post-hoc test and expressed as mean ± standard error of 6 animals per group. Statistical analyses were performed using the SAS 9.1 statistical program (SAS Institute Inc., Cary, NC, USA). All comparisons were considered significant at $P < 0.05$.

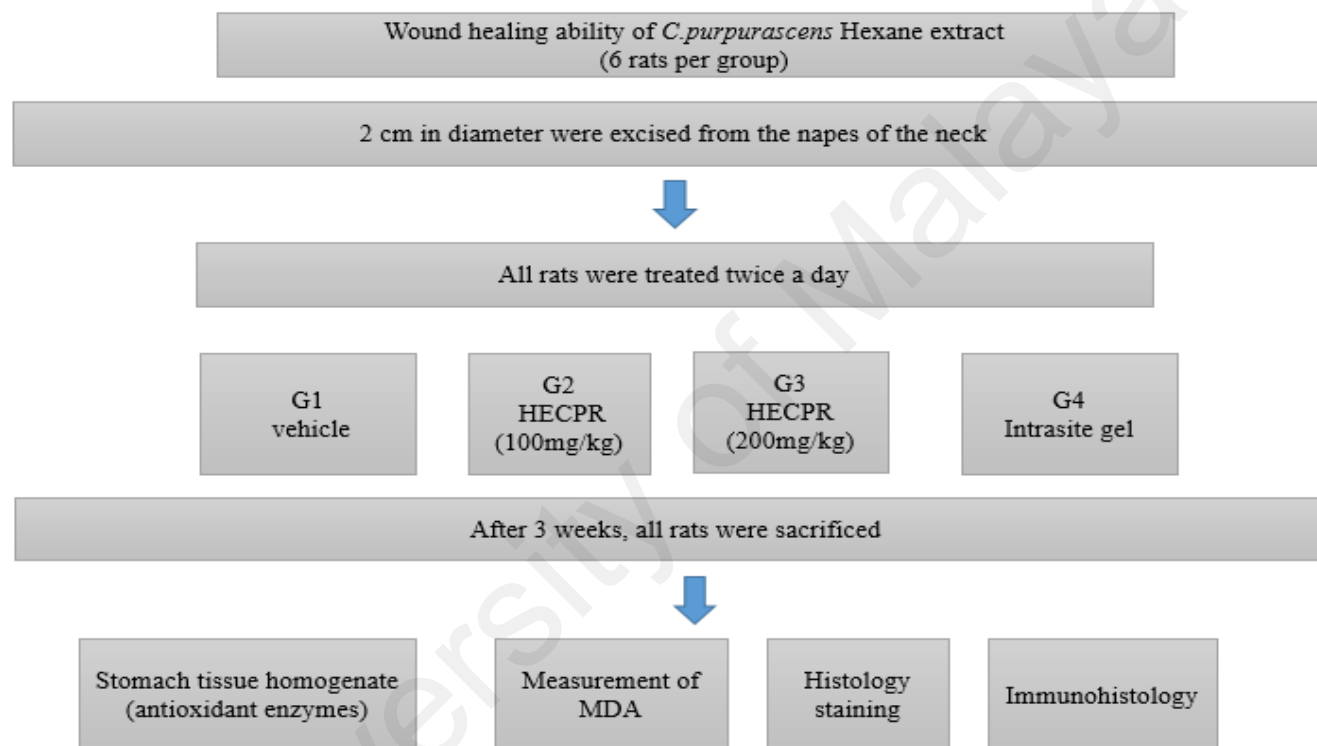


Figure 3.5: Study flow chart for the wound healing ability of the *C. purpurascens* extract

CHAPTER 1: RESULTS

4.1 Antioxidant Properties of DECPR and HECPR

4.1.1 DPPH Scavenging Activity of DECPR and HECPR

The percentage of DPPH inhibition of DECPR and HECPR extracts is illustrated in (Figure 4.1). Results showed that DECPR IC_{50} ($13.52 \pm 0.42 \mu\text{g/ml}$) which was higher than that of HECPR IC_{50} ($9.81 \pm 0.31 \mu\text{g/ml}$) and the standards ascorbic acid and trolox (4.67 ± 0.32 and $8.86 \pm 0.21 \mu\text{g/ml}$ respectively). Results indicate that the ability of DECPR to scavenge DPPH is lower than that of HECPR which has better scavenging activity that approaches the capacity of the standard trolox.

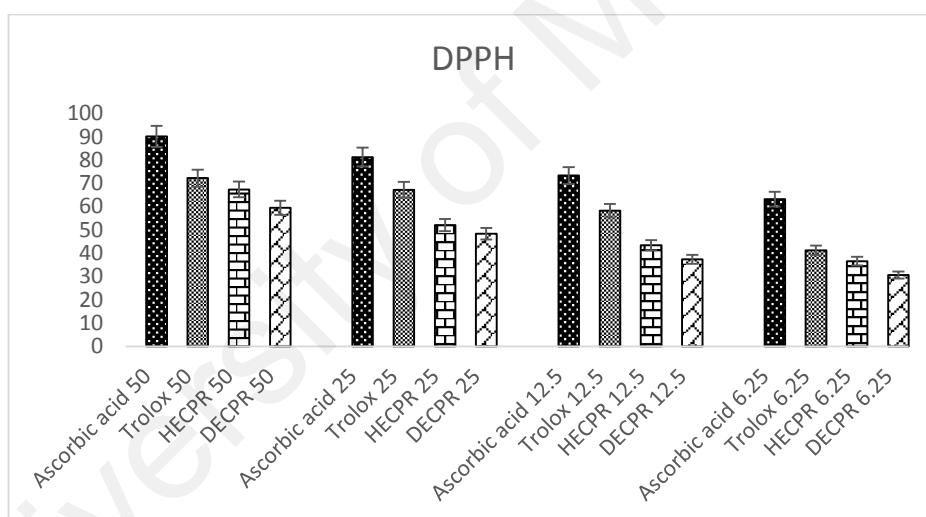


Figure 4.1: DPPH free radical scavenging activities of HECPR and DECPR compared with the standards, Ascorbic acid, and Trolox

4.1.2 FRAP Capacity of DECPR and HECPR

As illustrated in (Figure 4.2), the ferric reducing antioxidant power (FRAP) of HECPR was significantly higher ($p < 0.05$) ($2341.32 \pm 45.40 \text{ mmol/FeII/mg}$) than DECPR which measured $1501.38 \pm 25.12 \text{ mmol/FeII/mg}$.

The measured value from both extracts were significantly lower than ferric reducing power of the standards; gallic acid, quercetin, ascorbic acid, rutin, and butylated hydroxytoluene or BHT (24149.44 ± 45.40 , 19212.11 ± 35.31 , 10312.17 ± 29.81 , 5138.15 ± 15.40 , 3150.31 ± 11.40 mmol/FeII/mg, respectively) based on these readings, it is reasonable to extrapolate that HECPR has high antioxidant activity and DECPR must be containing sufficient acceptable level of anti-oxidant activity.

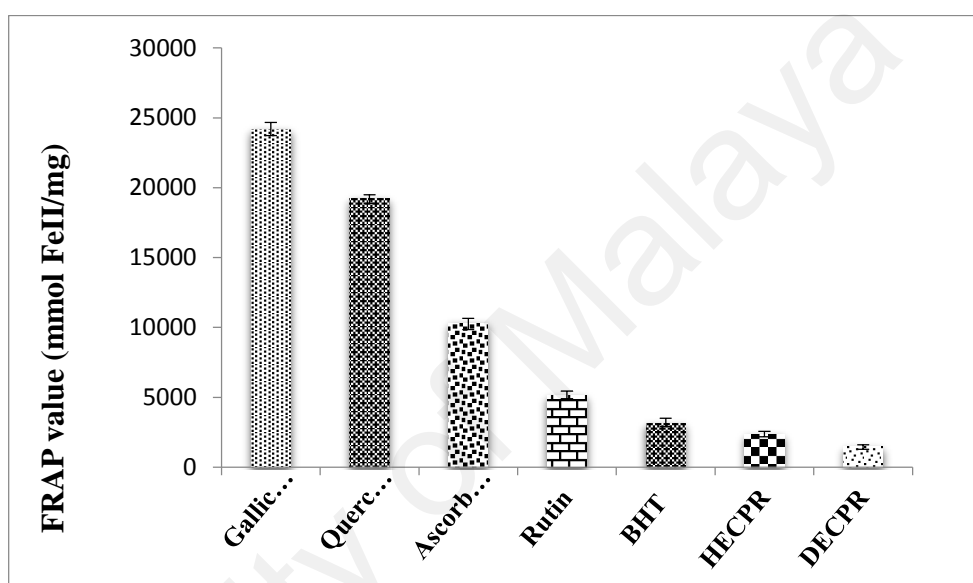


Figure 4.2: Ferric reducing power (FRAP) of the DECPR and HECPR

Ferric reducing power (FRAP) of the DECPR and HECPR as compared with the standards; gallic acid, quercetin, ascorbic acid, rutin, Trolox, BHT. Values were expressed as Mean ± SEM.

4.1.3 Total Phenolic Content of DECPR and HECPR

Figure 4.3 shows the total phenolic content (TPC) of 1 mg of DECPR and HECPR. Results showed that TPC of DECPR and HECPR were (450.32 ± 6.76 , 461.15 ± 7.32 mg GAE/mg extract respectively), moreover, there was no significant difference between the TPC value of DECPR and HECPR. These results showed that both plant extracts have high phenolic content.

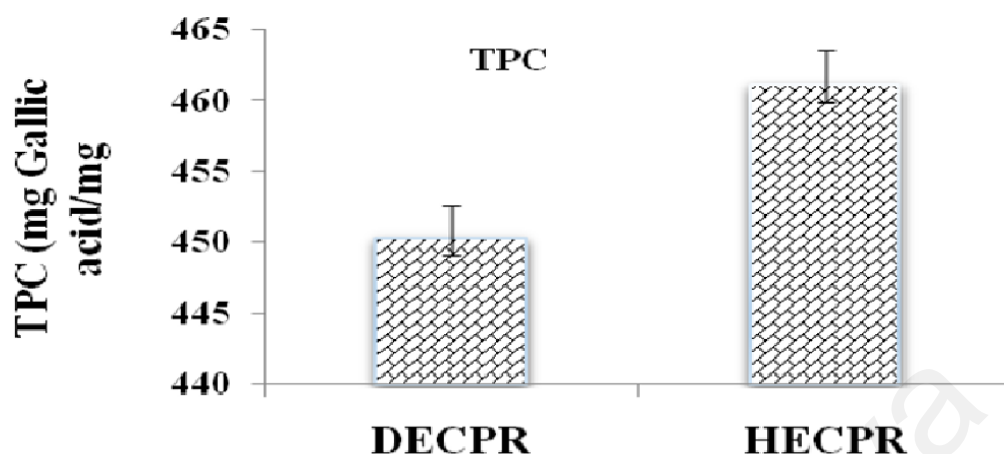


Figure 4.3: Total phenol content (TPC) of DECPR and HECPR

4.2 In vitro results

4.2.1 MTT Cell Viability Assay

To determine the effects of hexane and dichloromethane extracts of *C. purpurascens* rhizome on human cancer cells, the viability of eight different cancer cell lines after 24h treatment with the extract were examined using MTT assay. As shown in Table 4.1, hexane and dichloromethane extracts showed the extensive range of cytotoxic effects towards cancer cells (IC_{50} ranged from 5.43 ± 0.38 to 52.23 ± 1.31 $\mu\text{g/ml}$). The results showed that DECPR induced higher cytotoxic effects on cancer cells when compared with the hexane extract. Furthermore, DECPR elicited the strongest anti-proliferative effect on HT-29 colon cancer cells with the IC_{50} value of 5.43 ± 0.38 $\mu\text{g/ml}$. The relatively higher IC_{50} value of DECPR on WRL-68 and CCD841 compared to the cancer cells suggested the safety of this plant on normal human cells and its selective cytotoxic effects.

Table 4.1: Anti- proliferative activity of *Curcuma purpurascens* BI. on some normal and cancer cells

Extract	IC ₅₀ (µg/mL)					
	HT-29	HepG2	PC-3	MDA-MB-231	CCD841	WRL-68
Hexane µg/ml	11.83 ± 1.21	12.85 ± 1.18	13.43 ± 1.20	20.34 ± 1.02	49.77 ± 1.82	55.42 ± 1.79
Dichloromethane µg/ml	5.43 ± 0.38	7.36 ± 0.82	8.59 ± 0.93	12.39 ± 1.12	45.69 ± 1.77	52.23 ± 1.31

The data represent the means ± SEM of three independent experiments. **P* < 0.05 compared with the untreated group

4.2.2 Cytotoxic Effects of DECPR and HECPR by LDH Release Assay

Any kind of cell demise, including apoptosis and necrosis is associated with LDH release caused by irreversible cell membrane damage. Hence, measurement of the LDH leakage from cells into the medium is an easy marker to determine cytotoxic activity. In order to confirm the anti-proliferative effect of DECPR observed in MTT assay, we measured the level of released LDH from HT-29 cells after 24 h of treatment. As depicted in Figure 4.4, DECPR caused a significant and dose-dependent elevation in LDH release at 6.25 to 50 $\mu\text{g/ml}$ concentrations, compared to the control. The results of MTT and LDH assays together confirmed the noticeable antiproliferative effect of DECPR towards HT-29 cells.

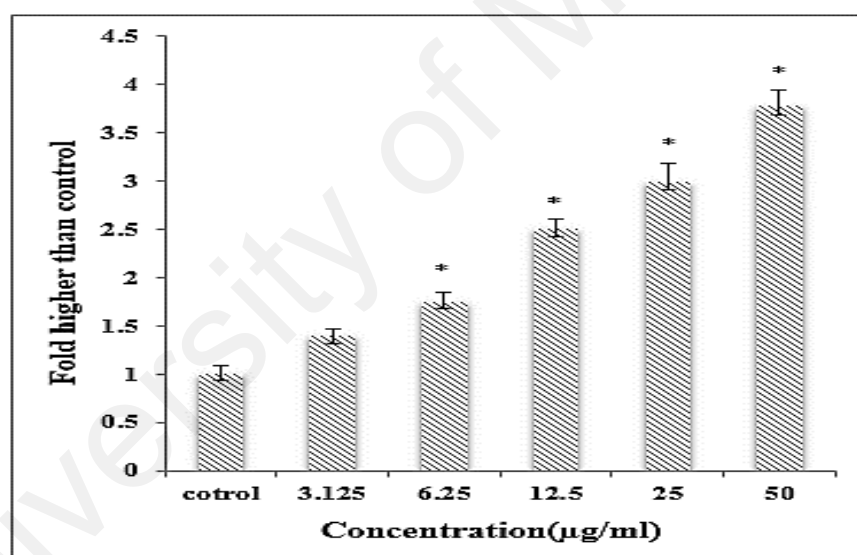


Figure 4.4: Lactate dehydrogenase (LDH) assay of DECPR on HT-29 cells

LDH assay elicited the cytotoxicity of DECPR towards HT-29 cells. The result showed significant LDH release at concentrations of 6.25 to 50 $\mu\text{g/ml}$, in a dose-dependent manner. The data represent the means \pm SEM of three independent experiments. * $P < 0.05$ compared with the untreated group.

4.2.3 Induction of Cytoskeletal Rearrangement and Nuclear Fragmentation by DECPR

Since DECPR showed a significant cytotoxic potential towards HT-29 cells, further mechanistic studies were carried out with this extract. To investigate the cytoskeletal and nuclear changes in HT-29 cells after DECPR treatment, Hoechst 33342 and phalloidin dyes were used to detect perturbation in nucleus and F-actin, respectively. As illustrated in (Figure 4.5A), HT-29 treated cells elicited clear sign of DNA shrinkage and fragmentation after 24 h of treatment. In addition, F-actin perturbations at the peripheral membrane of HT-29 cells revealed the cytoskeletal rearrangements induced by DECPR, which was significant at 12.5 to 50 $\mu\text{g/ml}$ concentrations (Figure 4-5B). These morphological changes suggest the induction of apoptosis by DECPR.

University of Malaya

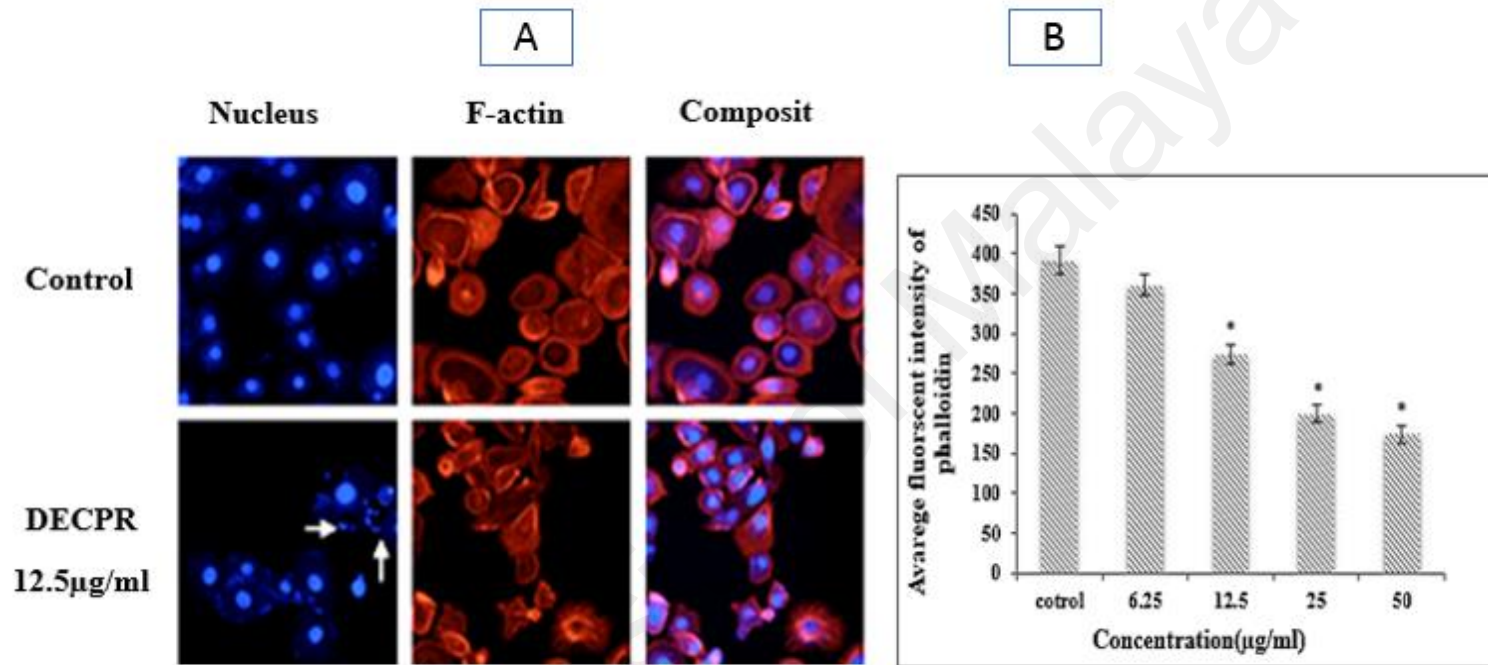


Figure 4.5: Induction of Cytoskeletal Rearrangement and Nuclear Fragmentation by DECPR

HT-29 cells were treated with different concentrations of DECPR for 24 h and stained with Hoechst 33342 (blue) for nucleus and phalloidin (red) for polymerized actin (F-actin). White arrows depict DNA fragmentation and shrinkage. Representative bar chart showed the significant reduction in fluorescent intensity of phalloidin at 12.5 to 50 µg/ml concentrations showing the cytoskeletal rearrangement induced by DECPR. The data represent the means \pm SEM of three independent experiments. *P < 0.05 compared with the untreated group.

4.2.4 Reactive Oxygen Species (ROS) Generation

The level of ROS in HT-29 cells after DECPR treatment was examined using the oxidative-sensitive dihydroethidium probe which converts to fluorescent ethidium and intercalates into DNA as a result of ROS generation. When HT-29 cells were treated with DECPR for 24 h, ethidium derived fluorescence dose-dependently increased showing the capacity of DECPR to cause intracellular oxidation (Figure 4-6A). Quantification of the fluorescence intensity with HCS system demonstrated significant ROS production at 6.25 to 50 $\mu\text{g/ml}$ concentrations (Figure 4.6B). The level of ROS was elevated to more than 2-fold at 12.5 $\mu\text{g/ml}$ concentration compared to the control. This result showed that DECPR promotes oxidative stress in HT-29 cells upon treatment.

University of Malaya

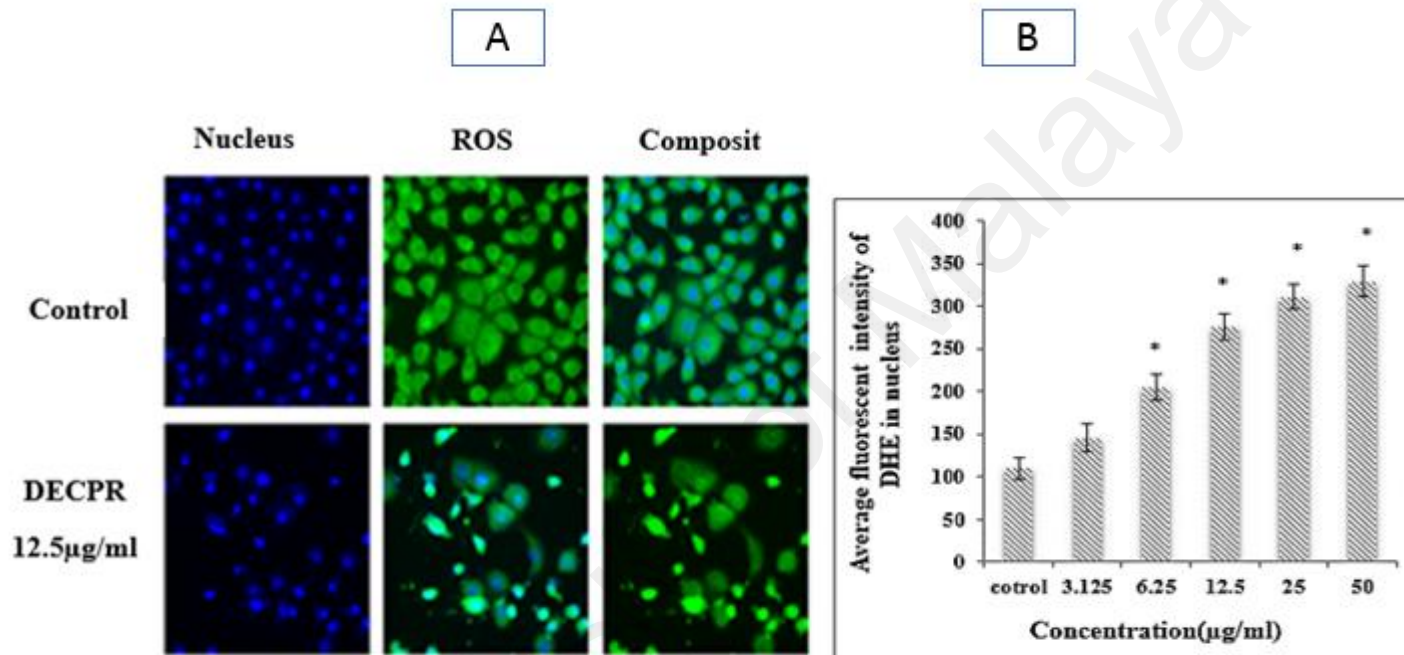


Figure 4.6: ROS generation in the presence of DECPR

HT-29 cells were treated with vehicle DMSO or DECPR at 12.5 µg/ml concentration, stained with Hoechst 33342 dye (blue) for nucleus and dihydroethidium for ROS detection. Representative bar chart showed significant ROS generation at 6.25 to 50 µg/ml concentrations after 24 h treatment with DECPR. The data represent the means \pm SEM of three independent experiments. * $P < 0.05$ compared with the untreated group.

4.2.5 Effect of DECPR on Nuclear Morphology, Membrane Permeability, Mitochondrial Membrane Potential (MMP) and Cytochrome C Release

To determine the possible mechanism of action in which DECPR suppressed the proliferation of HT-29 cells, we investigated the changes in the critical apoptosis-related factors, namely nuclear morphology cell membrane permeability, MMP and cytochrome C. As depicted in (Figure 4.7), cell membrane permeability in control cells was marked with green fluorescent dye, which was conspicuously elevated in DECPR-treated cells. Meanwhile, the red fluorescent intensity of control cells was noticeably attenuated after DECPR treatment showing in MMP (Figure 4.7). In addition, cyan fluorescent intensity in control cells presenting the cytochrome C leakage from mitochondria to cytosol was markedly lightened upon treatment with DECPR (Figure 4.7). The quantitative analysis of the fluorescent (Figure 4.8) intensity of three markers showed a dose-dependent and significant increase in cell membrane permeability and cytochrome C leakage at 6.25 to 50 $\mu\text{g/ml}$ concentrations. The MMP of treated HT-29 cells was also significantly reduced at these concentrations.

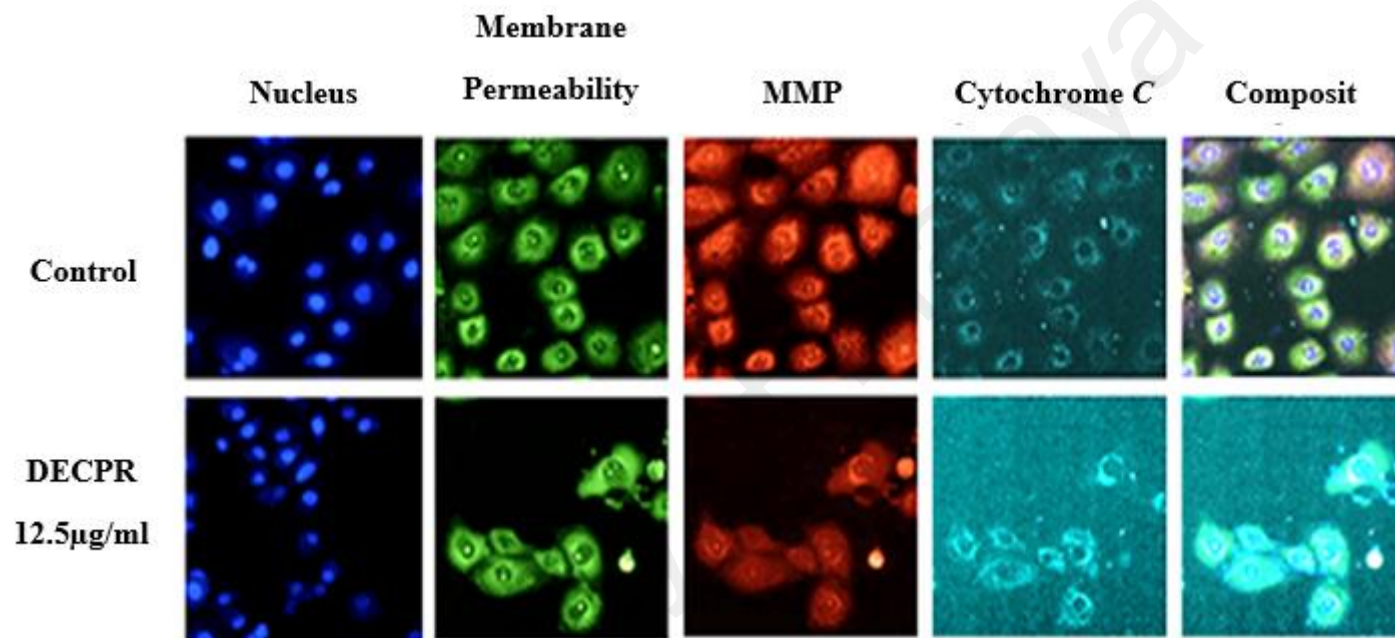


Figure 4.7: Effect of DECPR on nuclear morphology

Effect of DECPR on nuclear morphology, membrane permeability and mitochondrial membrane potential (MMP) and Cytochrome C release, HT-29 cells were treated with DECPR at different concentrations for 24 h. After fixing the cells, they were stained with Hoechst 33342, membrane permeability, MMP and cytochrome C dyes following with HCS analysis of the stained cells.

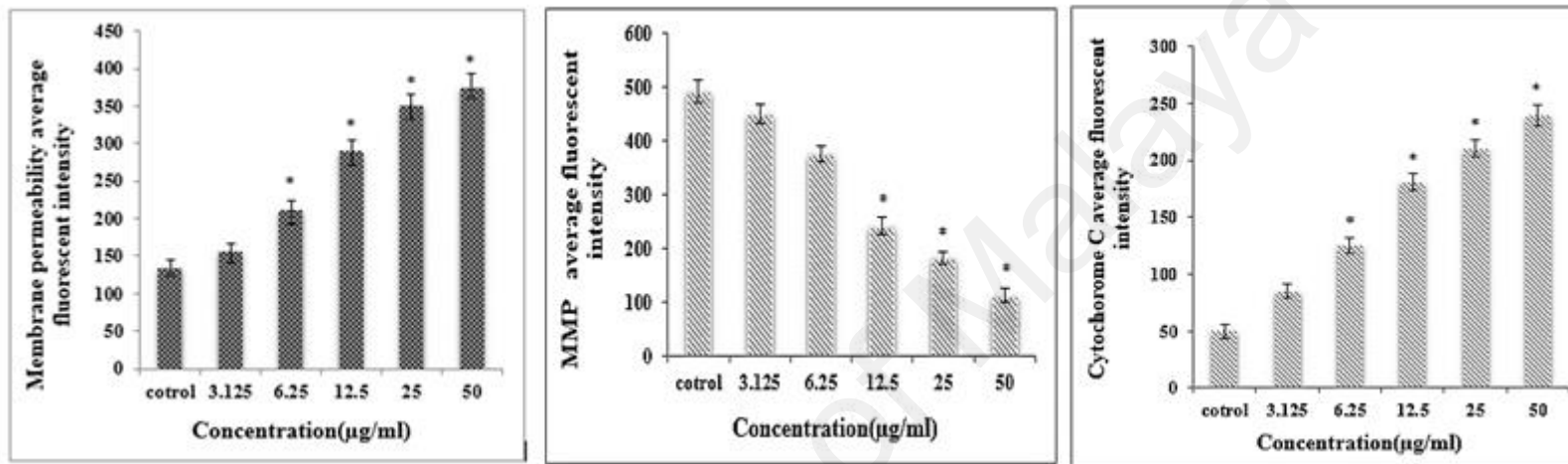


Figure 4.8: Effect of DECPR on membrane permeability mitochondrial membrane potential (MMP) and Cytochrome C release

Representative analysis of the figures showed that DECPR at 6.25 to 50 µg/ml concentrations significantly elevated the cell membrane permeability and cytochrome C release. Meanwhile, at 12.5 to 50 µg/ml concentrations, there was a significant collapse in MMP.

4.2.6 Induction of Caspases Activation by DECPR

Since morphological and biochemical characterizations of apoptosis were observed in DECPR-treated HT-29 cells, we measured the activity of different caspases as key mediators of apoptosis using an aminoluciferin-labeled caspase substrate. Between initiator caspase-8 and -9, DECPR only induced the activity of caspase-9 with dose-dependent and significant elevation at 6.25 to 50 $\mu\text{g/ml}$ concentrations. Meanwhile, the activity of initiator caspase-8 elicited no significant perturbation. In addition, the activation of executioner caspase-3/7 was significantly increased at the same concentrations (Figure 4.9). The results of caspases activity associated with MMP changes and cytochrome *C* release strongly suggest the induction of mitochondrial-mediated apoptosis by DECPR.

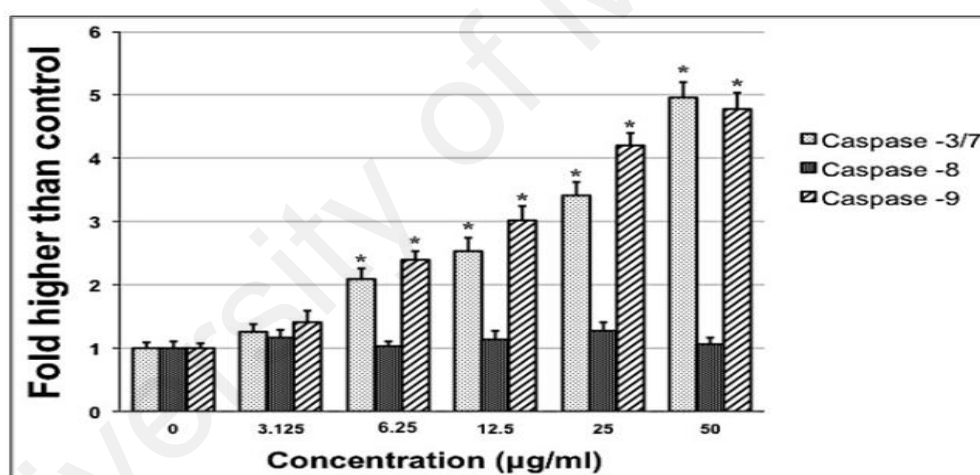


Figure 4.9: Effect of DECPR on caspase 3/7, 8, and 9 activation in HT-29 cells

Cells were treated with different concentrations of DECPR for 24 h following with bioluminescent analysis of caspases activities. The quantitative analysis showed the significant activation for caspase-3/7 and -9 at 6.25 to 50 $\mu\text{g/ml}$ concentrations, while there was no significant fold-change in caspase-8 activity.

4.2.7 Induction of DNA Fragmentation by DECPR

To elucidate late stage of apoptosis, DNA laddering assay was performed. The exposure of HT-29 cells to DECPR at 12.5 and 25 $\mu\text{g/ml}$ concentrations for 24 h led to apparent DNA fragmentation, as shown by the formation of DNA ladders in the agarose

gel (Figure 4.10), whereas the control did not reveal any DNA fragmentation. The ability to cause DNA fragmentation is one of the hallmarks of late apoptotic cell death.

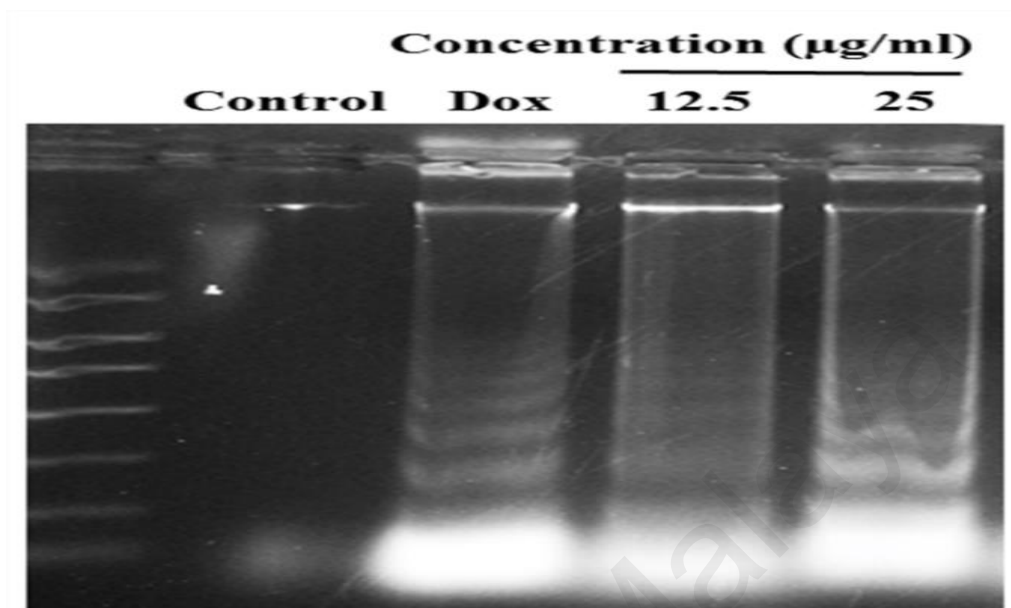


Figure 4.10: DECPR induced DNA fragmentation in HT-29

Cells were exposed to DECPR at 12.5 and 25 $\mu\text{g/ml}$ concentrations for 24 h. Doxorubicin (Dox, 10 $\mu\text{g/ml}$) was used as a positive control. After incubation, the extracted DNA samples were run on the 1.5% agarose gel in a Tris-acetic- EDTA buffer, stained and visualized with a UV light transilluminator.

4.2.8 Changes in Expression of Apoptosis-Associated Molecules by DECPR

Bcl-2 family of proteins has critical role in the regulation of mitochondrial-mediated apoptosis, and perturbation in the expression of these genes trigger a variety of biochemical changes. Hence, we examined the mRNA expression of the pro-apoptotic and anti-apoptotic molecules upon treatment with DECPR. Pro-apoptotic gene, Bax showed dose-dependent and significant mRNA up-regulation after 24 h treatment with DECPR at 12.5 to 50 $\mu\text{g/mL}$ concentrations. Meanwhile, at the same concentrations, there was a significant down-regulation in the mRNA expression of Bcl-2 and Bcl-xl (Figure 4.11). These changes were also confirmed at the protein level using a Western blot analysis (Figure 4.12).

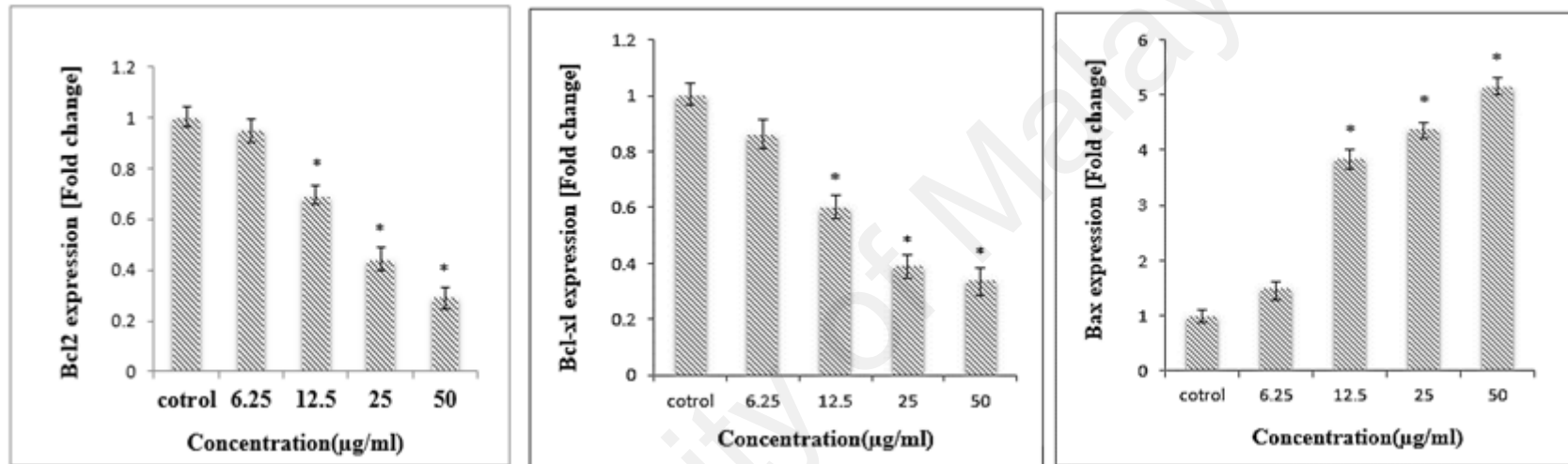


Figure 4.11: Quantitative RT-PCR analysis of apoptosis-associated genes in HT-29 cells

Shown significant up-regulation of Bax and down-regulation of Bcl-2 and Bcl-xl at the mRNA level. The data represent the means \pm SEM of three independent experiments. * $P < 0.05$ compared with the untreated group.

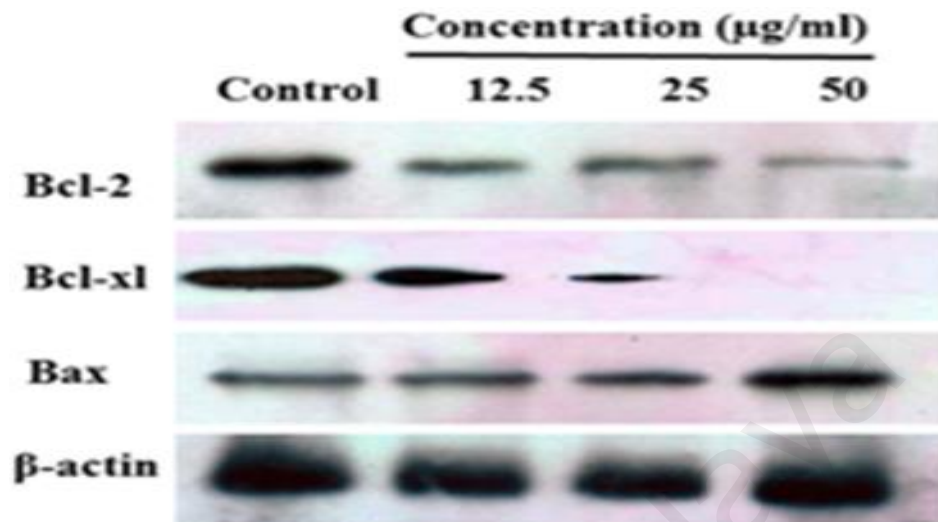


Figure 4.12: Western blot analysis of DECPR on HT-29 cells

DECPR induced changes in expression of mitochondrial-dependent proteins. Western blot analysis confirmed up-regulation of Bax and down-regulation of Bcl-2 and Bcl-xl at the protein level.

4.3 *In Vivo* Results

4.3.1 Safety of DECPR and CPRHE

In the acute toxicity analysis, the rats were orally administered with DECPR and HECPR at dosages of 2 g/kg and 5 g/kg and were monitored for 2 weeks. The result of study did not reveal any report for mortality or any sign of toxicity in rats. There was no detectable sign of toxicity in serum biochemical and hematological parameters of the treated groups compared with the vehicle group Table 4.2, 4.3, 4.4, 4.5, 4.6, and 4.7. The histological analysis showed the structures of the kidney and liver remain normal confirming the safety of DECPR and HECPR at the doses tested (Figure 4.13 and 4.14).

University of Malaya

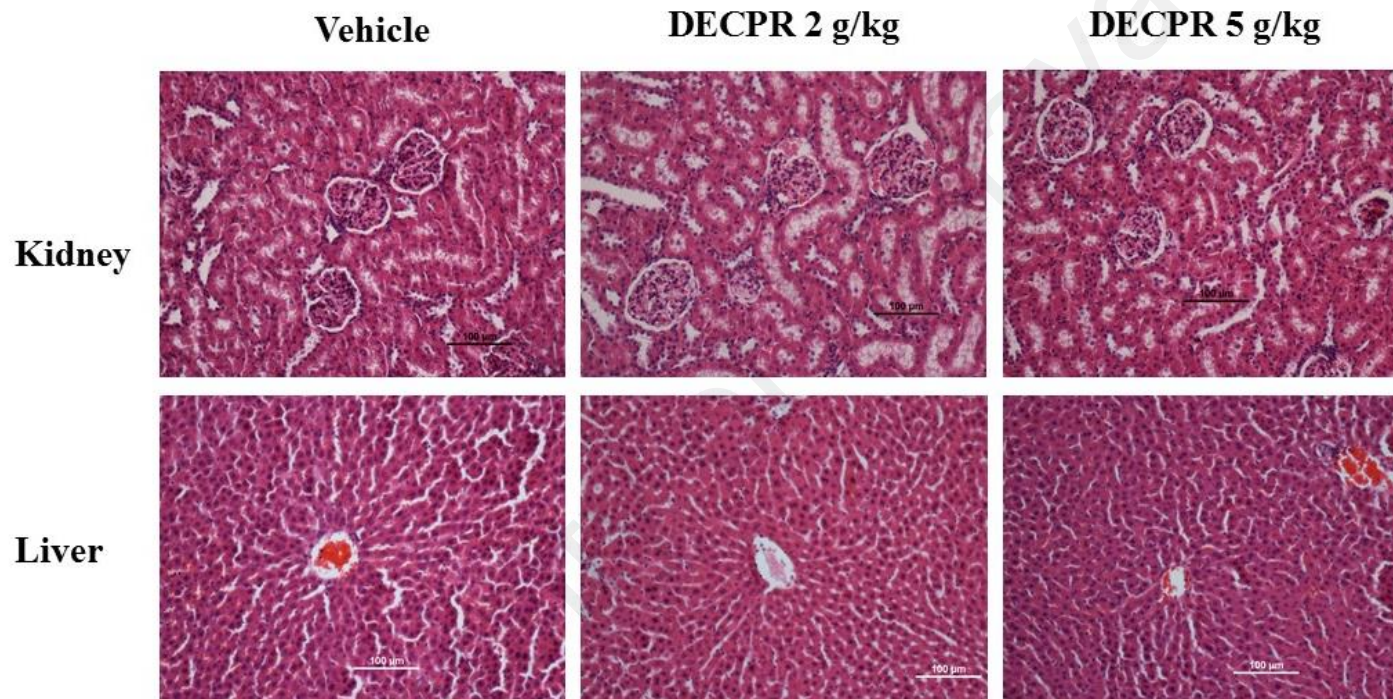


Figure 4.13: Histological sections of kidney and liver tissue treated with DECPR

Histopathology of kidney (first row) and liver (second row) in acute toxicity study representing the rats treated with vehicle (5% Tween 20), DECPR (2 g/kg) and (5 g/kg). The result did not show significant differences in the structures of kidney and liver between treated and control groups (H & E stain, 20× magnifications).

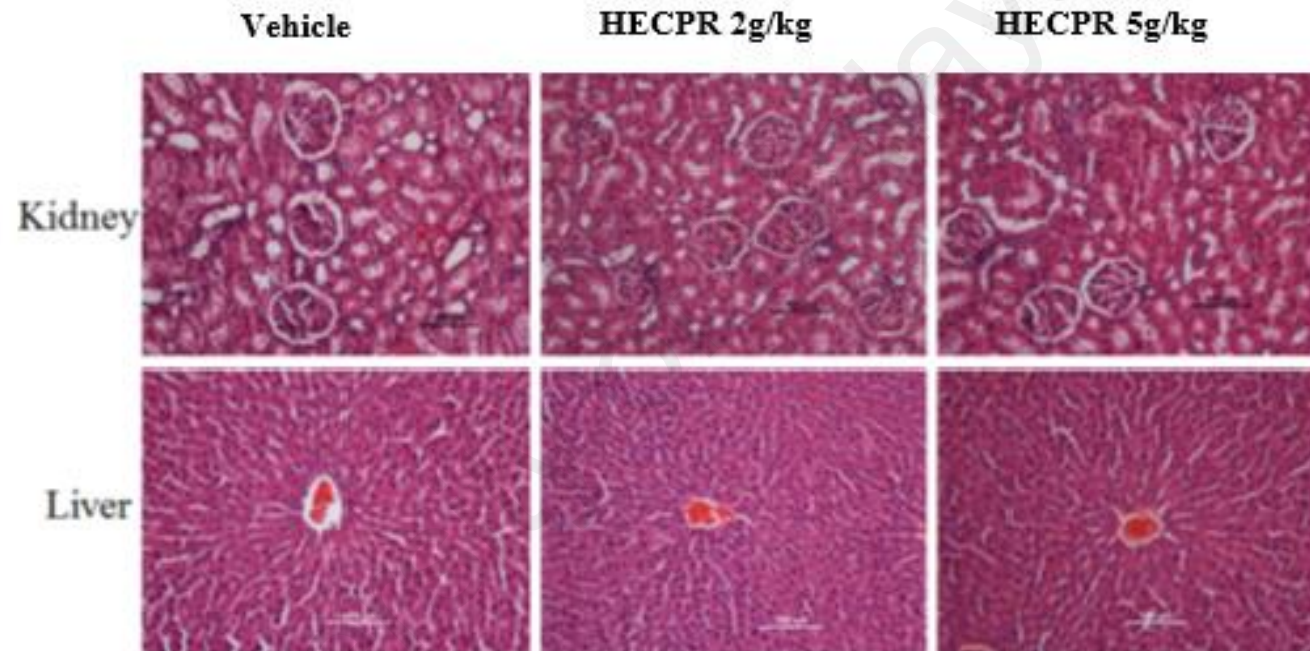


Figure 4.14: Histological sections of kidney and liver tissue treated with HECPR

Histopathology of kidney (first row) and liver (second row) in acute toxicity study representing the rats treated with vehicle (5% Tween 20), HECPR (2 g/kg) and (5 g/kg). The result did not show significant differences in the structures of kidney and liver between treated and control groups (H & E stain, 20× magnifications).

Table 4.2: Effects of DECPR on renal function test

Group	Sodium (mM/L)	Potassium (mM/L)	Chloride (mM/L)	CO₂ (mM/L)	Anion (mM/L)	Urea (mM/L)	Creatinine (μM/L)
Vehicle	138.25 ± 0.46	4.76 ± 0.07	102.67 ± 0.38	26.78 ± 0.53	13.37 ± 0.46	4.39 ± 0.27	30.68 ± 1.59
2 g/kg	139.56 ± 0.39	5.05 ± 0.63	104.37 ± 0.46	28.64 ± 0.54	14.68 ± 0.65	4.85 ± 0.36	29.87 ± 2.24
5 g/kg	140.87 ± 0.73	4.89 ± 0.035	103.47 ± 0.48	27.81 ± 0.42	14.78 ± 0.36	5.16 ± 0.29	31.48 ± 2.17

Values are expressed as mean ± S.E.M. There are no statistically significant differences between the measurements in different groups. The significant value was set at $p < 0.05$.

Table 4.3: Effects of HECPR on renal function test

Group	Sodium (mM/L)	Potassium (mM/L)	Chloride (mM/L)	CO₂ (mM/L)	Anion (mM/L)	Urea (mM/L)	Creatinine (μM/L)
Vehicle	142.23 ± 0.45	4.85± 0.06	104.45 ± 0.45	23.89 ± 0.64	19.36± 0.48	5.28 ± 0.58	30.75 ± 1.87
2g/kg	143.54 ± 0.37	5.12 ± 0.72	106.54 ± 0.54	21.49 ± 0.73	19.58 ± 0.75	5.93 ± 0.43	29.81 ± 2.27
5g/kg	143.85 ± 0.82	4.91 ± 0.034	105.27 ± 0.56	22.85 ± 0.48	19.95 ± 0.39	5.68 ± 0.37	31.46 ± 2.19

Values are expressed as mean ± S.E.M. There are no statistically significant differences between the measurements in different groups. The significant value was set at $p < 0.05$.

Table 4.4: Effects of the DECPR on liver function test

Group	Total protein (g/L)	Albumin (g/L)	Globulin (g/L)	TB (μmol/L)	AP (U/L)	ALT (U/L)	AST (U/L)	GGT(U/L)
Vehicle	67.52 \pm 0.76	9.48 \pm 0.21	51.39 \pm 1.41	2.25 \pm 0.17	151.64 \pm 5.49	47.54 \pm 1.27	170.21 \pm 5.28	2.39 \pm 0.35
2 g/kg	65.46 \pm 0.38	8.67 \pm 0.43	51.14 \pm 1.25	2.21 \pm 0.15	152.43 \pm 5.68	44.72 \pm 1.63	169.57 \pm 6.51	2.48 \pm 0.49
5 g/kg	63.78 \pm 0.82	8.68 \pm 0.29	50.32 \pm 1.27	2.23 \pm 0.16	154.56 \pm 6.75	43.69 \pm 1.35	171.35 \pm 6.49	2.65 \pm 0.37

Values are expressed as mean \pm S.E.M. There are no statistically significant differences between the measurements in different groups. The significant value was set at $p < 0.05$. TB: Total Bilirubin; AP: Alkaline Phosphatase; ALT: Alanine Aminotransferase; AST: Aspartate Aminotransferase; GGT: G-Glutamyl Transferase.

Table 4.5: Effects of the HECPR on liver function test

Group	Total Protein (g/L)	Albumin (g/L)	Globulin (g/L)	TB ($\mu\text{mol/L}$)	AP (U/L)	ALT (U/L)	AST (U/L)	GGT (U/L)
Vehicle	60.76 \pm 0.94	9.56 \pm 0.39	51.07 \pm 1.28	2.19 \pm 0.13	154.45 \pm 5.37	50.49 \pm 1.34	173.82 \pm 5.38	3.45 \pm 0.27
2 g/kg	58.57 \pm 0.57	8.35 \pm 0.53	50.68 \pm 1.32	2.14 \pm 0.16	153.23 \pm 5.87	45.65 \pm 1.74	175.48 \pm 6.49	3.37 \pm 0.53
5 g/kg	59.67 \pm 1.29	8.87 \pm 0.19	50.25 \pm 1.45	2.15 \pm 0.14	155.73 \pm 6.82	46.76 \pm 1.48	176.27 \pm 6.52	3.57 \pm 0.43

Values are expressed as mean \pm S.E.M. There are no statistically significant differences between the measurements in different groups. The significant value was set at $p < 0.05$. TB: Total Bilirubin; AP: Alkaline Phosphatase; ALT: Alanine Aminotransferase; AST: Aspartate Aminotransferase; GGT: G-Glutamyl Transferase.

Table 4.6: Effects of the DECPR on hematological parameters

Group	HGB (g/dL)	HCT (%)	RBC (10⁶ Cells/μL)	MCV(fL)	MCH (pg)	MCHC (g/dL)	RDW (%)	WBC (10³cells/μL)	Platelet (10³ cells/μL)
Vehicle	15.42 \pm 0.13	45 \pm 0.00	10.56 \pm 0.14	61.23 \pm 0.59	17.31 \pm 0.27	34.48 \pm 0.16	18.12 \pm 0.47	7.21 \pm 0.44	988.71 \pm 23.58
2 g/kg	15.23 \pm 0.12	44 \pm 0.00	10.63 \pm 0.17	62.65 \pm 0.48	17.79 \pm 0.27	34.45 \pm 0.33	19.25 \pm 0.61	7.26 \pm 0.36	996.41 \pm 25.34
5 g/kg	15.27 \pm 0.11	44 \pm 0.00	10.79 \pm 0.15	61.84 \pm 0.39	18.62 \pm 0.31	34.14 \pm 0.28	20.79 \pm 0.36	7.33 \pm 0.38	1012.64 \pm 23.21

Values are expressed as mean \pm SEM. There are no significant differences between groups. Significant value at $p < 0.05$. HGB: Haemoglobin; HCT: Haematocrit; RBC: Red Cell Count; MCV: Mean Corpuscular Volume; MCH: Mean crepuscular Haemoglobin; MCHC: Mean Corpuscular Haemoglobin Concentration; RDW, Red Cell Distribution Width; WBC, White C

Table 4.7: Effects of the HECPR on hematological parameters

Group	HGB (g/dL)	HCT (%)	RBC (10⁶ cells/μL)	MCV(fL)	MCH(pg)	MCHC (g/dL)	RDW (%)	WBC (10³cells/μ L)	Platelet (10³ ells/μL)
Vehicle	15.03 \pm 0.13	46 \pm 0.00	9.38 \pm 0.13	59.12 \pm 0.65	19.25 \pm 0.31	34.22 \pm 0.19	17.03 \pm 0.44	6.12 \pm 0.47	986.75 \pm 3.65
2 g/kg	15.47 \pm 0.13	46 \pm 0.00	9.64 \pm 0.18	58.54 \pm 0.63	18.89 \pm 0.36	34.04 \pm 0.35	18.23 \pm 0.58	6.23 \pm 0.34	995.36 \pm 5.32
5 g/kg	15.98 \pm 0.12	46 \pm 0.00	9.83 \pm 0.16	57.78 \pm 0.76	18.59 \pm 0.29	34.93 \pm 0.22	18.77 \pm 0.34	6.31 \pm 0.39	1011.52 \pm 23.18

Values are expressed as mean \pm SEM. There are no significant differences between groups. Significant value at $p < 0.05$. HGB: Haemoglobin; HCT: Haematocrit; RBC: Red Cell Count; MCV: Mean Corpuscular Volume; MCH: Mean Corpuscular Haemoglobin; MCHC: Mean Corpuscular Haemoglobin Concentration; RDW, Red Cell Distribution Width; WBC, White Cell.

4.3.2 Colon Cancer Chemoprevention Results

4.3.2.1 Analysis of Rat's Body Weight and Serum Biochemistry Parameter

The body weight of all rats were taken at the beginning (at 1st week) of the experiment then weekly up to 10 weeks table 4.8. Although there are differences between groups among the treatment but statistically there were no significant differences in the body weight among the groups. The parameters of liver and kidney function tested for all groups were analyzed and compared to their vehicle group and there was no significant difference observed in any of groups compared to their respective groups table 4.9 & 4.10.

Table 4.8: Effect of DECPR on rat's body weight in AOM-induced colon cancer

Group	Week 1	Week 10
Normal control group	182± 5.6	442± 9.12
Cancer control group	185± 4.7	436± 10.3
Drug control group	181± 4.1	452± 9.11
DECPR low dose	186± 6.2	461± 8.7
DECPR high dose	184± 3.3	455± 11.4

Values expressed as mean ± S.E.M. there are no statically difference between the measurements in different groups. The significant value was set at $P < 0.05$.

Group	Total protein (g/L)	Albumin (g/L)	AST (IU/L)	ALT (IU/L)	GGT (IU/L)
Normal control group	67.5± 3.2	11.5± 0.26	210.3± 3.23	61.4± 1.23	5.5± 0.3
Cancer control group	65.4± 2.1	11.3± 0.31	206.5± 4.27	65.3± 1.19	4.2± 0.23
Drug control group	69.8± 4.7	10.2± 0.43	209.5± 3.41	64.1± 1.28	4.3± 0.35
DECPR low dose	70.3± 0.61	11.12± 0.16	211.5± 4.51	62.5± 1.34	4.4± 0.26
DECPR high dose	68.7± 2.3	11.0± 0.35	214.5± 6.6	63.4± 1.25	5.3± 0.19

Table 4.9: Effect of DECPR on liver function test in AOM-induced colon cancer

Values expressed as mean ± SEM there are no statistically significant differences between groups. The significant value was set at P< 0.05, compared with cancer group. ALT: alanine aminotransferase; AST: aspartate aminotransferase GGT: G-glutamyl transferase.

Table 4.10: Effect of DECPR on renal function test in AOM-induced colon cancer study

Group	Urea(mmol/L)	Creatinine(μmol/L)
Normal control group	5.3 \pm 0.11	52.3 \pm 4.12
Cancer control group	5.2 \pm 0.15	50.8 \pm 5.23
Drug control group	4.31 \pm 0.17	52.1 \pm 4.11
DECPR low dose	4.54 \pm 0.14	49.3 \pm 5.17
DECPR high dose	5.1 \pm 0.12	51.4 \pm 4.24

Values expressed as mean \pm SEM there are no statistically significant differences between the measurements for all different groups. The significant value was set at $P < 0.05$

4.3.2.2 Counting the Aberrant Crypt Foci (ACF)

ACF were mostly observed in the proximal part of colon. ACF in the colon were counted and the average of the total number of ACF and the number crypts per focus were obtained. ACF were observed in the colon as well as in multicrypt clusters (more than four crypts / focus) of aberrant crypts table 4.11. Rats treated with AOM and fed with the low and high DECPR showed significant reduction of total ACF/colon compared with AOM-control rats (80 ± 6.13 and 57 ± 5.78) inhibition respectively, $P < 0.05$. The incidence of multiple aberrant crypts /focus was also significant inhibited in rats fed with compounds when compared with AOM-induced rats. As shown in Figure 4.15, ACF were mainly distributed in the middle of the colon in rats treated with AOM alone. DECPR significantly suppressed the number of ACF in the distal, middle and proximal colon compared to AOM treated group, $P < 0.05$.

Table 4.11. Effect of DECPR on AOM-induced colon ACF in rats

Group	No. of crypts per ACF					
	1 crypt	2 crypt	3 crypt	4 crypt and more	Total	Inhibition (%)
Normal control group	0	0	0	0	0	-
Cancer control group	46 ± 1.22	47 ± 1.89	55 ± 1.98	34 ± 1.40	182 ± 6.47	-
DECPR low dose	19 ± 1.03*	24 ± 1.28*	22 ± 2.62*	15 ± 1.20*	80 ± 6.13*	56.04
DECPR high dose	14 ± 2.08*	19 ± 1.79*	15 ± 1.24*	9 ± 0.67*	57 ± 5.78*	68.68
Drug control group	14 ± 0.50*	14 ± 1.39*	11 ± 1.22*	8 ± 0.58*	47 ± 3.69*	74.17

Values are expressed as mean ± S.E.M. the significant value was set at *P<0.05, compared with cancer control group.

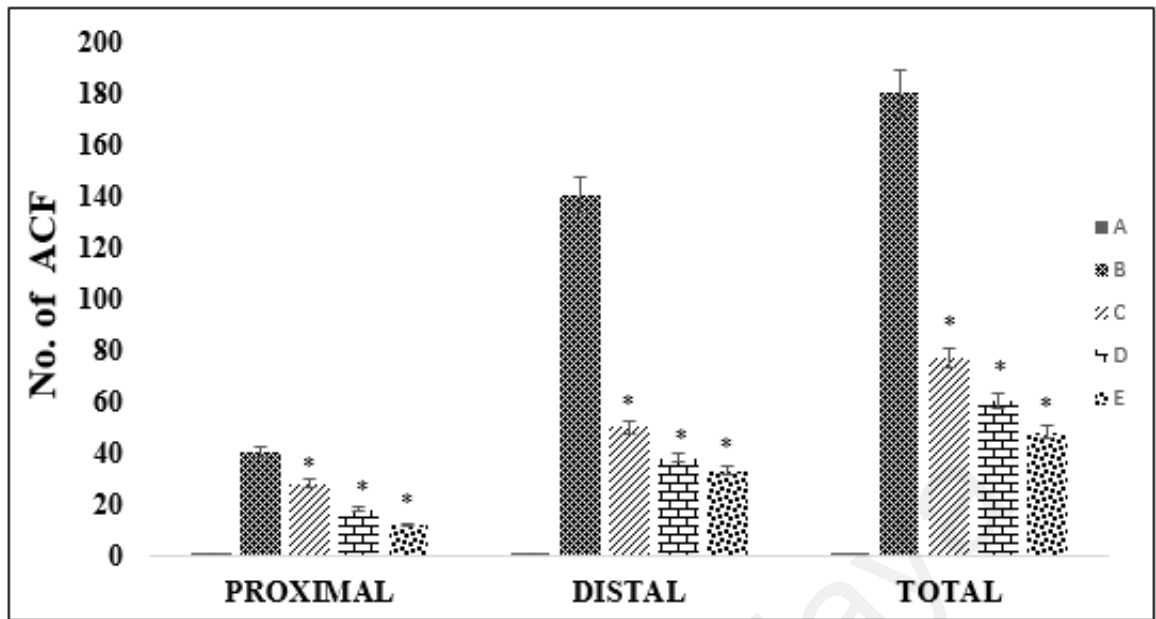


Figure 4.15. Effect of DECPR on ACF formation in proximal and distal parts of the colons separated from the treated rats

Five groups of rats included (A) normal control, (B) cancer control, (C) low dose of DECPR, (D) high dose of DECPR and (E) 5-FU treatment control. Data are shown as means \pm SEM; (n=6). Values are statistically significant at *P<0.05.

4.3.2.3 Topographic Views of Colon

As depicted in figure 4.16, no aberrant crypts were identified with methylene blue staining in the intact colons of normal control rats. The number of ACF per colon, which is considered as a marker for tumour initiation were significantly higher in AOM-control group compared to DECPR. The multiplicity of ACF (number of crypts per ACF), which is considered as a marker for tumour promotion, was significantly higher in the AOM group.

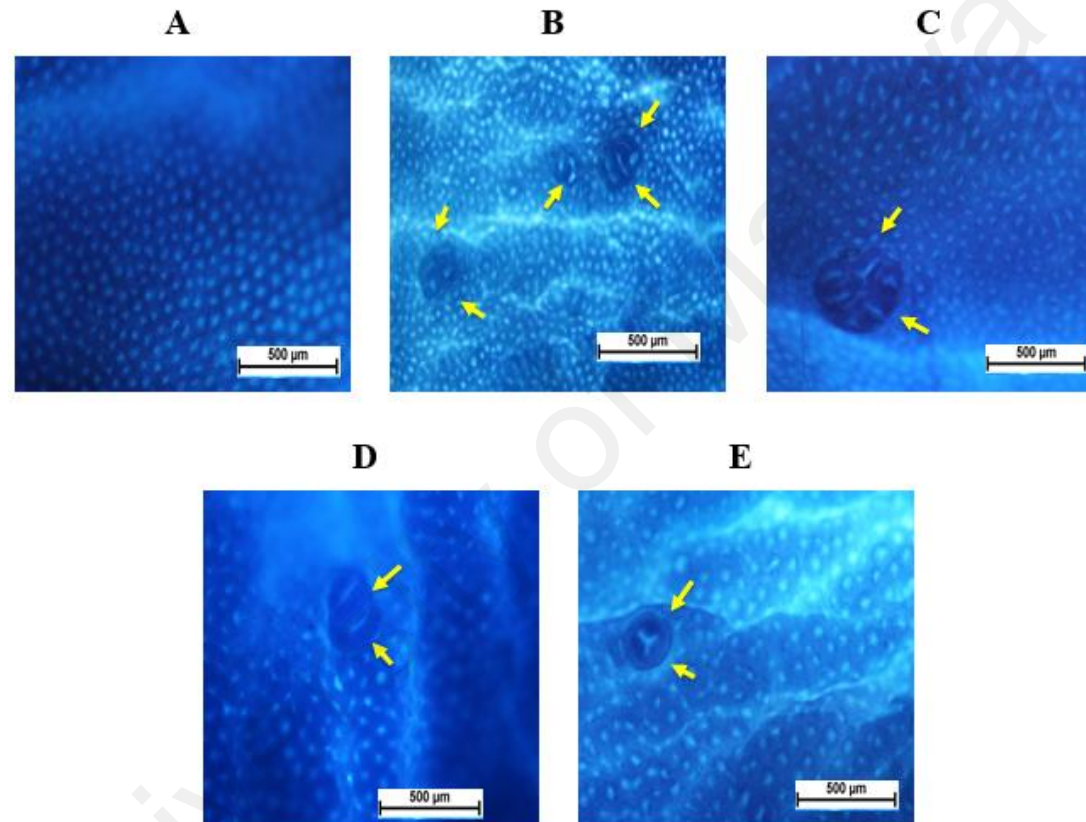


Figure 4.16: Topographic views of colon mucosa of group treated with DECPR

Effect of DECPR on gross appearances of ACF (arrows) on the colon mucosa separated from the treated rats and stained with methylene blue dye. Five groups of rats included (A) normal control, (B) cancer control, (C) low dose of DECPR, (D) high dose of DECPR and (E) 5-FU treatment control. Magnification 20X.

4.3.2.4 Histological Classification of ACF

Histological examination of haematoxylin and eosin-stained sections was performed to determine the extent of colon injury for each section. Example slides obtained from the histological examination under the light microscope were given in (Figure 4.17). In the control rats, there were no pathological abnormalities, the colon sections looked normal with regular cellular architecture and were clear of any pathology. Normal control group showed circular shape and basal location of the nuclei. According to H& E staining photos from dysplastic ACF, elongated nuclei loss, of cell polarity, increase in mitosis, lack of goblet cells and narrow lumen in epithelial cells of ACF were observed compared to the surrounding normal crypts. The rats in 5-flourouracil treated group exhibited significantly lesser pathology as compared to the extensive colon damage found in the AOM treated group. The histopathological examination of the colon sections from the rats treated with DECPR revealed reduced degree of pathology. These results provided microscopic evidence again demonstrating the significant inhibition of the compounds to counter balance the negative effects of AOM in the colon tissue.

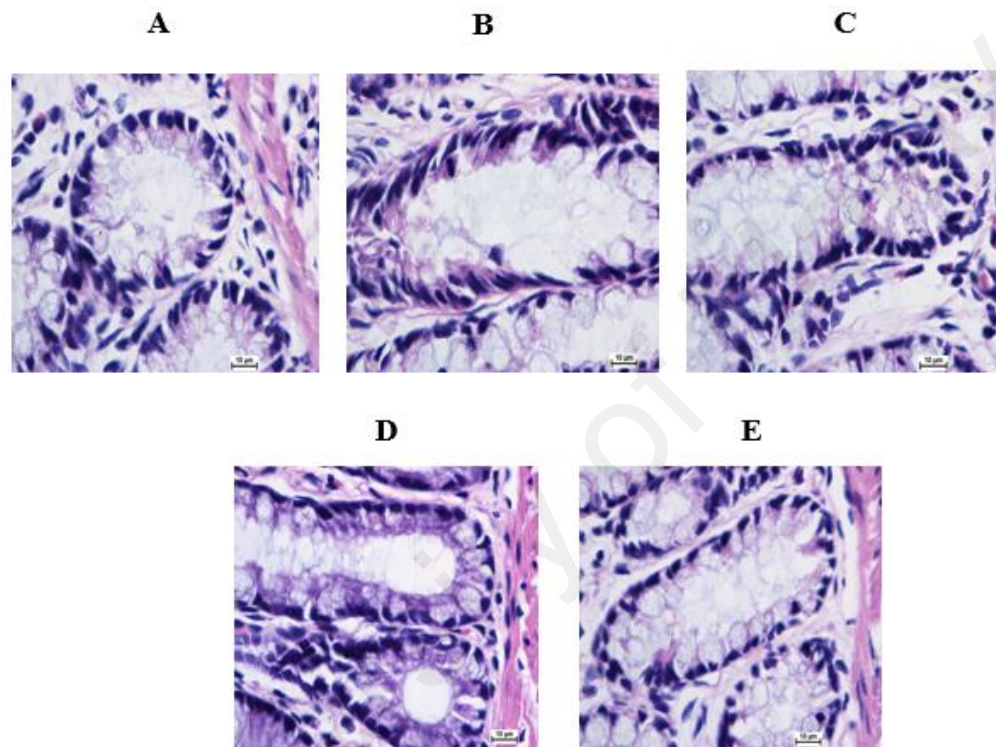


Figure 4.17: Histological study of colon cancer in the rat treated with DECPR

Five groups of rats were included (A) normal control, (B) cancer control, (C) low dose of DECPR, (D) high dose of DECPR and (E) 5-FU treatment control. The section was cut parallel to the muscle layer. (H & E stain; Magnification 100X).

4.3.2.5 Immunohistochemistry Analysis

Photomicrographs of ACF exhibiting grades of nuclear morphology from colons of rats receiving AOM were captured. All sections were cut parallel to the muscle layer. The presence of elongated and stratified nuclei were noted throughout the crypt.

4.3.2.5.1 Proliferating Cell Nuclear Antigen (PCNA) Staining of Colons and Cell Counting

The PCNA was evaluated as a marker for cell proliferation in the colon specimens. Sections of colon samples from the control group and the DECPR treated group are shown (Figure 4.18). The PCNA positive staining cells in the nucleus (brown) of mucosa of the colon tissue were much stronger in azoxymethane treated rats than in the DECPR group. PCNA negative cells (blue) were stained with haematoxylin. The PCNA labelling index is also shown in (Figure 4.19). The colon section from the AOM control group showed a higher number of positive cells than the treated group.

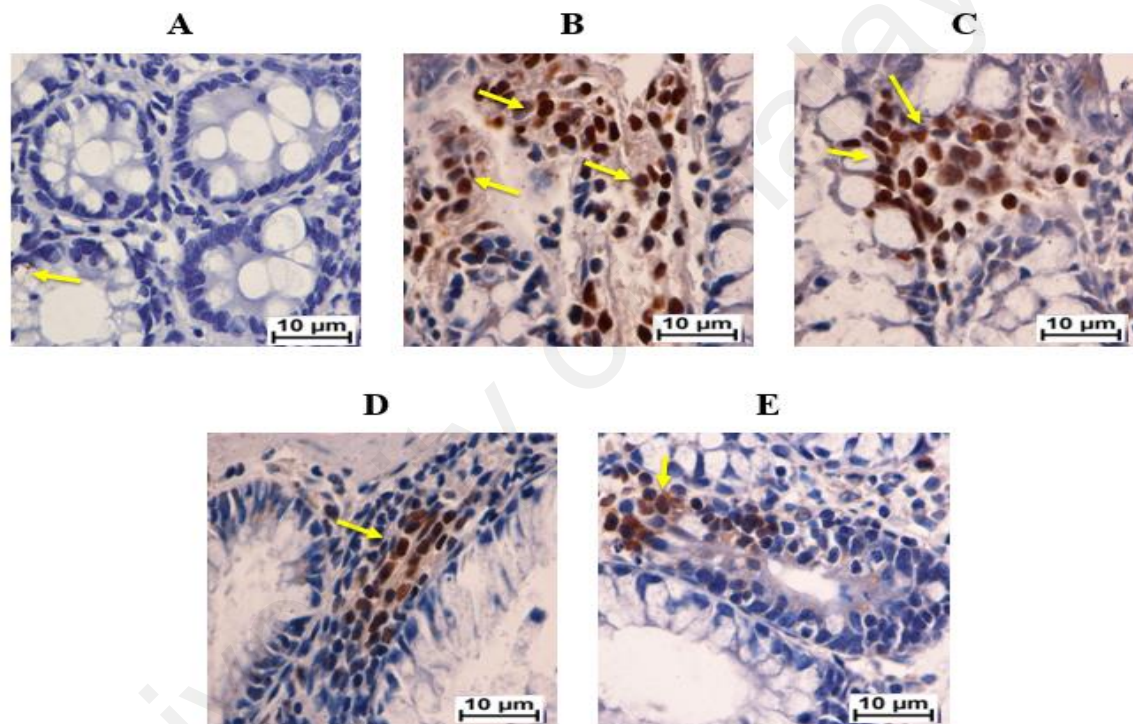


Figure 4.18: Immunohistochemical analyses of the expression of PCNA in the colon tissues treated with DECPR

Five groups of rats were included (A) normal control, (B) cancer control, (C) low dose of DECPR, (D) high dose of DECPR and (E) 5-FU treatment control. Immunohistochemical staining for PCNA protein revealed a down-regulation of PCNA proteins in the rats treated with DECPR (Magnification 100X).

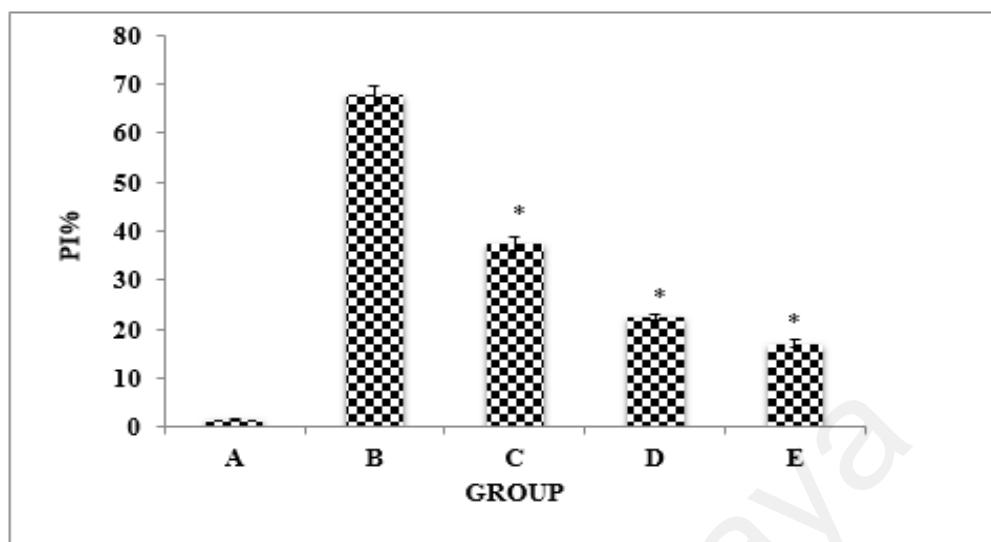


Figure 4.19: Immunohistochemical analyses of the expression of PCNA in the colon tissues treated with DECPR

Five groups of rats were included (A) normal control, (B) cancer control, (C) low dose of DECPR, (D) high dose of DECPR and (E) 5-FU treatment control. Immunohistochemical staining for PCNA protein revealed a down-regulation of PCNA protein in the rats treated with DECPR. All values are expressed as the mean \pm the SEM. The mean difference was significant at the $P < 0.05$ level compared to the cancer control group.

4.3.2.5.2 Bax Staining of Colons and Cell Counting

Since inhibition of higher dose of DECPR prevents the AOM-induced ACF formation, the proliferation index was measured by staining colon sections with anti-Bax antibodies. The Bax was evaluated as a marker for cell proliferation in the colon specimens. Sections of colon samples from the control groups and treatment groups with DECPR are shown in (Figure 4.20) respectively. The immunohistochemical Bax staining of the colon sections from the azoxymethan group revealed a lower number of positive cells than those from the azoxymethan plus treatment groups.

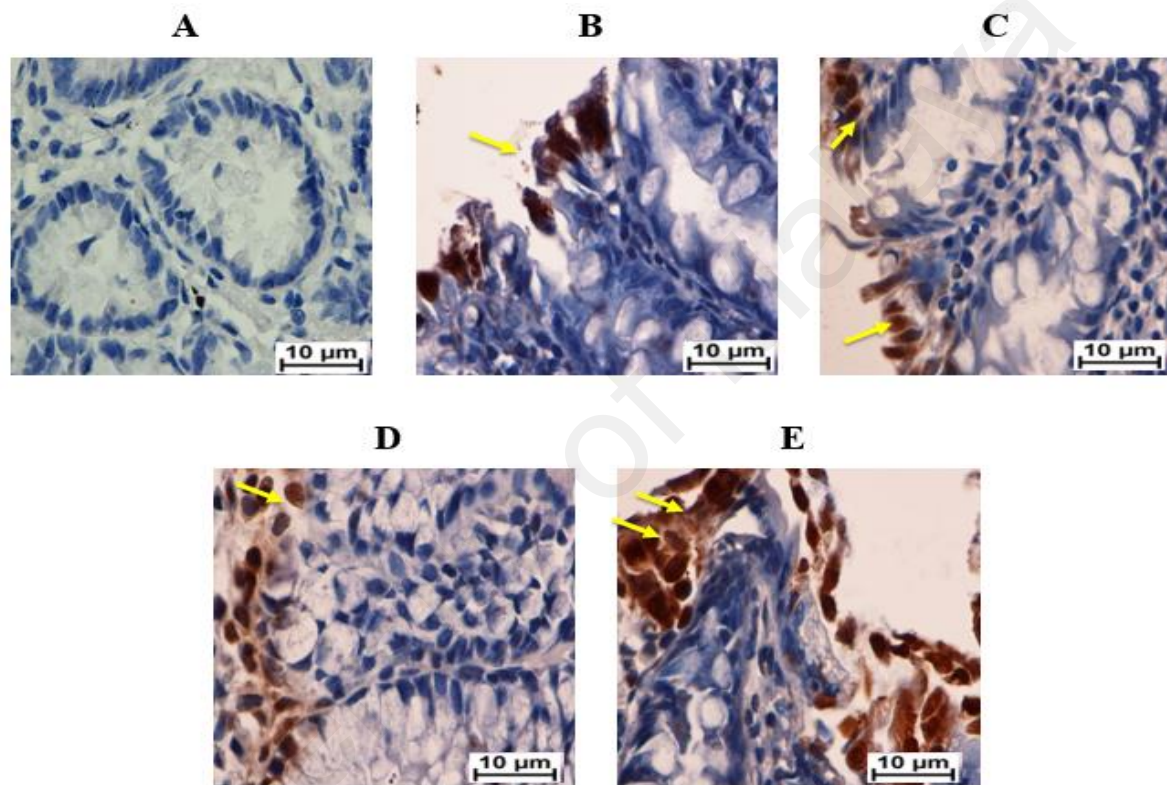


Figure 4.20: Immunohistochemical expression of Bax in colon tissues of control and experimental groups of rats

Five groups of rats were included (A) normal control, (B) cancer control, (C) low dose of DECPR, (D) high dose of DECPR and (E) 5-FU treatment control. Bax protein expression is illustrated as brown staining (Magnification 100X).

4.3.2.5.3 Bcl-2 Staining of Colons and Cell Counting

Since inhibition of higher dose of DECPR prevents the AOM-induced ACF formation, the proliferation index (PI) was measured by staining colon sections with anti-Bax antibodies. The Bcl-2 was evaluated as a marker for cell proliferation in the colon specimens. Sections of colon samples from the control groups and treatment groups with DECPR are shown in (Figure 4.21) respectively. The immunohistochemical Bcl-2 staining of the colon sections from the azoxymethan group revealed a higher number of positive cells than those from the azoxymethane plus treatment groups.

University of Malaya

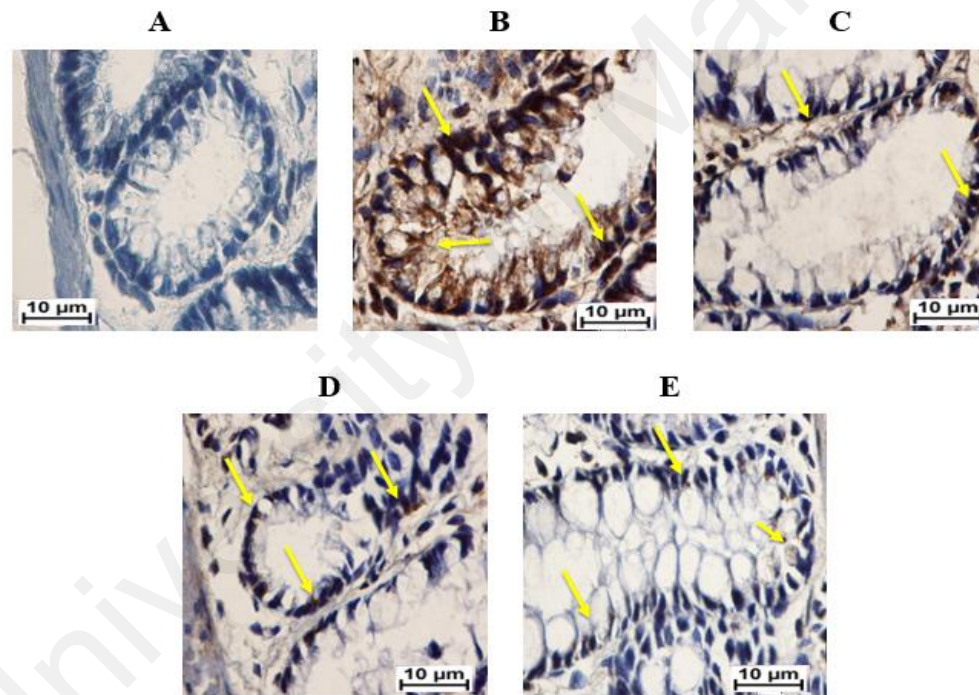


Figure 4.21: Immunohistochemical expression of Bcl-2 in colon tissues of control and experimental groups of rats

Five groups of rats were included (A) normal control, (B) cancer control, (C) low dose of DECPR, (D) high dose of DECPR and (E) 5-FU treatment control. Bcl-2 protein expression is illustrated as brown staining (Magnification 100X).

4.3.2.6 Western Blot

In order to investigate the mechanisms by which DECPR evoke apoptosis, proteins isolated from normal control group, AOM control group and colon mucosa of the rats fed with high and low dose of DECPR were subjected to western blot analysis. Western blots of colonic lysates from control, AOM alone and AOM induced treated groups with DECPR at 8 weeks are shown in (Figure 4.22). According to the western blot result, Bcl-2 and PCNA were up regulated in cancer control group. Bax protein was up-regulated in the AOM-induced group treated with DECPR compared to the AOM control group which was down-regulated.

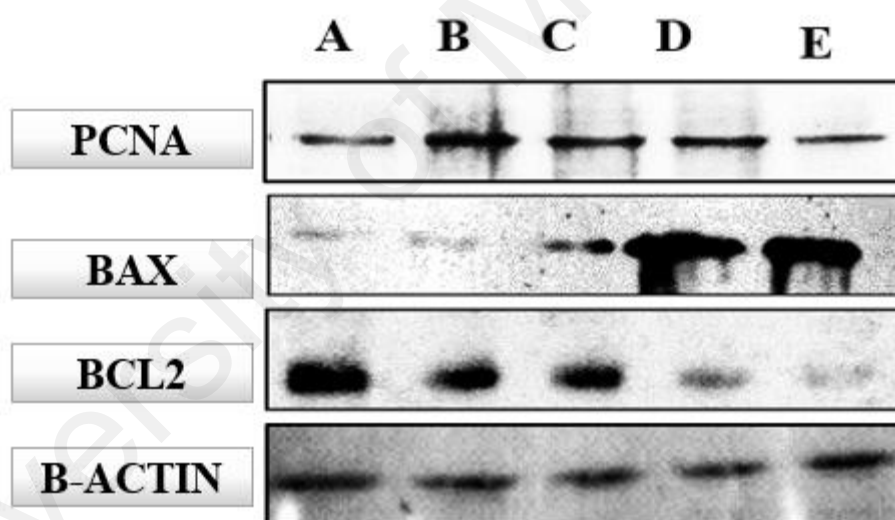


Figure 4.22: Western blot analysis of PCNA, Bax and Bcl-2

Five groups of rats were included (A) normal control, (B) cancer control, (C) low dose of DECPR, (D) high dose of DECPR and (E) 5-FU treatment control. B-actin western blotting was used as the control band.

4.3.2.7 Antioxidant Activities of Homogenized Colon

Measurement of antioxidant activities showed that the levels SOD, CAT and GPX in colon cancer homogenized samples treated with both doses significantly increased compared with cancer control group. The MDA level of the colon homogenized tissue

was significantly decreased in comparison with cancer control group. During oxidative stress the body uses its defence mechanism to minimize the process of lipid peroxidation by using these antioxidant enzymes, thus, the activity of those enzymes become higher in early stages of AOM induction, but when the insult continue for a long period, the enzymes become depleted and are unable to fight against free radicals, which means that in advance stages of peroxidation due to AOM, the activity of catalase and SOD declined as shown in (Figure 4.23). On the other hand, in the AOM control group, there is a significant increase of MDA level compared to the normal control group observed, indicating acute hepatocytes damage. Treatment of animals with DECPR and 5-fluorouracil significantly reduced the level of MDA and lipid peroxidation.

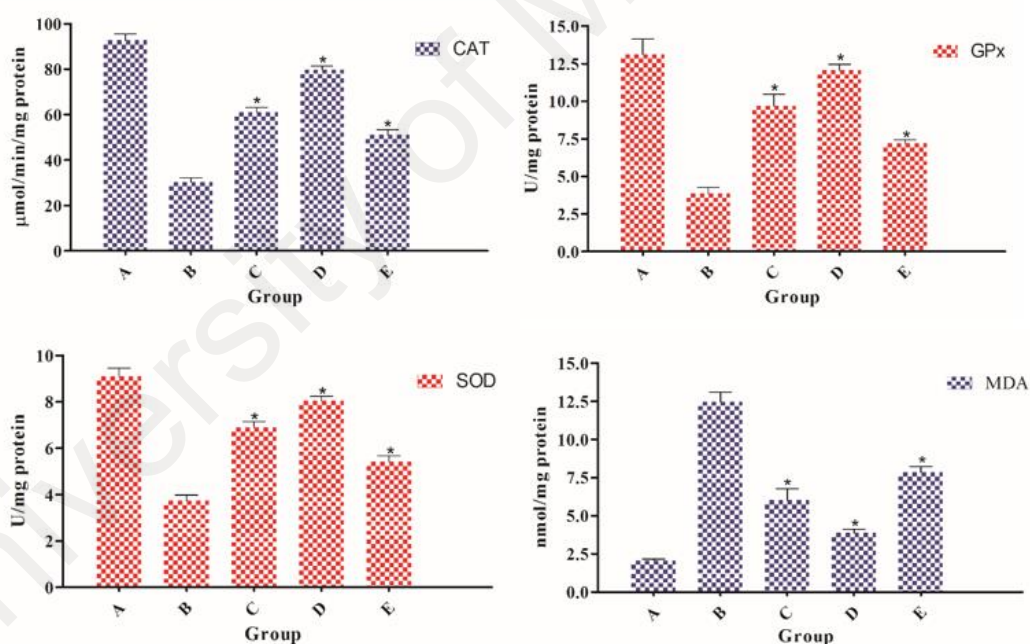


Figure 4.23: Effect of DECPR on antioxidant enzyme activities and on MDA

Five groups of rats were included (A) normal control, (B) cancer control, (C) low dose of DECPR, (D) high dose of DECPR and (E) 5-FU treatment control. All values are expressed as the mean \pm SEM. The mean difference was significant at the $P < 0.05$ level compared to the cancer control group.

4.3.3 Gastroprotective Ulcer

4.3.3.1 PH of Gastric Content and Determination of Mucus Production

The acidity of gastric content in rodents administered orally with ethanol was significantly increased compared to the normal control group, as shown in table 4.12. After treatment with omeprazole (positive control), the acidity was significantly attenuated ($P < 0.05$) and animals pre-treated with HECPR at high dose and low dose elicited significant ($P < 0.05$) elevation of PH. The gastric mucus content was significantly depleted in animals pre-treated with ethanol. Meanwhile, omeprazole and HECPR treatment significantly replenished the loss in mucosal content $P < 0.05$, table 4.12. The findings of both parameters suggested the anti-ulcer effect of HECPR.

Table 4.12. Gastroprotective effect of HECPR against ethanol-induced gastric injury

Animal Groups	PH of Gastric tissue	Mucus Weight (g)	Ulcer area (mm)²	Inhibition (%)	MDA (μmol/mg protein)	SOD(U/mg protein)	Nitric oxide (μmol/mg protein)
A) Normal control	4.02 ± .004	0.89 ± 0.03	-	-	10 ± 1.1	528 ± 16.51	10 ± 1.3
B) Lesion control (alcohol)	2.54 ± 0.17	0.41 ± 0.01	880 ± 16.23	-	28 ± 2.98	333 ± 9.98	5.9 ± 0.47
C) drug control (omeprazole)	5.60 ± 0.24*	0.79 ± 0.03*	195 ± 8.97*	77	13 ± 0.71*	481 ± 12.22*	9.1 ± 1.4*
D) HECPR (200 mg/kg)	4.47 ± 0.09*	0.68 ± 0.02*	455 ± 12.24*	48	21 ± 0.22*	393 ± 7.67*	7.6 ± 0.8*
E) HECPR (400 mg/kg)	5.12 ± 0.41*	0.72 ± 0.02*	325 ± 10.67*	63	17 ± 0.41*	459 ± 10.73*	8.4 ± 0.9*

4.3.3.2 Macroscopic Evaluation of Gastric Lesions

The administration of ethanol to the rats induced noticeable black hemorrhagic lesions in the gastric walls (Figure 4.24) (group B) with ulcer area of $880 \pm 16.23 \text{ mm}^2$ table 4.12. As shown in (Figure 4.24), rodents pre-treated with HECPR (group D and E) and omeprazole (group C) had markedly reduced areas of gastric ulcer formation in comparison with lesion control group (group B). Pre-treatment of rats with HECPR at doses of 200 mg/kg and 400 mg/kg suppressed the ulcer area formation to $455 \pm 12.24 \text{ mm}^2$ and $325 \pm 10.67 \text{ mm}^2$ respectively, which was comparable to the suppressive effect of omeprazole $195 \pm 8.97 \text{ mm}^2$. The incidence of ulcer was decreased by 48% and 63% after treatment with HECPR at doses of 200 mg/kg and 400 mg/kg, respectively table 4.12. It is worthy to note that HECPR treatment helped to flatten the gastric mucosal folds in rodents (group D and E).

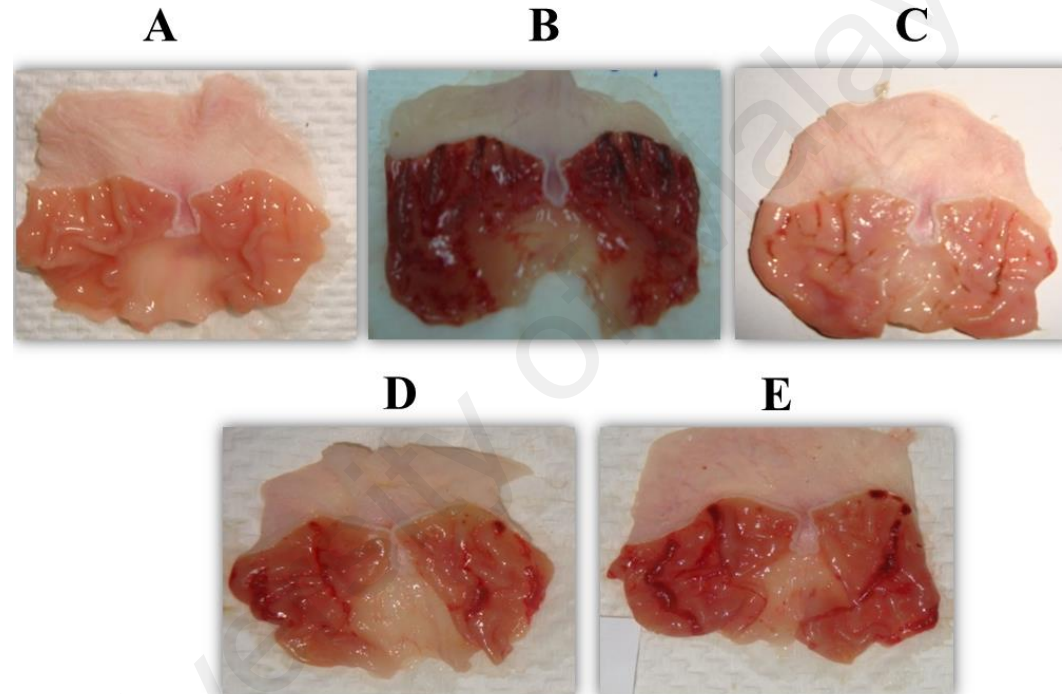


Figure 4.24. Gross evaluation of stomach in rats

Results demonstrated that the rodents pre-treated with (C) omeprazole and HECPR at doses of (D) 200 mg/kg and (E) 400 mg/kg had conspicuously decreased area of gastric ulcer formation compared to (B) ulcer control. (A) Normal control group demonstrated no gastric lesion formation.

4.3.3.3 Assessment of Stomach Malondialdehyde and Superoxide Dismutase

To determine the effects on lipid peroxidation and oxidative stress, we determined the level of MDA in gastric tissue homogenate. After treatment with ethanol, the MDA level ($28 \pm 2.98 \mu\text{mol/mg}$) was significantly ($P < 0.05$) elevated compared to the normal control group ($10 \pm 1.1 \mu\text{mol/mg}$). The results showed that administration of HECPR and omeprazole before ethanol significantly ($P < 0.05$) decreased the MDA level compared to the lesion control group (Figure 4-25 A) Ethanol treated rodents elicited a significantly lower SOD activity compared to the normal control group ($P < 0.05$), which was elevated upon treatment with HECPR (Figure 4.25 B).

4.3.3.4 Assessment of Nitric Oxide Level

The perturbation in nitric oxide levels of the stomach was investigated using Griess reagent, as shown in (Figure 4.25 C). In gastric tissue homogenate, the nitric oxide level in lesion control group was markedly ($P < 0.05$) lower ($5.9 \pm 0.47 \mu\text{mol/mg protein}$) compared to the normal control group ($10 \pm 1.3 \mu\text{mol/g protein}$). Administration of HECPR significantly ($P < 0.05$) elevated nitric oxide level, which was comparable to the nitric oxide-generation effect of omeprazole.

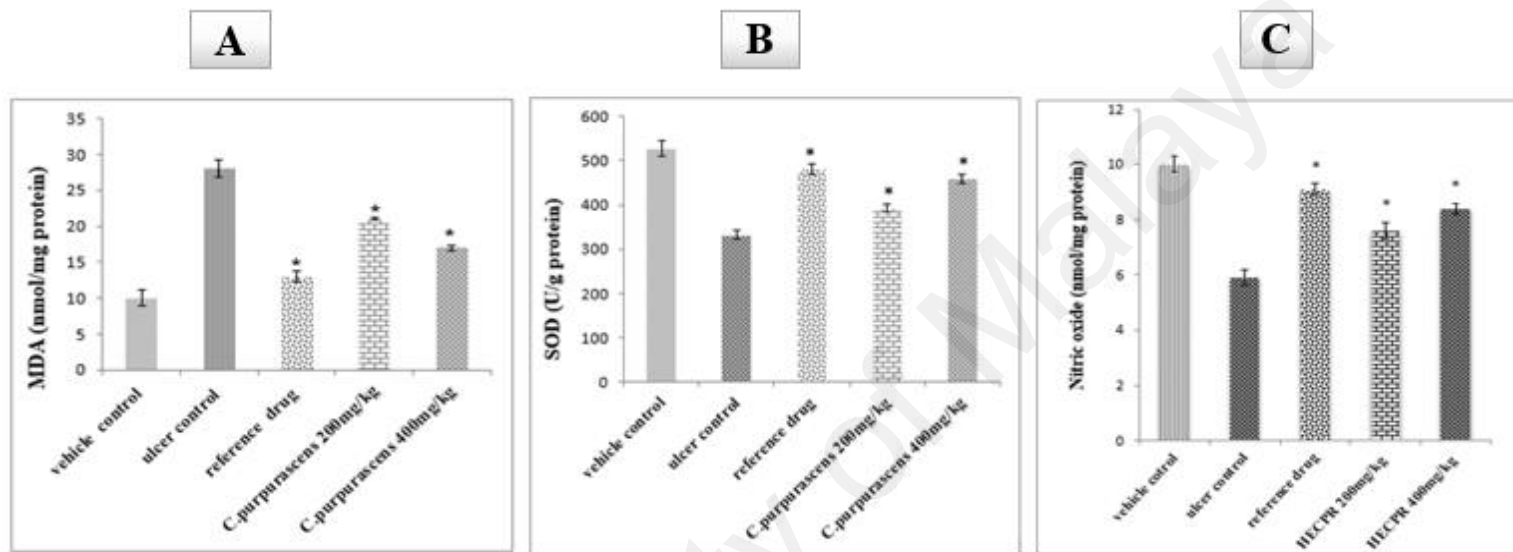


Figure 4.25: Effect of HECPR on the level of SOD, Nitric oxide, MDA in ethanol induces gastric ulcer, (6rats/group). Values are presented as mean \pm SD.*significant at $P < 0.05$ compared with ulcer control group.

4.3.3.5 Histological Assessment of Gastric Lesions by Haematoxylin and Eosin Staining

Microscopic analysis of the gastric lesions in the ulcer control group elicited extensive damage to the gastric mucosa of the rodents characterized by disrupted surface epithelium and deeply penetrated necrotic lesions into mucosa associated with conspicuous leucocytes infiltration and severe edema of submucosal layer (Figure 4.26) (group B). Pretreatment with HECPR (group D and E) and omeprazole (group C) revealed a protective effect by reduction in leucocytes infiltration and submucosal edema. The replenishment of the loss in mucus content by HECPR was evidenced by the stumpy amount of magenta color in the histological analysis as compared to the control group (group D and E). The results showed that HECPR pre-treatment at high dose and low dose markedly disrupted ethanol-induced destruction of gastric mucosa.

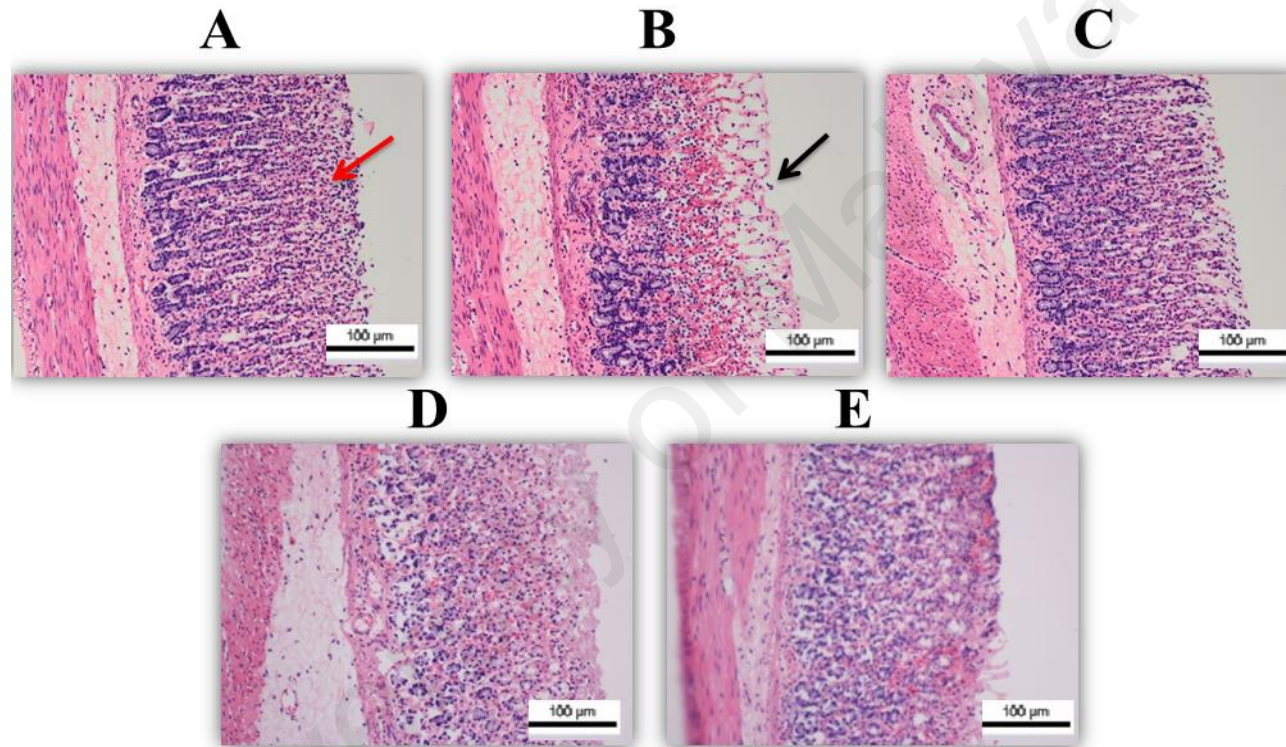


Figure 4.26: Histological study of ulcer in rats treated with HECPR

Histopathology of rodents pre-treated with (C) omeprazole or HECPR at the doses of (D) 200 mg/kg and (E) 400 mg/kg compared to the (B) lesion control group. (A) Normal control group demonstrated normal histological structure. (H and E stain 10 \times).

4.3.3.6 Histological Examination by Periodic Acid-Schif (PAS)

The histological examination by PAS staining was conducted to estimate the level of gastric mucus that coat the gastric mucosa in the ethanol-induced gastric lesion model. The gastric mucus is a gel –like substance produced and secreted by the surface epithelial cells of the gastric mucosa. Figure 4.27 shows the PAS staining results for the HECPR groups. PAS staining (violet color accumulation) at the surface cells and neck part the gastric glands was observed with moderate to strong color (depending on the administered dose) in the experimental rats from the pre-treated HECPR groups . By contrast, adequate PAS staining was not observed in the ulcer control group (B). In addition, observation of strong PAS staining at the surface epithelium and neck part of the gastric glands (violet granules) in the experimental rats pretreated with omeprazole (group C).

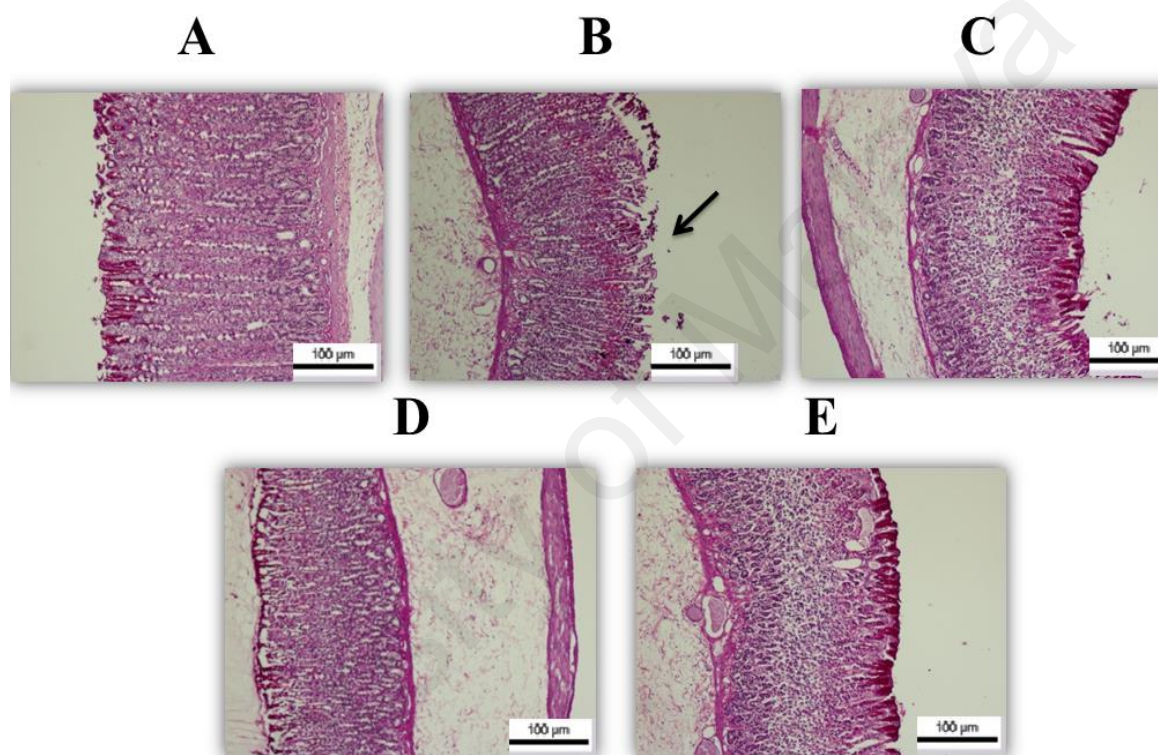


Figure 4.27: Stomach histological evaluation by Periodic Acid- Schiff (PAS)

Histopathology of rodents pre-treated with (C) omeprazole showed excellent accumulation of gastric mucous or HECPR at the doses of (D) 200 mg/kg and (E) 400 mg/kg exhibited mild to moderate mucous accumulation on the surface of gastric epithelial cells compared to the (B) lesion control group. (A) Normal control group demonstrated normal histological structure. (PAS stain10X).

4.3.3.7 Immunohistochemistry

Immunohistochemical analysis of the gastric injuries revealed that pre-treatment with HECPR at the doses of 200 mg/kg and 400 mg/kg caused conspicuous up-regulation of Hsp70 protein when compared with the ulcer control group (Figure 4.28). In addition, the expression of Hsp70 in normal control group was relatively higher than the expression in ulcer control group. Immunohistochemical examination of Bax protein indicated a down-regulation of this protein after administration of HECPR and omeprazole. Meanwhile, the expression of Bax was up-regulated in ulcer control group in comparison with normal control group.

University of Malaysia

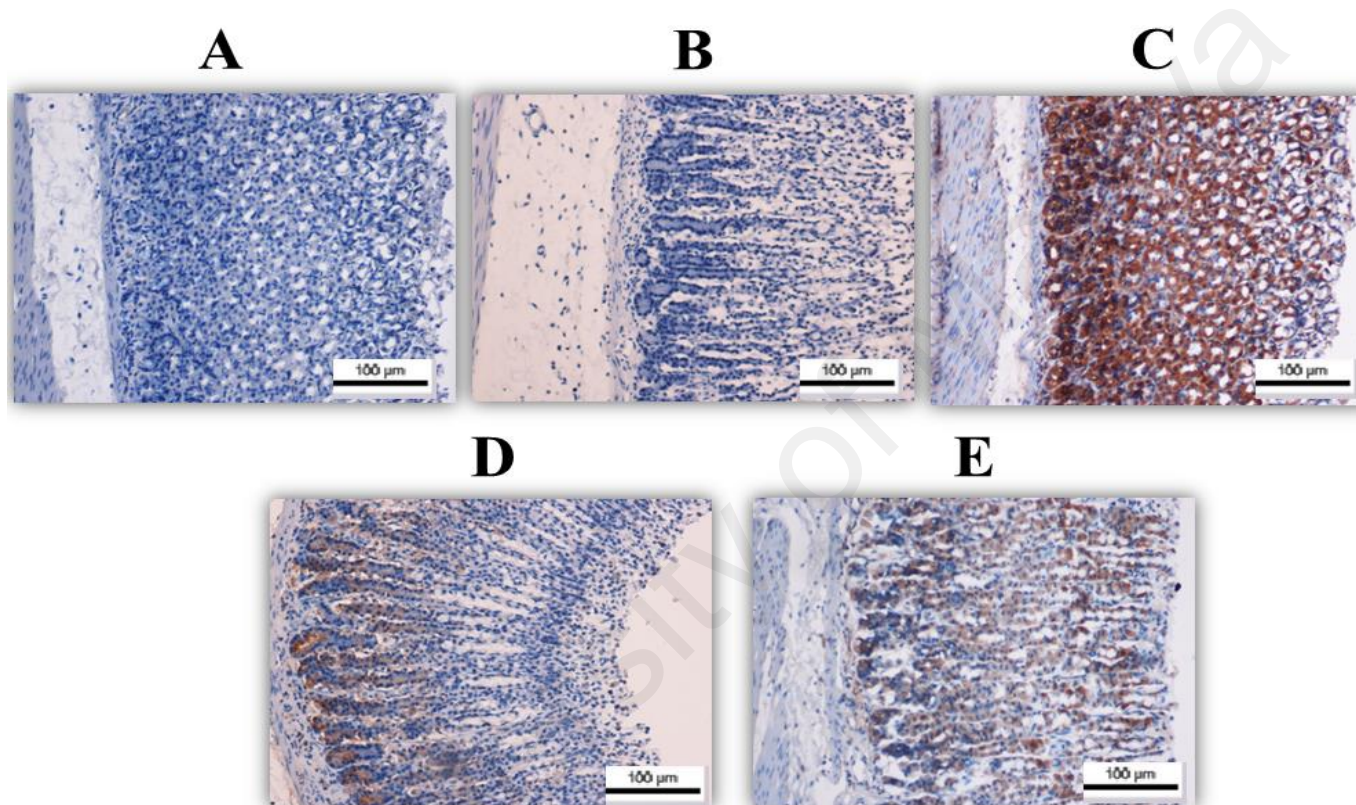


Figure 4.28: Immunohistochemical examination of Hsp70

The results depicted the up-regulation of Hsp70 proteins in rats pre-treated with (C) omeprazole and HECPR at the doses of (D) 200 mg/kg and (E) 400 mg/kg compared to the (B) lesion control group. (A) Normal control group demonstrated normal immunohistochemical structure.

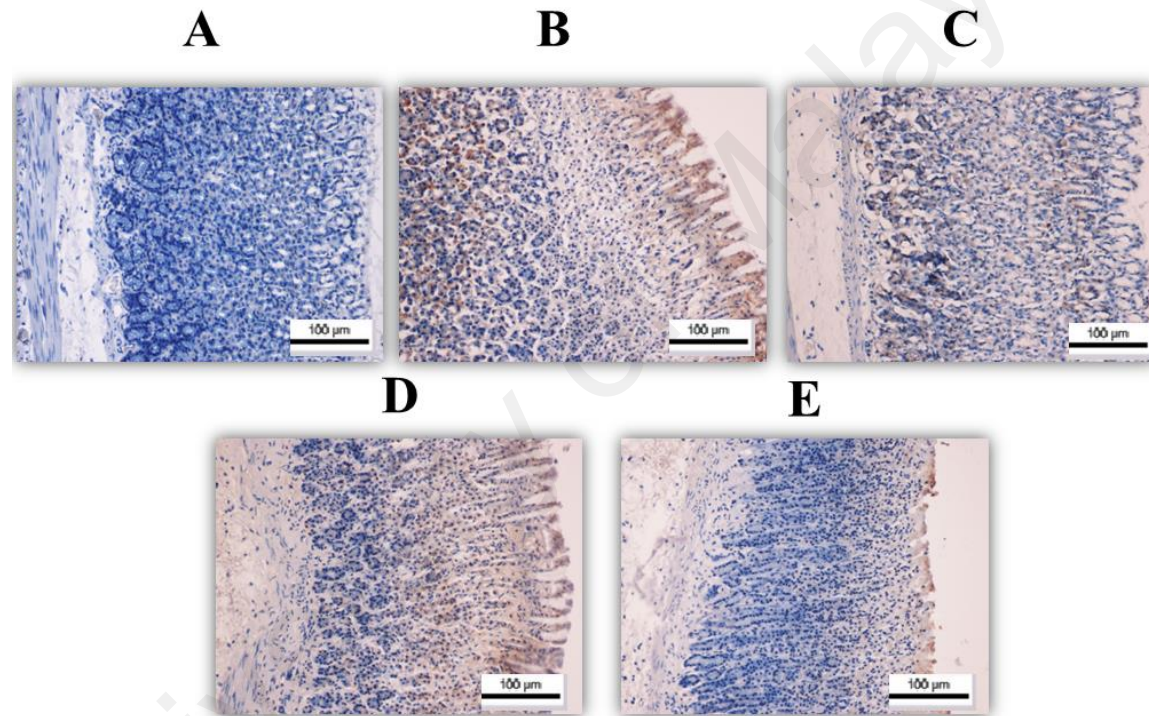


Figure 4.29: Immunohistochemical examination of Bax

The results depicted the down-regulation of Bax proteins in rats pre-treated with (C) omeprazole and HECPR at the doses of (D) 200 mg/kg and (E) 400 mg/kg compared to the (B) lesion control group. (A) Normal control group demonstrated normal immunohistochemical structure.

4.3.4 Wound Healing Evaluation Parameters

This study was carried out in order to verify the ability of HECPR to enhance the wound healing process. Circular excision wound model was employed for assessing the *in vivo* wound healing activity of these medicinal plants. Two percent concentration solution of gum acacia used to prepare plant extract at dose 100mg/ml and 200mg/ml applied on the experimentally created excision wounds of rats.

4.3.5 Wound Area Contraction

A blinded observer, who was unaware of the experimental protocol, evaluated the wound healing rate. Macroscopically the wounds dressed with HECPR showed considerable signs of dermal healing and healed significantly faster compared with the vehicle control group (gum acacia in normal saline) on the day 20th after the wounds were incurred (Figure 4.30). Grossly, wounds dressed with Intrasite gel (Group 4) revealed remarkable wound repair and significantly accelerated rate of healing compared with the control group (Group 1). Moreover, Group 4 exhibited the highest healing rate among all the groups.

The wound-healing rate of HECPR on the wounds dressed with 200mg/ml was almost equivalent to the healing rate in Group 4. Rats treated with 100mg/ml HECPR showed faster wound-healing rate than rats in Group 1, but this rate was slower than the wound healing rate of Groups 3 and 4. The above findings suggesting that a high dose of HECPR may be as effective as Intrasite gel in improving the progression of wound-healing. The estimation of wound closure in rats for HECPR are shown in (Figures 4.30). Wound closure was measured to determine the percentage of wound healing in each rat. During the course of the study, the wound closure percentage in the vehicle control group was significantly lower than any of the HECPR or Intrasite gel groups. Rats treated with

a high dose of HECPR 200mg/ml had a comparable level of healing with the rats given the Intracel gel, as well as slightly higher level of healing than the rats treated with a low dose of HECPR 100mg/kg. The above evaluations provide further independent confirmation that HECPR treatment effectively improves skin wounds in a dose-dependent manner. On the other hand, the results demonstrated that rats treated with HECPR had significantly ($P<0.05$) higher values of inhibition than the vehicle control group. Intracel gel induced a significant reduction in the wound area on the 5th day when compared with the other groups.

University of Malaya

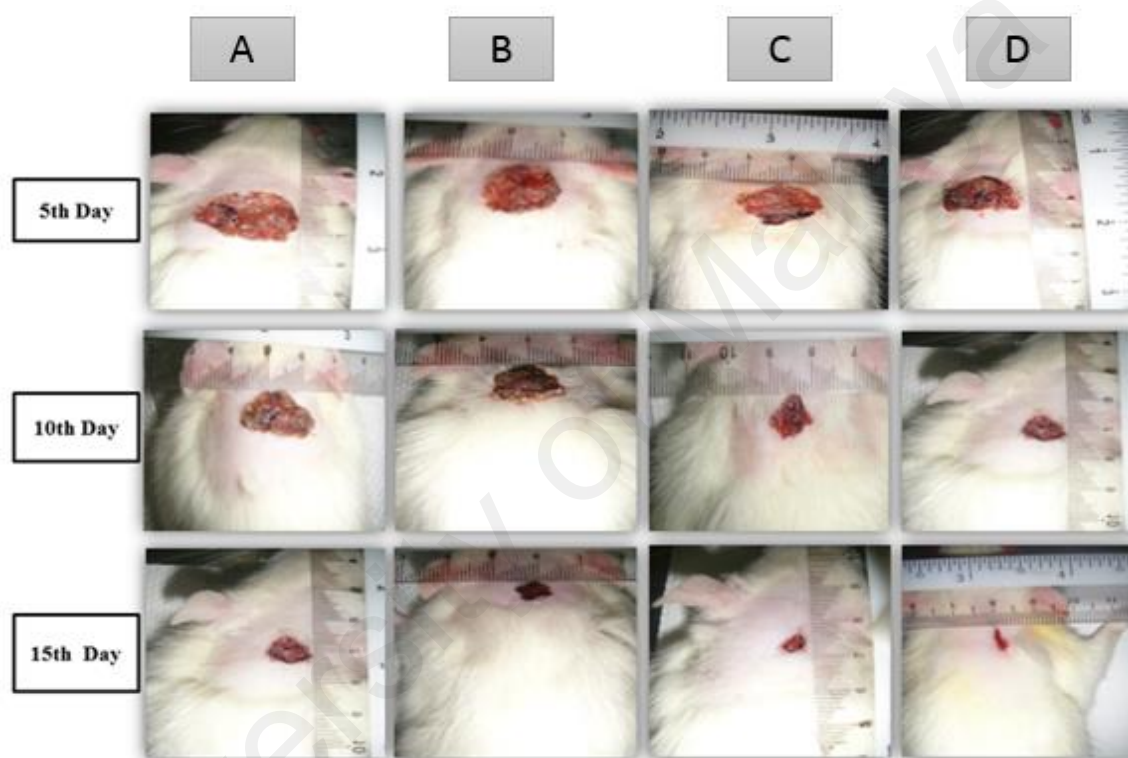


Figure 4.30: Gross appearance of excision wound healing area in rats

Gross appearance of the excision wound in rats after treatment (0.2 ml) with (A) blank placebo, (B) HECPR (100 mg/ml), (C) HECPR (200 mg/ml) and (D) intrasite gel on excision wound contraction.

Measurements of wound healing progression as induced by HECPR and the reference drug and the vehicle control groups are shown in (Figure 4.31). Wound margin was traced after wound creation using transparent paper and the wound area was measured using graph paper. Wound contraction was measured over an interval of 5 days until the 20th day. In the excision wound model, the wounds of animals treated with HECPR at doses (100 and 200) mg/ml contracted at a significantly higher rate by day 20 ($P < 0.05$) as compared with the vehicle control group.

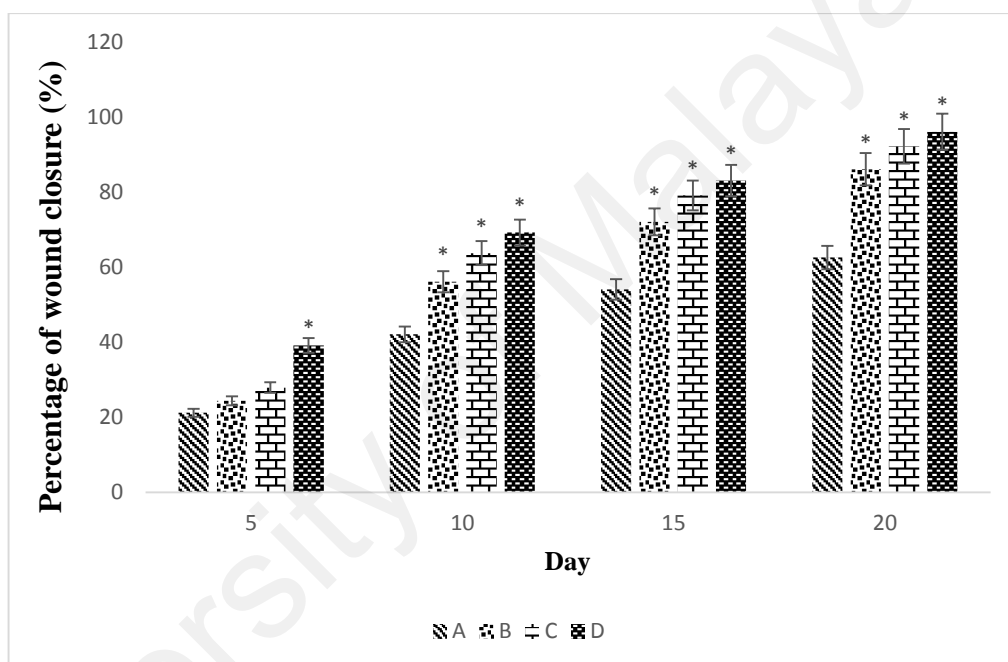


Figure 4.31. Effect of topical treatment of HECPR on rats

Effect of topical treatment (0.2 ml) with (A) blank vehicle, (B) HECPR (100 mg/ml), (C) HECPR (200 mg/ml) and (D) intrasite gel on excision wound contraction % wound closure after 5, 10, 15 and 20 days. Values are expressed as mean \pm SEM, $n = 6$ animals in each group. * $p < 0.05$ vs negative control rats (A).

4.3.5.1 Histological Evaluations of Healed Wound Area

The histology of the wound tissue on the 20th day after wounding was evaluated by an observer blinded to the experimental protocol. In the HECPR treated groups, the wound enclosure is smaller, and the granulation tissues contained comparatively less inflammatory cells and more collagen, fibroblast and blood proliferating capillaries compared with the vehicle control group (Figure 4.32).

Histological examination of haematoxylin and eosin (H & E) sections of the wound tissues treated with HECPR is shown in Figure 4.32. The microscopic appearance of the skin of the control group revealed greater scar width at 10X and 100X magnification. The granulation tissue had high amounts of inflammatory cell infiltrate fibroblasts, angiogenesis (blood vessel formation) was visible, and a few collagen fibers were formed. Skin from the intrasite gel and high dose of HECPR group had a smaller scar width at 10X magnification, with less inflammatory cell infiltrate, more fibroblasts, blood vessel formation and collagen deposition than other HECPR.

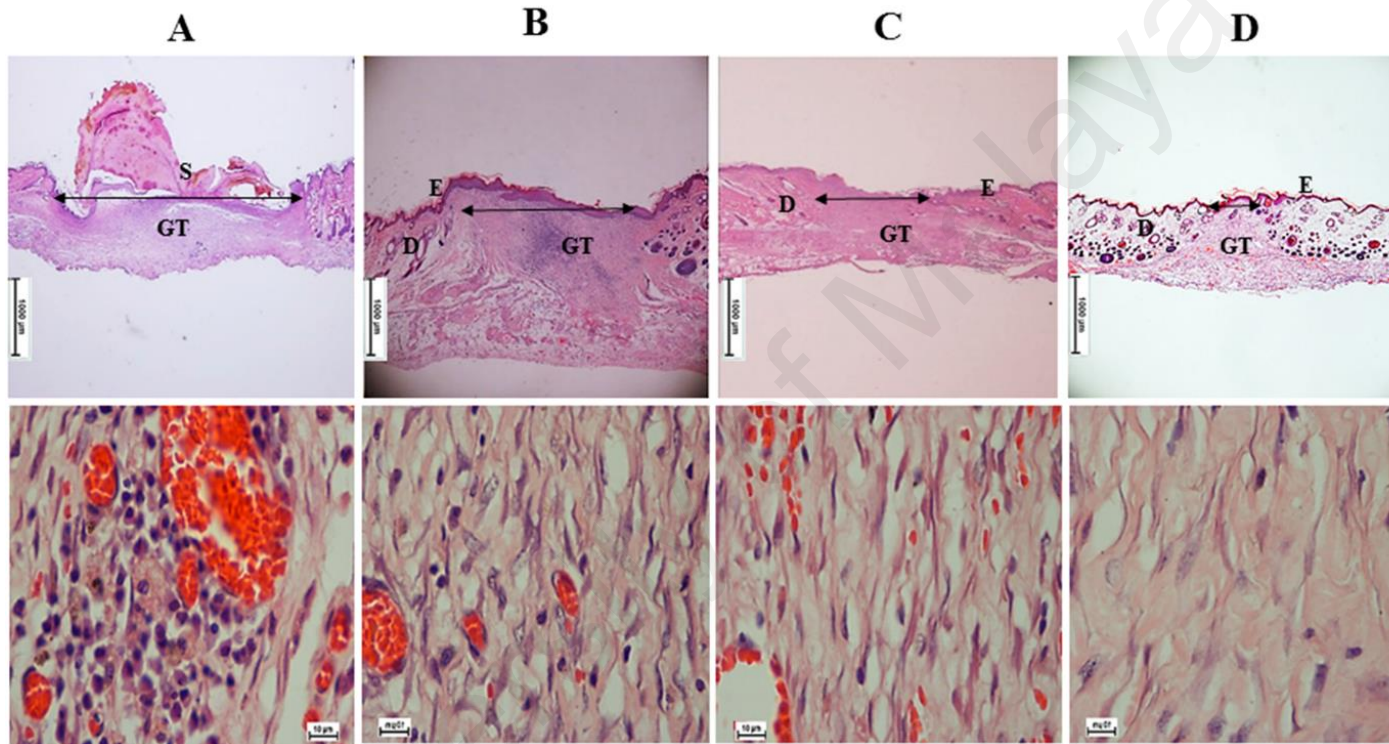


Figure 4.32: Histopathological view of excision wound healing after H & E staining at two magnifications

. On the 20th day of treatment, wound tissues were processed from (A) blank vehicle, (B) HECPR (100 mg/ml), (C) HECPR (200 mg/ml) and (D) intrasite gel administrated rats. Skin sections illustrating dermis (D), epidermis (E), GT, granulation tissue and scar width (S). Scale bar: 1000 μ m (low magnification) and 10 μ m (high magnification).

4.3.5.2 Masson's Trichrome Staining of Healed Wound in Rats

Masson's trichrome staining of wounds healed by HECPR are shown in Figure 4.33. The degree of collagen deposition as determined by Masson's trichrome staining is illustrated at magnification of 10X. Sections of skin tissue from the blank vehicle group appeared to be normal with minimal signs of collagen deposition. Skin tissue from the intrasite gel group showed high collagen accumulation, indicating that some level of healing had started. Section of skin tissue from the HECPR group 200mg/ml showed extensive collagen accumulation, whereas skin sections from the other HECPR group at doses of 100mg/ml showed mild to moderate collagen accumulation.

University of Malaysia

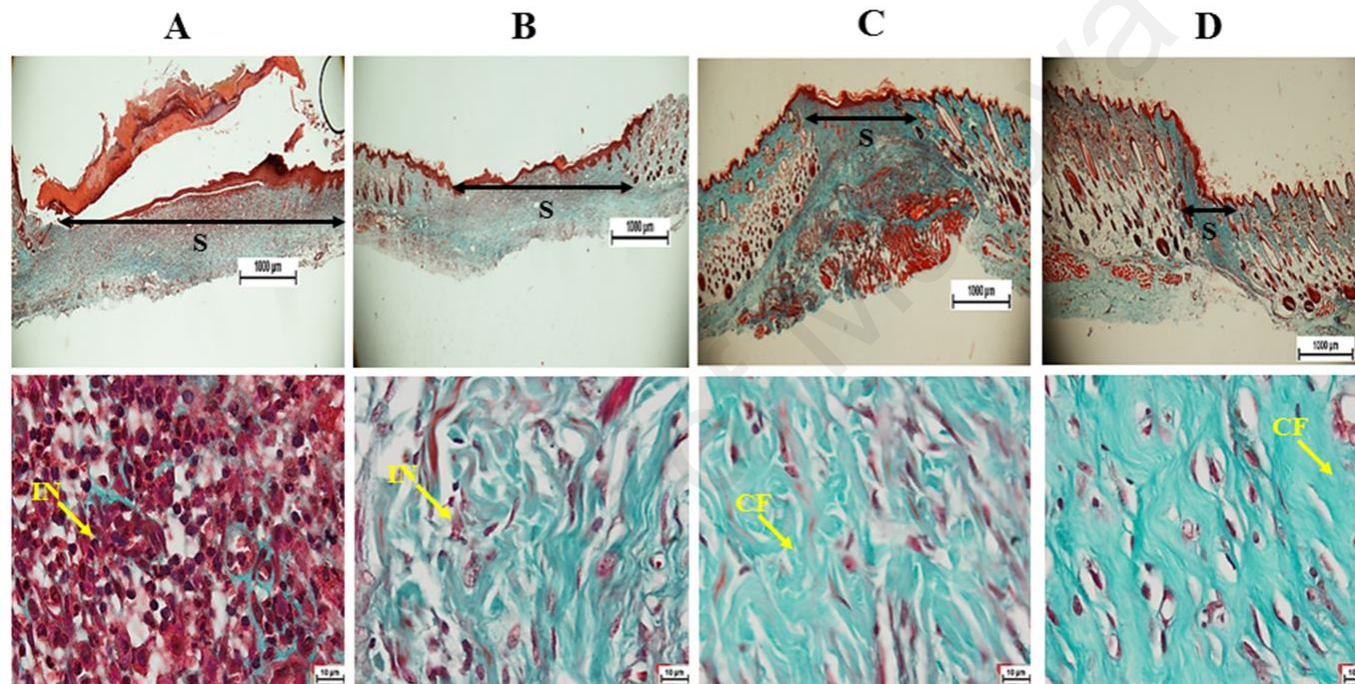


Figure 4.33: Photomicrographs of healed wound stained with Masson Trichrome at two magnifications

On the 20th day, wound tissues were taken from (A) blank vehicle, (B) HECPR (100 mg/ml), (C) HECPR (200 mg/ml) and (D) intrasite gel administrated rats. CF, collagen fibre; IN: inflammatory cell; S: scar width. Scale bar: 1000 μ m (low magnification) and 10 μ m (high magnification).

4.3.5.3 Immunohistochemistry

4.3.5.3.1 Topical Application of HECPR Effect on Bax Expression

Immunohistochemical analyses of the Bax expression of the HECPR in rat wounds are shown in (Figures 4.34B). Bcl-2-associated protein (Bax) staining of the wound from the HECPR group showed greater Bax staining. Histopathological examination of the intrasite gel group showed considerably less Bax staining compared with the control group. Furthermore, wounds from the HECPR-treated groups showed less Bax staining with few inflammatory cells, indicating improvement in healing. Sections of the healed wounds showed that the Bax protein expression was higher in the control group compared with the other groups that received treatment. The intrasite gel group and HECPR groups showed decreases of Bax protein expression when compared with the control group. Furthermore, 200 mg/ml of HECPR showed higher Bax protein expression compared with 100mg/ml of HECPR.

4.3.5.3.2 Topical Application of HECPR Induced Up-Regulation of Hsp70

Immunohistochemical analyses of the HSP70 expression in wounds healed with HECPR are shown in Figure 4.34A. The immunohistochemical reaction of heat shock protein 70 (HSP70) staining results showed that the control group had normal histological examination of healed wounds with lower HSP70, whereas the intrasite gel group showed fewer inflammatory cells with higher fibroblasts and an increase in HSP70 protein expression compared with the control group. The groups treated with HECPR showed fewer inflammatory cells and increased HSP70 protein expression levels compared with the vehicle group. Tissue sections of the healed wounds showed that HSP70 protein expression was lower in the control group compared with the other groups that received treatment. The Intrasite gel and HECPR groups had increased HSP70 protein expression

when compared with the control group. Furthermore, 200 mg/ml of HECPR showed the higher HSP70 protein expression compared with 100mg/ml of HECPR.

University of Malaya

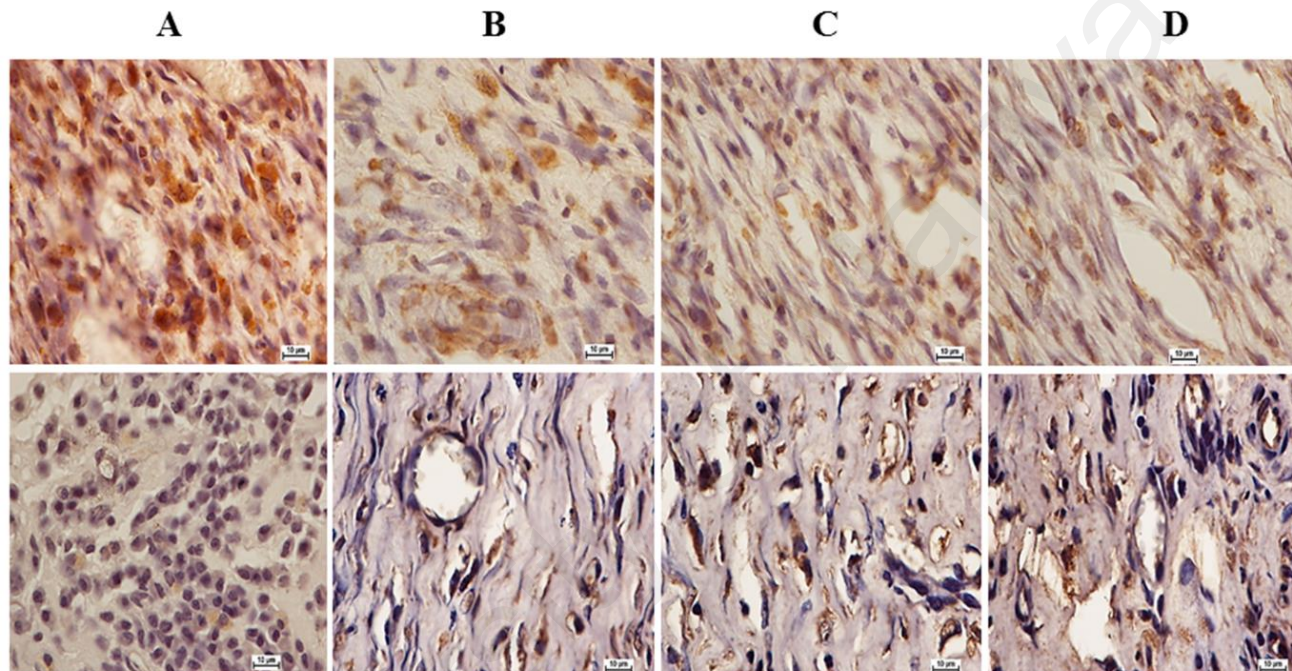


Figure 4.34: Bax and Hsp70 staining of wound area

Immunohistochemistry of wound tissue sections for Bax (first row) and Hsp70 (second row) proteins from four groups of rats treated with (A) blank placebo, (B) HECPR (100 mg/ml), (C) HECPR (200 mg/ml) and (D) intrasite gel after 20 days. Immunopositivity as shown by brown staining demonstrated down-regulation of Bax and up-regulation of Hsp70 in groups B-D. Scale bar: 10 µm.

4.3.5.4 Antioxidant Evaluation in the Healed Wound Area

Antioxidant enzymes (CAT, GPx, and SOD) were estimated in this study to evaluate the progression of the wound healing process and to determine the effect of HECPR. The results revealed that elevated CAT level was significant compared with vehicle control group (Figure 4.35A). A similar result was obtained with regard to GPx and SOD levels (Figure 4.35B and Figure 4.35C respectively).

Estimations of the effect of HECPR on catalase (CAT) in the tissue homogenate of dermal wounds in rats is shown in Figure 4.35 A. The effect of HECPR on CAT enzyme activity among the different experimental groups was analysed. In the tissue homogenization of the dermal wounds of the rats, the CAT levels were decreased in the control group compared with the other groups. On the other hand, the HECPR groups showed increases in CAT levels compared with the control group. The results indicate that treatment with HECPR increased CAT levels in the tissue homogenate, as shown in the intrasite gel groups, which demonstrated the possible protective property of HECPR against tissue damage. Intrasite gel group had the highest CAT levels at a value of (84.56 U/mg protein), which is higher than the value of the HECPR 200mg/ml group (79.55U/mg protein).

Antioxidant enzyme GPX was estimated in this study to evaluate the progression of the wound healing process and determine the effect of the HECPR. The results revealed that elevated GPX level was significant $p < 0.05$ compared with vehicle control group (Figure 4.35C). The results indicate that treatment with HECPR increased GPX levels in the tissue homogenate, as shown in the Intrasite gel groups, which demonstrated the possible protective property of HECPR against tissue damage. Intrasite gel group had the highest GPX levels at a value of $(3.08 \pm 0.12 \text{U/mg protein})$, which is higher than the value of the HECPR 200mg/ml group $(2.46 \pm 0.40 \text{U/mg protein})$.

Evaluation of SOD in the tissue homogenates of dermal rat wounds for HECPR is shown in table 4.13. The effect of HECPR on SOD among the different experimental groups was analyzed. SOD levels were decreased in the control group at a value of (13.67 U/mg protein). The groups treated with HECPR and Intrasite gel had increased the levels of SOD concentration U/mg protein compared with the negative control group. In addition, in terms of treatment, Intrasite gel had the highest SOD level at a value of 34.18 U/mg protein. The SOD results were higher in rats dressed with HECPR and Intrasite gel than blank placebo group. The above results collectively support the suggestion that HECPR may provide a favourable host environment for accelerating the wound healing process.

University of Malaya

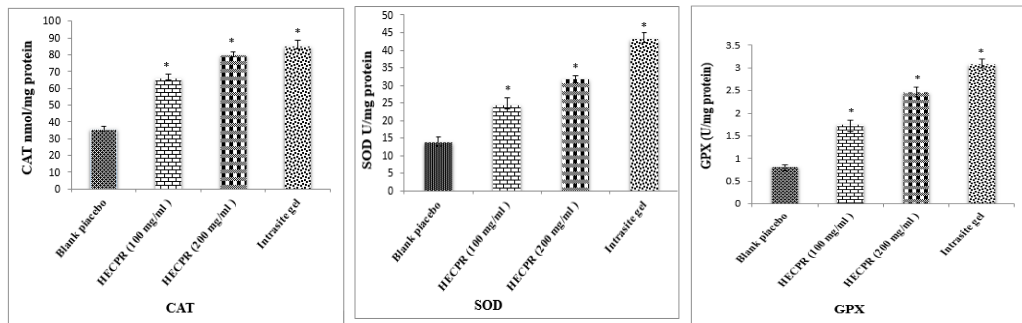


Figure 4.35: Effects of HECPR on CAT, GPX and SOD level in the healed wound area in the rats.

Values are presented as mean \pm SEM* Significant ($P < 0.05$) compared with the vehicle control. CAT, GPx and SOD from four groups of rats: (A) vehicle, (B) HECPR (100 mg/ml), (C) HECPR (200 mg/ml) and (D) intrastite gel, Values are expressed as mean \pm SEM, $n = 6$ animals in each group. * $p < 0.05$ vs negative control rats (A).

4.3.5.5 HECPR Attenuated the MDA Level

The estimation of lipid peroxidation index and TBARS-malondialdehyde (MDA) in tissue homogenates of dermal rat wounds is shown in Figure 4.36 for HECPR. MDA levels vary among different treatment groups. The intrasite gel group showed a significantly lower ($P < 0.05$) MDA level compared with control group. Generally rats dressed with gum acacia showed significantly increased levels of lipid peroxidation when compared with the groups treated with HECPR at doses 100mg/ml and 200mg/ml. Notably, among all the groups treated with HECPR and intrasite gel showed the lowest MDA levels at value of (22.12 ± 0.15 nmol/mg protein) at dose 100mg/ml in the wound homogenates. The above findings indicate that the skin of wounds dressed with HECPR may have been protected from lipid peroxidation during the course of the experiment.

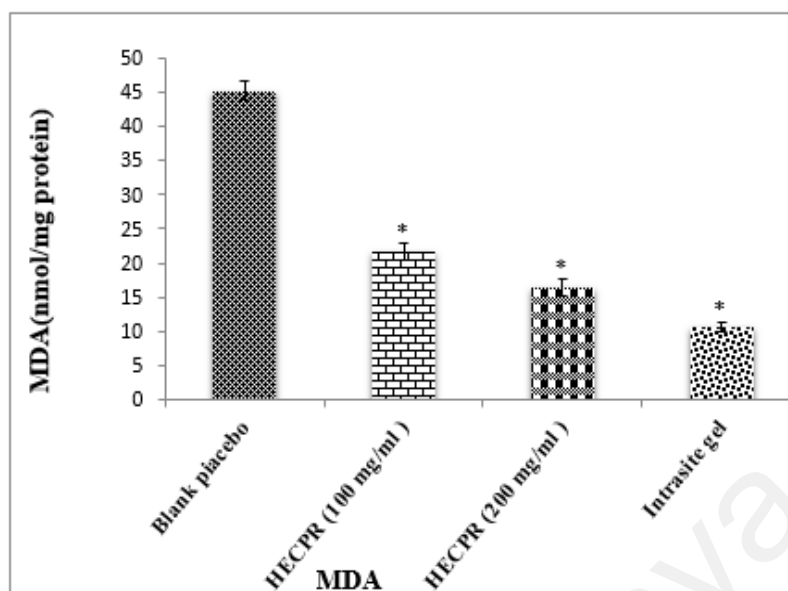


Figure 4.36: The MDA level in wounds tissues homogenates from four groups of rats

(A) Vehicle control, (B) HECPR (100 mg/ml), (C) HECPR (200 mg/ml) and (D) intrasite gel showed significant attenuation in topically treated rats with HECPR (100 mg/ml and 200 mg/ml) and Intrasite gel. Values are expressed as mean \pm SEM, $n = 6$ animals in each group. * $p < 0.05$ vs negative control rats (A).

4.3.6 Gas Chromatography Profile of DECPR and HECPR

As shown in Figure 4.39 and 4.40, the dichloromethane and hexane extract of *C. purpurascens* was characterized with a GC-MS-TOF analysis. The gas chromatography profile of DECPR and HECPR showed that the detected compounds in DECPR are c- Elemene (1), a-elemenone (2), ar-turmerone (3), turmerone (4) and curlone (5), with turmerone (4) as the major compound and the major compounds in HECPR are c-elemene (1), benzofuran, 6-ethenyl-4,5,6,7-tetrahydro-3,6-dimethyl-5-isopropenyl (2), 3,7-cyclodecadien-1-one,3,7-dimethyl-10-(1-methylethylidene) (3), turmerone (4) and curlone (5) table 4.14 and 4.15.

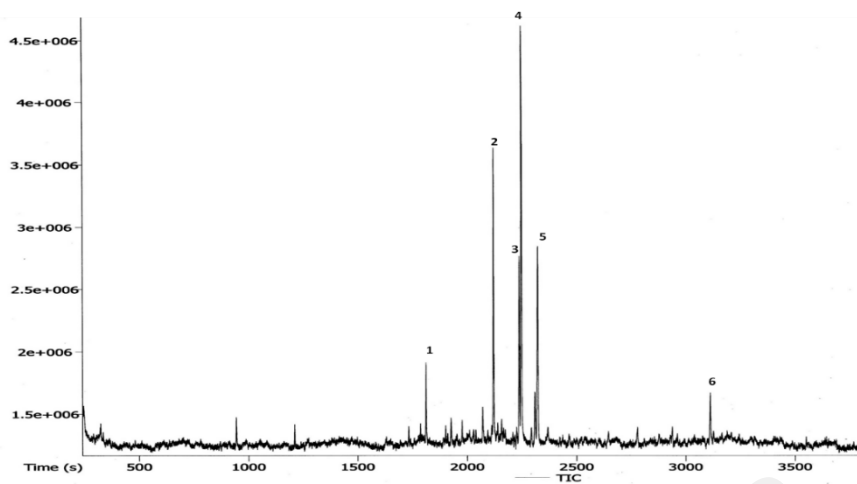


Figure 4.37 : A gas chromatogram of the chemical constituents of DECPR

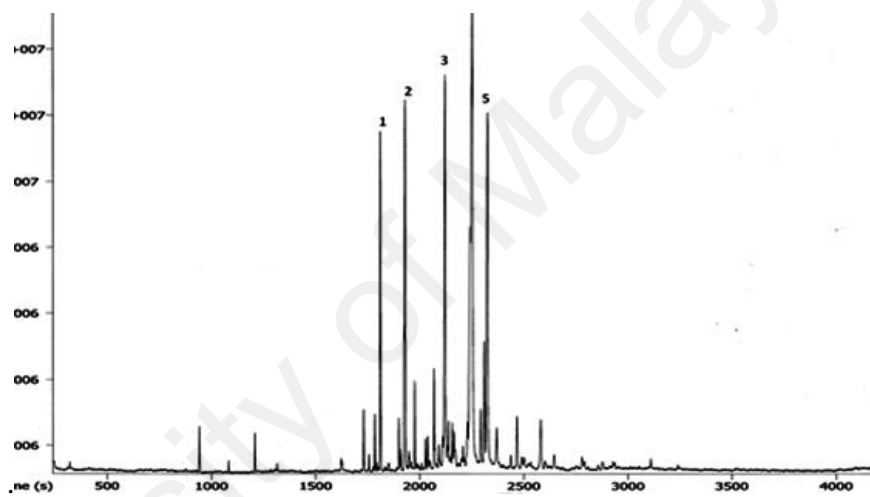


Figure 4.38: A gas chromatogram of the chemical constituents of HECPR

Table 4.13: The possible compounds in DECPR were characterized using a GC-MS-TOF analysis

Peak No.	Name of Compounds	Retention Time (s)	Mass
1	c-Elemene	1810.45	189
2	a-Elemenone	2119	218
3	ar-Turmerone	2235.55	216
4	Turmerone	2245.75	218
5	Curlone	2319.85	218

Table 4.14: The possible compounds in HECPR were characterized using a GC-MS-TOF analysis

Peak No.	Name of Compounds	Retention Time (s)	Mass
1	c-Elemene	1812.55	189
2	benzofuran, 6-ethenyl-4,5,6,7-tetrahydro-3,6-dimethyl-5-isopropenyl	1931.3	216
3	3,7-cyclodecadien-1-one,3,7-dimethyl-10-(1-methylethylidene)	2123.3	218
4	Turmerone	2254.45	218
5	Curlone	2326.55	218

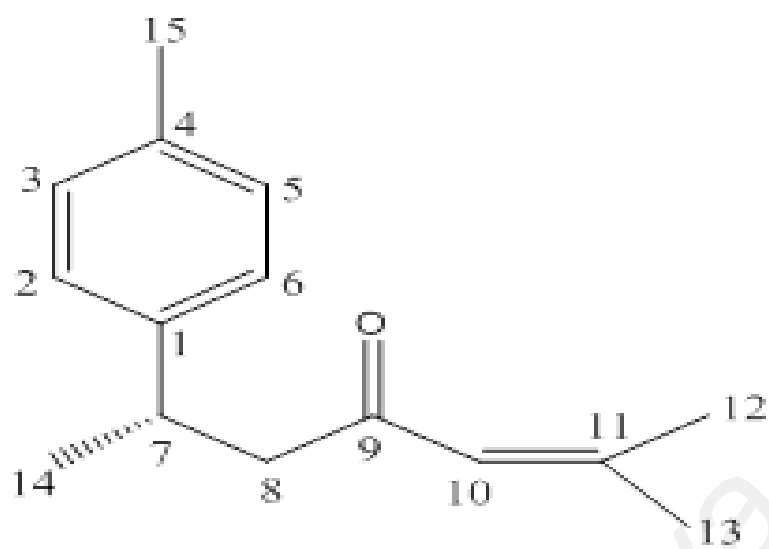


Figure 4.39: Chemical structure of Ar-turmerone (peak NO.4) Identified in DECPR

University of Malaya

CHAPTER 5: DISCUSSION

5.1 Antioxidant Activity

The presence of antioxidant activity in plants is important because of health by playing an important role in protecting the body cells from damage by oxidative stress. The secondary metabolites in plants are the most biologically active natural product compounds; therefore, plants are the sources of food antioxidants, and these include vitamin E, vitamin C, phenolic acids, carotenes and phytoestrogens. Polyphenol or phenolic compounds are a group of secondary metabolites; they are composed in the optimal structure from one aromatic ring, holding one or more hydroxyl groups. The simplest molecular form is phenolic acid and ranging from the flavonoids to more complex structure compounds (polymerized compounds) as lignin or tannins (Gupta et al., 2005). Plants are considerable the major natural sources to the polyphenols compounds (flavonoids and non- flavonoids); which gives the color and flavor in the plants (Barreto et al., 2009). Phenolic compounds play an important role in the life of the plant by contributing to the defense against microbial attacks. Flavonoids have been involved UV filtration, symbiotic nitrogen fixation and flora pigmentation. In addition, it acts as a chemical messenger and regulator to physiological functions. Finally, some flavonoids inhibit the growth of organisms that can cause diseases to plants (Chun et al., 2005). The antioxidant activity of DEPCR and HEPCR were evaluated by FRAP and DPPH tests are shown in Figure 4.2. HEPCR extract has statically significant high antioxidant potential when compared with DEPCR and standard ascorbic acid. The FRAP value of HEPCR extract is 2341.38 ± 45.40 mmole Fe⁺²/mg, while for DEPCR and standard ascorbic acid, the values are 1501.38 ± 25.12 , 10312.17 ± 29.81 mmole Fe⁺²/mg respectively. The total antioxidant activity is conducted by DPPH test that; detected DPPH inhibition % 86.79 ± 0.4 , as well as the IC₅₀ 14μg/ml for HEPCR, 9.81 ± 0.31 ; IC₅₀ 22 μg/ml for DEPCR and 13.52 ± 0.42 ; IC₅₀ 19 μg/ml for ascorbic acid. The total

phenolic contents are displayed in the Figure 4.3. The results revealed that the total phenolic content of HECPR is 461.15 ± 7.32 mg GAE/mg of dry rhizome weight while total phenolic content is 400.32 ± 6.76 mg GAE/mg in the DECPR.

5.2 *In vitro* studies

Plants from the *Curcuma* genus as represented by the turmeric spice, such as *C. longa*, *C. phaeocaulis*, *C. wenyujin* and *C. kwangsiensis* are well known to be valuable herbal medicines (Li et al., 2011). Due to the extensive biological activities reported for the chemical constituents of these plants, including anti-Alzheimer's disease (Ishrat et al., 2009), anti-inflammatory (Bansal et al., 2011), anti-angiogenesis (Li, et al., 2007) and anti-microbial (Zorofchian Moghadamtousi et al., 2014), a number of scientific works have been carried out on *Curcuma* species. The safety of these plants and their active compounds in animal studies in a number of species have been confirmed. However, some species were found to be susceptible to hepatotoxicity at high doses of turmeric (Chainani-Wu, 2003; Ireson et al., 2002). The present study demonstrated the safety of DECPR and HECPR in rats even at high dose of 5 g/kg without any signs of renal or hepatic dysfunction. In spite of numerous studies on *Curcuma* species, there is no report on biological activity of *C. purpurascens*, including its anti-cancer potential. Hence, in the current experiment, cytotoxic effect of *C. purpurascens* on different cancer cells was examined. Our results showed a promising suppressive effect of DECPR against HT-29 cells observed by MTT and LDH assays.

The growing body of experimental evidence supports the extensive anticancer effect of *Curcuma* species and their chemical constituents, known as curcuminoids, towards different cancer cells (Bar-Sela et al., 2010; Hu et al., 2011; Rao et al., 2012; Schaffer et al., 2011b; Wilken et al., 2011). *In vivo* studies and clinical trials for the treatment of various tumors have highlighted the role of curcuminoids and their analogues as promising therapeutic agents. Turmerone and its derivatives as major compounds

detected in DECPR were previously reported to have apoptotic effect towards different cancer cells, such as HL-60, MCF-7, MDA-MB-231 and HepG2 cancer cells (Aratanechemuge et al., 2002; Yue et al., 2010). However, the apoptotic effect of turmerone and its mechanism of action on HT-29 cells have not yet been fully elucidated.

Apoptosis is generally characterised by specific morphological characterizations, including cell shrinkage, nuclear or cytoplasmic fragmentations, chromatin condensation and formation of dense bodies that are phagocytosed by neighboring cells (Bottone et al., 2013). It is well established that restructuring of actin cytoskeleton has a critical role in the formation of morphological changes in apoptotic cells (May & Machesky, 2001). Our study indicated that DECPR treatment induced nuclear shrinkage and fragmentation after 24 h. This result was associated with alteration in actin filaments polymerizations in the treated HT-29 cells. Previous studies showed that standard anticancer drugs such as cisplatin and tamoxifen cause F-actin damages prior to the induction of nuclear changes in cancer cells (Acconcia et al., 2006; Kruidering et al., 1998).

ROS can generate nonradical derivatives of oxygen, such as H_2O_2 and free radicals, namely hydroxyl radical (OH^\cdot) and superoxide (O_2^\cdot) (Moustafa et al., 2004). The excessive production of free radicals has been demonstrated to accelerate cell death by inducing severe damages to DNA, lipid membranes and proteins of cells (Simon et al., 2000). In the current study, we found that DECPR significantly induced ROS generation in HT-29 cells.

A previous study showed that the primary initiating signaling factor of ROS was markedly involved in three different signaling pathways of apoptosis induced by curcumin in L929 cells showing the critical role of ROS generation in the suppressive effect of different anticancer agents (Thayyullathil et al., 2008). It is well-established that numerous apoptotic stimuli, including ROS generation, initiate apoptosis by disturbing mitochondrial function that is sufficient to trigger leakage of cytochrome *C* from

mitochondria (Nicholls, 2004). Production of MMP across the mitochondrial inner membrane is the result of utilization of oxidizable substrates, therefore excessive generation of ROS in cells may lead to the loss in MMP (Gottlieb et al., 2003). This is showed by High-content screening (HCS) analysis on HT-29 cells after DECPR treatment which demonstrated significant reduction in mitochondrial membrane potential (MMP) and elevation in cell membrane permeability and cytochrome *C* release.

Cytochrome *C* release from mitochondria to cytosol activates the initiator and executioner caspases involved in the intrinsic pathway of apoptosis (Budihardjo et al., 1999; Huang et al., 2011). The biochemical changes of this apoptotic pathway are mediated and tightly regulated by Bcl-2 family of proteins, including pro-apoptotic and anti-apoptotic proteins (Tsujimoto, 2003). Cytochrome *C* release is mediated through dimerization of Bax and Bak as a pro-apoptotic proteins (Scorrano & Korsmeyer, 2003). On the other hand, activity of pro-apoptotic proteins is facilitated through inhibition of anti-apoptotic proteins, e.g. Bcl-2 and Bcl-xl by intracellular stress signals (Youle & Strasser, 2008). In the present experiment, DECPR caused a dramatic cytochrome *C* leakage to cytosol in HT-29 cells as a key factor in apoptosome formation which leads to the cleavage of procaspase-9 to caspase-9 (Riedl & Salvesen, 2007). The investigation on the activation of caspases upon treatment with DECPR demonstrated the elevation in the activity of caspase-3 and -9.

According to these data, it is strongly conceivable that ROS production in HT-29 cells triggered the mitochondrial-initiated events leading to the cytochrome *C* release and activation of caspase cascade. Our investigations on the mRNA expression of apoptosis-associated proteins also supported the induction of apoptosis through mitochondrial-mediated pathway. Colon Cancer *In Vivo* to evaluate the chemopreventive effect of DECPR in animal model, ACF enumeration was applied as an easy indicator of colon neoplasia. Methylene blue dye was used to stain the proximal and distal parts of the

separated colons and quantitative results are reported in Table 4.11 and Figure 4.15. The rats that were treated with AOM experienced severe development of ACF, compared to the normal control group, which was evidenced by different numbers of crypts with increased sizes and by the reformed luminal epithelia (Figure 4.16). As shown in Table 4.11, the number of crypts were statistically significant in cancer control group (182 ± 6.47) compared to the treatment control (47 ± 3.69), and the low and high dose treatment with DECPR treated groups (80 ± 6.13 and 57 ± 5.78 respectively). The groups treated with the DECPR showed no significant difference with the treatment control. Figure 4.16 presents the scattering of the ACF formation in proximal and distal parts of the colons separated from the treated rats. The distal parts of the colons showed more aggregation of the ACF formation compared to the proximal part in all experimental groups (Figure 4.15).

The result of this study appears to be in line with previous studies which reported a higher number of ACF in distal parts of the colon compared to the proximal parts (Gourineni et al., 2011). The consequent ACF detriment was significantly attenuated by administration of DECPR at 250 mg/kg and 500 mg/kg concentrations with inhibitory percentage of 56.04% and 68.68%, respectively. A number of published findings on other *Curcuma* species and their isolated phytochemicals demonstrated similar suppressive and protective effect against paraneoplastic lesions of colon carcinogenesis (Bounaama et al., 2012; Kwon et al., 2004; Rao et al., 1995). This result demonstrates the promising chemopreventive potential of DECPR against chemical carcinogen-induced colon cancer in rats.

Due to its critical role in several biological pathways such as chromatin remodeling, cell cycle, DNA synthesis, repair and methylation, proliferating cell nuclear antigen (PCNA) is known to be a good index of cell proliferation (Maga & Hubscher, 2003; Mayer et al., 1993). An association between PCNA activity and tumour evolution

in clinical studies has indicated that this protein can be considered as a prognostic marker for cancer (Isozaki et al., 1994; Naryzhny & Lee, 2007). In addition, oncology investigations have found that excessive cell proliferation in epithelial colon tissues is inevitable in neoplasia development (De Leon et al., 1988; Lipkin et al., 1983).

Since development of ACF requires aberrant cell proliferation in colon tissues, we performed immunohistochemical analysis on PCNA protein. In the AOM-induced colon cancer model, this chemical carcinogen caused significant elevation in PCNA expression (PI: 67.68%), compared to the normal control group (PI: 1.5%). This observation was previously shown by other chemical carcinogens (Bishayee & Mandal, 2014; Deschner et al., 1983). After administration of DECPR to rats, PI was significantly reduced to 37.45% and 22.46% for low dose and high dose groups, respectively. The down regulation of PCNA protein expression was also detected in Western blot analysis (Figure 4.19). This result reveals that DECPR treatment causes a diminished proliferation zone in the colon tissues of rats and throws a light in involvement of proliferation pathways in the chemopreventive effect of DECPR.

The Bcl-2 family of proteins with 25 members has been established to be regulators and mediators of cellular life or death (Cory & Adams, 2002). This Bcl-2 family consists of two groups of proteins functioning as pro-apoptotic and anti-apoptotic molecules. In addition, these proteins have close relationship with mitochondria function. Therefore, changes in the expressions of these proteins can activate intrinsic or mitochondrial-mediated pathway of apoptosis (Green & Kroemer, 2004). For example, pro-apoptotic protein of Bax dimerizes and translocates to the outer mitochondrial membrane and provides a channel for release of several proteins including cytochrome C. However, this process can be suppressed by anti-apoptotic mediators, including Bcl-2, Bcl-x, Bcl-w and BAG (Ocker & Hopfner, 2012).

To determine the role of apoptosis in the chemopreventive potential of DECPR, we performed immunohistochemical analysis on Bax and Bcl-2 proteins. In the cancer control rats (group B), colon tissue sections revealed a small degree of immunostaining for Bax protein (Figure 4.20), while marked degree of immunostaining was depicted for Bcl-2 protein (Figure 4.21). A conspicuous increase in the Bax protein expression and decrease in the Bcl-2 protein expression were detected after administration of DECPR at 250 mg/kg (Group C) and 500 mg/kg (Group D) doses. The 5-FU drug group (Group E) showed a comparable result with groups treated with DECPR. Western blot analysis also confirmed the observed perturbations in the protein expression of Bax and Bcl-2 (Figure 4.22). It is previously reported that sufficient expression of Bax in cancer tissues may ameliorate the survival rate of cancer patients (Sturm et al., 2001). On the other hand, defect in Bax function has a substantial effect on cancer progression (Ionov et al., 2000). Our findings suggest that DECPR has a promising potential to activate mitochondrial-mediated apoptosis in cells exposed to chemical carcinogen. This result is in agreement with our previous *in vitro* investigation which showed induction of apoptosis in HT-29 cells through mitochondrial mediated apoptosis (Rouhollahi et al., 2015b).

A previous study showed that oxidative stress is involved in the pathogenesis of several diseases such as cancer and cardiovascular disorder (Granados-Principal et al., 2014). It has been shown previously that concomitant use of antioxidant drugs with anticancer agents such as doxorubicin can potentiate their therapeutic effects and ameliorate the survival rate of patients (Granados-Principal et al., 2014). Hence, development of new chemotherapeutic drugs with inborn antioxidant activity is in the best interests of cancer researchers. Moreover, identifying different potent antioxidants derived from natural products has stimulated significant scientific attentiveness in characterizing these phytochemicals to counteract the effects of oxidative stress (Zhang et al., 2012).

The antioxidant activity, including CAT, GPx and SOD in colon tissue homogenates from different groups of rats are depicted in (Figure 4.23). The level of CAT, GPx and SOD were significantly decreased in cancer-bearing animals (Group B) which shows similarity to previous studies (Moghadamtousi et al., 2015).

In rats treated with both doses of DECPR, these activities were significantly augmented compared to the cancer control group. As expected, DECPR elicited higher enzymic activities compared to the 5-FU chemotherapeutic drug group (Group E). This result was in line with a previous gastroprotective study on *C. purpurascens* rhizome which showed potent antioxidative potential of this plant (Rouhollahi, et al., 2014). Moreover, a number of investigations on other *Curcuma* species have established this genus as a source of phytochemicals with antioxidant and anti-inflammatory properties (Mau et al., 2003; Ramsewak et al., 2000; Srinivas et al., 1992). For instance, turmerone and its derivatives as the major phytochemicals of DECPR, have been shown to be potent antioxidants in previous studies (Jayaprakasha et al., 2002; Sacchetti et al., 2005; Tsai et al., 2011). Our result demonstrates that DECPR protect the colons of rats from oxidative stress which was provoked by AOM treatment.

Under cellular stress, neutrophils can cause the generation of superoxide radical anions which leads to the formation of lipid peroxides as a result of reaction with cellular lipids (Kobayashi et al., 2001). Several products, including lipid hydroperoxides, alkenes and MDA are degraded metabolites of this reaction, which eventually compromise the cell membrane integrity (Pandurangan et al., 2012; Vaca et al., 1988). Since MDA is a prime product of lipid peroxidation, it is defined as an effective marker of this process (Demircan et al., 2005; Moghadamtousi et al., 2015). As shown in Figure 4.23, AOM administration to rats provoked significant MDA production due to lipid peroxidation. This result was in agreement with previous reports showing the augmented MDA generation in tissue and plasma of patients suffering from colorectal cancer (Hendrickse

et al., 1994; Skrzydlewska et al., 2005). Administration of rats with DECPR at 250 and 500 mg/kg doses attenuated MDA production in tissue homogenates. This protective effect against lipid peroxidation was more effective than that produced by 5-FU. Our data verified the antioxidative potential of DECPR against the induced oxidative stress by a chemical carcinogen, which was reflected by decreased level of MDA.

5.3 Gastric ulcer

In the present study, one of the contributing factors in gastric ulcer formation is ethanol. Due to the rapid penetration of ethanol into the gastric mucosa, it is widely utilized to induce experimental gastric ulcer in numerous *in vivo* studies (Abdulaziz et al., 2013; Mahmood et al., 2005; Vieira et al., 2013). The elevation in mucosal permeability and release of vasoactive products by ethanol result in vascular damage and astric cell necrosis prior to the ulcer formation. Furthermore, it is believed that the generation of reactive oxygen species (ROS) by ethanol has a significant role in ulcer formation (Golbabapour et al., 2013). Therefore, in our study, the administration of ethanol to rats was used to induce gastric lesions. Our findings in this study showed that HECPR can effectively suppress gastric acidity and also suppress the destruction of gastric wall mucus. It was reported earlier that herbal products could elevate the gastro-defensive system, especially gastric wall mucus secretion in patients with gastric ulcer (Iijima et al., 2009). The depletion of mucus secretion is one of the pathogenic mechanisms accountable for gastric mucosal erosions (Alvarez-Suarez et al., 2011). Previous studies have explained the close correlation between suppression of gastric acidity and effectiveness of treatment. The ability to attenuate the gastric acid secretion is considered to be the mainstay of treatment for gastric ulceration (Howden & Hunt., 1990; Hunt et al., 2008). One of the standard drug, omeprazole, has shown remarkable healing rates among patients with peptic ulcer because of its ability to minimize the degree of gastric acidity through inhibition of the proton pump (Lin et al., 2006). The perturbation in balance

between gastro-protective mechanisms and gastrototoxicity of different agents is the basis of acute inflammation and secretion of several proinflammatory cytokines (Xu et al., 2010). It is reported earlier that acute inflammation induced by ethanol is accompanied by neutrophils infiltration of gastric wall mucus (La Casa et al., 2000). As shown in Figure 4.26, our results demonstrated that submucosal infiltration was effectively suppressed by pretreatment of rats with HECPR. An extensive generation of ROS and free radicals causes metabolic impairments and irreversible cell damages in the human body (Liao et al., 2013). As such, protecting the gastric tissue from oxidative damages can provide successful treatment approaches by natural products against ulcer formation (Chen et al., 2003). Superoxide dismutase by converting the superoxide to hydrogen peroxide has a critical role in this protecting effect (Van Raamsdonk & Hekimi, 2012). Superoxide radical anions such as ROS are generated by neutrophils, which results in the reaction with cellular lipids and the reduction of lipid peroxides (Demircan et al., 2005). An effective indicator of oxidative stress and mucosal injuries by ROS is malondialdehyde (MDA), which is a major metabolite of lipid peroxidation (Weismann et al., 2011). This is the first study to show that oral administration of HECPR could protect against gastric ulceration by elevating superoxide dismutase activity, which is reflected by decreased MDA production. In our study, the NO level is significantly increased after pre-treatment with HECPR. The important role of NO synthesis for the gastroprotective system and effectiveness of anti-ulcer agents has been elucidated earlier (Weismann et al., 2011). It has been shown that suppression of NO pathway by L-NAME markedly inhibited the gastroprotective activity of several anti-ulcer medications. Furthermore, formation of ethanol-induced gastric lesions is remarkably abolished by NO-stimulating drugs. Meanwhile, reduction in NO synthesis can increase the susceptibility of the gastric mucosa to the destructive effects of ethanol (Allami et al., 2011; Riano et al., 2011). Therefore, increasing NO level by HECPR treatment is beneficial in alleviating ethanol-

induced gastric wall destruction as shown in this study. Our findings showed that administration of HECPR to rats induced the up-regulation of Hsp70 protein associated with down-regulation of Bax protein. Hsp70 is a 70 kDa protein which belongs to the heat shock protein family. This protein is abundantly produced in response to various forms of stress, such as toxic agents, oxidative stress, infection and heat shock (Li et al., 2012). It is well known that the ethanol-triggered generation of ROS could suppress Hsp70 expression and intensifies the oxidative damages (Shichijo et al., 2003). Hence, natural products with the ability to induce the over-expression of Hsp70 may provide higher threshold of protection against gastric lesions (Shim et al., 2011). Previous studies have demonstrated that the suppression of Bax expression or its dysfunction can protect cells against programmed cell death through prevention of cytochrome C release from mitochondria to cytosol. A variety of stimuli, including heat, radiation and excessive production of ROS cause the dimerization of Bax protein and translocation to the outer mitochondrial membrane, which trigger cytochrome C release (Elmore, 2007; Hetz et al., 2005; Ocker & Höpfner, 2012). In our study, suppression of ROS production induced by HECPR seems to be the reason for the attenuation of Bax expression. Previous study done using *Curcuma longa* showed that hexane soluble fraction of the rhizome was effective against HCl-induced peptic ulcer, while the hexane non-soluble fraction was inactive (Nutakul, 2013). Therefore, in this study, the hexane extract was used to investigate the anti-ulcer potential of *C. purpurascens* rhizome. Furthermore, gas chromatography profile of HECPR suggested the presence of turmerone as the major active compound. Turmerone is an active constituent with powerful antioxidant activity, which has been previously isolated from other *Curcuma* species (Liao et al., 2013). A previous clinical trial suggested that turmerone is responsible for the anti-ulcer effect of *C. longa* (Prucksunand et al., 2001). However, insufficient research studies on the photochemistry

of this spice could not provide enough evidence to confirm the major role of turmerone for the observed anti-ulcer effect.

5.4 Wound healing

In ethno medicine of Indonesia, *C. purpurascens* rhizome has been employed for its wound healing effect with topical use on the skin (Koller, 2009a). A previous study on the essential oil content of the rhizome showed the presence of turmerone, germacrone, *ar*-turmerone as the major compounds (Hong et al., 2014). These sesquiterpenoids are well established as effective biological molecules with antioxidant property (Bakkali et al., 2008; Jayaprakasha et al., 2005). Despite the fact that the chemical constituents of *C. purpurascens* rhizome strongly support its application as the wound healing agent (Farahpour et al., 2014; Thakare et al., 2011), a scientific examination is still required to substantiate its use in folk medicine. Therefore, in the current study, we evaluated the effect of the topical administration of HECPR on excision wound model in rats.

The mean percentage of wound contraction was determined after 5, 10, 15 and 20 days of treatment in all four groups. The curative effect of HECPR at both doses (100 and 200 mg/ml) after 20 days is distinctly obvious in the gross appearance of excision wound, compared to the negative control group (Figure 4.30). During the initial 5 days, the healing rate was significantly higher than the negative control only in rats treated with Intracite gel (39.16%, positive control). However, after 10 days, topical treatment with HECPR at both doses showed significant wound healing activity (low dose: 56.21%, high dose: 63.8% and positive control, 69.31%). Similarly after 20 days, the percentage of wound closure was significantly higher in rats treated with HECPR (100 and 200 mg/ml) and intracite gel (Figure 4.31). No significant difference between wound healing effect of HECPR (100 and 200 mg/ml) groups and positive control group after 20 days

demonstrated their comparable effectiveness. These results showed the potential effect of HECPR in accelerating the process of excisional wound healing in rats.

Histological analysis of the wound tissues was carried out on day 20 after operation using H & E and Masson Trichrome stainings. As shown in Figure 4.32 and Figure 4.33, both stainings illustrated that the scar width was considerably reduced after topical administration of HECPR for 20 days, when compared with negative control group. The granulation tissues from rats treated with blank placebo contained high number of inflammatory cells (mononuclear cells), which were comparatively reduced after topical treatment with HECPR (both concentrations) or Intrasite gel (Figure 4.32 and Figure 4.33). Instead, the collagen fiber and fibroblast formations were conspicuously stimulated and enhanced in these three groups. In addition, as illustrated in Figure 4.33, new blood vessels were actively formed in rats treated with HECPR at both concentrations, comparable with the intrasite gel group.

Histological evaluations revealed a significant elevation in wound repair after topical administration of HECPR. Mechanisms underlying this effect could be due to an increase in angiogenesis and deposition of collagen fibers. Collagen, a principal component of connective tissue, is a critical contributing factor for the tensile strength of healing wounds (Al-Bayaty et al., 2012). Our results showed that apart from a decline in the number of inflammatory cells, collagen fiber synthesis was augmented in the wound site. Impairment of blood flow to the wound site cause severe deficiencies in the wound healing process, including decreased anabolic activity, impaired local immune and cell defences, oxidative stress, protein malnutrition and shortage of growth factors. All these factors amplify the collapse in collagen and fibroblast synthesis (Davidson et al., 1985; Longo et al., 2011). As a major determinant in the wound healing process, angiogenesis enables oxygen and nutrient deliveries to the wound area which result in the suppression

of ROS stress and the facilitation of the local collagen synthesis and reepithelialisation (Buemi et al., 2004).

The energy dependant mechanism of apoptosis has a pivotal role in the progression of wound healing process (Moghadamtousi, et al., 2015 & Rai et al., 2005). Neutrophils are the first cells that arrive at the wound site to eliminate microorganisms and initiate the inflammatory process (Ohta et al., 1994). Neutrophils and other recruited inflammatory cells could generate ROS in the wound area (Rai et al., 2005). Excessive production of reactive species oxygen at the wound site results in the induction of apoptosis of surrounding cells, including keratinocytes (Roberts & Sporn, 1993), through activation of pro-apoptotic protein such as Bax and further mitochondrial-initiated events (Ocker & Höpfner, 2012). Immunohistochemistry staining of the wound sections demonstrated marked Bax protein expression in rats treated with vehicle, indicating that the wound healing process is still at the inflammatory phase. However, the other three groups treated with HECPR (both doses) and intrasite gel showed a remarkable decrease in Bax protein expression, demonstrating that the wound healing process was at a later stage. This level of Bax protein expression and induction of apoptosis in these groups are possibly to remove the scar and as a part of normal homeostasis of the tissue cells.

Heat shock proteins (HSPs) are highly conserved family of proteins and amongst the most copious intracellular proteins (Benjamin & McMillan, 1998). Study show that the level of HSPs expression is elevated after exposure of cells to a wide variety of stress, including wound injury (Atalay et al., 2009). HSPs have a pivotal role in the wound healing process through attenuation of the inflammatory responses. Moreover, HSPs defend tissues against injuries by preserving synthesis and conformation of proteins, repairing damaged proteins and accelerating the healing process (Lamore et al., 2010). It was previously established that HSP70 is the most abundant inducible HSP in the wound bed, therefore its protein expression was determined in this study using

immunohistochemistry analysis (Wagstaff et al., 2007). As illustrated in Figure 4.34, topically treated rats with vehicle elicited the basal level of HSP70, however the inflammatory cells (mononuclear cells) clearly accumulated in the wound section. The brown staining representing the HSP70 protein expression was elevated after administration of HECPR at 100 and 200 mg/ml concentrations. The induction of HSP70 protein expression by HECPR was comparable with the effect of intrasite gel. These results strongly suggest that HECPR induced the protein expression of HSP70 in the wound tissue which subsequently accelerated wound healing process.

Free radicals or reactive oxygen species (ROS) play a pivotal role in wound healing process. Skin ischemia in the tissue site cause ROS production by activated leukocytes which can be amplified by positive feedback between the release of free radicals and accumulation of leukocytes (Bickers & Athar, 2006). Moreover, in the inflammation phase, phagocytosis and digestion of wound debris by neutrophils and macrophages led to the excessive ROS formation in the wound site (Clark & Moon, 1999). The human body regulates ROS homeostasis through enzymatic systems. The main class of cellular enzymatic antioxidants consists of CAT, GPx and SOD which play an important role in the vascular system by attenuation of oxidative stress (Singh et al., 2011). Nonetheless, excessive accumulation of highly reactive radicals could induce different structural changes, including damages to mitochondrial DNA, lipids and proteins, which result in further reversible or irreversible cell injuries (Valko et al., 2007).

As shown in Table 4.13, after topical administration of HECPR (100 and 200 mg/ml), CAT, GPx and SOD activities were significantly augmented in wound tissue homogenates compared with those treated with vehicle. The increased enzymatic antioxidants of HECPR in wound tissues, especially at 200 mg/ml, were comparable to the positive control. These results were in agreement with previous studies exploring the antioxidant effects of compounds and extracts from *Curcuma* species. An earlier study

on four species of *Curcuma* showed the major role of sesquiterpenoids in the antioxidant potential of *Curcuma* species (Zhao et al., 2010). Investigation on antioxidant capacity of curcumin-free turmeric oil with major compounds of ar-turmerone, turmerone and curlone introduced this oil as alternative natural antioxidants (Yu et al., 2008). Another *in vivo* study on antioxidant and anti-hyperlipidaemic effects of turmeric oil with turmerone as the most abundant compound, revealed the preventive effect of turmeric oil against oxidative stress generation in hyperlipidaemic rats (Ling et al., 2012). These findings showed that the marked enzymatic antioxidant effect of HECPR may be a contributing factor in the wound healing potential of HECPR. In biological systems, lipid peroxidation is generally defined as the free-radical oxidation of polyunsaturated fatty acids (Gutteridge, 1995). The excessive production of ROS, including hydroxyl radicals in wound tissues induces lipid peroxidation and causes damage to the cells (Muralikrishna Adibhatla & Hatcher, 2006). Impairment in the functions of collagen and fibroblast metabolism, endothelial cells and keratinocyte capillary permeability is one of the destructive effects of lipid peroxidation. Moreover, as a detrimental factor in the expression of vascular endothelial growth factor (VEGF), lipid peroxidation can negatively impact the progress of wound healing process (Altavilla et al., 2011). As one of the most copious carbonyl products of this process, MDA is an easy index of lipid peroxidation (Marnett, 2002). As shown in Figure 4.36, topical administration of HECPR (both doses) and intrasite gel significantly declined the MDA level in the wound tissues of rats, compared to the negative control group. However, there was no significant difference between MDA level in the HECPR treated rats and intrasite gel treated rats representing that HECPR at both doses attenuated lipid peroxidation with comparable results with the positive control.

CHAPTER 6: CONCLUSION

The results evidenced the occurrence of apoptotic death in the HT-29 cells treated with these extract, as illustrated by chromatin condensation, DNA fragmentation, and membrane blebbing. Furthermore, the treatment of HT-29 cells with both extracts significantly increased the generation of reactive oxygen species, which triggered further mitochondrial-initiated events. The collapse of the mitochondrial membrane potential and the elevated release of cytochrome *C* from the mitochondria to the cytosol indicate the involvement of the intrinsic pathway in the induction of apoptosis. The role of the mitochondria-dependent apoptotic pathway was further proven by the significant activation of the initiator caspase-9 and the executioner caspases-3 and -7. The DECPR extract chemopreventive effects against AOM-induced colon cancer that have been demonstrated by reductions in the numbers of ACFs in the distal, middle and proximal colon. Reductions in the damage induced by AOM in the treated rats supported the microscopic evidence and demonstrated the significant chemopreventive activity of extracts to reverse the negative effects of AOM in the colon. Possible mechanisms of this chemoprevention include the down-regulation of cell proliferation-promoting proteins in cancer cells (which was demonstrated by PCNA immunohistochemistry) and the elevation of the levels of antioxidant enzymes that protect colon cells from the oxidative injury caused by the injection of azoxymethane. Western blot analyses revealed that the complexes activated apoptosis via the mitochondrial pathway by down-regulating Bcl-2 and PCNA and up-regulating Bax.

Our results indicate that *Curcuma purpurascens* BI pretreatment has protective effects against ethanol induced gastric ulcer in rats. Moreover, these results provide evidence that these protective effects of the plant are carried out by a significant effect on some important antioxidant enzymes, such as SOD and CAT which are scavengers of ROS and can prevent gastric injury. Furthermore this plant extract can be associated with a protection

of gastric mucus excretion, by enhancing many mechanisms to protect the gastric mucosa from offensive factors by decreasing the gastric acidity, increasing production of mucus, decreasing the level of gastrin, pepsin and MDA.

The current study suggests that HECPR have significant excision wound-healing potential. Topical treatment with HECPR improved the activity of endogenous antioxidants through elevation of the activity of SOD and CAT that prevented free radical-mediated tissue injury. This extract also played an important role in the regulation of apoptosis protein and it is efficacious in the remodeling phase of wound healing. The effectiveness of HECPR in acceleration of wound healing in rats may be due to an effect on antioxidant enzymes and a decrease in the MDA level that indicate decrease in the damage of the cell. In addition, an important role in the regulation of apoptosis gene expression (Bax and Bcl-2) and its efficacy in the remodeling phase in wound healing. Besides, the results clearly indicate the effect of HECPR in accelerating the wound healing process to be due to acceleration to the proliferative phase and shortening of the inflammatory phase in order to enhance wound contraction.

To conclude, the results of our study clearly indicate that *Curcuma purpuracens* extracts are safe and have anti-cancer activity, cancer preventive and gastroprotective and wound healing potentials. Both extracts HECPR and DECPR have great potential, however, further pharmacological studies and development of the extracts need to be carried out in order to take it a step further as potential therapeutic agents.. This study is in line with development of traditional plants as treatment or supplementary treatment of diseases through scientific methodologies.

REFERENCES

- Abdelwahab, S. I., Mohan, S., Abdulla, M. A., Sukari, M. A., Abdul, A. B., Taha, M. M. E., Syam, S., Ahmad, S., & Lee, K.-H. (2011). The methanolic extract of *Boesenbergia rotunda* (L.) Mansf. and its major compound pinostrobin induces anti-ulcerogenic property in vivo: possible involvement of indirect antioxidant action. *Journal of ethnopharmacology*, *137*(2), 963-970.
- Abdulaziz B, D., Halabi, M. F., Abdullah, N. A., Rouhollahi, E., Hajrezaie, M., & Abdulla, M. A. (2013). In vivo evaluation of ethanolic extract of *Zingiber officinale* rhizomes for its protective effect against liver cirrhosis. *BioMed Research International*, *2013*(2013),10.
- Acconcia, F., Barnes, C. J., & Kumar, R. (2006). Estrogen and tamoxifen induce cytoskeletal remodeling and migration in endometrial cancer cells. *Endocrinology*, *147*(3), 1203-1212.
- Adelstein, B.-A., Macaskill, P., Chan, S. F., Katelaris, P. H., & Irwig, L. (2011). Most bowel cancer symptoms do not indicate colorectal cancer and polyps: a systematic review. *BMC gastroenterology*, *11*(1), 65.
- Adler, D. G. (2005). Aberrant crypt foci as biomarkers for colonic dysplasia. *Nature Clinical Practice Gastroenterology & Hepatology*, *2*(9), 390-391.
- Aihara, T., Nakamura, E., Amagase, K., Tomita, K., Fujishita, T., Furutani, K., & Okabe, S. (2003). Pharmacological control of gastric acid secretion for the treatment of acid-related peptic disease: past, present, and future. *Pharmacology & therapeutics*, *98*(1), 109-127.
- Al-Bayaty, F., & Abdulla, M. A. (2012). A comparison of wound healing rate following treatment with aftamed and chlorine dioxide gels in streptozotocin-induced diabetic rats. *Evidence-Based Complementary and Alternative Medicine*, *2012*.
- Alam, S., Asad, M., Asdaq, S. M. B., & Prasad, V. S. (2009). Antiulcer activity of methanolic extract of *Momordica charantia* L. in rats. *Journal of ethnopharmacology*, *123*(3), 464-469.
- Allami, N., Javadi-Paydar, M., Rayatnia, F., Sehat, K., Rahimian, R., Norouzi, A., & Dehpour, A. R. (2011). Suppression of nitric oxide synthesis by L-NAME reverses the beneficial effects of pioglitazone on scopolamine-induced memory impairment in mice. *European journal of pharmacology*, *650*(1), 240-248.
- AlRashdi, A. S., Salama, S. M., Alkiyumi, S. S., Abdulla, M. A., Hadi, A. H. A., Abdelwahab, S. I., Taha, M. M., Hussiani, J., & Asykin, N. (2012). Mechanisms of gastroprotective effects of ethanolic leaf extract of *Jasminum sambac* against HCl/ethanol-induced gastric mucosal injury in rats. *Evidence-Based Complementary and Alternative Medicine*, *2012*(2012), 786426.

- Altavilla, D., Squadrito, F., Polito, F., Irrera, N., Calò, M., Lo Cascio, P., Galeano, M., La Cava, L., Minutoli, L., & Marini, H. (2011). Activation of adenosine A_{2A} receptors restores the altered cell-cycle machinery during impaired wound healing in genetically diabetic mice. *Surgery*, *149*(2), 253-261.
- Alvarez-Suarez, J. M., Dekanski, D., Ristić, S., Radonjić, N. V., Petronijević, N. D., Giampieri, F., Astolfi, P., González-Paramás, A. M., Santos-Buelga, C., & Tulipani, S. (2011). Strawberry polyphenols attenuate ethanol-induced gastric lesions in rats by activation of antioxidant enzymes and attenuation of MDA increase. *PloS one*, *6*(10), e25878.
- Aratanechemuge, Y., Komiya, T., Moteki, H., Katsuzaki, H., Imai, K., & Hibasami, H. (2002). Selective induction of apoptosis by ar-turmerone isolated from turmeric (*Curcuma longa* L) in two human leukemia cell lines, but not in human stomach cancer cell line. *International Journal of Molecular Medicine*, *9*(5), 481-484.
- Asghar, Z., & Masood, Z. (2008). Evaluation of antioxidant properties of silymarin and its potential to inhibit peroxy radicals in vitro. *Pak J Pharm Sci*, *21*(3), 249-254.
- Ashcroft, G. S., Mills, S. J., Lei, K., Gibbons, L., Jeong, M.-J., Taniguchi, M., Burow, M., Horan, M. A., Wahl, S. M., & Nakayama, T. (2003). Estrogen modulates cutaneous wound healing by downregulating macrophage migration inhibitory factor. *Journal of Clinical Investigation*, *111*(9), 1309.
- Astin, M., Griffin, T., Neal, R. D., Rose, P., & Hamilton, W. (2011). The diagnostic value of symptoms for colorectal cancer in primary care: a systematic review. *The British Journal of General Practice*, *61*(586), e231.
- Atalay, M., Oksala, N., Lappalainen, J., Laaksonen, D. E., Sen, C. K., & Roy, S. (2009). HEAT SHOCK PROTEINS IN DIABETES AND WOUND HEALING. *Current protein & peptide science*, *10*(1), 85-95.
- Bagchi, D., Carryl, O., Tran, M., Krohn, R., Bagchi, D., Garg, A., Bagchi, M., Mitra, S., & Stohs, S. (1998). Stress, diet and alcohol-induced oxidative gastrointestinal mucosal injury in rats and protection by bismuth subsalicylate. *Journal of applied toxicology*, *18*(1), 3-13.
- Bakkali, F., Averbeck, S., Averbeck, D., & Idaomar, M. (2008). Biological effects of essential oils—a review. *Food and chemical toxicology*, *46*(2), 446-475.
- Bansal, S. S., Vadhanam, M. V., & Gupta, R. C. (2011). Development and in vitro-in vivo evaluation of polymeric implants for continuous systemic delivery of curcumin. *Pharmaceutical research*, *28*(5), 1121-1130.
- Bar-Sela, G., Epelbaum, R., & Schaffer, M. (2010). Curcumin as an anti-cancer agent: review of the gap between basic and clinical applications. *Current Medicinal Chemistry*, *17*(3), 190-197.
- Bardi, D. A., Halabi, M. F., Hassandarvish, P., Rouhollahi, E., Paydar, M., Moghadamtousi, S. Z., Al-Wajeeh, N. S., Ablat, A., Abdullah, N. A., & Abdulla, M. A. (2014). *Andrographis paniculata* Leaf Extract Prevents Thioacetamide-Induced Liver Cirrhosis in Rats. *PloS one*, *9*(10), e109424.

- Barkun, A., & Leontiadis, G. (2010). Systematic review of the symptom burden, quality of life impairment and costs associated with peptic ulcer disease. *The American journal of medicine*, 123(4), 358-366. e352.
- Barreto, G. P., Benassi, M. T., & Mercadante, A. Z. (2009). Bioactive compounds from several tropical fruits and correlation by multivariate analysis to free radical scavenger activity. *Journal of the brazilian chemical society*, 20(10), 1856-1861.
- Baum, C. L., & Arpey, C. J. (2005). Normal cutaneous wound healing: clinical correlation with cellular and molecular events. *Dermatologic surgery*, 31(6), 674-686.
- Béjar, L. M., Gili, M., Infantes, B., & Marcott, P. F. (2012). Incidence of colorectal cancer and influence of dietary habits in fifteen European countries from 1971 to 2002. *Gaceta Sanitaria*, 26(1), 69-73.
- Benjamin, I. J., & McMillan, D. R. (1998). Stress (heat shock) proteins molecular chaperones in cardiovascular biology and disease. *Circulation Research*, 83(2), 117-132.
- Benzie, I. F., & Strain, J. (1996). The ferric reducing ability of plasma (FRAP) as a measure of "antioxidant power": the FRAP assay. *Analytical biochemistry*, 239(1), 70-76.
- Bian, J., & Sun, Y. (1997). Transcriptional activation by p53 of the human type IV collagenase (gelatinase A or matrix metalloproteinase 2) promoter. *Molecular and cellular biology*, 17(11), 6330-6338.
- Bickers, D. R., & Athar, M. (2006). Oxidative stress in the pathogenesis of skin disease. *Journal of Investigative Dermatology*, 126(12), 2565-2575.
- Biesalski, H. (2010). Micronutrients, wound healing, and prevention of pressure ulcers. *Nutrition*, 26(9), 858.
- Bird, R. P. (1987). Observation and quantification of aberrant crypts in the murine colon treated with a colon carcinogen: preliminary findings. *Cancer letters*, 37(2), 147-151.
- Bird, R. P. (1995). Role of aberrant crypt foci in understanding the pathogenesis of colon cancer. *Cancer letters*, 93(1), 55-71.
- Bishayee, A., & Mandal, A. (2014). *Trianthema portulacastrum* Linn. exerts chemoprevention of 7, 12-dimethylbenz (a) anthracene-induced mammary tumorigenesis in rats. *Mutation Research/Fundamental and Molecular Mechanisms of Mutagenesis*, 768, 107-118.
- Bishop, A. (2008). Role of oxygen in wound healing. *Journal of wound care*, 17(9), 399.
- Blaser, M. J., & Atherton, J. C. (2004). *Helicobacter pylori* persistence: biology and disease. *Journal of Clinical Investigation*, 113(3), 321.
- Borrelli, F., & Izzo, A. A. (2000). The plant kingdom as a source of anti-ulcer remedies. *Phytotherapy Research*, 14(8), 581-591.

- Bosco, M. C., Puppo, M., Blengio, F., Fraone, T., Cappello, P., Giovarelli, M., & Varesio, L. (2008). Monocytes and dendritic cells in a hypoxic environment: Spotlights on chemotaxis and migration. *Immunobiology*, 213(9), 733-749.
- Bottone, M. G., Santin, G., Aredia, F., Bernocchi, G., Pellicciari, C., & Scovassi, A. I. (2013). Morphological features of organelles during apoptosis: an overview. *Cells*, 2(2), 294-305.
- Bounaama, A., Djerdjouri, B., Laroche-Clary, A., Le Morvan, V., & Robert, J. (2012). Short curcumin treatment modulates oxidative stress, arginase activity, aberrant crypt foci, and TGF- β 1 and HES-1 transcripts in 1, 2-dimethylhydrazine-colon carcinogenesis in mice. *Toxicology*, 302(2), 308-317.
- Brambilla, D., Mancuso, C., Scuderi, M. R., Bosco, P., Cantarella, G., Lempereur, L., Di Benedetto, G., Pezzino, S., & Bernardini, R. (2008). The role of antioxidant supplement in immune system, neoplastic, and neurodegenerative disorders: a point of view for an assessment of the risk/benefit profile. *Nutrition journal*, 7(1), 29.
- Brem, H., & Tomic-Canic, M. (2007). Cellular and molecular basis of wound healing in diabetes. *Journal of Clinical Investigation*, 117(5), 1219.
- Brew, K., Dinakarpanian, D., & Nagase, H. (2000). Tissue inhibitors of metalloproteinases: evolution, structure and function. *Biochimica et Biophysica Acta (BBA)-Protein Structure and Molecular Enzymology*, 1477(1), 267-283.
- Budihardjo, I., Oliver, H., Lutter, M., Luo, X., & Wang, X. (1999). Biochemical pathways of caspase activation during apoptosis. *Annual review of cell and developmental biology*, 15(1), 269-290.
- Buemi, M., Galeano, M., Sturiale, A., Ientile, R., Crisafulli, C., Parisi, A., Catania, M., Calapai, G., Impalà, P., & Aloisi, C. (2004). Recombinant human erythropoietin stimulates angiogenesis and healing of ischemic skin wounds. *Shock*, 22(2), 169-173.
- Chainani-Wu, N. (2003). Safety and anti-inflammatory activity of curcumin: a component of tumeric (*Curcuma longa*). *The Journal of Alternative & Complementary Medicine*, 9(1), 161-168.
- Challa, A., Rao, D. R., & Reddy, B. S. (1997). Interactive suppression of aberrant crypt foci induced by azoxymethane in rat colon by phytic acid and green tea. *Carcinogenesis*, 18(10), 2023-2026.
- Chan, F. K., & Leung, W. (2002). Peptic-ulcer disease. *The Lancet*, 360(9337), 933-941.
- Chaturvedi, A., Kumar, M. M., Bhawani, G., Chaturvedi, H., Kumar, M., & Goel, R. (2007). Effect of ethanolic extract of *Eugenia jambolana* seeds on gastric ulceration and secretion in rats. *Indian Journal of physiology and Pharmacology*, 51(2), 131.
- Chen, J., & Huang, X.-F. (2009a). The signal pathways in azoxymethane-induced colon cancer and preventive implications. *Cancer Biology & Therapy*, 8(14), 1313-1317.

- Chen, J., & Huang, X. F. (2009b). The signal pathways in azoxymethane-induced colon cancer and preventive implications. *Cancer Biology & Therapy*, 8(14), 1313-1317.
- Chen, W., Weng, Y.-M., & Tseng, C.-Y. (2003). Antioxidative and antimutagenic activities of healthy herbal drinks from Chinese medicinal herbs. *The American journal of Chinese medicine*, 31(04), 523-532.
- Cheng, L., & Lai, M.-D. (2003). Aberrant crypt foci as microscopic precursors of colorectal cancer. *World Journal of Gastroenterology*, 9(12), 2642-2649.
- Chernyshev, A., Fleischmann, T., & Kohen, A. (2007). Thymidyl biosynthesis enzymes as antibiotic targets. *Applied microbiology and biotechnology*, 74(2), 282-289.
- Chisholm, M. A. (1998). Pharmacotherapy of duodenal and gastric ulcerations. *American Journal of Pharmaceutical Education*, 62, 196-203.
- Chun, O. K., Kim, D. O., Smith, N., Schroeder, D., Han, J. T., & Lee, C. Y. (2005). Daily consumption of phenolics and total antioxidant capacity from fruit and vegetables in the American diet. *Journal of the Science of Food and Agriculture*, 85(10), 1715-1724.
- Cines, D. B., Pollak, E. S., Buck, C. A., Loscalzo, J., Zimmerman, G. A., McEver, R. P., Pober, J. S., Wick, T. M., Konkle, B. A., & Schwartz, B. S. (1998). Endothelial cells in physiology and in the pathophysiology of vascular disorders. *Blood*, 91(10), 3527-3561.
- Clark, L., & Moon, R. (1999). Hyperbaric oxygen in the treatment of life-threatening soft-tissue infections. *Respiratory Care Clinics of North America*, 5(2), 203-219.
- Corpet, D. E., & Taché, S. (2002). Most effective colon cancer chemopreventive agents in rats: a systematic review of aberrant crypt foci and tumor data, ranked by potency. *Nutrition and cancer*, 43(1), 1-21.
- Cory, S., & Adams, J. M. (2002). The Bcl2 family: regulators of the cellular life-or-death switch. *Nature Reviews Cancer*, 2(9), 647-656.
- Cui, Y. F., Xia, G. W., Fu, X. B., Yang, H., Peng, R. Y., Zhang, Y., Gu, Q. Y., Gao, Y. B., Cui, X. M., & Hu, W. H. (2003). Relationship between expression of Bax and Bcl-2 proteins and apoptosis in radiation compound wound healing of rats. *Chin J Traumatol*, 6(3), 135-138.
- Daferera, D. J., Ziogas, B. N., & Polissiou, M. G. (2000). GC-MS analysis of essential oils from some Greek aromatic plants and their fungitoxicity on *Penicillium digitatum*. *Journal of Agricultural and Food Chemistry*, 48(6), 2576-2581.
- Dahlbäck, B. (2005). Blood coagulation and its regulation by anticoagulant pathways: genetic pathogenesis of bleeding and thrombotic diseases. *Journal of internal medicine*, 257(3), 209-223.
- Danenbergh, P. V. (1977). Thymidylate synthetase-a target enzyme in cancer chemotherapy. *Biochimica et biophysica acta*, 473(2), 73-92.

- Danese, S., & Mantovani, A. (2010). Inflammatory bowel disease and intestinal cancer: a paradigm of the Yin–Yang interplay between inflammation and cancer. *Oncogene*, *29*(23), 3313-3323.
- Darby, I. A., Bisucci, T., Hewitson, T. D., & MacLellan, D. G. (1997). Apoptosis is increased in a model of diabetes-impaired wound healing in genetically diabetic mice. *The international journal of biochemistry & cell biology*, *29*(1), 191-200.
- Das, N. P. (1989). Effects of vitamin A and its analogs on nonenzymatic lipid peroxidation in rat brain mitochondria. *Journal of neurochemistry*, *52*(2), 585-588.
- Davidson, J. M., Klagsbrun, M., Hill, K. E., Buckley, A., Sullivan, R., Brewer, P. S., & Woodward, S. C. (1985). Accelerated wound repair, cell proliferation, and collagen accumulation are produced by a cartilage-derived growth factor. *The Journal of Cell Biology*, *100*(4), 1219-1227.
- De Leon, M. P., Roncucci, L., Di Donato, P., Tassi, L., Smerieri, O., Amorico, M. G., Malagoli, G., De Maria, D., Antonioli, A., & Chahin, N. J. (1988). Pattern of epithelial cell proliferation in colorectal mucosa of normal subjects and of patients with adenomatous polyps or cancer of the large bowel. *Cancer research*, *48*(14), 4121-4126.
- Demircan, B., Çelik, G., Süleyman, H., & Akçay, F. (2005). Effects of indomethacin, celecoxib and meloxicam on glutathione, malondialdehyde and myeloperoxidase in rat gastric tissue. *The Pain Clinic*, *17*(4), 383-388.
- Deschner, E. E., Long, F. C., Hakissian, M., & Herrmann, S. L. (1983). Differential susceptibility of AKR, C57BL/6J, and CF1 mice to 1, 2-dimethylhydrazine-induced colonic tumor formation predicted by proliferative characteristics of colonic epithelial cells. *Journal of the National Cancer Institute*, *70*(2), 279-282.
- Desmoulière, A., Badid, C., Bochaton-Piallat, M.-L., & Gabbiani, G. (1997). Apoptosis during wound healing, fibrocontractive diseases and vascular wall injury. *The international journal of biochemistry & cell biology*, *29*(1), 19-30.
- Desmoulière, A., Redard, M., Darby, I., & Gabbiani, G. (1995). Apoptosis mediates the decrease in cellularity during the transition between granulation tissue and scar. *The American journal of pathology*, *146*(1), 56.
- Diegelmann, R. F., & Evans, M. C. (2004). Wound healing: an overview of acute, fibrotic and delayed healing. *Front Biosci*, *9*(1), 283-289.
- Dipple, A. (1995). DNA adducts of chemical carcinogens. *Carcinogenesis*, *16*(3), 437-441.
- Draper, H., Squires, E., Mahmoodi, H., Wu, J., Agarwal, S., & Hadley, M. (1993). A comparative evaluation of thiobarbituric acid methods for the determination of malondialdehyde in biological materials. *Free Radical Biology and Medicine*, *15*(4), 353-363.

- Dryden, S. V., Shoemaker, W. G., & Kim, J. H. (2013). Wound management and nutrition for optimal wound healing. *Atlas of the oral and maxillofacial surgery clinics of North America*, 21(1), 37-47.
- Durani, P., & Bayat, A. (2008). Levels of evidence for the treatment of keloid disease. *Journal of Plastic, Reconstructive & Aesthetic Surgery*, 61(1), 4-17.
- Ebert, M. P., Mooney, S. H., Tonnes-Priddy, L., Lograsso, J., Hoffmann, J., Chent, J., Rocken, C., Schulz, H.-U., Malfertheiner, P., & Lofton-Day, C. (2005). Hypermethylation of the TPEF/HPP1 Gene in Primary, Metastatic Colorectal Cancers. *Neoplasia*, 7(8), 771-778.
- Eid, S. M., Boueiz, A., Paranji, S., Mativo, C., BA, R. L., & Abougergi, M. S. (2010). Patterns and predictors of proton pump inhibitor overuse among academic and non-academic hospitalists. *Internal medicine*, 49(23), 2561-2568.
- Eisenbud, D., Hunter, H., Kessler, L., & Zulkowski, K. (2003). Hydrogel wound dressings: where do we stand in 2003? *Ostomy Wound Management*, 49(10), 52-56.
- Elmore, S. (2007). Apoptosis: a review of programmed cell death. *Toxicologic Pathology*, 35(4), 495-516.
- Epstein, F. H., & Ross, R. (1999). Atherosclerosis—an inflammatory disease. *New England Journal of Medicine*, 340(2), 115-126.
- Epstein, F. H., Singer, A. J., & Clark, R. A. (1999). Cutaneous wound healing. *New England Journal of Medicine*, 341(10), 738-746.
- Faisal Thayyullathil, Shahanas Chathoth, Abdulkader Hago, Mahendra Patel, & Galadari, S. (2008). Rapid reactive oxygen species (ROS) generation induced by curcumin leads to caspase-dependent and -independent apoptosis in L929 cells. *Free Radical Biology and Medicine*, 45, 1403-1412.
- Farahpour, M. R., Emami, P., & Ghayour, S. J. (2014). vitro antioxidant properties and wound healing activity of hydroethanolic turmeric rhizome extract (zingiberaceae). *International Journal of Pharmacy and Pharmaceutical Sciences*, 6(8), 474-478.
- Farinella, E., Soobrah, R., Phillips, R. K. S., & Clark, S. K. (2010). Familial adenomatous polyposis (FAP) and gender. Does gender influence the genetic transmission of FAP? *Familial cancer*, 9(3), 405-406.
- Fattaha, N. A. A., & Abdel-Rahman, M. S. (2000). Effects of omeprazole on ethanol lesions. *Toxicology letters*, 118(1), 21-30.
- Fedirko, V., Tramacere, I., Bagnardi, V., Rota, M., Scotti, L., Islami, F., Negri, E., Straif, K., Romieu, I., & La Vecchia, C. (2011). Alcohol drinking and colorectal cancer risk: an overall and dose-response meta-analysis of published studies. *Annals of oncology*, 22(9), 1958-1972.

- Fenoglio-Preiser, C. M., & Noffsinger, A. (1999). Review article: Aberrant crypt foci: A Review. *Toxicologic Pathology*, 27(6), 632-642.
- Ferlay, J., Shin, H. R., Bray, F., Forman, D., Mathers, C., & Parkin, D. M. (2010). Estimates of worldwide burden of cancer in 2008: GLOBOCAN 2008. *International journal of cancer*, 127(12), 2893-2917.
- Fraga, C. G., Leibovitz, B. E., & Tappel, A. L. (1988). Lipid peroxidation measured as thiobarbituric acid-reactive substances in tissue slices: characterization and comparison with homogenates and microsomes. *Free Radical Biology and Medicine*, 4(3), 155-161.
- Fuchs, Y., & Steller, H. (2011). Programmed cell death in animal development and disease. *Cell*, 147(4), 742-758.
- Fujimitsu, Y., Nakanishi, H., Inada, K., Yamachika, T., Ichinose, M., Fukami, H., & Tatematsu, M. (1996). Development of aberrant crypt foci involves a fission mechanism as revealed by isolation of aberrant crypts. *Cancer Science*, 87(12), 1199-1203.
- Gawronska-Kozak, B. (2011). Scarless skin wound healing in FOXN1 deficient (nude) mice is associated with distinctive matrix metalloproteinase expression. *Matrix Biology*, 30(4), 290-300.
- Goel, R., & Sairam, K. (2002). Anti-ulcer drugs from indigenous sources with emphasis on *Musa sapientum*, *tamrahabasma*, *Asparagus racemosus* and *Zingiber officinale*. *Indian Journal of Pharmacology*, 34(2), 100-110.
- Goh, K. L., Quek, K. F., Yeo, G., Hilmi, I., LEE, C. K., Hasnida, N., Aznan, M., KWAN, K. L., & Ong, K. T. (2005). Colorectal cancer in Asians: a demographic and anatomic survey in Malaysian patients undergoing colonoscopy. *Alimentary pharmacology & therapeutics*, 22(9), 859-864.
- Golbabapour, S., Gwaram, N. S., Hassandarvish, P., Hajrezaie, M., Kamalidehghan, B., Abdulla, M. A., Ali, H. M., Hadi, A. H. A., & Majid, N. A. (2013). Gastroprotection studies of Schiff base zinc (II) derivative complex against acute superficial hemorrhagic mucosal lesions in rats. *PloS one*, 8(9), e75036.
- Gordon, K. J., & Blobel, G. C. (2008). Role of transforming growth factor- β superfamily signaling pathways in human disease. *Biochimica et Biophysica Acta (BBA)-Molecular Basis of Disease*, 1782(4), 197-228.
- Gorinstein, S., Martin-Belloso, O., Katrich, E., Lojek, A., Číž, M., Gligelmo-Miguel, N., Haruenkit, R., Park, Y.-S., Jung, S.-T., & Trakhtenberg, S. (2003). Comparison of the contents of the main biochemical compounds and the antioxidant activity of some Spanish olive oils as determined by four different radical scavenging tests. *The Journal of nutritional biochemistry*, 14(3), 154-159.
- Gosain, A., & DiPietro, L. A. (2004). Aging and wound healing. *World journal of surgery*, 28(3), 321-326.

- Gottlieb, E., Armour, S., Harris, M., & Thompson, C. (2003). Mitochondrial membrane potential regulates matrix configuration and cytochrome c release during apoptosis. *Cell Death & Differentiation*, 10(6), 709-717.
- Gourineni, V., Verghese, M., Boateng, J., Shackelford, L., & Bhat, K. (2011). Chemopreventive potential of synergy1 and soybean in reducing azoxymethane-induced aberrant crypt foci in Fisher 344 male rats. *Journal of nutrition and metabolism*, 2011.
- Granados-Principal, S., El-azem, N., Pamplona, R., Ramirez-Tortosa, C., Pulido-Moran, M., Vera-Ramirez, L., Quiles, J. L., Sanchez-Rovira, P., Naudí, A., & Portero-Otin, M. (2014). Hydroxytyrosol ameliorates oxidative stress and mitochondrial dysfunction in doxorubicin-induced cardiotoxicity in rats with breast cancer. *Biochemical Pharmacology*, 90(1), 25-33.
- Green, D. R., & Kroemer, G. (2004). The pathophysiology of mitochondrial cell death. *Science*, 305(5684), 626-629.
- Greenhalgh, D. G. (1998). The role of apoptosis in wound healing. *The international journal of biochemistry & cell biology*, 30(9), 1019-1030.
- Grem, J. L. (2000). 5-Fluorouracil: forty-plus and still ticking. A review of its preclinical and clinical development. *Investigational new drugs*, 18(4), 299-313.
- Griendling, K. K., Sorescu, D., Lassègue, B., & Ushio-Fukai, M. (2000). Modulation of protein kinase activity and gene expression by reactive oxygen species and their role in vascular physiology and pathophysiology. *Arteriosclerosis, thrombosis, and vascular biology*, 20(10), 2175-2183.
- Grisham, M. B., Von Ritter, C., Smith, B. F., Lamont, J. T., & Granger, D. N. (1987). Interaction between oxygen radicals and gastric mucin. *American Journal of Physiology-Gastrointestinal and Liver Physiology*, 253(1), G93-G96.
- Grose, R., Werner, S., Kessler, D., Tuckermann, J., Huggel, K., Durka, S., Reichardt, H. M., & Werner, S. (2002). A role for endogenous glucocorticoids in wound repair. *EMBO reports*, 3(6), 575-582.
- Guo, S., & DiPietro, L. A. (2010). Factors affecting wound healing. *Journal of dental research*, 89(3), 219-229.
- Gupta, A. K., Pinsky, P., Rall, C., Mutch, M., Dry, S., Seligson, D., & Schoen, R. E. (2009). Reliability and accuracy of the endoscopic appearance in the identification of aberrant crypt foci. *Gastrointestinal endoscopy*, 70(2), 322-330.
- Gupta, A. K., Pretlow, T. P., & Schoen, R. E. (2007). Aberrant crypt foci: what we know and what we need to know. *Clinical Gastroenterology and Hepatology*, 5(5), 526-533.
- Gupta, M., Mazumder, U., Manikandan, L., Bhattacharya, S., Senthilkumar, G., & Suresh, R. (2005). Anti-ulcer activity of ethanol extract of *Terminalia pallida* Brandis. in Swiss albino rats. *Journal of ethnopharmacology*, 97(2), 405-408.

- Gupta, S. C., Sung, B., Kim, J. H., Prasad, S., Li, S., & Aggarwal, B. B. (2013). Multitargeting by turmeric, the golden spice: From kitchen to clinic. *Molecular nutrition & food research*, 57(9), 1510-1528.
- Gutteridge, J. (1995). Lipid peroxidation and antioxidants as biomarkers of tissue damage. *Clinical Chemistry*, 41(12), 1819-1828.
- Hajiaghaalipour, F., Kanthimathi, M., Abdulla, M. A., & Sanusi, J. (2013). The effect of *Camellia sinensis* on wound healing potential in an animal model. *Evidence-Based Complementary and Alternative Medicine*, 2013.
- Hajiaghaalipour, F., Kanthimathi, M., Sanusi, J., & Rajarajeswaran, J. (2015). White tea (*Camellia sinensis*) inhibits proliferation of the colon cancer cell line, HT-29, activates caspases and protects DNA of normal cells against oxidative damage. *Food Chemistry*, 169, 401-410.
- Hajrezaie, M., Golbabapour, S., Hassandarvish, P., Gwaram, N. S., Hadi, A. H. A., Ali, H. M., Majid, N., & Abdulla, M. A. (2012). Acute toxicity and gastroprotection studies of a new schiff base derived copper (II) complex against ethanol-induced acute gastric lesions in rats. *PloS one*, 7(12), e51537.
- Hajrezaie, M., Hassandarvish, P., Moghadamtousi, S. Z., Gwaram, N. S., Golbabapour, S., NajiHussien, A., Almagrabi, A. A., Zahedifard, M., Rouhollahi, E., & Karimian, H. (2014). Chemopreventive evaluation of a Schiff base derived copper (II) complex against azoxymethane-induced colorectal cancer in rats. *PloS one*, 9(3), e91246.
- Half, E., Bercovich, D., & Rozen, P. (2009). Familial adenomatous polyposis. *Orphanet journal of rare diseases*, 4(1), 22.
- Han, J., Hughes, M., & Cherry, G. (2004). Effect of glucose concentration on the growth of normal human dermal fibroblasts in vitro. *Journal of wound care*, 13(4), 150-153.
- Hao, X., Du, M., Bishop, A. E., & Talbot, I. (1998). Imbalance between proliferation and apoptosis in the development of colorectal carcinoma. *Virchows Archiv*, 433(6), 523-527.
- Haroon, Z. A., Raleigh, J. A., Greenberg, C. S., & Dewhirst, M. W. (2000). Early wound healing exhibits cytokine surge without evidence of hypoxia. *Annals of surgery*, 231(1), 137.
- Harrop, A., Ghahary, A., Scott, P., Forsyth, N., Uji-Friedland, R., & Tredget, E. (1995). Regulation of collagen synthesis and mRNA expression in normal and hypertrophic scar fibroblasts in vitro by interferon- γ . *Journal of Surgical Research*, 58(5), 471-477.
- Hartree, E. F. (1972a). Determination of protein: a modification of the Lowry method that gives a linear photometric response. *Analytical biochemistry*(48), 422-427.
- Hartree, E. F. (1972b). Determination of protein: a modification of the Lowry method that gives a linear photometric response. *Analytical biochemistry*, 48(2), 422-427.

- Hayouni, E., Miled, K., Boubaker, S., Bellasfar, Z., Abedrabba, M., Iwaski, H., Oku, H., Matsui, T., Limam, F., & Hamdi, M. (2011). Hydroalcoholic extract based-ointment from *Punica granatum* L. peels with enhanced *in vivo* healing potential on dermal wounds. *Phytomedicine*, 18(11), 976-984.
- He, Y. F., Wei, W., Zhang, X., Li, Y. H., Li, S., Wang, F. H., Lin, X. B., Li, Z. M., Zhang, D. S., & Huang, H. Q. (2008). Analysis of the DPYD gene implicated in 5-fluorouracil catabolism in Chinese cancer patients. *Journal of clinical pharmacy and therapeutics*, 33(3), 307-314.
- Hendrickse, C., Kelly, R., Radley, S., Donovan, I., Keighley, M., & Neoptolemos, J. (1994). Lipid peroxidation and prostaglandins in colorectal cancer. *British journal of surgery*, 81(8), 1219-1223.
- Heng, M. C. (2011). Wound healing in adult skin: aiming for perfect regeneration. *International Journal of Dermatology*, 50(9), 1058-1066.
- Hentschel, E., Brandstatter, G., Dragosics, B., Hirschl, A. M., Nemeč, H., Schutze, K., Taufer, M., & Wurzer, H. (1993). Effect of ranitidine and amoxicillin plus metronidazole on the eradication of *Helicobacter pylori* and the recurrence of duodenal ulcer. *New England Journal of Medicine*, 328(5), 308-312.
- Hetz, C., Vitte, P.-A., Bombrun, A., Rostovtseva, T. K., Montessuit, S., Hiver, A., Schwarz, M. K., Church, D. J., Korsmeyer, S. J., & Martinou, J.-C. (2005). Bax channel inhibitors prevent mitochondrion-mediated apoptosis and protect neurons in a model of global brain ischemia. *Journal of Biological Chemistry*, 280(52), 42960-42970.
- Hirose, Y., Yoshimi, N., Makita, H., Kara, A., Tanaka, T., & Mori, H. (1996). Early alterations of apoptosis and cell proliferation in azoxymethane-initiated rat colonic epithelium. *Cancer Science*, 87(6), 575-582.
- Hong, S.-L., Lee, G.-S., Syed Abdul Rahman, S. N., Ahmed Hamdi, O. A., Awang, K., Aznam Nugroho, N., & Abd Malek, S. N. (2014a). Essential Oil Content of the Rhizome of *Curcuma purpurascens* Bl.(Temu Tis) and Its Antiproliferative Effect on Selected Human Carcinoma Cell Lines. *The Scientific World Journal*, 2014.
- Hong, S.-L., Lee, G.-S., Syed Abdul Rahman, S. N., Ahmed Hamdi, O. A., Awang, K., Aznam Nugroho, N., & Abd Malek, S. N. (2014b). Essential Oil Content of the Rhizome of *Curcuma purpurascens* Bl.(Temu Tis) and Its Antiproliferative Effect on Selected Human Carcinoma Cell Lines. *The Scientific World Journal*, 2014, doi: 10.1155/2014/397430.
- Horvitz, H. R. (1999). Genetic control of programmed cell death in the nematode *Caenorhabditis elegans*. *Cancer research*, 59(7 Supplement), 1701s-1706s.
- Houghton, P., Hylands, P., Mensah, A., Hensel, A., & Deters, A. (2005). In vitro tests and ethnopharmacological investigations: wound healing as an example. *Journal of ethnopharmacology*, 100(1), 100-107.

- Howden, C., & Hunt, R. (1990). The relationship between suppression of acidity and gastric ulcer healing rates. *Alimentary pharmacology & therapeutics*, 4(1), 25-33.
- Hu, B., Shen, K.-P., An, H.-M., Wu, Y., & Du, Q. (2011). Aqueous extract of *Curcuma aromatica* induces apoptosis and G2/M arrest in human colon carcinoma LS-174-T cells independent of p53. *Cancer biotherapy & radiopharmaceuticals*, 26(1), 97-104.
- Huang, Q., Li, F., Liu, X., Li, W., Shi, W., Liu, F.-F., O'Sullivan, B., He, Z., Peng, Y., & Tan, A.-C. (2011). Caspase 3-mediated stimulation of tumor cell repopulation during cancer radiotherapy. *Nature medicine*, 17(7), 860-866.
- Huebener, P., & Schwabe, R. F. (2013). Regulation of wound healing and organ fibrosis by toll-like receptors. *Biochimica et Biophysica Acta (BBA)-Molecular Basis of Disease*, 1832(7), 1005-1017.
- Hulme, A. T., Price, S. L., & Tocher, D. A. (2005). A new polymorph of 5-fluorouracil found following computational crystal structure predictions. *Journal of the American Chemical Society*, 127(4), 1116-1117.
- Hunt, R., Armstrong, D., Yaghoobi, M., James, C., Chen, Y., Leonard, J., Shin, J., Lee, E., Tang-Liu, D., & Sachs, G. (2008). Predictable prolonged suppression of gastric acidity with a novel proton pump inhibitor, AGN 201904-Z. *Alimentary pharmacology & therapeutics*, 28(2), 187-199.
- Iijima, K., Ichikawa, T., Okada, S., Ogawa, M., Koike, T., Ohara, S., & Shimosegawa, T. (2009). Rebamipide, a cytoprotective drug, increases gastric mucus secretion in human: evaluations with endoscopic gastrin test. *Digestive diseases and sciences*, 54(7), 1500-1507.
- Iocono, J. A., Colleran, K. R., Remick, D. G., Gillespie, B. W., Ehrlich, H. P., & Garner, W. L. (2000). Interleukin-8 levels and activity in delayed-healing human thermal wounds. *Wound Repair and Regeneration*, 8(3), 216-225.
- Ionov, Y., Yamamoto, H., Krajewski, S., Reed, J. C., & Perucho, M. (2000). Mutational inactivation of the proapoptotic gene BAX confers selective advantage during tumor clonal evolution. *Proceedings of the National Academy of Sciences*, 97(20), 10872-10877.
- Ireson, C. R., Jones, D. J., Orr, S., Coughtrie, M. W., Boocock, D. J., Williams, M. L., Farmer, P. B., Steward, W. P., & Gescher, A. J. (2002). Metabolism of the cancer chemopreventive agent curcumin in human and rat intestine. *Cancer Epidemiology Biomarkers & Prevention*, 11(1), 105-111.
- Ishrat, T., Hoda, M. N., Khan, M. B., Yousuf, S., Ahmad, M., Khan, M. M., Ahmad, A., & Islam, F. (2009). Amelioration of cognitive deficits and neurodegeneration by curcumin in rat model of sporadic dementia of Alzheimer's type (SDAT). *European Neuropsychopharmacology*, 19(9), 636-647.
- Isozaki, H., Okajima, K., Ichinona, T., Tanimura, M., Morita, S., Takada, Y., Ishibashi, T., & Hara, H. (1994). The significance of proliferating cell nuclear antigen

- (PCNA) expression in cancer of the ampulla of Vater in terms of prognosis. *Surgery today*, 24(6), 494-499.
- Jamal, A., Javed, K., Aslam, M., & Jafri, M. (2006). Gastroprotective effect of cardamom, *Elettaria cardamomum* Maton. fruits in rats. *Journal of ethnopharmacology*, 103(2), 149-153.
- Jass, J., Ajioka, Y., Radojkovic, M., Allison, L., & Lane, M. (2003). Failure to detect colonic mucosal hyperproliferation in mutation positive members of a family with hereditary non-polyposis colorectal cancer. *Histopathology*, 30(3), 201-207.
- Jawad, N., Direkze, N., & Leedham, S. J. (2011). Inflammatory bowel disease and colon cancer. *Inflammation and Gastrointestinal Cancers*, 2011(185), 99-115.
- Jayaprakasha, G., Jagan Mohan Rao, L., & Sakariah, K. (2005). Chemistry and biological activities of *C. longa*. *Trends in Food Science and Technology*, 16(12), 533-548.
- Jayaprakasha, G. K., Jena, B. S., Negi, P. S., & Sakariah, K. K. (2002). Evaluation of antioxidant activities and antimutagenicity of turmeric oil: a byproduct from curcumin production. *Zeitschrift fur Naturforschung C-Journal of Biosciences*, 57(9-10), 828-835.
- Karimian, H., Mohan, S., Moghadamtousi, S. Z., Fadaeinasab, M., Razavi, M., Arya, A., Kamalidehghan, B., Ali, H. M., & Noordin, M. I. (2014). Tanacetum polycephalum (L.) Schultz-Bip. Induces mitochondrial-mediated apoptosis and inhibits migration and invasion in MCF7 cells. *Molecules*, 19(7), 9478-9501.
- Kobayashi, T., Ohta, Y., Yoshino, J., & Nakazawa, S. (2001). Teprenone promotes the healing of acetic acid-induced chronic gastric ulcers in rats by inhibiting neutrophil infiltration and lipid peroxidation in ulcerated gastric tissues. *Pharmacological Research*, 43(1), 23-30.
- Koller, E. (2009a). *Javanese medical plants used in rural communities*. uniwiien.
- Koller, E. (2009b). *Javanese medical plants used in rural communities*. (Master), uniwiien.
- Kotani, T., Murashima, Y., Kobata, A., Amagase, K., & Takeuchi, K. (2007). Pathogenic importance of pepsin in ischemia/reperfusion-induced gastric injury. *Life sciences*, 80(21), 1984-1992.
- Kraus, S., & Arber, N. (2009). Inflammation and colorectal cancer. *Current opinion in pharmacology*, 9(4), 405-410.
- Kruidering, M., van de Water, B., Zhan, Y., Baelde, J. J., de Heer, E., Mulder, G. J., Stevens, J. L., & Nagelkerke, J. (1998). Cisplatin effects on F-actin and matrix proteins precede renal tubular cell detachment and apoptosis in vitro. *Cell Death and Differentiation*, 5(7), 601-614.
- Kumar, M., Gautam, M. K., Singh, A., & Goel, R. K. (2013). Healing effects of *Musa sapientum* var. *paradisiaca* in diabetic rats with co-occurring gastric ulcer:

- cytokines and growth factor by PCR amplification. *BMC complementary and alternative medicine*, 13(1), 305.
- Kushi, L., & Giovannucci, E. (2002). Dietary fat and cancer. *The American journal of medicine*, 113(9), 63-70.
- Kwon, Y., Malik, M., & Magnuson, B. A. (2004). Inhibition of colonic aberrant crypt foci by curcumin in rats is affected by age. *Nutrition and cancer*, 48(1), 37-43.
- La Casa, C., Villegas, I., De La Lastra, C. A., Motilva, V., & Calero, M. M. (2000). Evidence for protective and antioxidant properties of rutin, a natural flavone, against ethanol induced gastric lesions. *Journal of ethnopharmacology*, 71(1), 45-53.
- Laine, L., Takeuchi, K., & Tarnawski, A. (2008). Gastric mucosal defense and cytoprotection: bench to bedside. *Gastroenterology*, 135(1), 41-60.
- Lamore, S. D., Cabello, C. M., & Wondrak, G. T. (2010). The topical antimicrobial zinc pyrithione is a heat shock response inducer that causes DNA damage and PARP-dependent energy crisis in human skin cells. *Cell Stress and Chaperones*, 15(3), 309-322.
- Larsson, J., Serrander, L., Stendahl, O., & Lundqvist-Gustafsson, H. (2000). Involvement of the β 2-integrin CD18 in apoptosis signal transduction in human neutrophils. *Inflammation Research*, 49(9), 452-459.
- Lawrence, W. T. (1998). Physiology of the acute wound. *Clinics in plastic surgery*, 25(3), 321-340.
- Lee, I. M., Shiroma, E. J., Lobelo, F., Puska, P., Blair, S. N., & Katzmarzyk, P. T. (2012). Effect of physical inactivity on major non-communicable diseases worldwide: an analysis of burden of disease and life expectancy. *The Lancet* 380(9838), 219-29.
- Li, J., Chen, J., & Kirsner, R. (2007). Pathophysiology of acute wound healing. *Clinics in dermatology*, 25(1), 9-18.
- Li, L., Ahmed, B., Mehta, K., & Kurzrock, R. (2007). Liposomal curcumin with and without oxaliplatin: effects on cell growth, apoptosis, and angiogenesis in colorectal cancer. *Molecular cancer therapeutics*, 6(4), 1276-1282.
- Li, R., Xiang, C., Ye, M., Li, H.-F., Zhang, X., & Guo, D.-A. (2011). Qualitative and quantitative analysis of curcuminoids in herbal medicines derived from *Curcuma* species. *Food Chemistry*, 126(4), 1890-1895.
- Li, W., Khor, T. O., Xu, C., Shen, G., Jeong, W.-S., Yu, S., & Kong, A.-N. (2008). Activation of Nrf2-antioxidant signaling attenuates NF κ B-inflammatory response and elicits apoptosis. *Biochemical Pharmacology*, 76(11), 1485-1489.
- Li, W., O'Brien, K., Woodley, D. T., & Chen, M. (2012). Heat shock protein 90 versus conventional growth factors in acute and diabetic wound healing *Cellular Trafficking of Cell Stress Proteins in Health and Disease* (pp. 259-277): Springer.

- Liao, J.-C., Tsai, J.-C., Liu, C.-Y., Huang, H.-C., Wu, L.-Y., & Peng, W.-H. (2013). Antidepressant-like activity of turmerone in behavioral despair tests in mice. *BMC complementary and alternative medicine*, *13*(1), 299.
- Liew, S. Y., Looi, C. Y., Paydar, M., Cheah, F. K., Leong, K. H., Wong, W. F., Mustafa, M. R., Litaudon, M., & Awang, K. (2014). Subditine, a new monoterpenoid indole Alkaloid from bark of *Nauclea subdita* (Korth.) Steud. Induces apoptosis in human prostate cancer cells. *Plos one*, *9*(2), e87286.
- Lim, G. C. C. (2002). Overview of cancer in Malaysia. *Japanese Journal of Clinical Oncology*, *32*(suppl 1), S37-S42.
- Lin, H.-J., Lo, W.-C., Cheng, Y.-C., & Perng, C.-L. (2006). Role of intravenous omeprazole in patients with high-risk peptic ulcer bleeding after successful endoscopic epinephrine injection: a prospective randomized comparative trial. *The American journal of gastroenterology*, *101*(3), 500-505.
- Ling, J., Wei, B., Lv, G., Ji, H., & Li, S. (2012). Anti-hyperlipidaemic and antioxidant effects of turmeric oil in hyperlipidaemic rats. *Food Chemistry*, *130*(2), 229-235.
- Lipkin, M., Blattner, W. E., Fraumeni, J. F., Lynch, H. T., Deschner, E., & Winawer, S. (1983). Tritiated thymidine labeling distribution as a marker for hereditary predisposition to colon cancer. *Cancer research*, *43*(4), 1899-1904.
- Longley, D. B., Latif, T., Boyer, J., Allen, W. L., Maxwell, P. J., & Johnston, P. G. (2003). *The interaction of thymidylate synthase expression with p53-regulated signaling pathways in tumor cells*. Paper presented at the Seminars in oncology.
- Longo, U. G., Lamberti, A., Maffulli, N., & Denaro, V. (2011). Tissue engineered biological augmentation for tendon healing: a systematic review. *British Medical Bulletin*, *98*(1), 31-59.
- Maga, G., & Hübscher, U. (2003). Proliferating cell nuclear antigen (PCNA): a dancer with many partners. *Journal of Cell Science*, *116*(15), 3051-3060.
- Magnuson, B., South, E., Exon, J., Dashwood, R., Xu, M., Hendrix, K., & Hubele, S. (2000). Increased susceptibility of adult rats to azoxymethane-induced aberrant crypt foci. *Cancer letters*, *161*(2), 185-193.
- Mahmood, A., Sidik, K., Salmah, I., Suzainor, K., & Philip, K. (2005). Antiulcerogenic activity of *Ageratum conyzoides* leaf extract against ethanol-induced gastric ulcer in rats as animal model. *International journal of molecular medicine and Advance sciences*, *1*(4), 402-405.
- Malfertheiner, P., Megraud, F., O'Morain, C., Bazzoli, F., El-Omar, E., Graham, D., Hunt, R., Rokkas, T., Vakil, N., & Kuipers, E. J. (2007). Current concepts in the management of *Helicobacter pylori* infection: the Maastricht III Consensus Report. *Gut*, *56*(6), 772-781.
- Marnett, L. J. (2002). Oxy radicals, lipid peroxidation and DNA damage. *Toxicology*, *181*, 219-222.

- Marotta, F., Tajiri, H., Safran, P., Fesce, E., & Ideo, G. (1999). Ethanol-related gastric mucosal damage: evidence of a free radical-mediated mechanism and beneficial effect of oral supplementation with bionormalizer, a novel natural antioxidant. *Digestion*, *60*(6), 538-543.
- Mau, J.-L., Lai, E. Y., Wang, N.-P., Chen, C.-C., Chang, C.-H., & Chyau, C.-C. (2003). Composition and antioxidant activity of the essential oil from *Curcuma zedoaria*. *Food Chemistry*, *82*(4), 583-591.
- May, R. C., & Machesky, L. M. (2001). Phagocytosis and the actin cytoskeleton. *Journal of Cell Science*, *114*(6), 1061-1077.
- Mayer, A., Takimoto, M., Fritz, E., Schellander, G., Kofler, K., & Ludwig, H. (1993). The prognostic significance of proliferating cell nuclear antigen, epidermal growth factor receptor, and *mdr* gene expression in colorectal cancer. *Cancer*, *71*(8), 2454-2460.
- Medlin, S. (2012). Nutrition for wound healing. *British Journal of Nursing*, *21*(Sup12), S11-S15.
- Menke, N. B., Ward, K. R., Witten, T. M., Bonchev, D. G., & Diegelmann, R. F. (2007). Impaired wound healing. *Clinics in dermatology*, *25*(1), 19-25.
- Messersmith, W., Oppenheimer, D., Peralba, J., Sebastiani, V., Amador, M., Jimeno, A., Embuscado, E. E., Hidalgo, M., & Iacobuzio-Donahue, C. A. (2005). Assessment of epidermal growth factor receptor (EGFR) signaling in paired colorectal cancer and normal colon tissue samples using computer-aided immunohistochemical analysis. *Cancer Biology & Therapy*, *4*(12), 1381-1386.
- Moghadamtousi, S. Z., Kamarudin, M. N. A., Chan, C. K., Goh, B. H., & Kadir, H. A. (2014). Phytochemistry and biology of *Loranthus parasiticus* Merr, a commonly used herbal medicine. *The American journal of Chinese medicine*, *42*(01), 23-35.
- Moghadamtousi, S. Z., Rouhollahi, E., Hajrezaie, M., Karimian, H., Abdulla, M. A., & Kadir, H. A. (2015a). *Annona muricata* leaves accelerate wound healing in rats via involvement of Hsp70 and antioxidant defence. *International Journal of Surgery* *2015*(1), 55-63.
- Moghadamtousi, S. Z., Rouhollahi, E., Karimian, H., Fadaeinasab, M., Firoozinia, M., Abdulla, M. A., & Kadir, H. A. (2015b). The Chemopotential Effect of *Annona muricata* Leaves against Azoxymethane-Induced Colonic Aberrant Crypt Foci in Rats and the Apoptotic Effect of Acetogenin Annonuricin E in HT-29 Cells: A Bioassay-Guided Approach. *PloS one*, *10*(4), 0122288.
- Monaco, J. L., & Lawrence, W. T. (2003). Acute wound healing: an overview. *Clinics in plastic surgery*, *30*(1), 1-12.
- Mosmann, T. (1983). Rapid colorimetric assay for cellular growth and survival: application to proliferation and cytotoxicity assays. *Journal of immunological methods*, *65*(1), 55-63.

- Moustafa, M. H., Sharma, R. K., Thornton, J., Mascha, E., Abdel-Hafez, M. A., Thomas, A. J., & Agarwal, A. (2004). Relationship between ROS production, apoptosis and DNA denaturation in spermatozoa from patients examined for infertility. *Human Reproduction*, *19*(1), 129-138.
- Muralikrishna A, R., & Hatcher, J. (2006). Phospholipase A₂, reactive oxygen species, and lipid peroxidation in cerebral ischemia. *Free Radical Biology and Medicine*, *40*(3), 376-387.
- Nakazono-Kusaba, A., Takahashi-Yanaga, F., Miwa, Y., Morimoto, S., Furue, M., & Sasaguri, T. (2004). PKC412 induces apoptosis through a caspase-dependent mechanism in human keloid-derived fibroblasts. *European journal of pharmacology*, *497*(2), 155-160.
- Naryzhny, S. N., & Lee, H. (2007). Characterization of proliferating cell nuclear antigen (PCNA) isoforms in normal and cancer cells: there is no cancer-associated form of PCNA. *FEBS Letters*, *581*(25), 4917-4920.
- Newby, Z., Lee, T. T., Morse, R. J., Liu, Y., Liu, L., Venkatraman, P., Santi, D. V., Finer-Moore, J. S., & Stroud, R. M. (2006). The role of protein dynamics in thymidylate synthase catalysis: variants of conserved 2'-deoxyuridine 5'-monophosphate (dUMP)-binding Tyr-261. *Biochemistry*, *45*(24), 7415-7428.
- Nicholls, D. G. (2004). Mitochondrial membrane potential and aging. *Aging Cell*, *3*(1), 35-40.
- Noli, C., & Miolo, A. (2001). The mast cell in wound healing. *Veterinary dermatology*, *12*(6), 303-313.
- Nutakul, W. (2013). NMR Analysis of Antipeptic Ulcer Principle from *Curcuma longa* L. *Bulletin of the Department of Medical Sciences*, *36*(4), 211-218.
- Ocker, M., & Höpfner, M. (2012). Apoptosis-modulating drugs for improved cancer therapy. *European Surgical Research*, *48*(3), 111-120.
- Ohta, H., Yatomi, Y., Sweeney, E. A., Hakomori, S.-i., & Igarashi, Y. (1994). A possible role of sphingosine in induction of apoptosis by tumor necrosis factor- α , in human neutrophils. *FEBS Letters*, *355*(3), 267-270.
- Pan, J.-S., He, S.-Z., Xu, H.-Z., Zhan, X.-J., Yang, X.-N., Xiao, H.-M., Shi, H.-X., & Ren, J.-L. (2008). Oxidative stress disturbs energy metabolism of mitochondria in ethanol-induced gastric mucosa injury. *World journal of gastroenterology: WJG*, *14*(38), 5857.
- Pandurangan, A. K., Dharmalingam, P., Anandasadagopan, S., & Ganapasam, S. (2012). Effect of luteolin on the levels of glycoproteins during azoxymethane-induced colon carcinogenesis in mice. *Asian Pac J Cancer Prev*, *13*(4), 1569-1573.
- Pena, J. C., Fuchs, E., & Thompson, C. B. (1997). Bcl-x expression influences keratinocyte cell survival but not terminal differentiation. *Cell growth & differentiation: the molecular biology journal of the American Association for Cancer Research*, *8*(6), 619-629.

- Pignone, M., Saha, S., Hoerger, T., & Mandelblatt, J. (2002). Cost-effectiveness analyses of colorectal cancer screening: a systematic review for the US Preventive Services Task Force. *Annals of Internal Medicine*, 137(2), 96-104.
- Power, E., Miles, A., Von Wagner, C., Robb, K., & Wardle, J. (2009). Uptake of colorectal cancer screening: system, provider and individual factors and strategies to improve participation. *Future Oncology*, 5(9), 1371-1388.
- Pretlow, T. P., Barrow, B. J., Ashton, W. S., O'Riordan, M. A., Pretlow, T. G., Jurcisek, J. A., & Stellato, T. A. (1991). Aberrant crypts: putative preneoplastic foci in human colonic mucosa. *Cancer research*, 51(5), 1564-1567.
- Prucksunand, C., Indrasukhsri, B., Leethochawalit, M., & Hungspreugs, K. (2001). Phase II clinical trial on effect of the long turmeric (*Curcuma longa* Linn) on healing of peptic ulcer 32(1), 208-15 .
- Qiao, J., Kang, J., Ko, T. C., Evers, B. M., & Chung, D. H. (2006). Inhibition of transforming growth factor- β /Smad signaling by phosphatidylinositol 3-kinase pathway. *Cancer letters*, 242(2), 207-214.
- Rai, N. K., Tripathi, K., Sharma, D., & Shukla, V. K. (2005). Apoptosis: a basic physiologic process in wound healing. *The International Journal of Lower Extremity Wounds*, 4(3), 138-144.
- Raj, S. M., Yap, K., Haq, J., Singh, S., & Hamid, A. (2001). Further evidence for an exceptionally low prevalence of *Helicobacter pylori* infection among peptic ulcer patients in north-eastern peninsular Malaysia. *Transactions of the Royal Society of Tropical Medicine and Hygiene*, 95(1), 24-27.
- Ramsewak, R., DeWitt, D., & Nair, M. (2000). Cytotoxicity, antioxidant and anti-inflammatory activities of curcumins I–III from *Curcuma longa*. *Phytomedicine*, 7(4), 303-308.
- Rao, C. V., Rivenson, A., Simi, B., & Reddy, B. S. (1995). Chemoprevention of colon carcinogenesis by dietary curcumin, a naturally occurring plant phenolic compound. *Cancer research*, 55(2), 259-266.
- Rao, K., Samikkannu, T., Dakshayani, K., Zhang, X., Sathaye, S., Indap, M., & Nair, M. P. (2012). Chemopreventive potential of an ethyl acetate fraction from *Curcuma longa* is associated with upregulation of p57 kip2 and Rad9 in the PC-3M prostate cancer cell line. *Asian Pacific Journal of Cancer Prevention*, 13(3), 1031-1038.
- Raskin, C. A. (1997). Apoptosis and cutaneous biology. *Journal of the American Academy of Dermatology*, 36(6), 885-896.
- Riano, A., Ortiz-Masia, D., Velázquez, M., Calatayud, S., Esplugues, J., & Barrachina, M. D. (2011). Nitric oxide induces HIF-1 α stabilization and expression of intestinal trefoil factor in the damaged rat jejunum and modulates ulcer healing. *Journal of gastroenterology*, 46(5), 565-576.

- Rickardson, L., Fryknäs, M., Dhar, S., Lövborg, H., Gullbo, J., Rydåker, M., Nygren, P., Gustafsson, M. G., Larsson, R., & Isaksson, A. (2005). Identification of molecular mechanisms for cellular drug resistance by combining drug activity and gene expression profiles. *British journal of cancer*, 93(4), 483-492.
- Riedl, S. J., & Salvesen, G. S. (2007). The apoptosome: signalling platform of cell death. *Nature Reviews Molecular Cell Biology*, 8(5), 405-413.
- Robert, A., Leung, F., & Guth, P. (1992). Morphological and functional gastric cytoprotection by prostaglandin in rats receiving absolute ethanol orally. *Gut*, 33(4), 444-451.
- Roberts, A. B., & Sporn, M. B. (1993). Physiological actions and clinical applications of transforming growth factor- β (TGF- β). *Growth factors*, 8(1), 1-9.
- Roberts, S. A., Hyatt, D. C., Honts, J. E., Changchien, L., Maley, G. F., Maley, F., & Montfort, W. R. (2006). Structure of the Y94F mutant of Escherichia coli thymidylate synthase. *Acta Crystallographica Section F: Structural Biology and Crystallization Communications*, 62(9), 840-843.
- Rodero, M. P., & Khosrotehrani, K. (2010). Skin wound healing modulation by macrophages. *International journal of clinical and experimental pathology*, 3(7), 643.
- Rodriguez, P. G., Felix, F. N., Woodley, D. T., & Shim, E. K. (2008). The role of oxygen in wound healing: a review of the literature. *Dermatologic surgery*, 34(9), 1159-1169.
- Rouhollahi, E., Moghadamtousi, S. Z., Hamdi, O. A., Fadaeinasab, M., Hajrezaie, M., Awang, K., Looi, C. Y., Abdulla, M. A., & Mohamed, Z. (2014). Evaluation of acute toxicity and gastroprotective activity of curcuma purpurascens BI. rhizome against ethanol-induced gastric mucosal injury in rats. *BMC complementary and alternative medicine*, 14(1), 378.
- Rouhollahi, E., Moghadamtousi, S. Z., Paydar, M., Fadaeinasab, M., Zahedifard, M., Hajrezaie, M., Hamdi, O. A. A., Looi, C. Y., Abdulla, M. A., & Awang, K. (2015). Inhibitory effect of Curcuma purpurascens BI. rhizome on HT-29 colon cancer cells through mitochondrial-dependent apoptosis pathway. *BMC complementary and alternative medicine*, 15(1), 15.
- Rouhollahi, E., Zorofchian Moghadamtousi, S., Hamdi, O. A. A., Fadaeinasab, M., Hajrezaie, M., Awang, K., Looi, C. Y., Abdulla, M. A., & Zahurin, M. (2014). Evaluation of acute toxicity and gastroprotective activity of curcuma purpurascens BI. rhizome against ethanol-induced gastric mucosal injury in rats. *BMC complementary and alternative medicine*, 14, 378.
- Ruberg, R. (1984). Role of nutrition in wound healing. *The Surgical clinics of North America*, 64(4), 705-714.
- Sacchetti, G., Maietti, S., Muzzoli, M., Scaglianti, M., Manfredini, S., Radice, M., & Bruni, R. (2005). Comparative evaluation of 11 essential oils of different origin

as functional antioxidants, antiradicals and antimicrobials in foods. *Food Chemistry*, 91(4), 621-632.

Schaffer, M., Schaffer, P. M., Zidan, J., & Sela, G. B. (2011a). Curcuma as a functional food in the control of cancer and inflammation. *Current Opinion in Clinical Nutrition and Metabolic Care*, 14(6), 588-597.

Schmid, P., Itin, P., Cherry, G., Bi, C., & Cox, D. A. (1998). Enhanced expression of transforming growth factor-beta type I and type II receptors in wound granulation tissue and hypertrophic scar. *The American journal of pathology*, 152(2), 485.

Schreml, S., Szeimies, R.-M., Prantl, L., Landthaler, M., & Babilas, P. (2010). Wound healing in the 21st century. *Journal of the American Academy of Dermatology*, 63(5), 866-881.

Schwentker, A., Vodovotz, Y., Weller, R., & Billiar, T. R. (2002). Nitric oxide and wound repair: role of cytokines. *Nitric oxide*, 7(1), 1-10.

Scorrano, L., & Korsmeyer, S. J. (2003). Mechanisms of cytochrome c release by proapoptotic BCL-2 family members. *Biochemical and Biophysical Research Communications*, 304(3), 437-444.

Scott, K. M., Alonso, J., de Jonge, P., Viana, M. C., Liu, Z., O'Neill, S., Aguilar-Gaxiola, S., Bruffaerts, R., Caldas-de-Almeida, J. M., & Stein, D. J. (2013). Associations between DSM-IV mental disorders and onset of self-reported peptic ulcer in the World Mental Health Surveys. *Journal of psychosomatic research*, 75(2), 121-127.

Shichijo, K., Ihara, M., Matsuu, M., Ito, M., Okumura, Y., & Sekine, I. (2003). Overexpression of heat shock protein 70 in stomach of stress-induced gastric ulcer-resistant rats. *Digestive diseases and sciences*, 48(2), 340-348.

Shim, S., Kim, S., Choi, D.-S., Kwon, Y.-B., & Kwon, J. (2011). Anti-inflammatory effects of [6]-shogaol: potential roles of HDAC inhibition and HSP70 induction. *Food and chemical toxicology*, 49(11), 2734-2740.

Shingel, K. I., Faure, M. P., Azoulay, L., Roberge, C., & Deckelbaum, R. J. (2008). Solid emulsion gel as a vehicle for delivery of polyunsaturated fatty acids: implications for tissue repair, dermal angiogenesis and wound healing. *Journal of tissue engineering and regenerative medicine*, 2(7), 383-393.

Shwter, A. N., Abdullah, N. A., Alshawsh, M. A., Alsalahi, A., Hajrezaei, M., Almaqrami, A. A., Salem, S. D., & Abdulla, M. A. (2014). Chemoprevention of colonic aberrant crypt foci by *Gynura procumbens* in rats. *Journal of ethnopharmacology*, 151(3), 1194-1201.

Sillars-Hardebol, A. H., Carvalho, B., De Wit, M., Postma, C., Delis-van Diemen, P. M., Mongera, S., Ylstra, B., van de Wiel, M. A., Meijer, G. A., & Fijneman, R. J. A. (2010). Identification of key genes for carcinogenic pathways associated with colorectal adenoma-to-carcinoma progression. *Tumor Biology*, 31(2), 89-96.

- Simon, H.-U., Haj-Yehia, A., & Levi-Schaffer, F. (2000). Role of reactive oxygen species (ROS) in apoptosis induction. *Apoptosis*, 5(5), 415-418.
- Singh, M., Sandhir, R., & Kiran, R. (2011). Effects on antioxidant status of liver following atrazine exposure and its attenuation by vitamin E. *Experimental and Toxicologic Pathology*, 63(3), 269-276.
- Siu, I.-M., Robinson, D. R., Schwartz, S., Kung, H.-J., Pretlow, T. G., Petersen, R. B., & Pretlow, T. P. (1999). The identification of monoclonality in human aberrant crypt foci. *Cancer research*, 59(1), 63-66.
- Skrzydłewska, E., Sulkowski, S., Koda, M., Zalewski, B., Kanczuga-Koda, L., & Sulkowska, M. (2005). Lipid peroxidation and antioxidant status in colorectal cancer. *World journal of gastroenterology: WJG*, 11(3), 403-406.
- Slichenmyer, W. J., & Von Hoff, D. D. (1991). Taxol: a new and effective anti-cancer drug. *Anti-Cancer Drugs*, 2(6), 519-530.
- Solis-Herruzo, J., Brenner, D., & Chojkier, M. (1988). Tumor necrosis factor alpha inhibits collagen gene transcription and collagen synthesis in cultured human fibroblasts. *Journal of Biological Chemistry*, 263(12), 5841-5845.
- Sotelo-Mundo, R. R., Changchien, L., Maley, F., & Montfort, W. R. (2006). Crystal structures of thymidylate synthase mutant R166Q: structural basis for the nearly complete loss of catalytic activity. *Journal of biochemical and molecular toxicology*, 20(2), 88-92.
- Srinivas, L., Shalini, V., & Shylaja, M. (1992). Turmerin: a water soluble antioxidant peptide from turmeric [*Curcuma longa*]. *Archives of biochemistry and biophysics*, 292(2), 617-623.
- Sturm, I., Petrowsky, H., Volz, R., Lorenz, M., Radetzki, S., Hillebrand, T., Wolff, G., Hauptmann, S., Dörken, B., & Daniel, P. T. (2001). Analysis of p53/BAX/p16ink4a/CDKN2 in esophageal squamous cell carcinoma: High BAX and p16ink4a/CDKN2 identifies patients with good prognosis. *Journal of clinical oncology*, 19(8), 2272-2281.
- Sun, Y., Oberley, L. W., & Li, Y. (1988). A simple method for clinical assay of superoxide dismutase. *Clinical Chemistry*, 34(3), 497-500.
- Sung, J., Lau, J., Goh, K., & Leung, W. (2005). Increasing incidence of colorectal cancer in Asia: implications for screening. *The lancet oncology*, 6(11), 871.
- Sung, J., Lau, J., Young, G. P., Sano, Y., Chiu, H., Byeon, J., Yeoh, K., Goh, K., Sollano, J., & Rerknimitr, R. (2008). Asia Pacific consensus recommendations for colorectal cancer screening. *Gut*, 57(8), 1166-1176.
- Süntar, I., Akkol, E. K., Nahar, L., & Sarker, S. D. (2012). Wound healing and antioxidant properties: do they coexist in plants? *Free Radicals and Antioxidants*, 2(2), 1-7.
- Suzuki, H., Matsuzaki, J., & Hibi, T. (2011). Ghrelin and oxidative stress in gastrointestinal tract. *Journal of clinical biochemistry and nutrition*, 48(2), 122.

- Suzuki, H., Nishizawa, T., Tsugawa, H., Mogami, S., & Hibi, T. (2012). Roles of oxidative stress in stomach disorders. *Journal of clinical biochemistry and nutrition*, 50(1), 35.
- Takayama, T., Katsuki, S., Takahashi, Y., Ohi, M., Nojiri, S., Sakamaki, S., Kato, J., Kogawa, K., Miyake, H., & Niitsu, Y. (1998). Aberrant crypt foci of the colon as precursors of adenoma and cancer. *New England Journal of Medicine*, 339(18), 1277-1284.
- Takeshita, S., Zheng, L., Brogi, E., Kearney, M., Pu, L., Bunting, S., Ferrara, N., Symes, J., & Isner, J. (1994). Therapeutic angiogenesis. A single intraarterial bolus of vascular endothelial growth factor augments revascularization in a rabbit ischemic hind limb model. *Journal of Clinical Investigation*, 93(2), 662.
- Tamri, P., Hemmati, A., & Boroujerdnia, M. G. (2014). Wound healing properties of quince seed mucilage: In vivo evaluation in rabbit full-thickness wound model. *International Journal of Surgery*, 12(8), 843-847.
- Tarnawski, A., Szabo, I., Husain, S., & Soreghan, B. (2001). Regeneration of gastric mucosa during ulcer healing is triggered by growth factors and signal transduction pathways. *Journal of Physiology-Paris*, 95(1), 337-344.
- Thakare, V., Chaudhari, R., & Patil, V. (2011). Wound Healing Evaluation of Some Herbal Formulations Containing Curcuma Longa and Cynodon Dactalon Extract. *International Journal of Phytomedicine*, 3(3), 325-332.
- Thayyullathil, F., Chathoth, S., Hago, A., Patel, M., & Galadari, S. (2008). Rapid reactive oxygen species (ROS) generation induced by curcumin leads to caspase-dependent and-independent apoptosis in L929 cells. *Free Radical Biology and Medicine*, 45(10), 1403-1412.
- Triantafyllidis, J. K., Nasioulas, G., & Kosmidis, P. A. (2009). Colorectal cancer and inflammatory bowel disease: epidemiology, risk factors, mechanisms of carcinogenesis and prevention strategies. *Anticancer research*, 29(7), 2727-2737.
- Tsai, S.-Y., Huang, S.-J., Chyau, C.-C., Tsai, C.-H., Weng, C.-C., & Mau, J.-L. (2011). Composition and antioxidant properties of essential oils from Curcuma rhizome. *Asian J. Arts Sci*, 2, 57-66.
- Tsikas, D., Gutzki, F.-M., Rossa, S., Bauer, H., Neumann, C., Dockendorff, K., Sandmann, J., & Frölich, J. C. (1997). Measurement of nitrite and nitrate in biological fluids by gas chromatography–mass spectrometry and by the Griess assay: problems with the Griess assay—solutions by gas chromatography–mass spectrometry. *Analytical biochemistry*, 244(2), 208-220.
- Tsujimoto, Y. (2003). Cell death regulation by the Bcl-2 protein family in the mitochondria. *Journal of Cellular Physiology*, 195(2), 158-167.
- Vaca, C., Wilhelm, J., & Harms-Ringdahl, M. (1988). Interaction of lipid peroxidation products with DNA. A review. *Mutation Research/Reviews in Genetic Toxicology*, 195(2), 137-149.

- Vainio, H., & Miller, A. B. (2003). Primary and secondary prevention in colorectal cancer. *Acta oncologica*, 42(8), 809-815.
- Valko, M., Leibfritz, D., Moncol, J., Cronin, M. T., Mazur, M., & Telser, J. (2007). Free radicals and antioxidants in normal physiological functions and human disease. *The International Journal of Biochemistry and Cell Biology*, 39(1), 44-84.
- Van Raamsdonk, J. M., & Hekimi, S. (2012). Superoxide dismutase is dispensable for normal animal lifespan. *Proceedings of the National Academy of Sciences*, 109(15), 5785-5790.
- Velmurugan, B., Singh, R. P., Tyagi, A., & Agarwal, R. (2008). Inhibition of azoxymethane-induced colonic aberrant crypt foci formation by silibinin in male Fisher 344 rats. *Cancer Prevention Research*, 1(5), 376-384.
- Velnar, T., Bailey, T., & Smrkolj, V. (2009). The wound healing process: an overview of the cellular and molecular mechanisms. *Journal of International Medical Research*, 37(5), 1528-1542.
- Verghese, M., Rao, D., Chawan, C., Williams, L., & Shackelford, L. (2002). Dietary inulin suppresses azoxymethane-induced aberrant crypt foci and colon tumors at the promotion stage in young Fisher 344 rats. *The Journal of nutrition*, 132(9), 2809-2813.
- Verma, G., Marella, A., Shaquiquzzaman, M., & Alam, M. M. (2013). Immunoinflammatory responses in gastrointestinal tract injury and recovery. *Acta Biochim Pol*, 60(2), 143-149.
- Vieira, A., Araujo, G., Galassi, C., Rodrigues, R., Cassalli, G., Kaiser, M., Dalla Costa, T., Beraldo, H., & Tagliati, C. (2013). Toxicological, toxicokinetic and gastroprotective evaluation of the benzaldehyde semicarbazone. *Food and chemical toxicology*, 55, 434-443.
- Visse, R., & Nagase, H. (2003). Matrix metalloproteinases and tissue inhibitors of metalloproteinases structure, function, and biochemistry. *Circulation Research*, 92(8), 827-839.
- Vogelstein, B., Fearon, E. R., Hamilton, S. R., Kern, S. E., Preisinger, A. C., Leppert, M., Nakamura, Y., White, R., Smits, A., & Bos, J. (1988). Genetic alterations during colorectal-tumor development. *The New England journal of medicine*, 319(9), 525-532.
- Wagstaff, M., Shah, M., McGrouther, D., & Latchman, D. (2007). The heat shock proteins and plastic surgery. *Journal of Plastic, Reconstructive and Aesthetic Surgery*, 60(9), 974-982.
- Wallace, J. L. (2005). Recent advances in gastric ulcer therapeutics. *Current opinion in pharmacology*, 5(6), 573-577.

- Wallace, J. L., & McKnight, G. W. (1990). The mucoid cap over superficial gastric damage in the rat. A high-pH microenvironment dissipated by nonsteroidal antiinflammatory drugs and endothelin. *Gastroenterology*, *99*(2), 295-304.
- Walsh, J. M. E., & Terdiman, J. P. (2003). Colorectal cancer screening. *JAMA: the journal of the American Medical Association*, *289*(10), 1288-1296.
- Wargovich, M. J., Brown, V. R., & Morris, J. (2010). Aberrant Crypt Foci: The Case for Inclusion as a Biomarker for Colon Cancer. *Cancers*, *2*(3), 1705-1716.
- Watson, A. J. M., & Collins, P. D. (2011). Colon cancer: a civilization disorder. *Digestive Diseases*, *29*(2), 222-228.
- Weil, J., Langman, M., Wainwright, P., Lawson, D., Rawlins, M., Logan, R., Brown, T., Vessey, M., Murphy, M., & Colin-Jones, D. (2000). Peptic ulcer bleeding: accessory risk factors and interactions with non-steroidal anti-inflammatory drugs. *Gut*, *46*(1), 27-31.
- Weismann, D., Hartvigsen, K., Lauer, N., Bennett, K. L., Scholl, H. P., Issa, P. C., Cano, M., Brandstätter, H., Tsimikas, S., & Skerka, C. (2011). Complement factor H binds malondialdehyde epitopes and protects from oxidative stress. *Nature*, *478*(7367), 76-81.
- White, J. R., Harris, R. A., Lee, S. R., Craigon, M. H., Binley, K., Price, T., Beard, G. L., Mundy, C. R., & Naylor, S. (2004). Genetic amplification of the transcriptional response to hypoxia as a novel means of identifying regulators of angiogenesis. *Genomics*, *83*(1), 1-8.
- Widenhouse, T. V., Lester, G. D., & Merritt, A. M. (2002). Effect of hydrochloric acid, pepsin, or taurocholate on bioelectric properties of gastric squamous mucosa in horses. *American journal of veterinary research*, *63*(5), 744-749.
- Wild, T., Rahbarnia, A., Kellner, M., Sobotka, L., & Eberlein, T. (2010). Basics in nutrition and wound healing. *Nutrition*, *26*(9), 862-866.
- Wilken, R., Veena, M. S., Wang, M. B., & Srivatsan, E. S. (2011). Curcumin: A review of anti-cancer properties and therapeutic activity in head and neck squamous cell carcinoma. *Mol Cancer*, *10*(12), 1-19.
- Wills, E. (1966). Mechanisms of lipid peroxide formation in animal tissues. *Biochemical Journal*, *99*, 667-676.
- Xie, J., & Itzkowitz, S. H. (2008). Cancer in inflammatory bowel disease. *World journal of gastroenterology: WJG*, *14*(3), 378.
- Xu, S., Kojima-Yuasa, A., Azuma, H., Kennedy, D. O., Konishi, Y., & Matsui-Yuasa, I. (2010). Comparison of glutathione reductase activity and the intracellular glutathione reducing effects of 13 derivatives of 1'-acetoxychavicol acetate in Ehrlich ascites tumor cells. *Chemico-biological interactions*, *185*(3), 235-240.
- Yadav, D. K., Singh, N., Dev, K., Sharma, R., Sahai, M., Palit, G., & Maurya, R. (2011). Anti-ulcer constituents of *Annona squamosa* twigs. *Fitoterapia*, *82*(4), 666-675.

- Youle, R. J., & Strasser, A. (2008). The BCL-2 protein family: opposing activities that mediate cell death. *Nature Reviews Molecular Cell Biology*, 9(1), 47-59.
- Yu, Y., Chen, F., Wang, X., Adelberg, J., Barron, F. H., Chen, Y., & Chung, H. Y. (2008). Evaluation of antioxidant activity of curcumin-free turmeric (*Curcuma longa* L.) oil and identification of its antioxidant constituents. *ACS Symposium Series*, 993, 152-164.
- Yue, G. G., Chan, B. C., Hon, P.-M., Lee, M. Y., Fung, K.-P., Leung, P.-C., & Lau, C. B. (2010). Evaluation of in vitro anti-proliferative and immunomodulatory activities of compounds isolated from *Curcuma longa*. *Food and chemical toxicology*, 48(8), 2011-2020.
- Yusoff, H. M., Daud, N., Noor, N. M., & Rahim, A. A. (2012). Participation and Barriers to Colorectal Cancer Screening in Malaysia. *Asian Pacific Journal of Cancer Prevention*, 13, 3983-3987.
- Zhang, X.-Q., Kim, J.-H., Lee, G.-S., Pyo, H.-B., Shin, E.-Y., Kim, E.-G., & Zhang, Y.-H. (2012). In vitro antioxidant and in vivo anti-inflammatory activities of *Ophioglossum thermale*. *The American journal of Chinese medicine*, 40(02), 279-293.
- Zhao, J., Zhang, J.-s., Yang, B., Lv, G.-P., & Li, S.-P. (2010). Free radical scavenging activity and characterization of sesquiterpenoids in four species of *Curcuma* using a TLC bioautography assay and GC-MS analysis. *Molecules*, 15(11), 7547-7557.
- Zorofchian Moghadamtousi, S., Abdul Kadir, H., Hassandarvish, P., Tajik, H., Abubakar, S., & Zandi, K. (2014). A review on antibacterial, antiviral, and antifungal activity of curcumin. *BioMed Research International*, 2014(2014), 12.

PUBLICATION

- **Rouhollahi E**, Moghadamtousi SZ, Paydar M, Fadaeinasab M, Zahedifard M, Hajrezaie M, Hamdi OA, et al. (2015) Inhibitory effect of *Curcuma purpurascens* BI. Rhizome on HT-29 colon cancer cells through mitochondrial-dependent apoptosis pathway. *BMC Complementary and Alternative Medicine*, 15: 15 (ISI-Cited Publication).
- **Rouhollahi E**, Moghadamtousi SZ, Al-Henhena N, Kunasegaran T, Al-HenhenaM, et al. (2015) The Chemopreventive Potential of *Curcuma purpurascens* Rhizome in Reducing Azoxy methane-Induced Aberrant Crypt Foci in Rats. *Drug Design, Development and Therapy*, In Press (ISI-Cited Publication).
- **Rouhollahi E**, Moghadamtousi SZ, Hajiaghaalipour F, Tayeby F, et al. (2015) *Curcuma purpurascens* BI. Rhizome accelerates rat excisional wound healing; involvement of HSP70/Bax proteins, antioxidant defence and angiogenesis activity. *Drug Design, Development and Therapy*, In Press (ISI-Cited Publication).
- **Rouhollahi E**, Moghadamtousi SZ, Hamdi OA, Fadaeinasab M, Hajrezaie M, et al. (2014) Evaluation of acute toxicity and gastroprotective activity of *Curcuma purpurascens* BI. rhizome against ethanol-induced gastric mucosal injury in rats. *BMC Complementary and Alternative Medicine* 14: 378 (ISI-Cited Publication).

SEMINARS

- Elham Rouhollahi, Soheil Zorofchian Moghadamtousi, Mahmood Ameen Abdulla, Zahurin Mohamed. Evaluation of Wound Healing Activity of *Curcuma purpurascens* BI. Rhizomes in Rats. ICPPM 2014: International Conference on Pharmacology and Pharmaceutical Medicine. Kuala Lumpur, Malaysia.
- Elham Rouhollahi, Soheil Zorofchian Moghadamtousi, Mahmood Ameen Abdulla, Zahurin Mohamed. Apoptosis Effect of *Curcuma Purpurascens* BI. Rhizome on HT-29 colon cancer cells. ICBENS 2015: International Conference on Biological Engineering and Natural Sciences. Singapore.
- Elham Rouhollahi, Soheil Zorofchian Moghadamtousi, Mahmood Ameen Abdulla, Zahurin Mohamed. Dichloromethane *Curcuma purpurascens* BI rhizome extract Prevents Thioacetamide-Induced Liver Cirrhosis in Rats. International Conference GOLDEN HELIX SYMPOSIA 2015. Kuala Lumpur, Malaysia.
- Elham Rouhollahi, Soheil Zorofchian Moghadamtousi, Mahmood Ameen Abdulla, Zahurin Mohamed. The chemopreventive potential of *Curcuma purpurascens* rhizome in reducing azoxymethane-induced aberrant crypt foci in rats. ICBENS 2015: International Conference Asian Oncology Summit 2015 Shanghai, China

Appendix A

Preparation of Reagents:

10% Tween - 20

100 ml of the stock solution was prepared by dissolving 10ml of 10% Tween-20 in 90 ml of distilled water.

0.9% Normal saline

9 g of NaCl was added to 1 L of distilled water.

(PBS) PH 7.3+ 0.2

1 Liter PBS was prepared as follows: sodium chloride 8.0 g, potassium chloride 0.2 g , di-sodium phosphate 1.15 g and potassium di-hydrogen phosphate 0.2 g were dissolved in distilled water at 25°C.

10% fresh formalin (Buffered formalin)

1 L of fresh formalin was prepared by dissolving 6.5 g di-sodium hydrogen phosphate with 4 g sodium di-hydrogen phosphate monohydrate and 100 ml concentrated formalin (38 - 40%) in 900 ml of phosphate buffer saline (PBS).

Appendix B

Routine histology slide preparation

a- Tissue trimming and fixation

The tissue processing started with trimming and excising the tissues into small pieces of about 1 cm in size and then put in cassettes containing fresh 10% buffered formalin of 10:1 ratio of fixative to tissue for 48 hr. The purpose of fixation is to preserve tissues permanently in life - like state as possible after removal of the tissues.

b- Processing

The technique of getting fixed tissue into paraffin is called tissue processing. This process have been done by using automatic tissue processor. The main steps in this process were: dehydration, clearing and infiltration in a programmed sequence.

c- Embedding

After the above processes, the tissues were manually transferred from the cassettes and put into the blocks with molten paraffin over them, with proper orientation of tissue in the block of paraffin.

d- Sectioning

Once the melted paraffin was cooled and hardened, the blocks were trimmed into an appropriately sized block and put into freezer under -4°C for 1 hr before sectioning. Each block was then mounted in a specially designed slicing machine, a microtome. They were cut with steel knife into sections of $5\ \mu\text{m}$ thickness. These sections were floated in a 40°C warm water bath to avoid wrinkling, then they were picked up on a labeled glass microscopic slides. All these slides were then dried less than 50°C temperature.

e- Staining

Before staining, all the slides were deparaffinized by running them through xylenes I, II for 5 min each, in order to remove the paraffin wax out of the tissues and allow water soluble dyes to penetrate the sections. The stains which were used in our experiment were H and E stains. Thick paraffin sections (5 μm) of colon were de-waxed in xylene, dehydrated in series of alcohol to water then immersed in hematoxylin for 15 min. Sections were then differentiated with 1% acid alcohol and washed in tap water, followed by staining with eosin for 5 min.

f- Mounting

Finally, to protect the stained sections from damage, the stained sections were dehydrated in series of alcohol, cleared in xylene and mounted with the mounting media DPX and the use of coverslip in 45° angle then bubbles were removed carefully and left to dry overnight at room temperature.

Appendix C

Histopathology H and E Techniques

Reagents required:

- 1- Harris haematoxylin working solution
- 2- Eosin working solution
- 3- 0.5 % acid alcohol
- 4- 2 % sodium acetate
- 5- 80 % alcohol
- 6- 95 % alcohol
- 7- Absolute alcohol

Procedure:

- 1- Bring section to water
- 2- Stain in Harris haematoxylin 10 min.
- 3- Wash in running water until excess blue color goes off
- 4- Differentiation: Dip 2 to 3X in 0.5% acid alcohol and wash in running tap water
- 5- Wash well in running tap water 2-3 min.
- 6- Blue section with 2% sodium acetate 2 sec.
- 7- Wash again in running tap water 2-3 min.
- 8- Rinse in 80% alcohol
- 9- Stain in eosin solution 5 min.
- 10- Dehydration: 95 % alcohol I 5 sec
95 % alcohol II 2 min.
Absolute alcohol I 2 min.
Absolute alcohol II 2 min.
- 11- Clear in xylene 2 min. x3

12- Mount with DPX

13- Wipe slide to remove excess xylene

14- Label slide appropriately.

Results: Nuclei blue Cytoplasm various shades of pink and red.

University of Malaya

Appendix D

Catalase antioxidant assay kit (Item no.707002 cayman)

Precautions

Please read these instructions carefully before beginning this assay.

For research use only. Not for human or diagnostic use.

It is recommended to take appropriate precautions when using the kit reagents (i.e., lab coat, gloves, eye goggles, etc.) as some of them can be harmful.

Catalase Hydrogen Peroxide is corrosive and is harmful if swallowed. Contact with skin may cause burns. In case of contact with skin or eyes, rinse immediately with plenty of water for 15 minutes. Keep away from combustible materials.*

Catalase Formaldehyde Standard is carcinogenic. It is toxic if inhaled, ingested, or if in contact with skin. In case of contact with skin or eyes, rinse immediately with plenty of water for 15 minutes. Keep away from combustible materials.*

Catalase Potassium Hydroxide is corrosive and is harmful if swallowed. Contact with skin may cause burns. In case of contact with skin or eyes, rinse immediately with plenty of water for 15 minutes. Keep away from combustible materials. Heat is generated when Catalase Potassium Hydroxide pellets are dissolved in water.*

Catalase Purpald (Chromagen) is an irritant. In case of contact with skin or eyes, rinse immediately with plenty of water for 15 minutes.*

Catalase Potassium Periodate is an oxidizer and an irritant. In case of contact with skin or eyes, rinse immediately with plenty of water for 15 minutes.*

Hydrochloric acid is corrosive and is harmful if swallowed. Contact with skin may cause burns. In case of contact with skin or eyes, rinse immediately with plenty of water for 15 minutes.*

*Before use the user must review the complete Material Safety Data Sheet.

If You Have Problems

Technical Service Contact Information

Phone: 888-526-5351 (USA and Canada only) or 734-975-3888

Fax: 734-971-3641

Email: techserv@caymanchem.com

Hours: M-F 8:00 AM to 5:30 PM EST

In order for our staff to assist you quickly and efficiently, please be ready to supply the lot number of the kit (found on the outside of the box).

Storage and Stability

This kit will perform as specified if stored at 4°C and used before the expiration date indicated on the outside of the box.

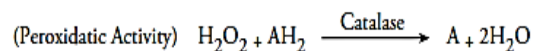
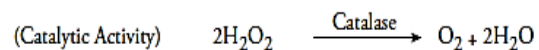
Materials Needed But Not Supplied

1. A plate reader with a 540 nm filter.
2. An adjustable pipettor and a repeat pipettor.
3. A source of pure water. Glass distilled water or HPLC-grade water is acceptable.
4. A 5 ml vial of methanol can be purchased from Cayman (Item No. 707016).

INTRODUCTION

Background

Catalase (EC 1.11.1.6; 2H₂O₂ oxidoreductase) is an ubiquitous antioxidant enzyme that is present in most aerobic cells. Catalase (CAT) is involved in the detoxification of hydrogen peroxide (H₂O₂), a reactive oxygen species (ROS), which is a toxic product of both normal aerobic metabolism and pathogenic ROS production. This enzyme catalyzes the conversion of two molecules of H₂O₂ to molecular oxygen and two molecules of water (catalytic activity). CAT also demonstrates peroxidatic activity, in which low molecular weight alcohols can serve as electron donors. While aliphatic alcohols serve as specific substrates for CAT, other enzymes with peroxidatic activity do not utilize these substrates.



In humans, the highest levels of CAT are found in liver, kidney, and erythrocytes, where it is believed to account for the majority of H₂O₂ decomposition.

About This Assay

Cayman's Catalase Assay Kit utilizes the peroxidatic function of CAT for determination of enzyme activity. The method is based on the reaction of the enzyme with methanol in the presence of an optimal concentration of H₂O₂. The formaldehyde produced is measured colorimetrically with 4-amino-3-hydrazino-5-mercapto-1,2,4-triazole (Purpald) as the chromogen.^{1,2} Purpald specifically forms a bicyclic heterocycle with aldehydes, which upon oxidation changes from colorless to a purple color.^{1,2} The assay can be used to measure CAT activity in plasma, serum, erythrocyte lysates, tissue homogenates, and cell lysates.

PRE-ASSAY PREPARATION

Reagent Preparation

NOTE: Methanol is no longer supplied in this kit. It can be purchased separately under Item No. 707016 or you can supply your own.

1. Catalase Assay Buffer (10X) – (Item No. 707010)

Each vial contains 5 ml of Assay Buffer. Dilute 2 ml of Catalase Assay Buffer concentrate with 18 ml of HPLC-grade water. This final Assay Buffer (100 mM potassium phosphate, pH 7.0) should be used in the assay. When stored at 4°C, this diluted Assay Buffer is stable for at least two months. Prepare the additional vial as needed.

2. Catalase Sample Buffer (10X) – (Item No. 707012)

Each vial contains 10 ml of Sample Buffer. Dilute 5 ml of Catalase Sample Buffer concentrate with 45 ml of HPLC-grade water. This final Sample Buffer (25 mM potassium phosphate, pH 7.5, containing 1 mM EDTA and 0.1% BSA) should be used to dilute the formaldehyde standards, Catalase (Control), and CAT samples prior to assaying. When stored at 4°C, this diluted Sample Buffer is stable for at least two months. Prepare the additional vial as needed.

3. Catalase Formaldehyde Standard - (Item No. 707014)

The vial contains 4.25 M formaldehyde. The reagent is ready to use as supplied.

4. Catalase (Control) – (Item No. 707013)

Each vial contains a lyophilized powder of bovine liver CAT and is used as a positive control. Reconstitute the Catalase (Control) by adding 2 ml of diluted Sample Buffer to the vial and vortex well. Take 100 µl of the reconstituted enzyme and dilute with 1.9 ml of diluted Sample Buffer. A 20 µl aliquot of this diluted enzyme per well causes an absorbance of approximately 0.29 after subtracting the background absorbance. The diluted enzyme is stable for 30 minutes. The reconstituted Catalase (Control) is stable for one month at -20°C.

5. Catalase Potassium Hydroxide – (Item No. 707015)

Each vial contains potassium hydroxide (KOH) pellets. Place the vial on ice, add 4 ml of cold HPLC-grade water, and vortex to yield a 10 M solution. *CAUTION: Heat is generated when Catalase Potassium Hydroxide pellets are dissolved in water. The diluted Potassium Hydroxide solution is stable for at least three months if stored at 4°C.*

6. Catalase Hydrogen Peroxide – (Item No. 707011)

The vial contains an 8.82 M solution of H₂O₂. Dilute 40 µl of Catalase Hydrogen Peroxide with 9.96 ml of HPLC-grade water. The diluted Hydrogen Peroxide solution is stable for two hours.

7. Catalase Purpald (Chromagen) – (Item No. 707017)

Each vial contains 4 ml of 4-amino-3-hydrazino-5-mercapto-1,2,4-triazole (Purpald) in 0.5 M hydrochloric acid. The reagent is ready to use as supplied.

8. Catalase Potassium Periodate – (Item No. 707018)

Each vial contains 1.5 ml of potassium periodate in 0.5 M potassium hydroxide. The reagent is ready to use as supplied.

Sample Preparation

Overheating can inactivate catalase. The enzyme should be kept cold during sample preparation and assaying. In general, catalase is very unstable at high dilution. It is recommended to store samples concentrated and assay within 30 minutes after dilution.

Tissue Homogenate

1. Prior to dissection, either perfuse tissue or rinse tissue with a phosphate buffered saline (PBS) solution, pH 7.4, to remove any red blood cells and clots.
2. Homogenize the tissue on ice in 5-10 ml of cold buffer (*i.e.*, 50 mM potassium phosphate, pH 7.0, containing 1 mM EDTA) per gram tissue.
3. Centrifuge at 10,000 x g for 15 minutes at 4°C.
4. Remove the supernatant for assay and store on ice. If not assaying on the same day, freeze the sample at -80°C. The sample will be stable for at least one month.

Cell Lysate

1. Collect cells by centrifugation (*i.e.*, 1,000-2,000 x g for 10 minutes at 4°C). For adherent cells, do not harvest using proteolytic enzymes; rather use a rubber policeman.
2. Homogenize or sonicate the cell pellet on ice in 1-2 ml of cold buffer (*i.e.*, 50 mM potassium phosphate, pH 7.0, containing 1 mM EDTA).
3. Centrifuge at 10,000 x g for 15 minutes at 4°C.
4. Remove the supernatant for assay and store on ice. If not assaying on the same day, freeze the sample at -80°C. The sample will be stable for at least one month.

Plasma and Erythrocyte Lysate

1. Collect blood using an anticoagulant such as heparin, citrate, or EDTA.
2. Centrifuge the blood at 700-1,000 x g for 10 minutes at 4°C. Pipette off the top yellow plasma layer without disturbing the white buffy layer. Store plasma on ice until assaying or freeze at -80°C. The plasma sample will be stable for at least one month.
3. Remove the white buffy layer (leukocytes) and discard.
4. Lyse the erythrocytes (red blood cells) in four times its volume of ice-cold HPLC-grade water.
5. Centrifuge at 10,000 x g for 15 minutes at 4°C.
6. Collect the supernatant (erythrocyte lysate) for assaying and store on ice. If not assaying the same day, freeze at -80°C. The sample will be stable for at least one month.

Serum

1. Collect blood without using an anticoagulant. Allow blood to clot for 30 minutes at 25°C.
2. Centrifuge the blood at 2,000 x g for 15 minutes at 4°C. Pipette off the top yellow serum layer without disturbing the white buffy layer. Store serum on ice. If not assaying the same day, freeze at -80°C. The sample will be stable for at least one month.

Tissue Homogenization using the Precellys 24 Homogenizer

- Prior to dissection, either perfuse or rinse tissue with phosphate buffered saline (PBS), pH 7.4, to remove any red blood cells and clots.
- Freeze organs immediately upon collection and then store at -80°C. Snap-freezing of tissues in liquid nitrogen is preferred.
- Add cold 50 mM potassium phosphate, pH 7.0, containing 1 mM EDTA.
- Homogenize the tissue sample using the Precellys 24 according to appropriate settings.
- Spin the tissue homogenates at 10,000 x g for 15 minutes at 4°C.
- Collect supernatant and assay samples according to the kit booklet protocol. Samples may need to be diluted appropriately for assay and should be normalized using a protein assay.

ASSAY PROTOCOL

Plate Set Up

There is no specific pattern for using the wells on the plate. We suggest that there be at least two wells designated as positive controls. A typical layout of formaldehyde standards and samples to be measured in duplicate is shown in Figure 1. We suggest you record the contents of each well on the template sheet provided on page 23.

	1	2	3	4	5	6	7	8	9	10	11	12
A	(A)	(A)	(S1)	(S1)	(S9)	(S9)	(S17)	(S17)	(S25)	(S25)	(S33)	(S33)
B	(B)	(B)	(S2)	(S2)	(S10)	(S10)	(S18)	(S18)	(S26)	(S26)	(S34)	(S34)
C	(C)	(C)	(S3)	(S3)	(S11)	(S11)	(S19)	(S19)	(S27)	(S27)	(S35)	(S35)
D	(D)	(D)	(S4)	(S4)	(S12)	(S12)	(S20)	(S20)	(S28)	(S28)	(S36)	(S36)
E	(E)	(E)	(S5)	(S5)	(S13)	(S13)	(S21)	(S21)	(S29)	(S29)	(S37)	(S37)
F	(F)	(F)	(S6)	(S6)	(S14)	(S14)	(S22)	(S22)	(S30)	(S30)	(S38)	(S38)
G	(G)	(G)	(S7)	(S7)	(S15)	(S15)	(S23)	(S23)	(S31)	(S31)	(S39)	(S39)
H	(+)	(+)	(S8)	(S8)	(S16)	(S16)	(S24)	(S24)	(S32)	(S32)	(S40)	(S40)

A-G = Standards

+ = Positive Controls

S1-S40 = Sample Wells

Figure 1. Sample plate format

Pipetting Hints

- It is recommended that an adjustable pipette be used to deliver reagents to the wells.
- Before pipetting each reagent, equilibrate the pipette tip in that reagent (*i.e.*, slowly fill the tip and gently expel the contents, repeat several times).
- Do not expose the pipette tip to the reagent(s) already in the well.

General Information

- The final volume of the assay is 240 μ l in all the wells.
- All reagents except samples must be equilibrated to room temperature before beginning the assay.
- It is not necessary to use all the wells on the plate at one time.
- If the expected CAT activity of the sample is not known or if it is expected to be beyond the range of the standard curve, it is prudent to assay the sample at several dilutions.
- It is recommended that the samples and formaldehyde standards be assayed at least in duplicate.
- Use the diluted Assay Buffer in the assay.
- Monitor the absorbance at 540 nm using a plate reader.

Standard Preparation

1. Preparation of the Formaldehyde Standards - Dilute 10 μl of Catalase Formaldehyde Standard (Item No. 707014) with 9.99 ml of diluted Sample Buffer to obtain a 4.25 mM formaldehyde stock solution. Take seven clean glass test tubes and mark them A-G. Add the amount of formaldehyde stock and diluted Sample Buffer to each tube as described in Table 1 (below).

Tube	Formaldehyde (μl)	Sample Buffer (μl)	Final Concentration (μM formaldehyde)*
A	0	1,000	0
B	10	990	5
C	30	970	15
D	60	940	30
E	90	910	45
F	120	880	60
G	150	850	75

Table 1

*Final formaldehyde concentration in the 170 μl reaction.

Performing the Assay

1. **Formaldehyde Standard Wells** - Add 100 μl of diluted Assay Buffer, 30 μl of methanol, and 20 μl of standard (tubes A-G) per well in the designated wells on the plate (see sample plate format, Figure 1, page 12).
2. **Positive Control Wells (bovine liver CAT)** - Add 100 μl of diluted Assay Buffer, 30 μl of methanol, and 20 μl of diluted Catalase (Control) to two wells.
3. **Sample Wells** - Add 100 μl of diluted Assay Buffer, 30 μl of methanol, and 20 μl of sample to two wells. To obtain reproducible results, the amount of CAT added to the well should result in an activity between 2-35 nmol/min/ml. When necessary, samples should be diluted with diluted Sample Buffer or concentrated with an Amicon centrifuge concentrator with a molecular weight cut-off of 100,000 to bring the enzymatic activity to this level.
4. Initiate the reactions by adding 20 μl of diluted Hydrogen Peroxide to all the wells being used. Make sure to note the precise time the reaction is initiated and add the diluted Hydrogen Peroxide as quickly as possible.
5. Cover the plate with the plate cover and incubate on a shaker for 20 minutes at room temperature.
6. Add 30 μl of diluted Potassium Hydroxide to each well to terminate the reaction and then add 30 μl of Catalase Purpald (Chromagen) (Item No. 707017) to each well.
7. Cover the plate with the plate cover and incubate for 10 minutes at room temperature on the shaker.
8. Add 10 μl of Catalase Potassium Periodate (Item No. 707018) to each well. Cover with plate cover and incubate five minutes at room temperature on a shaker.
9. Read the absorbance at 540 nm using a plate reader.

ANALYSIS

Calculations

Determination of the Reaction Rate

1. Calculate the average absorbances of each standard and sample.
2. Subtract the average absorbance of standard A from itself and all other standards and samples.
3. Plot the corrected absorbance of standards (from step 2 above) as a function of final formaldehyde concentration (μM) from Table 1. See Figure 2 for a typical standard curve.

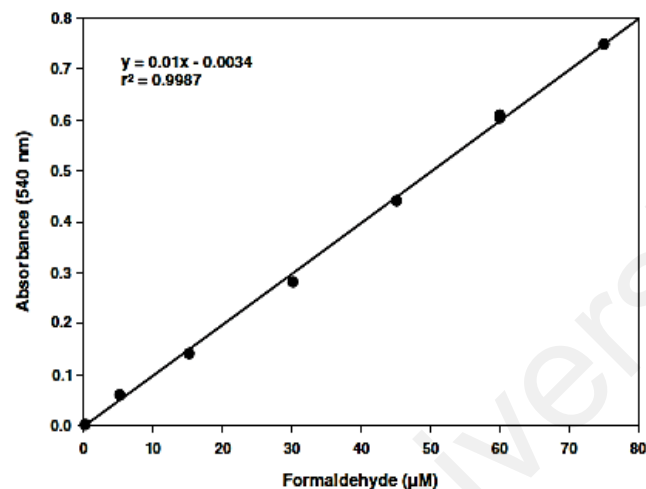


Figure 2. Formaldehyde standard curve

4. Calculate the formaldehyde concentration of the samples using the equation obtained from the linear regression of the standard curve substituting corrected absorbance values for each sample.

$$\text{Formaldehyde } (\mu\text{M}) = \left[\frac{\text{sample absorbance} - (\text{y-intercept})}{\text{slope}} \right] \times \frac{0.17 \text{ ml}}{0.02 \text{ ml}}$$

5. Calculate the CAT activity of the sample using the following equation. One unit is defined as the amount of enzyme that will cause the formation of 1.0 nmol of formaldehyde per minute at 25°C.

$$\text{CAT Activity} = \frac{\mu\text{M of sample}}{20 \text{ min.}} \times \text{Sample dilution} = \text{nmol/min/ml}$$

Performance Characteristics

Sensitivity:

The dynamic range of the assay is limited only by the accuracy of the absorbance measurement. Most plate readers are linear to an absorbance of 1.2. Samples containing CAT activity between 2-35 nmol/min/ml can be assayed without further dilution or concentration.

Precision:

When a series of 45 CAT measurements were performed on the same day, the intra-assay coefficient of variation was 3.8%. When a series of 45 CAT measurements were performed on five different days under the same experimental conditions, the inter-assay coefficient of variation was 9.9%.

Appendix E

Superoxide Dismutase Assay Kit (Item no.706002 cayman)

Precautions

Please read these instructions carefully before beginning this assay.

For research use only. Not for human or diagnostic use.

If You Have Problems

Technical Service Contact Information

Phone: 888-526-5351 (USA and Canada only) or 734-975-3888

Fax: 734-971-3641

Email: techserv@caymanchem.com

Hours: M-F 8:00 AM to 5:30 PM EST

In order for our staff to assist you quickly and efficiently, please be ready to supply the lot number of the kit (found on the outside of the box).

Storage and Stability

This kit will perform as specified if stored as directed at -20°C and used before the expiration date indicated on the outside of the box.

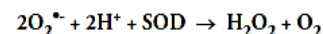
Materials Needed But Not Supplied

1. A plate reader capable of measuring an absorbance at 440–460 nm
2. Adjustable pipettes and a repeat pipettor
3. A source of pure water; glass distilled water or HPLC-grade water is acceptable

INTRODUCTION

Background

Superoxide dismutases (SODs) are metalloenzymes that catalyze the dismutation of the superoxide anion to molecular oxygen and hydrogen peroxide and thus form a crucial part of the cellular antioxidant defense mechanism.¹



Three types of SODs have been characterized according to their metal content: copper/zinc (Cu/Zn), manganese (Mn), and iron (Fe). SOD is widely distributed in both plants and animals. It occurs in high concentrations in brain, liver, heart, erythrocytes, and kidney. In humans, there are three forms of SOD: cytosolic Cu/Zn-SOD, mitochondrial MnSOD, and extracellular SOD.² Extracellular SOD is found in the interstitial spaces of tissues and also in extracellular fluids, accounting for the majority of the SOD activity in plasma, lymph, and synovial fluid.^{3,4}

The amount of SOD present in cellular and extracellular environments is crucial for the prevention of diseases linked to oxidative stress. Mutations in SOD account for approximately 20% of familial amyotrophic lateral sclerosis (ALS) cases. SOD also appears to be important in the prevention of other neurodegenerative disorders such as Alzheimer's, Parkinson's, and Huntington's diseases.^{5,6} The reaction catalyzed by SOD is extremely fast, having a turnover of $2 \times 10^9 \text{ M}^{-1}\text{sec}^{-1}$ and the presence of sufficient amounts of the enzyme in cells and tissues typically keeps the concentration of superoxide ($\text{O}_2^{\bullet -}$) very low.¹ However, in a competing reaction, nitric oxide (NO) reacts with $\text{O}_2^{\bullet -}$ with a rate constant of $6.7 \times 10^9 \text{ M}^{-1}\text{sec}^{-1}$ to form the powerful oxidizing and nitrating agent, peroxynitrite.⁷ Under conditions in which SOD activity is low or absent (*i.e.*, SOD mutation) or which favor the synthesis of μM concentrations of NO (*i.e.*, ischemia/reperfusion, iNOS upregulation, etc.), NO outcompetes SOD for superoxide, resulting in the formation of peroxynitrite. The presence of nitrotyrosine as a "footprint" for peroxynitrite, and hence the prior co-existence of both $\text{O}_2^{\bullet -}$ and NO, has been observed in a variety of medical conditions, including atherosclerosis, sepsis, and ALS.⁷

About This Assay

Cayman's Superoxide Dismutase Assay Kit utilizes a tetrazolium salt for detection of superoxide radicals generated by xanthine oxidase and hypoxanthine (see scheme 1, below). One unit of SOD is defined as the amount of enzyme needed to exhibit 50% dismutation of the superoxide radical. The SOD assay measures all three types of SOD (Cu/Zn, Mn, and FeSOD). The assay provides a simple, reproducible, and fast tool for assaying SOD activity in plasma, serum, erythrocyte lysates, tissue homogenates, and cell lysates. Mitochondrial MnSOD can be assayed separately following the procedure outlined under sample preparation (see page 8).

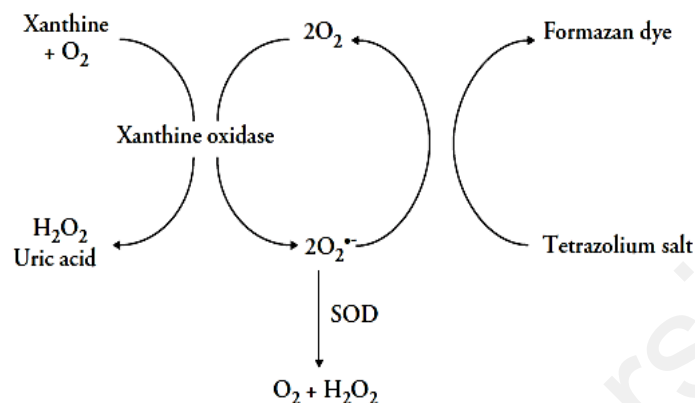


Figure 1. Scheme of the Superoxide Dismutase Assay

PRE-ASSAY PREPARATION

Reagent Preparation

1. Assay Buffer (10X) - (Item No. 706001)

Dilute 3 ml of Assay Buffer concentrate with 27 ml of HPLC-grade water for assaying 96 wells. Prepare additional Assay Buffer as needed. This final Assay Buffer (50 mM Tris-HCl, pH 8.0, containing 0.1 mM diethylenetriaminepentaacetic acid (DTPA) and 0.1 mM hypoxanthine) should be used to dilute the radical detector. When stored at 4°C, this diluted Assay Buffer is stable for at least two months.

2. Sample Buffer (10X) - (Item No. 706003)

Dilute 2 ml of Sample Buffer concentrate with 18 ml of HPLC-grade water for assaying 96 wells. Prepare additional Sample Buffer as needed. This final Sample Buffer (50 mM Tris-HCl, pH 8.0) should be used to prepare the SOD standards and dilute the xanthine oxidase and SOD samples prior to assaying. When stored at 4°C, this diluted Sample Buffer is stable for at least six months.

3. Radical Detector - (Item No. 706004)

The vials contain 250 µl of a tetrazolium salt solution. Prior to use, transfer 50 µl of the supplied solution to another vial and dilute with 19.95 ml of diluted Assay Buffer. Cover with tin foil. The diluted Radical Detector is stable for two hours. This is enough Radical Detector for 96 wells. Prepare additional detector as needed. Store unused Radical Detector at -20°C.

4. SOD Standard - (Item No. 706005)

The vials contain 100 µl of bovine erythrocyte SOD (Cu/Zn). Store the thawed enzyme on ice and see **Standard Preparation** on page 13 for preparing the standard curve. Store unused enzyme at -20°C. The enzyme is stable for at least two freeze/thaw cycles.

5. Xanthine Oxidase - (Item No. 706006)

These vials contain 150 μ l of Xanthine Oxidase. Prior to use, thaw one vial and transfer 50 μ l of the supplied enzyme to another vial and dilute with 1.95 ml of Sample Buffer (dilute). Store the thawed and diluted xanthine oxidase on ice. The diluted enzyme is stable for one hour. This is enough Xanthine Oxidase for 96 wells. Prepare additional Xanthine Oxidase as needed. Do not refreeze the thawed enzyme. Any unused enzyme should be thrown away.

Sample Preparation

The procedures listed below for tissue homogenates and cell lysates will result in assaying total SOD activity (cytosolic and mitochondrial). To separate the two enzymes, centrifuge the 1,500 x g supernatant at 10,000 x g for 15 minutes at 4°C. The resulting 10,000 x g supernatant will contain cytosolic SOD and the pellet will contain mitochondrial SOD.⁸ Homogenize the mitochondrial pellet in cold buffer (*i.e.*, 20 mM HEPES, pH 7.2, containing 1 mM EGTA, 210 mM mannitol, and 70 mM sucrose). If not assaying on the same day, freeze the samples at -80°C. The samples will be stable for at least one month.

The addition of 1-3 mM potassium cyanide to the assay will inhibit both Cu/Zn-SOD and extracellular SOD, resulting in the detection of only Mn-SOD activity.^{3,9}

Samples can be assayed in the absence of Xanthine Oxidase to generate a sample background. This sample background absorbance should be subtracted from the sample absorbance generated in the presence of Xanthine Oxidase thus correcting for non-SOD generated absorbance.

Tissue Homogenate

1. Prior to dissection, either perfuse or rinse tissue with phosphate buffered saline (PBS), pH 7.4, to remove any red blood cells and clots.
2. Homogenize the tissue in 5-10 ml of cold 20 mM HEPES buffer, pH 7.2, containing 1 mM EGTA, 210 mM mannitol, and 70 mM sucrose per gram tissue.
3. Centrifuge at 1,500 x g for five minutes at 4°C.
4. Remove the supernatant for assay and store on ice. If not assaying on the same day, freeze the sample at -80°C. The sample will be stable for at least one month.

Cell Lysate

1. Collect cells by centrifugation at 1,000-2,000 x g for 10 minutes at 4°C. For adherent cells, do not harvest using proteolytic enzymes; rather use a rubber policeman.
2. Homogenize or sonicate the cell pellet in cold 20 mM HEPES buffer, pH 7.2, containing 1 mM EGTA, 210 mM mannitol, and 70 mM sucrose.
3. Centrifuge at 1,500 x g for five minutes at 4°C.
4. Remove the supernatant for assay and store on ice. If not assaying on the same day, freeze the sample at -80°C. The sample will be stable for at least one month.

Plasma and Erythrocyte Lysate

1. Collect blood using an anticoagulant such as heparin, citrate, or EDTA.
2. Centrifuge the blood at 700-1,000 x g for 10 minutes at 4°C. Pipette off the top yellow plasma layer without disturbing the white buffy layer. Store plasma on ice until assaying or freeze at -80°C. The plasma sample will be stable for at least one month. Plasma should be diluted 1:5 with Sample Buffer before assaying for SOD activity.
3. Remove the white buffy layer (leukocytes) and discard.
4. Lyse the erythrocytes (red blood cells) in four times its volume of ice-cold HPLC-grade water.
5. Centrifuge at 10,000 x g for 15 minutes at 4°C.
6. Collect the supernatant (erythrocyte lysate) for assaying and store on ice. If not assaying the same day, freeze at -80°C. The sample will be stable for at least one month. The erythrocyte lysate should be diluted 1:100 with Sample Buffer before assaying for SOD activity.

Serum

1. Collect blood without using an anticoagulant such as heparin, citrate, or EDTA. Allow blood to clot for 30 minutes at 25°C.
2. Centrifuge the blood at 2,000 x g for 15 minutes at 4°C. Pipette off the top yellow serum layer without disturbing the white buffy layer. Store serum on ice. If not assaying the same day, freeze at -80°C. The sample will be stable for at least one month.
3. Serum should be diluted 1:5 with Sample Buffer before assaying for SOD activity.

Tissue Homogenization using the Precellys 24 Homogenizer

- Prior to dissection, either perfuse or rinse tissue with phosphate buffered saline (PBS), pH 7.4, to remove any red blood cells and clots.
- Freeze organs immediately upon collection and then store at -80°C. Snap-freezing of tissues in liquid nitrogen is preferred.
- Add cold 20 mM HEPES buffer, pH 7.2, containing 1mM EGTA, 210 mM mannitol, and 70mM sucrose.
- Homogenize the tissue sample using the Precellys 24 according to appropriate settings:
- Spin the tissue homogenates at 10,000 x g for 15 minutes at 4°C.
- Collect supernatant and assay samples according to the kit booklet protocol. Samples may need to be diluted appropriately for assay and should be normalized using a protein assay.

ASSAY PROTOCOL

Plate Set Up

There is no specific pattern for using the wells on the plate. A typical layout of SOD standards and samples to be measured in duplicate is given below in Figure 2. We suggest you record the contents of each well on the template sheet provided (see page 23).

	1	2	3	4	5	6	7	8	9	10	11	12
A	A	A	S2	S2	S10	S10	S18	S18	S26	S26	S34	S34
B	B	B	S3	S3	S11	S11	S19	S19	S27	S27	S35	S35
C	C	C	S4	S4	S12	S12	S20	S20	S28	S28	S36	S36
D	D	D	S5	S5	S13	S13	S21	S21	S29	S29	S37	S37
E	E	E	S6	S6	S14	S14	S22	S22	S30	S30	S38	S38
F	F	F	S7	S7	S15	S15	S23	S23	S31	S31	S39	S39
G	G	G	S8	S8	S16	S16	S24	S24	S32	S32	S40	S40
H	S1	S1	S9	S9	S17	S17	S25	S25	S33	S33	S41	S41

A-G = Standards

S1-S41 = Sample Wells

Figure 2. Sample plate format

Pipetting Hints

- It is recommended that an adjustable pipette be used to deliver reagents to the wells.
- Before pipetting each reagent, equilibrate the pipette tip in that reagent (*i.e.*, slowly fill the tip and gently expel the contents, repeat several times).
- Do not expose the pipette tip to the reagent(s) already in the well.

General Information

- The final volume of the assay is 230 μ l in all the wells.
- It is not necessary to use all the wells on the plate at one time.
- The assay temperature is 25°C.
- All reagents except samples and Xanthine Oxidase must be equilibrated to room temperature before beginning the assay.
- It is recommended that the samples and SOD standards be assayed at least in duplicate.
- Monitor the absorbance at 440–460 nm using a plate reader.

Standard Preparation

Dilute 20 μ l of the SOD Standard (Item No. 706005) with 1.98 ml of Sample Buffer (dilute) to obtain the SOD stock solution. Take seven clean glass test tubes and mark them A-G. Add the amount of SOD stock and Sample Buffer (dilute) to each tube as described in Table 1 below.

Tube	SOD Stock (μ l)	Sample Buffer (μ l)	Final SOD Activity (U/ml)
A	0	1,000	0
B	20	980	0.025
C	40	960	0.05
D	80	920	0.1
E	120	880	0.15
F	160	840	0.2
G	200	800	0.25

Table 1. Superoxide Dismutase standards

Performing the Assay

1. **SOD Standard Wells** - add 200 μ l of the diluted Radical Detector and 10 μ l of Standard (tubes A-G) per well in the designated wells on the plate (see sample plate format, Figure 2, page 11).
2. **Sample Wells**- add 200 μ l of the diluted Radical Detector and 10 μ l of sample to the wells. *NOTE: If using an inhibitor, add 190 μ l of the diluted Radical Detector, 10 μ l of inhibitor, and 10 μ l of sample to the wells. The amount of sample added to the well should always be 10 μ l. Samples should be diluted with Sample Buffer (dilute) or concentrated with an Amicon centrifuge concentrator with a molecular weight cut-off of 10,000 to bring the enzymatic activity to fall within the standard curve range.*
3. Initiate the reactions by adding 20 μ l of diluted Xanthine Oxidase to all the wells you are using. Make sure to note the precise time you started and add the Xanthine Oxidase as quickly as possible. *NOTE: If assaying sample backgrounds, add 20 μ l of Sample Buffer instead of Xanthine Oxidase.*
4. Carefully shake the 96-well plate for a few seconds to mix. Cover with the plate cover.
5. Incubate the plate on a shaker for 20 minutes at room temperature. Read the absorbance at 440-460 nm using a plate reader.

ANALYSIS

Calculations

1. Calculate the average absorbance of each standard and sample. If assayed, subtract sample background absorbance from the sample.
2. Divide standard A's absorbance by itself and divide standard A's absorbance by all the other standards and samples absorbances to yield the linearized rate (LR) (*i.e.*, LR for Std A = Abs Std A/Abs Std A; LR for Std B = Abs Std A/Abs Std B).
3. Plot the linearized SOD standard rate (LR) (from step 2 above) as a function of final SOD Activity (U/ml) from Table 1. See Figure 3 (on page 17) for a typical standard curve.
4. Calculate the SOD activity of the samples using the equation obtained from the linear regression of the standard curve substituting the linearized rate (LR) for each sample. One unit is defined as the amount of enzyme needed to exhibit 50% dismutation of the superoxide radical. SOD activity is standardized using the cytochrome c and xanthine oxidase coupled assay

$$\text{SOD (U/ml)} = \left[\left(\frac{\text{sample LR} - \text{y-intercept}}{\text{slope}} \right) \times \frac{0.23 \text{ ml}}{0.01 \text{ ml}} \right] \times \text{sample dilution}$$

Appendix F

Glutathione Peroxidase Assay Kit (Item no.703102 cayman)

Precautions

Please read these instructions carefully before beginning this assay.

For research use only. Not for human or diagnostic use.

If You Have Problems

Technical Service Contact Information

Phone: 888-526-5351 (USA and Canada only) or 734-975-3888

Fax: 734-971-3641

Email: techserv@caymanchem.com

Hours: M-F 8:00 AM to 5:30 PM EST

In order for our staff to assist you quickly and efficiently, please be ready to supply the lot number of the kit (found on the outside of the box).

Storage and Stability

This kit will perform as specified if stored as directed at -20°C and used before the expiration date indicated on the outside of the box.

Materials Needed But Not Supplied

1. A plate reader capable of measuring absorbance at 340 nm
2. Adjustable pipettes and a repeat pipettor
3. A source of pure water; glass distilled water or HPLC-grade water is acceptable

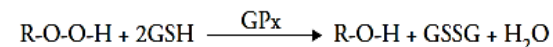
INTRODUCTION

Background

Glutathione peroxidase (GPx) catalyzes the reduction of hydroperoxides, including hydrogen peroxide, by reduced glutathione and functions to protect the cell from oxidative damage. With the exception of phospholipid-hydroperoxide GPx, a monomer, all of the GPx enzymes are tetramers of four identical subunits.^{1,2} Each subunit contains a selenocysteine in the active site which participates directly in the two-electron reduction of the peroxide substrate.^{1,2} The enzyme uses glutathione as the ultimate electron donor to regenerate the reduced form of the selenocysteine.^{1,2}

About This Assay

Cayman's GPx Assay measures GPx activity indirectly by a coupled reaction with glutathione reductase (GR). Oxidized glutathione (GSSG), produced upon reduction of hydroperoxide by GPx, is recycled to its reduced state by GR and NADPH:



The oxidation of NADPH to NADP⁺ is accompanied by a decrease in absorbance at 340 nm. Under conditions in which the GPx activity is rate limiting, the rate of decrease in the A₃₄₀ is directly proportional to the GPx activity in the sample.³ The Cayman GPx Assay Kit can be used to measure all of the glutathione-dependent peroxidases in plasma, erythrocyte lysates, tissue homogenates, and cell lysates.

PRE-ASSAY PREPARATION

Reagent Preparation

1. GPx Assay Buffer (10X) - (Item No. 703110)

Each vial contains 3 ml of Assay Buffer. Dilute the contents of the vial with 27 ml of HPLC-grade water. This final Assay Buffer (50 mM Tris-HCl, pH 7.6, containing 5 mM EDTA) should be used in the assay. When stored at 4°C, this diluted Assay Buffer is stable for at least six months. Prepare the additional vial as needed.

2. GPx Sample Buffer (10X) - (Item No. 703112)

Dilute 2 ml of Sample Buffer concentrate with 18 ml of HPLC-grade water. This final Sample Buffer (50 mM Tris-HCl, pH 7.6, containing 5 mM EDTA and 1 mg/ml BSA) should be used to dilute the GPx control and the GPx samples prior to assaying. When stored at 4°C, this diluted Sample Buffer is stable for at least one month.

3. Glutathione Peroxidase (Control) - (Item No. 703114)

This vial contains 50 µl of bovine erythrocyte GPx. To avoid repeated freezing and thawing, the GPx should be aliquoted into several small vials and stored at -20°C. Prior to use, transfer 10 µl of the supplied enzyme to another vial and dilute with 490 µl of diluted Sample Buffer and keep on ice. The diluted enzyme is stable for four hours on ice. A 20 µl aliquot of this diluted enzyme per well causes a decrease of approximately 0.051 absorbance unit/minute under the standard assay conditions described in Performing the Assay (see page 11).

4. GPx Co-Substrate Mixture - (Item No. 703116)

The 96-well kit contains three 40 well size of Co-Substrate Mixture. These vials contain a lyophilized powder of NADPH, glutathione, and glutathione reductase. Each reconstituted vial will be enough reagent for 40 wells. Reconstitute the number of vials that you will need by adding 2 ml of HPLC-grade water to each vial and vortex well. The 480-well kit contains five 96 well size of Co-Substrate Mixture. Reconstitute the number of vials that you will need by adding 6 ml of HPLC-grade water to each vial and vortex well. Each reconstituted vial will be enough reagent for 96 wells. The reconstituted reagent should be kept at 25°C while assaying and then stored at 4°C. If stored at 4°C, the reconstituted reagent is stable for two days. *NOTE: Do not freeze the reconstituted reagent.*

5. GPx Cumene Hydroperoxide - (Item No. 703118)

The 96-well kit contains one 2.5 ml vial of cumene hydroperoxide. The 480-well kit contains one 12 ml vial of cumene hydroperoxide. The vials should be stored at -20°C when not being used. The reagent is ready to use as supplied.

Sample Preparation

Tissue Homogenate

1. Prior to dissection, perfuse or rinse tissue with a PBS (phosphate buffered saline) solution, pH 7.4, to remove any red blood cells and clots.
2. Homogenize the tissue in 5-10 ml of cold buffer (*i.e.*, 50 mM Tris-HCl, pH 7.5, 5 mM EDTA, and 1 mM DTT) per gram tissue.
3. Centrifuge at 10,000 x g for 15 minutes at 4°C.
4. Remove the supernatant for assay and store on ice. If not assaying on the same day, freeze the sample at -80°C. The sample will be stable for at least one month.

Cell Lysate

1. Collect cells by centrifugation (*i.e.*, 1,000-2,000 x g for 10 minutes at 4°C). For adherent cells, do not harvest using proteolytic enzymes, rather use a rubber policeman.
2. Homogenize cell pellet in cold buffer (*i.e.*, 50 mM Tris-HCl, pH 7.5, 5 mM EDTA, and 1 mM DTT).
3. Centrifuge at 10,000 x g for 15 minutes at 4°C.
4. Remove the supernatant for assay and store on ice. If not assaying on the same day, freeze the sample at -80°C. The sample will be stable for at least one month.

Plasma and Erythrocyte Lysate

1. Collect blood using an anticoagulant such as heparin, citrate, or EDTA.
2. Centrifuge the blood at 700-1,000 x g for 10 minutes at 4°C. Pipette off the top yellow plasma layer without disturbing the white buffy layer. Store plasma on ice until assaying or freeze at -80°C. The plasma sample will be stable for at least one month. Dilute the plasma 1:2 with Sample Buffer before assaying.
3. Remove the white buffy layer (leukocytes) and discard.
4. Lyse the erythrocytes (red blood cells) in 4 volumes of ice-cold HPLC-grade water.
5. Centrifuge at 10,000 x g for 15 minutes at 4°C.
6. Collect the supernatant (erythrocyte lysate) for assaying and store on ice. If not assaying the same day, freeze at -80°C. The sample will be stable for at least one month. Dilute the erythrocyte lysate 1:10-1:20 with Sample Buffer before assaying.

NOTE: It has been reported that heme peroxidase activity of hemoglobin can lead to falsely elevated GPx activity in erythrocyte lysates. There was no significant effect in the GPx activity when assayed with Cumene Hydroperoxide as the substrate. Therefore, it is not necessary to treat the sample with Drabkin's Reagent (potassium ferricyanide/potassium cyanide) to convert hemoglobin to cyanmethemoglobin before assaying.

Tissue Homogenization using the Precellys 24 Homogenizer

- Freeze organs immediately upon collection and then store at -80°C. Snap-freezing of tissues in liquid nitrogen is preferred.
- Add 1 ml of homogenization buffer (50 mM Tris-HCl, pH 7.5, 5 mM EDTA and 1 mM DTT) per 100 milligrams of tissue.
- Homogenize the sample using the Precellys 24 according to appropriate settings:

Organ	Speed (rpm)	Cycle Length (seconds)	Cycle Break (seconds)	Number of Cycles	Beads
Heart (aorta)	5,000	30	30	3	CK28 Large Ceramic

- Spin the tissue homogenates at 10,000 x g for 15 minutes at 4°C.
- Collect supernatant and assay samples according to the kit booklet protocol. Samples may need to be diluted appropriately for assay and should be normalized using a protein assay.

ASSAY PROTOCOL

Plate Set Up

There is no specific pattern for using the wells on the plate. However, it is necessary to have three wells designated as non-enzymatic or background wells. The absorbance rate of these wells must be subtracted from the absorbance rate measured in the GPx sample and control wells. We suggest that there be at least three wells designated as positive controls and that you record the contents of each well on the template sheet provided on page 19.

	1	2	3	4	5	6	7	8	9	10	11	12
A	B	B	B	7	7	7	15	15	15	23	23	23
B	C	C	C	8	8	8	16	16	16	24	24	24
C	1	1	1	9	9	9	17	17	17	25	25	25
D	2	2	2	10	10	10	18	18	18	26	26	26
E	3	3	3	11	11	11	19	19	19	27	27	27
F	4	4	4	12	12	12	20	20	20	28	28	28
G	5	5	5	13	13	13	21	21	21	29	29	29
H	6	6	6	14	14	14	22	22	22	30	30	30

B - Background Wells
 C - Positive Control Wells
 1-30 - Sample Wells

Figure 2. Sample plate format

Pipetting Hints

- It is recommended that an adjustable pipette be used to deliver reagents to the wells.
- Use different tips to pipette the Assay Buffer (dilute), Co-Substrate Mixture, enzymes, and Cumene Hydroperoxide.
- Before pipetting each reagent, equilibrate the pipette tip in that reagent (*i.e.*, slowly fill the tip and gently expel the contents, repeat several times).
- Do not expose the pipette tip to the reagent(s) already in the well.

General Information

- The final volume of the assay is 190 μ l in all the wells.
- It is not necessary to use all the wells on the plate at one time.
- The assay temperature is 25°C.
- Use the Assay Buffer (dilute) in the assay.
- Monitor the decrease in absorbance at 340 nm using a plate reader.

Performing the Assay

1. **Background or Non-enzymatic Wells** - add 120 μ l of Assay Buffer and 50 μ l of co-substrate mixture to three wells.
2. **Positive Control Wells (bovine erythrocyte GPx)** - add 100 μ l of Assay Buffer, 50 μ l of Co-Substrate Mixture, and 20 μ l of diluted GPx (control) to three wells.
3. **Sample Wells** - add 100 μ l of Assay Buffer, 50 μ l of Co-Substrate Mixture, and 20 μ l of sample to three wells. To obtain reproducible results, the amount of GPx added to the well should cause an absorbance decrease between 0.02 and 0.135/min. When necessary, samples should be diluted with Sample Buffer or concentrated with an Amicon centrifuge concentrator with a molecular weight cut-off of 10,000 to bring the enzymatic activity to this level. *NOTE: The amount of sample added to the well should always be 20 μ l. To determine if an additional sample control should be performed see the Interferences section (page 14).*
4. Initiate the reactions by adding 20 μ l of Cumene Hydroperoxide to all the wells being used. Make sure to note the precise time the reaction is initiated and add the Cumene Hydroperoxide as quickly as possible.
5. Carefully shake the plate for a few seconds to mix.
6. Read the absorbance once every minute at 340 nm using a plate reader to obtain at least 5 time points. *NOTE: The initial absorbance of the sample wells should not be above 1.2 or below 0.5.*

ANALYSIS

Calculations

- Determine the change in absorbance (ΔA_{340}) per minute by:
 - Plotting the absorbance values as a function of time to obtain the slope (rate) of the linear portion of the curve (a graph is shown on page 13 using bovine erythrocyte GPx) -or-
 - Select two points on the linear portion of the curve and determine the change in absorbance during that time using the following equation:

$$\Delta A_{340}/\text{min.} = \frac{|A_{340}(\text{Time 2}) - A_{340}(\text{Time 1})|}{\text{Time 2 (min.)} - \text{Time 1 (min.)}}$$

*Use the absolute value.

- Determine the rate of $\Delta A_{340}/\text{min.}$ for the background or non-enzymatic wells and subtract this rate from that of the sample wells.
- Use the following formula to calculate the GPx activity. The reaction rate at 340 nm can be determined using the NADPH extinction coefficient of $0.00373 \mu\text{M}^{-1}\text{cm}^{-1}$ *. One unit is defined as the amount of enzyme that will cause the oxidation of 1.0 nmol of NADPH to NADP^+ per minute at 25°C.

$$\text{GPx activity} = \frac{\Delta A_{340}/\text{min.}}{0.00373 \mu\text{M}^{-1}} \times \frac{0.19 \text{ ml}}{0.02 \text{ ml}} \times \text{Sample dilution} = \text{nmol/min/ml}$$

*The actual extinction coefficient for NADPH at 340 nm is $0.00622 \mu\text{M}^{-1}\text{cm}^{-1}$. This value has been adjusted for the pathlength of the solution in the well (0.6 cm).

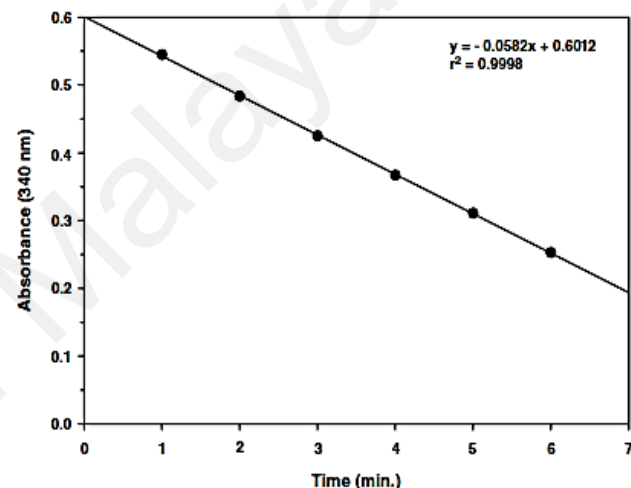


Figure 1. Activity of bovine erythrocyte GPx

Performance Characteristics

Precision:

When a series of seventy-seven GPx measurements were performed on the same day, the intra-assay coefficient of variation was 5.7%. When a series of seventy-seven GPx measurements were performed on five different days under the same experimental conditions, the inter-assay coefficient of variation was 7.2%.

Assay Range:

The dynamic range of the assay is limited only by the accuracy of the absorbance measurement. Most plate readers are linear to an absorbance of 1.2. Samples containing GPx activity between 50-344 nmol/min/ml can be assayed without further dilution or concentration. This GPx activity is equivalent to an absorbance decrease of 0.02 to 0.135 per minute.

Appendix G

TBARS Assay Kit(Item no.10009055 cayman)

Precautions

Please read these instructions carefully before beginning this assay.

For research use only. Not for human or diagnostic use.

It is recommended to take appropriate precautions when using the kit reagents (*i.e.*, lab coat, gloves, eye goggles, etc.), as some of them may be harmful.

The sodium hydroxide and acid solutions are corrosive and harmful if swallowed. Contact with skin may cause burns. In case of contact with skin or eyes, rinse immediately with plenty of water for 15 minutes.

Care should be exercised when removing samples from boiling water.

If You Have Problems

Technical Service Contact Information

Phone: 888-526-5351 (USA and Canada only) or 734-975-3888

Fax: 734-971-3641

Email: techserv@caymanchem.com

Hours: M-F 8:00 AM to 5:30 PM EST

In order for our staff to assist you quickly and efficiently, please be ready to supply the lot number of the kit (found on the outside of the box).

Storage and Stability

This kit will perform as specified if stored at 4°C and used before the expiration date indicated on the outside of the box.

Materials Needed But Not Supplied

1. A plate reader capable of measuring absorbance between 530-540 nm or a fluorometer with the capacity to measure fluorescence using an excitation wavelength of 530 nm and an emission wavelength of 550 nm
2. Adjustable pipettes and a repeat pipettor
3. A source of pure water; glass distilled water or HPLC-grade water is acceptable
4. Container sufficient to boil samples and standards
5. 5 ml polypropylene screw-cap centrifuge tubes (*i.e.*, VWR Item No. 16465-262)
6. Centrifuge capable of spinning 5 ml centrifuge tubes at 1,600 x g at 4°C

INTRODUCTION

Background

Malondialdehyde (MDA) is a naturally occurring product of lipid peroxidation. Lipid peroxidation is a well-established mechanism of cellular injury in both plants and animals and is used as an indicator of oxidative stress in cells and tissues.^{1,2} Lipid peroxides, derived from polyunsaturated fatty acids, are unstable and decompose to form a complex series of compounds, which include reactive carbonyl compounds, such as MDA. In human platelets, thromboxane synthase also catalyzes the conversion of PGH₂ to thromboxane A₂, 12(S)-HHTrE, and MDA in a ratio of 1:1:1.³

The measurement of Thiobarbituric Acid Reactive Substances (TBARS) is a well-established method for screening and monitoring lipid peroxidation.^{1,2} Modifications of the TBARS assay by many researchers have been used to evaluate several types of samples including human and animal tissues and fluids, drugs, and foods.⁴⁻⁸ Even though there remains a controversy cited in literature regarding the specificity of TBARS toward compounds other than MDA, it still remains the most widely employed assay used to determine lipid peroxidation.² If lipoprotein fractions are first acid precipitated from the sample, interfering soluble TBARS are minimized, and the test becomes quite specific for lipid peroxidation.² Lipids with greater unsaturation will yield higher TBARS values. It is recommended that if high TBARS values are obtained, a more specific assay such as HPLC should be performed.

About This Assay

Cayman's TBARS Assay Kit provides a simple, reproducible, and standardized tool for assaying lipid peroxidation in plasma, serum, urine, tissue homogenates, and cell lysates. The MDA-TBA adduct formed by the reaction of MDA and TBA under high temperature (90-100°C) and acidic conditions is measured colorimetrically at 530-540 nm or fluorometrically at an excitation wavelength of 530 nm and an emission wavelength of 550 nm. Although this reaction has a much higher sensitivity when measured fluorometrically, protocols for both methods are provided (see Figure 1 below).

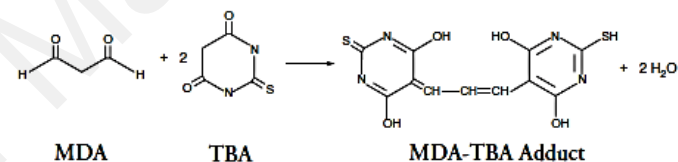


Figure 1.

PRE-ASSAY PREPARATION

Reagent Preparation

1. Thiobarbituric Acid - (Item No. 10009199)

The vial contains 2 g of thiobarbituric acid (TBA). It is ready to use to prepare the Color Reagent.

2. TBA Acetic Acid - (Item No. 10009200)

Each vial contains 20 ml of concentrated acetic acid. Slowly add both vials (40 ml) of TBA Acetic Acid to 160 ml of HPLC-grade water. This diluted Acetic Acid Solution is used in preparing the Color Reagent. The diluted Acetic Acid Solution is stable for at least three months at room temperature.

3. TBA Sodium Hydroxide (10X) - (Item No. 10009201)

The vial contains a solution of sodium hydroxide (NaOH). Dilute 20 ml of TBA NaOH with 180 ml of HPLC-grade water. This diluted NaOH Solution is used in preparing the Color Reagent. The diluted NaOH Solution is stable for at least three months at room temperature. Store the diluted NaOH Solution in a plastic container suitable for corrosive materials.

4. TBA Malondialdehyde Standard - (Item No. 10009202)

The vial contains 500 μM malondialdehyde (MDA) in water. It is ready to use to prepare the standard curve.

5. TBA SDS Solution - (Item No. 10009203)

The vial contains a solution of sodium dodecyl sulfate (SDS). The solution is ready to use as supplied.

6. To prepare the Color Reagent:

The following amount of Color Reagent is sufficient to evaluate 24 samples. Adjust the volumes accordingly if more or less samples are going to be assayed. Weigh 530 mg of TBA (Item No. 10009199) and add to ≥ 150 ml beaker containing 50 ml of diluted TBA Acetic Acid solution. Add 50 ml of diluted TBA Sodium Hydroxide and mix until the TBA is completely dissolved. The solution is stable for 24 hours.

Sample Preparation

Plasma

Typically, normal human plasma has a lipid peroxide level (expressed in terms of MDA) of 1.86-3.94 μM .^{1,8}

1. Collect blood using an anticoagulant such as heparin, EDTA, or citrate.
2. Centrifuge the blood at 700-1,000 x g for 10 minutes at 4°C. Pipette off the top yellow plasma layer without disturbing the white buffy layer. Store plasma on ice. If not assaying the same day, freeze at -80°C. The plasma sample will be stable for one month while stored at -80°C.
3. Plasma does not need to be diluted before assaying.

Serum

Typically, normal human serum has a lipid peroxide level (expressed in terms of MDA) of 1.86-3.94 μM .¹

1. Collect blood without using an anticoagulant.
2. Allow blood to clot for 30 minutes at 25°C.
3. Centrifuge the blood at 2,000 x g for 15 minutes at 4°C. Pipette off the top yellow serum layer without disturbing the white buffy layer. Store serum on ice. If not assaying the same day, freeze at -80°C. The serum sample will be stable for one month while stored at -80°C.
4. Serum does not need to be diluted before assaying.

Urine

Typically, normal human urine has a lipid peroxide level (expressed in terms of MDA) of 0.8-2 $\mu\text{mol/g}$ creatinine.^{9,10}

1. Urine does not require any special treatments. If not assaying the same day, freeze at -80°C.

Tissue Homogenates

1. Weigh out approximately 25 mg of tissue into a 1.5 ml centrifuge tube.
2. Add 250 μ l of RIPA Buffer (Item No. 10010263) with protease inhibitors of choice (see **Interferences** section on page 19).
3. Sonicate for 15 seconds at 40V over ice.
4. Centrifuge the tube at 1,600 x g for 10 minutes at 4°C. Use the supernatant for analysis. Store supernatant on ice. If not assaying the same day, freeze at -80°C. The sample will be stable for one month.
5. Tissue homogenates do not need to be diluted before assaying.

Cell Lysates

1. Collect 2×10^7 cells in 1 ml of cell culture medium or buffer of choice, such as PBS.
2. Sonicate 3X for five second intervals at 40V setting over ice.
3. Use the whole homogenate in the assay, being sure to use the culture medium as a sample blank.
4. Cell lysates do not need to be diluted before assaying.

ASSAY PROTOCOL

Plate Set Up

There is no specific pattern for using the wells on the plate. A typical layout of standards and samples to be measured in duplicate is shown below in Figure 2. We suggest you record the contents of each well on the template sheet provided (see page 23).

	1	2	3	4	5	6	7	8	9	10	11	12
A	(A)	(A)	(S1)	(S1)	(S9)	(S9)	(S17)	(S17)	(S25)	(S25)	(S33)	(S33)
B	(B)	(B)	(S2)	(S2)	(S10)	(S10)	(S18)	(S18)	(S26)	(S26)	(S34)	(S34)
C	(C)	(C)	(S3)	(S3)	(S11)	(S11)	(S19)	(S19)	(S27)	(S27)	(S35)	(S35)
D	(D)	(D)	(S4)	(S4)	(S12)	(S12)	(S20)	(S20)	(S28)	(S28)	(S36)	(S36)
E	(E)	(E)	(S5)	(S5)	(S13)	(S13)	(S21)	(S21)	(S29)	(S29)	(S37)	(S37)
F	(F)	(F)	(S6)	(S6)	(S14)	(S14)	(S22)	(S22)	(S30)	(S30)	(S38)	(S38)
G	(G)	(G)	(S7)	(S7)	(S15)	(S15)	(S23)	(S23)	(S31)	(S31)	(S39)	(S39)
H	(H)	(H)	(S8)	(S8)	(S16)	(S16)	(S24)	(S24)	(S32)	(S32)	(S40)	(S40)

A-H = Standards

S1-S40 = Sample Wells

Figure 2. Sample plate format

Pipetting Hints

- It is recommended that an adjustable pipette be used to deliver reagents to the wells.
- Before pipetting each reagent, equilibrate the pipette tip in that reagent (*i.e.*, slowly fill the tip and gently expel the contents, repeat several times).
- Do not expose the pipette tip to the reagent(s) already in the well.

General Information

- All reagents except samples must be equilibrated to room temperature before beginning the assay. The SDS Solution will take at least one hour to equilibrate to room temperature if stored at 2-8°C. Briefly heating the SDS Solution at 37°C will re-dissolve the precipitated SDS. The SDS Solution can then be stored at room temperature.
- The final volume of the assay is 150 μ l in all wells.
- The assay is performed at room temperature.
- It is not necessary to use all the wells on the plate at one time.
- It is recommended that the samples and standards be assayed at least in duplicate.
- It is recommended that the samples and standards be kept at 4°C after preparation to increase sensitivity and reproducibility.
- Monitor the absorbance at 530-540 nm or read fluorescence at an excitation wavelength of 530 nm and an emission wavelength of 550 nm.

Colorimetric Standard Preparation

Dilute 250 μ l of the MDA Standard (Item No. 10009202) with 750 μ l of water to obtain a stock solution of 125 μ M. Take eight clean glass test tubes and label them A-H. Add the amount of 125 μ M MDA stock solution and water to each tube as described in Table 1.

Tube	MDA (μ l)	Water (μ l)	MDA Concentration (μ M)
A	0	1,000	0
B	5	995	0.625
C	10	990	1.25
D	20	980	2.5
E	40	960	5
F	80	920	10
G	200	800	25
H	400	600	50

Table 1. MDA colorimetric standards

Fluorometric Standard Preparation

Dilute 25 μl of the MDA Standard (Item No. 10009202) with 975 μl of water to obtain a stock solution of 12.5 μM . Take eight clean glass test tubes and label them A-H. Add the amount of 12.5 μM MDA stock solution and water to each tube as described in Table 2.

Tube	MDA (μl)	Water (μl)	MDA Concentration (μM)
A	0	1,000	0
B	5	995	0.0625
C	10	990	0.125
D	20	980	0.25
E	40	960	0.5
F	80	920	1
G	200	800	2.5
H	400	600	5

Table 2. MDA fluorometric standards

Performing the Assay

1. Label vial caps with standard number or sample identification number.
2. Add 100 μl of sample or standard to appropriately labeled 5 ml vial.
3. Add 100 μl of SDS Solution to vial and swirl to mix.
4. Add 4 ml of the Color Reagent forcefully down side of each vial.
5. Cap vials and place vials in foam or some other holder to keep the tubes upright during boiling.
6. Add vials to vigorously boiling water. Boil vials for one hour.
7. After one hour, immediately remove the vials and place in ice bath to stop reaction. Incubate on ice for 10 minutes.
8. After 10 minutes, centrifuge the vials for 10 minutes at 1,600 x g at 4°C. Vials may appear clear or cloudy. Cloudiness will clear upon warming to room temperature.
9. Vials are stable at room temperature for 30 minutes.
10. Load 150 μl (in duplicate) from each vial to either the clear plate (colorimetric version) or to the black plate (fluorometric version).
11. Read the absorbance at 530-540 nm or read fluorescence at an excitation wavelength of 530 nm and an emission wavelength of 550 nm.

ANALYSIS

Colorimetric Calculations

1. Calculate the average absorbance of each standard and sample.
2. Subtract the absorbance value of the standard A (0 μM) from itself and all other values (both standards and samples). This is the corrected absorbance.
3. Plot the corrected absorbance values (from step 2 above) of each standard as a function of MDA concentration (see Table 1, on page 13).
4. Calculate the values of MDA for each sample from the standard curve. An example of the MDA standard curve is shown below in Figure 3.

$$\text{MDA } (\mu\text{M}) = \left[\frac{(\text{Corrected absorbance}) - (y\text{-intercept})}{\text{Slope}} \right]$$

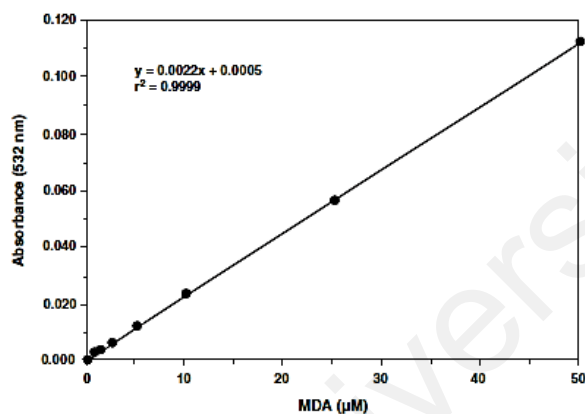


Figure 3. MDA colorimetric standard curve

Fluorometric Calculations

1. Calculate the average fluorescence of each standard and sample.
2. Subtract the fluorescence value of the standard A (0 μM) from itself and all other values (both standards and samples). This is the corrected fluorescence.
3. Plot the corrected fluorescence values (from step 2 above) of each standard as a function of MDA concentration (see Table 2, on page 14).
4. Calculate the values of MDA for each sample from the standard curve. An example of the MDA standard curve is shown below in Figure 4.

$$\text{MDA } (\mu\text{M}) = \left[\frac{(\text{Corrected fluorescence}) - (y\text{-intercept})}{\text{Slope}} \right]$$

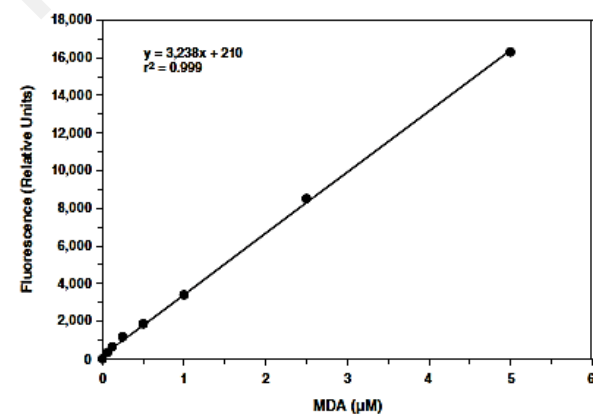


Figure 4. MDA fluorometric standard curve